

5-1-2010

# Identification and characterization of steroid receptor ligands

Megan Dennis

Follow this and additional works at: [https://digitalrepository.unm.edu/biom\\_etds](https://digitalrepository.unm.edu/biom_etds)

---

## Recommended Citation

Dennis, Megan. "Identification and characterization of steroid receptor ligands." (2010). [https://digitalrepository.unm.edu/biom\\_etds/11](https://digitalrepository.unm.edu/biom_etds/11)

This Dissertation is brought to you for free and open access by the Electronic Theses and Dissertations at UNM Digital Repository. It has been accepted for inclusion in Biomedical Sciences ETDs by an authorized administrator of UNM Digital Repository. For more information, please contact [disc@unm.edu](mailto:disc@unm.edu).

Megan Kathleen Dennis

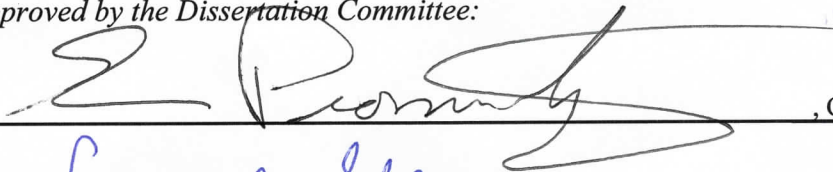
*Candidate*

Biomedical Sciences

*Department*

This dissertation is approved, and it is acceptable in quality and form for publication:

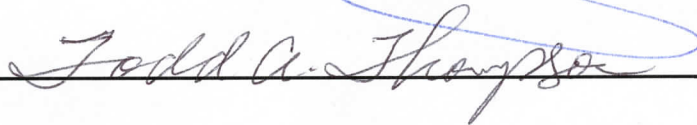
*Approved by the Dissertation Committee:*



, Chairperson

Larry A. Shear





**by**

DISSERTATION

Submitted in Partial Fulfillment of the  
Requirements for the Degree of

The University of New Mexico  
Albuquerque, New Mexico

## ACKNOWLEDGEMENTS

First, I would like to thank my parents, Mary and Greg. Without their guidance and support throughout the years this document would not exist. Thank you.

Secondly, I would like to thank my mentor, Dr. Eric Prossnitz. Eric has always been involved to the perfect degree in my research, staying out of the way and letting me learn to be an independent researcher but also always there to give advice and help me find my way. Throughout my career, I hope to be as effective a mentor to students as Eric has been for me.

Next, I would like to acknowledge my committee members, who have all been involved extensively with different parts of this work. Dr. Larry Sklar taught me a great many things about flow cytometry, presenting data and fielding questions. He also told me very early in my graduate work to keep my computer files organized and as I near the end of my time as a student, I realize that this may be the most valuable lesson of all. Dr. Todd Thompson has introduced me to the world of the androgen receptor and developing the MARS assay with his group restored my faith in my own ability to be a successful scientist when estrogen research appeared bleak. His Star Trek references and conversations with Eric also provided me with endless entertainment during meetings. Finally, I must thank Dr. Helen Hathaway, who has always provided a view from the 'mouse people' and has helped keep me grounded in the bigger physiological picture beyond chemical compounds and cell lines.

Finally, I would like to thank all of my co-workers, who are too numerous to name but who have all helped me with techniques, problems and making sense of the whole grad school experience.

**by**

**ABSTRACT OF DISSERTATION**

Submitted in Partial Fulfillment of the  
Requirements for the Degree of

The University of New Mexico  
Albuquerque, New Mexico

# IDENTIFICATION AND CHARACTERIZATION OF STEROID RECEPTOR LIGANDS

by

Megan Kathleen Dennis

B.S., Biology, Gonzaga University, 2004

Ph.D., Biomedical Sciences, University of New Mexico, 2010

## ABSTRACT

This work focuses on steroid receptors, including the androgen receptor (AR), the estrogen receptors (ERs) ER $\alpha$  and ER $\beta$ , known as the classical ERs, and GPR30, a recently described G protein-coupled estrogen receptor. Each of these receptors plays a role in many normal tissues and disease pathologies and signaling through steroid receptors is required for growth of many cancers. Additionally, many tissues express more than one estrogen receptor, making delineation of the functions of individual receptors difficult.

We have previously identified a GPR30-selective agonist, G-1, and this small molecule has been shown to mediate GPR30 function in a range of *in vitro* and *in vivo* systems. Thus, selective mediators of steroid receptor function do exist and will be useful in characterizing receptor function and in investigating therapeutic potential of each receptor individually. We hypothesize that the identification of novel estrogen and androgen receptor ligands will result in further elucidation of steroid receptor function in complex systems.

To address the possibility that additional selective ligands for steroid receptors exist, we first optimized a series of AR assays for investigation of a

library of small molecules to search for novel AR-mediating functions. Subsequently, high-throughput screening was used to search for selective estrogen receptor ligands and this search identified a small molecule antagonist of GPR30, G15. Follow-up characterization of G15 as well as synthetic chemistry based on the structural similarities resulted in a second-generation GPR30 antagonist, G36, which has increased specificity for GPR30 versus ER $\alpha$ /ER $\beta$ . These compounds were used to probe the function of GPR30 in glioma and we find that GPR30 is the functionally important estrogen receptor in this system, regulating the response of glioma cells to both estrogen and tamoxifen. Finally, two series of GPR30-targeted *in vivo* imaging agents were generated and characterized for biological activity prior to small animal imaging.

This work demonstrates the necessary processes involved for small molecule discovery and characterization, as well as several applications for receptor-specific small molecules beyond their initial identification.

## TABLE OF CONTENTS

ACKNOWLEDGEMENTS .....	iii
ABSTRACT.....	v
TABLE OF CONTENTS .....	vii
LIST OF FIGURES .....	xiii
ABBREVIATIONS .....	xvi
1 INTRODUCTION.....	1
1.1 Physiological importance of steroid hormones .....	2
1.2 Receptors for E2 and DHT .....	5
1.3 Genomic signaling through estrogen and androgen receptors.....	9
1.4 Non-genomic signaling through estrogen and androgen receptors . .....	11
1.5 Introduction to aberrant signaling of steroid receptors in cancer.	16
1.6 Introduction to estrogen and androgen receptor ligands.....	23
1.7 Introduction to high throughput screening .....	25
1.8 Introduction to <i>in vivo</i> tumor imaging.....	28
1.9 Rationale for project.....	32
2 ANDROGEN RECEPTOR SCREENING.....	35
2.1 Introduction .....	35
2.2 A multifunctional androgen receptor screening (MARS) assay using the high-throughput HyperCyt® flow cytometry system .....	40
2.2.1 ABSTRACT.....	41
2.2.2 INTRODUCTION.....	43
2.2.3 RESULTS.....	47
2.2.4 DISCUSSION.....	53
2.2.5 MATERIALS & METHODS .....	61
2.2.5.1 Chemicals.....	61
2.2.5.2 Expression vectors.....	61
2.2.5.3 Cell culture & transfection.....	61
2.2.5.4 Transcriptional activation assays .....	62
2.2.5.5 Microscopic analysis .....	62
2.2.5.6 HyperCyt® analysis.....	63
2.2.6 FIGURE LEGENDS.....	64
2.2.6.1 Figure 2.1. Methods of analysis using the MARS assay ...	64
2.2.6.2 Figure 2.2. MARS assay analyzed by microscopy .....	64
2.2.6.3 Figure 2.3. Chemical structures of the test set of compounds used for MARS assay validation .....	65
2.2.6.4 Figure 2.4. Androgenic activity of compounds in a single- dose MARS assay .....	65
2.2.6.5 Figure 2.5. Dose-response curves for AR agonists in the MARS assay.....	66
2.2.6.6 Figure 2.6. Dose-response curves for AR antagonists in the MARS assay .....	66
2.2.6.7 Table 2.1. EC <sub>50</sub> and IC <sub>50</sub> Values for MARS .....	66
2.3 Segue.....	74



2.4	AR / ICCVAM Screening Section.....	75
2.4.1	ABSTRACT.....	75
2.4.2	INTRODUCTION.....	76
2.4.3	RESULTS AND DISCUSSION.....	78
2.4.3.1	The MARS assay identifies AR transcriptional agonists and antagonists.....	78
2.4.3.2	Translocation of AR-GFP.....	79
2.4.4	MATERIALS & METHODS.....	82
2.4.4.1	Chemicals.....	82
2.4.4.2	Expression vectors.....	82
2.4.4.3	Cell culture & transfection.....	82
2.4.4.4	Transcriptional activation assays.....	83
2.4.4.5	HyperCyt® analysis.....	84
2.4.4.6	AR translocation assays.....	84
2.4.5	FIGURE LEGENDS.....	86
2.4.5.1	Figure 2.8. AR transcriptional activity of ICCVAM compounds.....	86
2.4.5.2	Figure 2.9. AR-GFP Translocation assay.....	86
2.4.5.3	Table 2.2. Summary of AR-GFP translocation induced by ICCVAM compounds.....	87
2.5	Overall Conclusions.....	94
3	ESTROGEN RECEPTOR SCREENING.....	96
3.1	ABSTRACT.....	96
3.2	INTRODUCTION.....	97
3.3	RESULTS & DISCUSSION.....	100
3.3.1	ER $\alpha$ and ER $\beta$ primary screen assay development.....	100
3.3.2	Primary ER $\alpha$ and ER $\beta$ screening.....	102
3.3.3	Secondary screening of ER $\alpha$ /ER $\beta$ hits.....	104
3.3.4	GPR30 preliminary screening and counterscreen of ER $\alpha$ , ER $\beta$ hits.....	104
3.3.5	Identification of GPR30/ER $\alpha$ /ER $\beta$ selective compounds.....	105
3.4	MATERIALS & METHODS.....	107
3.4.1	Cell culture and transfection.....	107
3.4.2	ER $\alpha$ and ER $\beta$ ligand binding assays.....	107
3.4.3	Intracellular calcium mobilization.....	108
3.4.4	PI3K activation.....	108
3.5	FIGURE LEGENDS.....	109
3.5.1	Figure 3.1. Optimization of ER $\alpha$ /ER $\beta$ ligand binding assay ...	109
3.5.2	Figure 3.2. Preliminary ER $\alpha$ /ER $\beta$ binding screen.....	109
3.5.3	Figure 3.3. Examples of results from ER $\alpha$ /ER $\beta$ dose-response screening.....	110
3.5.4	Figure 3.4. Example data from GPR30 calcium mobilization primary and counter screens.....	110
3.5.5	Figure 3.5. Venn diagram of selective compounds identified in roadmap screening of ER $\alpha$ , ER $\beta$ and GPR30.....	111
4	CHARACTERIZATION OF GPR30 ANTAGONISTS.....	119

4.1	Introduction .....	120
4.2	<i>In vivo</i> Effects of a GPR30 Antagonist.....	121
4.2.1	ABSTRACT.....	122
4.2.2	INTRODUCTION.....	123
4.2.3	RESULTS.....	126
4.2.3.1	Virtual & biomolecular screening and chemical synthesis ..	126
4.2.3.2	G15 inhibits cellular signaling through GPR30 .....	128
4.2.3.3	G15 inhibits GPR30-mediated function in vivo .....	130
4.2.4	DISCUSSION.....	133
4.2.5	METHODS.....	137
4.2.5.1	Chemical synthesis and characterization of G15. ....	137
4.2.5.2	Ligand binding assays .....	137
4.2.5.3	Intracellular calcium mobilization .....	138
4.2.5.4	PI3K activation.....	138
4.2.5.5	Mouse uterine estrogenicity assay .....	138
4.2.5.6	Mouse depression assay .....	139
4.2.6	ACKNOWLEDGEMENTS .....	141
4.2.7	FIGURE LEGENDS.....	142
4.2.7.1	Figure 4.1. Structures of G-1 and G15.....	142
4.2.7.2	Figure 4.2. Ligand binding properties of G15.....	142
4.2.7.3	Figure 4.3. G15 antagonism of intracellular calcium mobilization by GPR30 .....	142
4.2.7.4	Figure 4.4. G15 antagonism of PI3K activation by GPR30....	143
4.2.7.5	Figure 4.5. Effects of G15 on physiological responses mediated by GPR30.....	143
4.3	Segue.....	152
4.4	G36 Manuscript .....	153
4.4.1	ABSTRACT.....	153
4.4.2	INTRODUCTION.....	154
4.4.3	RESULTS & DISCUSSION.....	156
4.4.3.1	Identification of G36 .....	156
4.4.3.2	G36 exhibits decreased binding to ER $\alpha$ and ER $\beta$ at high doses compared to G15 .....	156
4.4.3.3	G36 effectively blocks E2-induced PI3K activation in GPR30 expressing cells .....	157
4.4.3.4	G36 blocks E2-induced calcium mobilization .....	158
4.4.4	MATERIALS & METHODS .....	159
4.4.4.1	Ligand binding assays .....	159
4.4.4.2	Intracellular calcium mobilization .....	159
4.4.4.3	PI3K activation.....	159
4.4.5	FIGURE LEGENDS.....	161
4.4.5.1	Figure 4.6. Structures of G-1, G15 and G36 .....	161
4.4.5.2	Figure 4.7. G36 Binding to ER $\alpha$ / $\beta$ .....	161

4.4.5.3	Figure 4.8. G36 Blocks PI3K activity mediated by GPR30 ....	161
4.4.5.4	Figure 4.9. G36 Blocks E2-induced calcium mobilization in cells expressing GPR30 .....	161
4.5	Summary .....	167
5	GPR30 SIGNALING IN CANCER .....	168
5.1	Introduction .....	169
5.2	A Role for GPR30 in Glioblastoma .....	171
5.2.1	ABSTRACT.....	172
5.2.2	INTRODUCTION.....	173
5.2.3	RESULTS.....	176
5.2.3.1	Expression of GPR30 in U87-MG cells.....	176
5.2.3.2	Functional characterization of GPR30 in U87-MG cells ..	176
5.2.3.3	Expression of GPR30 in patient tumor samples .....	178
5.2.4	DISCUSSION.....	179
5.2.5	MATERIALS & METHODS .....	182
5.2.5.1	Reagents.....	182
5.2.5.2	Cell culture and transfection .....	182
5.2.5.3	Immunofluorescence staining.....	183
5.2.5.4	PI3K Activation .....	183
5.2.5.5	Inhibitors .....	184
5.2.6	ACKNOWLEDGEMENTS .....	185
5.2.7	FIGURE LEGENDS.....	186
5.2.7.1	Figure 5.1. Expression of GPR30 in U87-MG cells.....	186
5.2.7.2	Figure 5.2. GPR30 activates PI3K in U87-MG cells .....	186
5.2.7.3	Figure 5.3. GPR30 is expressed in astrocytes in human glioblastoma.....	186
5.2.6	CONCLUSION.....	193
6	GPR30 <i>in vivo</i> IMAGING AGENTS .....	194
6.1	Introduction .....	195
6.2	Characterization of Iodinated GPR30 Imaging Agents .....	198
6.2.1	ABSTRACT.....	198
6.2.2	INTRODUCTION.....	199
6.2.3	RESULTS AND DISCUSSION .....	203
6.2.4	CONCLUSIONS.....	207
6.2.5	MATERIALS & METHODS .....	209
6.2.5.1	Intracellular calcium mobilization .....	209
6.2.5.2	PI3K activation.....	209
6.2.5.3	Ligand binding assays .....	209
6.2.5.4	Cell culture.....	210
6.2.5.5	Statistical analysis.....	210
6.2.6	ACKNOWLEDGEMENTS .....	211
6.2.7	FIGURE LEGENDS.....	212
6.2.7.1	Figure 6.1. Structures of 17 $\beta$ -estradiol (E2), GPR30-selective agonist (G-1) and antagonist (G-15).....	212

6.2.7.2	Figure 6.2. Structure of direct and pendant iodo-substituted tetrahydro-cyclopenta[c]quinoline derivatives .....	212
6.2.7.3	Table 6.1. Binding and functional characterization of GPR30-targeted compounds (summary).....	212
6.2.7.4	Table 6.2. Binding and functional characterization of GPR30-targeted compounds (raw data).....	212
6.3	Segue.....	217
6.4	Synthesis and Characterization of Indium Labeled GPR30 Imaging Agents.....	218
6.4.1	ABSTRACT.....	218
6.4.2	INTRODUCTION.....	219
6.4.3	RESULTS AND DISCUSSION.....	223
6.4.4	MATERIALS & METHODS.....	225
6.4.4.1	Cell culture.....	225
6.4.4.2	Intracellular calcium mobilization.....	225
6.4.4.3	PI3K activation.....	225
6.4.4.4	Receptor binding.....	226
6.4.4.5	Statistical analysis.....	226
6.4.5	CONCLUSION.....	227
6.4.6	FIGURE LEGENDS.....	228
6.4.6.1	Figure 6.3. Structure of G-1 based Indium labeled polyamino-polycarboxylate derivatives.....	228
6.4.6.2	Figure 6.4. Mobilization of intracellular calcium by <sup>113</sup> In labeled derivatives.....	228
6.4.6.3	Figure 6.5. Activation of PI3K via GPR30 by <sup>113</sup> In labeled derivatives.....	228
6.5	Conclusions.....	232
7	SUMMARY, IMPLICATIONS AND FUTURE DIRECTIONS.....	235
7.1	SUMMARY.....	236
7.1.1	Chapter 2.....	236
7.1.2	Chapter 3.....	240
7.1.3	Chapter 4.....	243
7.1.4	Chapter 5.....	245
7.1.5	Chapter 6.....	247
7.3	FUTURE DIRECTIONS.....	250
7.3.1	Androgen screen follow-up.....	250
7.3.2	Identification of important functional groups for GPR30-selective molecules.....	253
7.3.3	Characterization of additional roadmap compounds.....	254
7.3.4	Investigating GPR30 function in glioma.....	255
7.4	CONCLUDING REMARKS.....	256
APPENDIX:	Supplemental Figures.....	258
Figure S1.	ICCVAM MARS Agonists.....	259
Figure S2.	ICCVAM MARS Antagonists.....	260
Figure S3A.	ER Roadmap Primary Screening.....	261
Figure S3B.	ER Roadmap Primary Screening.....	262

Figure S3C.	ER Roadmap Primary Screening .....	263
Figure S3D.	ER Roadmap Primary Screening .....	264
Figure S3E.	ER Roadmap Primary Screening .....	265
Figure S3F.	ER Roadmap Primary Screening .....	266
Figure S3G.	ER Roadmap Primary Screening .....	267
Figure S3H.	ER Roadmap Primary Screening .....	268
Figure S3I.	ER Roadmap Primary Screening .....	269
Figure S4A. compounds	ER Roadmap Screening dose-responses of selected .....	270
Figure S4B. compounds	ER Roadmap Screening dose-responses of selected .....	271
Figure S4C. compounds	ER Roadmap Screening dose-responses of selected .....	272
Figure S4D. compounds	ER Roadmap Screening dose-responses of selected .....	273
Figure S4E. compounds	ER Roadmap Screening dose-responses of selected .....	274
Figure S4F. compounds	ER Roadmap Screening dose-responses of selected .....	275
Figure S4G. compounds	ER Roadmap screening dose-responses of selected .....	276
Figure S4H. compounds	ER Roadmap Screening dose-responses of selected .....	277
Figure S5.	Calcium mobilization assay data for G-scaffold Roadmap compounds .....	278
Figure S6.	G-Scaffold compounds.....	279
REFERENCES	.....	292

## LIST OF FIGURES

Figure 1.1.	Schematic of steroid hormone receptor superfamily members	6
Figure 1.2.	Schematic of classical ER subdomains	10
Figure 1.3.	Estrogen receptor signaling	14
Figure 1.4.	GPR30 Signaling	15
Figure 2.1.	Methods of analysis using the MARS assay	67
Figure 2.2.	MARS assay analyzed by microscopy	68
Figure 2.3.	Chemical structures of the test set of compounds used for MARS assay validation	69
Figure 2.4.	Androgenic activity of compounds in a single-dose MARS assay	70
Figure 2.5.	Dose-response curves for AR agonists in the MARS assay	71
Figure 2.6.	Dose-response curves for AR antagonists in the MARS assay	72
Table 2.1.	EC <sub>50</sub> and IC <sub>50</sub> Values for MARS	73
Figure 2.8A.	AR transcriptional activity of ICCVAM compounds	88
Figure 2.8B.	AR transcriptional activity of ICCVAM compounds	89
Figure 2.9A.	AR-GFP Translocation assay	90
Figure 2.9B and C.	AR-GFP Translocation assay	91
Figure 2.9D and E.	AR-GFP Translocation assay	92
Table 2.2.	Summary of AR-GFP translocation induced by ICCVAM compounds	93
Figure 3.1A and B.	Optimization of ER $\alpha$ /ER $\beta$ ligand binding assay	112
Figure 3.1C and D.	Optimization of ER $\alpha$ /ER $\beta$ ligand binding assay	113
Figure 3.1E.	Optimization of ER $\alpha$ /ER $\beta$ ligand binding assay	114
Figure 3.2.	Preliminary ER $\alpha$ /ER $\beta$ binding screen	115
Figure 3.3.	Examples of results from ER $\alpha$ /ER $\beta$ dose-response screening	116
Figure 3.4.	Example data from GPR30 calcium mobilization primary and counter screens	117
Figure 3.5.	Venn diagram of selective compounds identified in Roadmap screening of ER $\alpha$ , ER $\beta$ and GPR30	118
Figure 4.1.	Structures of G-1 and G15	145
Figure 4.2.	Ligand binding properties of G15	146
Figure 4.3.	G15 antagonism of intracellular calcium mobilization by GPR30	147
Figure 4.4A.	G15 antagonism of PI3K activation by GPR30	148
Figure 4.4B.	G15 antagonism of PI3K activation by GPR30	149
Figure 4.4C.	G15 antagonism of PI3K activation by GPR30	150
Figure 4.5.	Effects of G15 on physiological responses mediated by GPR30	151
Figure 4.6.	Structures of G-1, G15 and G36	162
Figure 4.7.	G36 Binding to ER $\alpha$ / $\beta$	163
Figure 4.8A.	G36 Blocks PI3K activity mediated by GPR30	164

Figure 4.8B.	G36 Blocks PI3K activity mediated by GPR30 .....	165
Figure 4.9.	G36 Blocks E2-induced calcium mobilization in cells expressing GPR30 .....	167
Figure 5.1.	Expression of GPR30 in U87-MG cells .....	187
Figure 5.2A.	GPR30 activates PI3K in U87-MG cells .....	188
Figure 5.2B.	GPR30 activates PI3K in U87-MG cells .....	189
Figure 5.2C.	GPR30 activates PI3K in U87-MG cells .....	190
Figure 5.3A.	GPR30 is expressed in astrocytes in human glioblastoma	191
Figure 5.3B.	GPR30 is expressed in astrocytes in human glioblastoma	192
Figure 6.1.	Structures of 17 $\beta$ -estradiol (E2), GPR30-selective agonist (G-1) and antagonist (G-15).....	213
Figure 6.2.	Structure of direct and pendant iodo-substituted tetrahydro-cyclopenta[c]quinoline derivatives .....	214
Table 6.1.	Binding and functional characterization of GPR30-targeted compounds (summary) .....	215
Table 6.2.	Binding and functional characterization of GPR30-targeted compounds (raw data).....	216
Figure 6.3.	Structure of G-1 based Indium labeled polyamino-polycarboxylate derivatives .....	229
Figure 6.4.	Mobilization of intracellular calcium by <sup>113</sup> In labeled derivatives .....	230
Figure 6.5.	Activation of PI3K via GPR30 by <sup>113</sup> In labeled derivatives..	231
Figure 6.6.	SPECT/CT Imaging of <sup>125</sup> I-labeled GPR30-targeted radioligand .....	232
Figure 6.7.	SPECT/CT Imaging of <sup>111</sup> In-labeled GPR30-targeted radioligand .....	233
Figure 6.8.	Focused SPECT/CT imaging of <sup>111</sup> In-labeled GPR30-targeted radioligand .....	234
Figure S1.	ICCVAM MARS Agonists.....	259
Figure S2.	ICCVAM MARS Antagonists.....	260
Figure S3A.	ER Roadmap Primary Screening .....	261
Figure S3B.	ER Roadmap Primary Screening .....	262
Figure S3C.	ER Roadmap Primary Screening .....	263
Figure S3D.	ER Roadmap Primary Screening .....	264
Figure S3E.	ER Roadmap Primary Screening .....	265
Figure S3F.	ER Roadmap Primary Screening .....	266
Figure S3G.	ER Roadmap Primary Screening .....	267
Figure S3H.	ER Roadmap Primary Screening .....	268
Figure S3I.	ER Roadmap Primary Screening .....	269
Figure S4A.	ER Roadmap Screening dose-responses of selected compounds .....	270
Figure S4B.	ER Roadmap Screening dose-responses of selected compounds .....	271
Figure S4C.	ER Roadmap Screening dose-responses of selected compounds .....	272

<b>Figure S4D.</b>	<b>ER Roadmap Screening dose-responses of selected</b>	
<b>compounds</b>	.....	273
<b>Figure S4E.</b>	<b>ER Roadmap Screening dose-responses of selected</b>	
<b>compounds</b>	.....	274
<b>Figure S4F.</b>	<b>ER Roadmap Screening dose-responses of selected</b>	
<b>compounds</b>	.....	275
<b>Figure S4G.</b>	<b>ER Roadmap screening dose-responses of selected</b>	
<b>compounds</b>	.....	276
<b>Figure S4H.</b>	<b>ER Roadmap Screening dose-responses of selected</b>	
<b>compounds</b>	.....	277
<b>Figure S5.</b>	<b>Calcium mobilization assay data for G-scaffold Roadmap</b>	
<b>compounds</b>	.....	278
<b>Figure S6.</b>	<b>G-Scaffold compounds</b> .....	279



## ABBREVIATIONS

3D—3 dimensional  
AF-1—activation function 1 domain  
AF-2—activation function 2 domain  
AR—androgen receptor  
ARE—androgen response element  
ATCC—American type culture collection  
ATP—adenosine triphosphate  
BC—bicalutamide  
BPA—bisphenol A  
BPB—bisphenol B  
BPC2—bisphenol C2  
Co-IP—co-immunoprecipitate  
CPA—cyproterone acetate  
CREB—cAMP response element binding  
CT—computed tomography  
CTGF—connective tissue growth factor  
DAPI—4',6-diamidino-2-phenylindole  
DBD—DNA binding domain  
DDT—dichlorodiphenyltrichloroethane  
DES—diethylstilbestrol  
DHT—5 $\alpha$ -dihydrotestosterone  
DOTA—1,4,7,10-tetraazacyclododecane-1,4,7,10-tetraacetic acid  
DPN—diarylpropionitrile  
dsEGFP—destabilized enhanced green fluorescent protein  
DTPA—diethylenetriaminepentaacetic acid  
E2—17 $\beta$ -estradiol  
EC50—half maximal effective concentration  
EGF—epidermal growth factor  
EGFR—epidermal growth factor receptor  
ER—estrogen receptor  
ERE—estrogen response element  
ERK—extracellular signal-regulated kinases  
ER $\alpha$ —estrogen receptor  $\alpha$   
ER $\beta$ —estrogen receptor  $\beta$   
FDG—2-[18F]-deoxy-D-Glucose  
FES—18F-fluoroestradiol  
GFAP— Glial fibrillary acidic protein  
EGFP—enhanced green fluorescent protein  
GPCR—G protein-coupled receptor  
GR—glucocorticoid receptor  
HER2—human epidermal growth factor receptor 2  
hr—hour  
HTS—high throughput screening  
IBC—inflammatory breast cancer

IC50—half maximal inhibitory concentration  
ICCVAM—Interagency Coordinating Committee on the Validation of Alternative Methods  
IGF—Insulin-like growth factor  
IGFR—Insulin-like growth factor receptor  
LDB—ligand binding domain  
LHRH—luteinizing hormone-releasing hormone  
MAPK—mitogen-activated protein kinase  
MARS—multifunctional androgen receptor screen  
MI—myocardial ischaemia  
min—minute  
MLSMR—Molecular Libraries Small Molecule Repository  
ms—millisecond  
MR—mineralocorticoid receptor  
NICETAM—The NTP (National Toxicology Program) Interagency Center for the Evaluation of Alternative Toxicological Methods  
NIH—National Institutes of Health  
PBS—Phosphate buffered saline  
PCa—Prostate cancer  
PET—positron emission tomography  
PFA—paraformaldehyde  
PH—pleckstrin homology  
PI3K—phosphoinositide 3-kinase  
PLC—phospholipase C  
PM—plasma membrane  
PMT—photomultiplier tube  
PPT—44',4''-(4-Propyl-[1H]-pyrazole-1,3,5-triyl)trisphenol  
PR<sub>A</sub>—progesterone receptor isoform A  
PR<sub>B</sub>—progesterone receptor isoform B  
RFP—red fluorescent protein  
SARM—selective androgen receptor modulator  
sec—second  
SERM—selective estrogen receptor modulator  
SHBG—sex hormone binding globulin  
SPECT—Single photon emission computed tomography

1

# INTRODUCTION

## 1.1 Physiological importance of steroid hormones

Steroid hormones, including  $17\beta$ -estradiol (E2), androgens, mineralocorticoids and glucocorticoids, regulate a wide range of physiological processes involved in the development and maintenance of an array of tissue types in both males and females. Estrogen plays a key role in development and general function of female reproductive organs and has also been shown to play a role in inflammation (Dai et al. 2009), cardioprotection (Guzzo 2000; Friedrich et al. 2006), maintenance of bone structure and strength (Termine and Wong 1998) and in the central nervous system (Hurn and Macrae 2000). Androgens play similar roles in normal male physiology; promoting reproductive organ development and maintaining organ function and regulating a number of other physiological processes.

Three classical roles for estrogen in female reproductive physiology are: reproductive organ development, regulation of estrus and menstrual cycling and establishing pregnancies and maintaining the pregnancy to term (Hewitt et al. 2005).  $ER\alpha$  is critical to mammary gland development, as shown in mice lacking  $ER\alpha$ , the branching ductal structures typically seen in mature mammary glands are not seen at the end of puberty, rather, mice have the rudimentary, non-branching mammary gland that they are born with (Visvader and Lindeman 2003). Estrogen, also signaling through  $ER\alpha$ , is required for implantation in mice (Curtis et al. 1999; Hewitt et al. 2002), whereas both  $ER\alpha$  and  $ER\beta$  are involved in regulating the estrus cycle in the mouse (Couse and Korach 1999). Estrogen is

also critical to male fertility, shown by ER $\alpha$  knockout mice, which are infertile due to breakdown of testicular structures (Couse and Korach 1999).

E2 also plays a well defined role in osteoporosis, wherein E2 normally acts to prevent osteoclast-mediated bone loss and promotes bone formation by osteoblasts; when E2 levels are deficient, such as following menopause, the rate of bone loss increases, resulting in osteoporosis (Rossouw et al. 2002). In patients with defective ER $\alpha$  or aromatase, bone density is decreased, supporting the role of E2 in maintenance of bone density (Smith et al. 1994; Herrmann et al. 2002).

Estrogen has also been shown to play a neuroprotective role in a range of conditions, including Parkinson's disease and Alzheimer's disease. In both diseases, postmenopausal hormone replacement therapy has been shown to be protective against disease onset, although E2 is not therapeutically useful after disease onset (Sherwin 2003; Currie et al. 2004). The mechanism of E2 neuroprotection in preventing the onset of Parkinson's has been suggested by culturing of rat neurons in E2-containing media, which prevents apoptosis and this effect is abrogated by ICI182,780 (Sawada et al. 1998; Sawada et al. 2000; Liu et al. 2005). In the case of Alzheimer's disease, the effects of E2 are less clear; however, E2 treatment of ovariectomized rats increases synthesis of acetylcholine, which has been shown to be reduced in Alzheimer's patients (Luine 1985).  $\beta$ -amyloid plaques are a major histological component seen in Alzheimer's patients and E2 treatment reduces cell death due to  $\beta$ -amyloid plaques in cholinergic cell lines, an effect that can be reversed by treatment with

ICI182,780 (Marin et al. 2003). Finally, in cell culture models, E2 promotes synapse formation and branching of dendritic cells; the loss of both of these structures is seen in Alzheimer's (Pinkerton and Henderson 2005).

Estrogen can also protect against stroke and cardiovascular disease in premenopausal women. The initial insight that E2 is protective against stroke comes from epidemiological data suggesting that premenopausal, but not postmenopausal, women have a lower incidence of stroke than men (Dhandapani and Brann 2002). This data led to the hypothesis that postmenopausal women who are on hormone therapy may also have a decreased risk of cardiovascular disease, but evidence from two large trials does not indicate that hormone replacement therapy decreases the risk of stroke in these women (Simon et al. 2001; Brass 2004). ERs, including ER $\alpha$ , ER $\beta$  and GPR30 are expressed in the brain, and in ER $\beta$ , but not ER $\alpha$  knockout mice, E2 is protective against brain injury, suggesting that ER $\alpha$  is involved in E2-mediated protection against injury (Dubal et al. 2001). However, in a different mouse stroke model, ER $\beta$  null mice were protected against stroke, suggesting a role for a protective mechanism independent of ER $\alpha$  or ER $\beta$  (Sampei et al. 2000), which could possibly be via GPR30.

As with stroke, premenopausal women exhibit significantly lower rates of cardiovascular disease, whereas postmenopausal women have higher rates of disease, similar to men (Deroo and Korach 2006). As with stroke, hormone replacement therapy in postmenopausal women does not decrease risk of cardiovascular disease, although this may have to do with the time elapsed

between the onset of menopause and the start of treatment with hormone replacement in many women (Mosca 2001). E2 also induces rapid vasodilatation via the release of nitric oxide and reduces the adhesion of inflammatory cells to atherosclerotic plaques (Mendelsohn 2000).

The roles for androgen in normal physiology are varied. 5 $\alpha$ -dihydrotestosterone (DHT) is required for building large amounts of muscle mass; hence, younger men tend to have larger muscles than older men who exercise a similar amount (Baumgartner et al. 1999). Additionally, as with estrogen, testosterone levels correlate positively with bone density measurements, although E2 levels seem to be more important (Barrett-Connor et al. 2000; Khosla et al. 2001). Increased testosterone levels also correlate with increased aggression, although the molecular basis for this observation is not known (Brooks and Reddon 1996). High levels of testosterone are also correlated with increased risk of atherosclerosis (Gyllenberg et al. 2001) and increased risk of prostate cancer (Gann et al. 1996) although, as for aggression, these correlations have not been exhaustively studied with regard to molecular mechanisms involving androgens.

## **1.2 Receptors for E2 and DHT**

Estrogen and androgen action in the body are mediated by a range of receptors, most of which are members of the steroid hormone receptor superfamily (**Fig. 1.1.**). Androgen signaling is controlled by the androgen receptor (AR), a 110 kD soluble protein, and possibly another type(s) of androgen receptor. This protein is resident in the cytoplasm prior to androgen

binding, at which point it translocates into the nucleus and dimerizes followed by receptor-mediated regulation of transcription of androgen responsive genes by binding to androgen response elements in

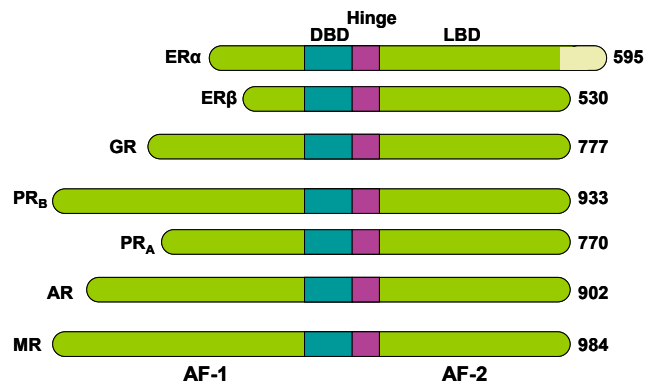


**Figure 1.1 Schematic of steroid hormone receptor superfamily members**

1999; Heinlein and Chang 2002). Other putative androgen receptors include an unknown receptor for androgen-bound sex hormone binding globulin (SHBG), which is either a G protein-coupled receptor (GPCR) or GPCR-linked (Nakhla et al. 1990; Nakhla et al. 1999) or a membrane androgen receptor, either the classical AR with a palmitoylation modification allowing membrane insertion or another unrelated membrane receptor (Benten et al. 1999; Christian et al. 2000; Kampa et al. 2002; Hall et al. 2006). This document will focus on the classical AR unless otherwise stated.

Mutations in the AR can result in altered specificity for ligand as well as altered signaling when a given ligand binds to the receptor. This aberrant signaling can result in compounds such as bicalutamide, which is an antagonist of wild type AR, acting as an agonist of the mutant AR and resulting in dysregulated signaling and disease. This results in the loss of sensitivity to anti-androgens and is a significant hurdle in the therapy of androgen-dependent tumors.



Estrogen signals through at least three receptors; the classical estrogen receptors (ERs) ER $\alpha$  and ER $\beta$  and the recently described 7 transmembrane G protein-coupled receptor GPR30 (Revankar et al. 2005; Thomas et al. 2005). The presence of multiple receptors, each with varying pharmacological properties and physiological roles, makes untangling the web of estrogenic signaling difficult.

The classical ERs, like the AR, are soluble hormone receptors of approximately 67 kD and 110 kD, respectively. Also, like the AR, the ER has a C-terminal ligand-binding domain (containing activation factor 2 or AF-2), a DNA binding domain and an N-terminal activation factor 1 (AF-1) domain containing Ser/Thr phosphorylation sites (Beato and Klug 2000). The N-terminal domains of ER $\alpha$  and ER $\beta$  are not well conserved, with ER $\alpha$  having a much longer N-terminal domain, which may account for, in part, the different physiological activities of the classical ERs (Edwards 2005). The phosphorylation sites in the N-terminal domain may regulate downstream signaling events and the interactions of classical ERs with cofactors (Lannigan 2003). The LBD is fairly well conserved between ER $\alpha$  and ER $\beta$ , although ER $\alpha$  has a slightly larger ligand binding pocket than ER $\beta$  (Zeng et al. 2008). The DNA binding domain of the classical ERs is highly conserved, with approximately 94% homology (Edwards 2005). Unlike the AR, the ERs reside predominantly in the nucleus regardless of ligand binding. Upon diffusion of E2 to the nucleus, it binds to ERs and the receptors dissociate from their chaperone protein, Hsp90, and dimerize to form the active transcription factor and bind to estrogen response elements (EREs) in the DNA to promote transcription (Song 2007). In addition to their role as transcription factors, the

classical ERs also mediate rapid signaling via other downstream pathways (Losel et al. 2003).

As a GPCR, GPR30 has significantly different physical properties than the classical ERs. Rather than being a soluble receptor, GPR30 is a membrane receptor with seven transmembrane domains and is localized predominantly to and active at the endoplasmic reticulum (Revankar et al. 2005; Revankar et al. 2007). GPR30 also does not act directly as a transcription factor but downstream signaling from GPR30 results in transcription of a variety of genes (Maggiolini et al. 2004; Albanito et al. 2007). GPR30 also initiates a wide range of rapid signaling events, via adenylyl cyclase (Filardo et al. 2002), transactivation of epidermal growth factor receptor (EGFR) via release of extracellular heparin-bound epidermal growth factor (EGF) (Filardo et al. 2000) and other pathways (Prossnitz et al. 2008).

There has been evidence for several other membrane estrogen receptors. The most well-defined of these is a modified classical ER which has a hydrophobic palmitoyl tail or another modification that allows insertion into the plasma membrane and thus localizes the classical ER to the inner leaflet of the plasma membrane (PM) (Pappas et al. 1995). A 46 kD truncated form of ER $\alpha$  has been shown to localize to the PM via palmitoylation; whereas a 36 kD truncated form of ER $\alpha$  has been shown to associate with the PM, most likely via myristoylation, although this mechanism is not completely defined (Song 2007). The membrane-localized classical ER is postulated to signal via rapid signaling pathways including mitogen-activated protein kinase (MAPK), Akt and activation

of cyclin D1 promoter (Song 2007) in a similar manner to nuclear-localized classical ERs and may also couple to G proteins to propagate downstream signaling (Razandi et al. 2003). In addition to modified classical ER there may exist another type of membrane ER, known as ER-X (Toran-Allerand et al. 2002; Toran-Allerand 2004).

### **1.3 Genomic signaling through estrogen and androgen receptors**

The classical activity attributed to steroid hormone receptors is that of ligand-activated transcription factors. Transcription via androgen response elements (AREs) and estrogen response elements (EREs) is responsible for the expression of many genes critical to male and female sexual development, respectively. Following development, estrogen and androgen driven transcription is critical for maintenance of a range of tissues including bone, reproductive tissues and neuronal function.

The mechanism for transcription via the classical ERs and the AR is well established. Upon binding of ligand to AR, the receptor dissociates from molecular chaperones, dimerizes and translocates to the nucleus where they bind to response elements in the DNA and promote transcription. ER-mediated transcription is very similar, except the ERs are resident in the nucleus prior to ligand binding so no receptor-ligand complex translocation is required.

Structurally, the classical ERs and the AR are relatively similar, containing the DNA-binding domain (DBD) at which ER/AR bind to AREs and EREs, respectively, in addition to a ligand binding domain (LBD) and domains for dimerization and cofactor binding. (**Fig. 1.2**). The binding of receptor dimers to

their cognate response elements results in coactivator or corepressor recruitment to DNA, with these cofactors binding to receptors at the AF-1 or AF-2 domains, and subsequent enhancement or repression of target gene expression (Edwards 2005).

In addition to ARE- or ERE-dependent gene transcription, AR and the classical ERs can also promote (or impair) transcription via non-ERE dependent mechanisms. In this modality, the AR/ER binds ligand, dissociates from HSP chaperones and dimerizes as in ARE-/ERE-dependent transcription but rather than the DBD of the receptor dimer binding to an ARE/ERE, the receptors bind to transcription factors such as AP-1, NF- $\kappa$ B or Sp1. The transcription factor bound to the AR/ER then binds directly to DNA and promotes or represses transcription (Kato et al. 2005). The interaction of transcription factors and AR/ER is facilitated by conformational changes, which occur upon ligand binding/HSP dissociation. The most well defined pathway for non-ERE-dependent classical ER-mediated transcription is that involving AP-1 sites, where ER $\alpha$  and ER $\beta$  act to mediate transcription via Jun/Fos (Kushner et al. 2000). ARE-independent, AR-mediated

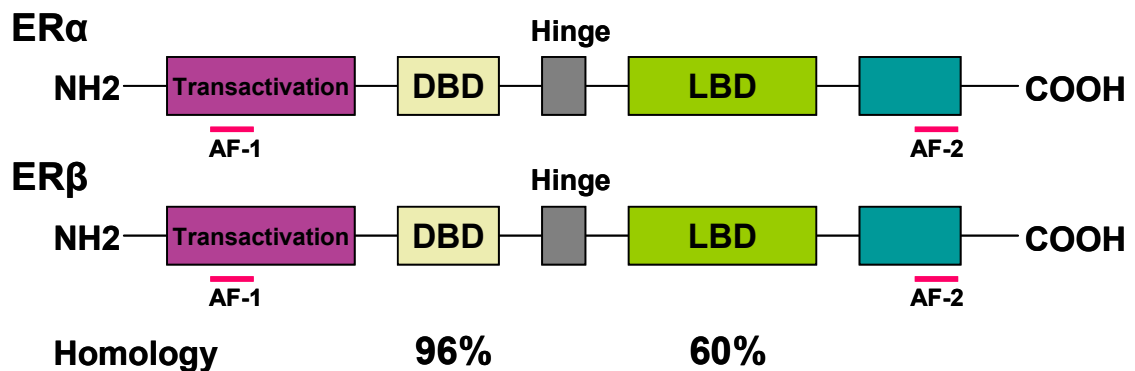


Figure 1.2 Schematic of classical ER subdomains.

transcription has been shown to occur in genes including EGFR (Brass et al. 1995; Lange et al. 1998) and *c-fos* (Richer et al. 1998; Church et al. 2005).

GPR30 also has the ability to influence transcription as a consequence of downstream signaling, one of the early reports of GPR30 function demonstrates that the proto-oncogene *c-fos* is upregulated following stimulation of GPR30 with estrogen and occurs downstream of extracellular signal-regulated kinase (ERK) activation (Maggiolini et al. 2004). This study was followed up using the selective GPR30 agonist, G-1, and similar results were seen for *c-fos* using this ligand as well as GPR30-dependent upregulation in cyclin D1, cyclin E and cyclin A expression (Albanito et al. 2007). GPR30 has also been reported to enhance transcription of nerve growth factor, cyclin D2 and Bcl-2 (Kanda and Watanabe 2003; Kanda and Watanabe 2003; Kanda and Watanabe 2004). Recently, connective tissue growth factor (CTGF) has been shown to be upregulated by GPR30 in response to both estrogen and tamoxifen and appears to promote proliferation (Pandey et al. 2009).

#### **1.4 Non-genomic signaling through estrogen and androgen receptors**

In addition to their important roles as transcription factors, steroid receptors have been shown to modulate a range of rapid signaling events. These signaling events are required for physiological effects of steroid hormones during development and for maintenance of reproductive capabilities.

The AR is capable of mediating a wide variety of rapid, non-classical signaling pathways. For example, acute application of testosterone to Sertoli cells results in a rapid AR-mediated increase in intracellular calcium

concentrations via phospholipase C (PLC) mediated opening of L-type calcium channels and an influx of extracellular calcium (Lyng et al. 2000; Loss et al. 2004). This increase in intracellular calcium may prompt cytoskeletal rearrangements and other events involved in Sertoli cell function (Loss et al. 2004). The MAPK pathway is also activated in Sertoli cells via Src-mediated transactivation of the EGFR by membrane bound AR, resulting in phosphorylation of ERK1/2 and CREB, leading to alterations in gene transcription (Cheng et al. 2007). This example of non-classical AR signaling indicates that while rapid AR signaling is via non-genomic mechanisms, the final downstream target of these pathways is often genomic in nature. Non-classical AR signaling can also involve other receptors, including the classical ER as seen in LNCaP cells, a human prostate cancer cell line, where the AR, ER and Src form an anti-apoptotic complex in response to androgen treatment (Migliaccio et al. 2000). Non-classical AR signaling may also play a crucial function in female reproduction, wherein androgen signaling via AR is required to overcome meiotic arrest in *Xenopus* oocytes *in vivo* and mouse oocytes *in vitro* (Lutz et al. 2001; Gill et al. 2004; White et al. 2005). Rapid androgen signaling also results in vasodilatation and rapid treatment (within 30 min) of patients with testosterone reduces myocardial ischaemia (Rosano et al. 1999; Webb et al. 1999; Webb et al. 1999). The sum total of these signaling pathways results in complex outcomes, including many aspects of male sexual development and physiological function.

Like the AR, classical ERs as well as GPR30 are capable of rapid, non-classical signaling. This network of signaling pathways mediates both non-genomic events including adhesion and activation of MAPK, Akt and other proteins, in addition to regulating pathways which result in the enhancement or repression of downstream transcription.

Classical ERs are capable of modulating phosphorylation of target proteins via an indirect mechanism utilizing other intracellular kinases, such as Src. The SH2 domain of Src binds to a site on ER $\alpha$  containing phosphotyrosine-537, and this interaction is stabilized when ER $\alpha$  is bound to estrogen (Castoria et al. 2001; Barletta et al. 2004). This activation of Src by ER $\alpha$  leads to the Src-mediated phosphorylation of Shc and insulin-like growth factor receptor (IGFR) and propagation of downstream signaling (Song et al. 2005). ER $\alpha$ , but not ER $\beta$ , can also bind directly to P85 $\alpha$ , the regulatory subunit of phosphoinositide 3-kinase (PI3K), which allows activation of p110, the catalytic subunit of PI3K and

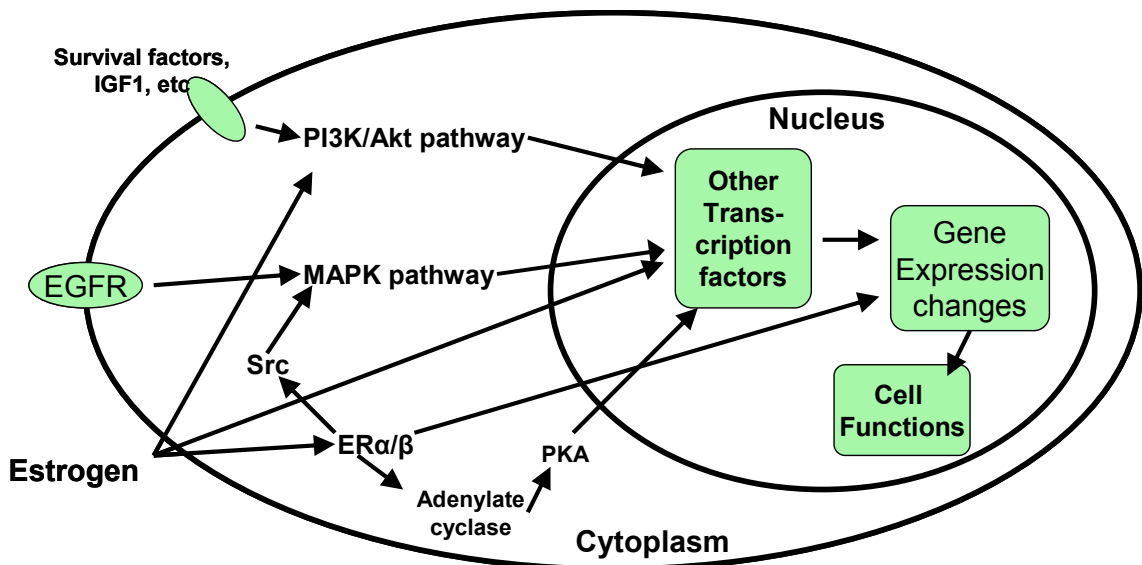


Figure 1.3 Estrogen receptor signaling

downstream activation of Akt and eNOS in an ER $\alpha$ -dependent response to estrogen stimulation (Simoncini et al. 2000) (**Fig. 1.3**). ER $\alpha$  can also directly interact with the G protein G $\alpha$ i in an estrogen-dependent manner and this interaction mediates downstream Src signaling (Kumar et al. 2007). Other steroid receptors show similar ligand-dependent interactions with G $\alpha$ i, including ER $\beta$  and the AR, although downstream signaling of these complexes was not investigated (Kumar et al. 2007). ER $\alpha$  also interacts directly with G $\beta$  $\gamma$  in a ligand-independent manner and both G $\alpha$ i and G $\beta$  $\gamma$  interactions are required for the downstream signaling of ER $\alpha$  through ERK, Src and eNOS (Kumar et al. 2007).

Rapid estrogen signaling may also be partially responsible for the cardioprotective effects of estrogen seen in premenopausal women. It is known that adhesion of circulating monocytes at atherosclerotic lesions plays a role in lesion progression (Ross 1999). The adhesion of monocytes at lesions is followed by chemotaxis and migration into the vessel wall as the lesion progresses. Estrogen signaling in monocytes decreases the activity of the small GTPase Rac1 and inhibits monocyte adhesion (Friedrich et al. 2006). Additionally, estrogen treatment of monocytes can prevent increases in adhesion seen following application of SDF-1, a chemokine commonly seen in atherosclerotic lesions and thought to play a key role in monocyte adhesion (Friedrich et al. 2006). These events may help to explain the cardioprotective role of estrogen, which occurs via a rapid signaling pathway.

As a GPCR, GPR30 is capable of mediating a wide range of downstream rapid signaling events. In fact, the initial activity attributed to GPR30 was its



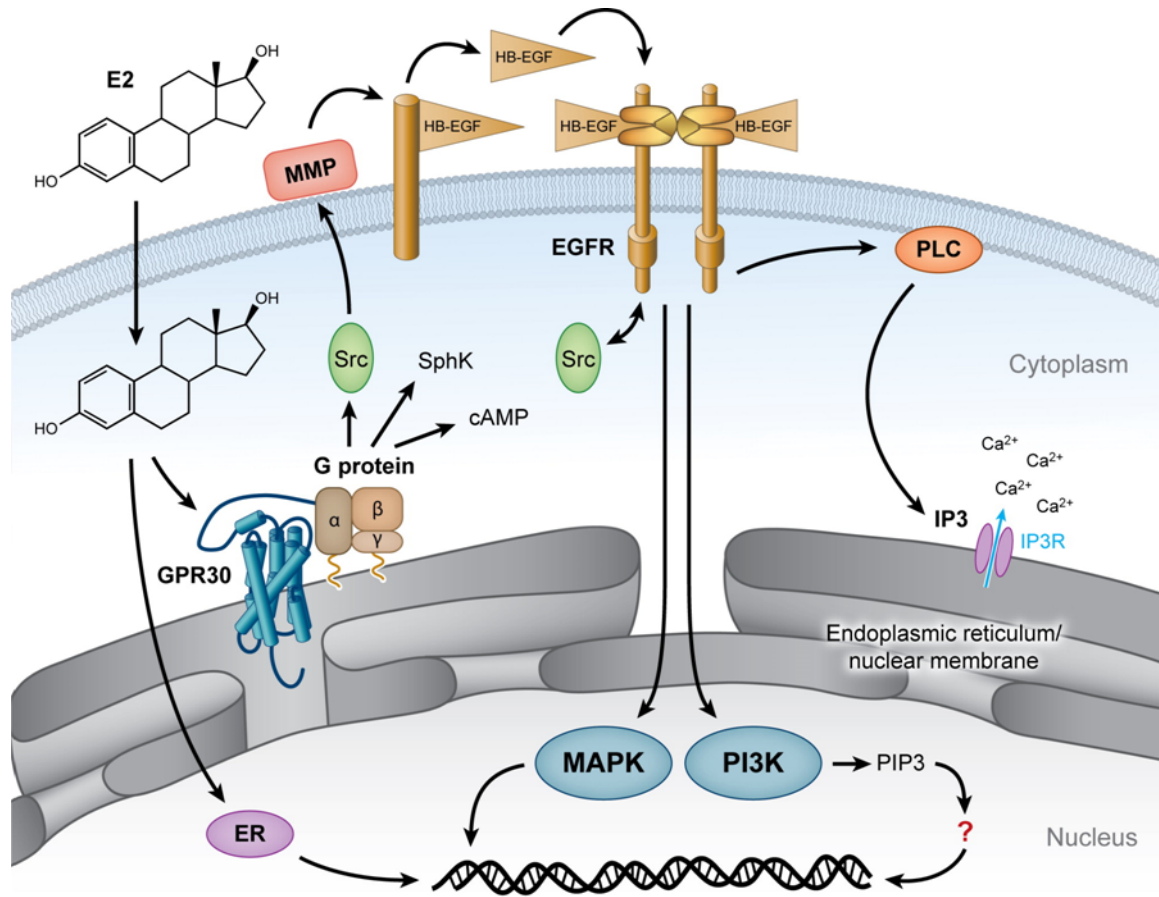


**Figure 1.4 GPR30 Signaling.**

ability to transactivate EGFR via the release of extracellular heparin-bound EGF and activation of ERK downstream of EGFR (Filardo et al. 2000). In this study, Filardo and colleagues demonstrated that estrogen-induced activation of ERK occurs in a GPR30-expression-dependent manner and does not require expression of either ER $\alpha$  or ER $\beta$ . Additionally, this ERK activation by GPR30 was shown to require Src kinase activity and involve G $\beta\gamma$ . In a subsequent report from the same group, estrogen signaling downstream of GPR30 was further investigated; they found that ERK activation by GPR30 is attenuated by stimulation of adenylyl cyclase and generation of cAMP (Filardo et al. 2002) (**Fig. 1.4**). In 2005, Revankar et al further elucidated the rapid signaling of GPR30, showing that GPR30, as well as the classical ERs, rapidly activated PI3K/Akt and

led to the generation of PIP3 in the nucleus although the signaling involved downstream of the classical ERs was EGFR-independent, whereas GPR30-mediated PI3K activation was EGFR-dependent (Revankar et al. 2005). Additionally, this study demonstrated that estrogen signaling via GPR30 results in rapid calcium mobilization via an EGFR-dependent, PLC-dependent mechanism.

### **1.5 Introduction to aberrant signaling of steroid receptors in cancer**

Aberrant signaling of both estrogen and androgen receptors plays a role in disease, including hormone-dependent cancers such as breast, ovarian, endometrial and prostate cancers.

Cancers of female reproductive organs are often dependent on estrogen, including breast, endometrial and ovarian cancer. These cancers tend to display variable expression of ER $\alpha$ , ER $\beta$  and GPR30, as well as of various growth factor receptors including the epidermal growth factor receptor (EGFR).

The development of breast cancer is a poorly understood process, and the progression from healthy breast cells to cancer most likely can occur via a number of mechanisms. Estrogen exposure may play a role in breast cancer development (Henderson and Feigelson 2000) and several mechanisms for the role of E2 in cancer progression have been suggested. For instance, E2 exposure over time may stimulate proliferation of mammary epithelium and, as more cells are dividing than in normal epithelium, there may be more errors in DNA replication, laying the groundwork for later tumor progression (Yue et al. 2005). An additional hypothesis for the role of E2 in tumor initiation involves E2

metabolism by cells generating products which can damage DNA, leading to tumor initiation or progression (Deroo and Korach 2006).

In breast tumors, ER $\alpha$  expression is often determined in order to choose the best course of treatment. Cancers which express high levels of ER $\alpha$  or the progesterone receptor are most likely to respond to hormonal treatment with anti-estrogens including tamoxifen or aromatase inhibitors. Additionally, ER-positive tumors generally have a better prognosis than ER-negative tumors, in part due to the ability to treat ER-positive tumors with anti-estrogens (Rocheffort et al. 2003). It is not known whether most ER-negative tumors begin as ER-positive tumors that lose ER expression via a range of possible mechanisms, including promoter methylation or genetic mutation, or if some tumors arise via an E2-independent mechanism and are ER-negative from the point of tumor initiation (Korach 1994; Ferguson et al. 1995). GPR30 and ER $\alpha$  expression is correlated in breast tumor samples and GPR30 also correlates with Her2/neu expression and positively correlates with metastasis (Filardo et al. 2006). Inflammatory breast cancer (IBC) is a very aggressive form of breast cancer, which is typically hormone-independent and expresses ER $\alpha$  at lower rates than other breast tumors (Yamauchi et al. 2009). In IBC, coexpression of GPR30 and ER $\alpha$  is predictive of better survival, whereas GPR30-negative, ER $\alpha$ -negative tumors are correlated with lower survival (Arias-Pulido et al. 2009).

In ovarian cancer, ER $\alpha$  and ER $\beta$  are commonly expressed by tumors, with expression of one or both classical ERs in approximately 2/3 of tumors (Deroo and Korach 2006). Ovarian cancer is the most serious gynecological malignancy

and survival rates are low, with most patients relapsing within 2 years (Hensley 2002; Tummala and McGuire 2005). The correlation between estrogen exposure and ovarian cancer is unclear, as some studies have reported that hormone replacement therapy in postmenopausal women increases ovarian cancer risk (Rodriguez et al. 2001; Riman et al. 2002) while others have found no correlation (Coughlin et al. 2000; Bakken et al. 2004). In cell culture systems with ovarian cell lines, E2 stimulates cell growth and this effect can be blocked by anti-estrogens (Nash et al. 1989; Syed et al. 2001); this enhanced proliferation may lead to genetic instability and tumorigenesis (Ho 2003). E2 also regulates the cytoskeleton in ovarian cancer cell lines, which can promote invasion and metastasis (Moll et al. 2002; O'Donnell et al. 2005). GPR30 has been found to be overexpressed in ovarian cancers, with expression seen more often in epithelial ovarian cancers than in low malignant potential tumors; GPR30 expression is predictive of lower survival rates in epithelial ovarian cancer (Smith et al. 2009). Additionally, ER $\alpha$  is overexpressed relative to ER $\beta$  in many ovarian cancers, suggesting that ER $\beta$  may protect against ovarian cancer and when expression of ER $\beta$  is lost, the tumor progresses (Li et al. 2003). Supporting this hypothesis is the finding that E2, via ER $\alpha$ , downregulates E-cadherin and promotes the epithelial mesenchymal transition crucial to metastasis of tumors (Park et al. 2008).

Extended exposure to unopposed E2 has been implicated in the development of type I endometrial cancer, which constitutes approximately 80% of endometrial cancer cases (Grady et al. 1995; Lax 2004). Studies investigating

the use of hormone replacement therapy containing E2 and progestin, compared to E2 replacement therapy alone, demonstrated that endometrial cancer risk increased with extended E2 replacement therapy; however, combined E2 and progestin hormone replacement therapy decreased the risk of endometrial cancer (Ito 2007). Endometrial cancers caused by unopposed E2 exposure such as these are type I endometrial cancers that typically overexpress ER $\alpha$  and ER $\beta$ , whereas type II endometrial cancers are not associated with unopposed E2 treatment and either express low levels of ER $\alpha$ /ER $\beta$  or do not express classical ERs (Lax 2004). In addition to changes in ER $\alpha$  and ER $\beta$ , GPR30 has been shown to be overexpressed in high grade, invasive endometrial cancers, with GPR30 overexpression also correlated with poorer survival rates (Smith et al. 2007).

In addition to cancers of the female reproductive system, E2 and ERs play a role in colon cancer. In colon tissue, both normal and tumor, ER $\beta$  is the predominant ER expressed; however, as colon tumors advance, ER $\beta$  expression is slowly lost and lack of ER $\beta$  is associated with advanced stage tumors (Foley et al. 2000). Supporting the role for ER $\beta$  as the major ER in the colon, an ER $\beta$ -selective agonist has been developed for the treatment of Crohn's disease (Harris et al. 2003).

Prostate cancer (PCa) is a hormone-dependent cancer and, as such, expression and activation of the AR is a survival mechanism for prostate cancer cells. Thus, anti-androgen therapy, including treatment with AR antagonists such as bicalutamide (BC) and flutamide, is the first-line treatment for advanced

prostate cancer. While anti-androgen therapy is effective initially in slowing the growth of PCa cells, most prostate cancers eventually develop an androgen-independent phenotype and are able to resume metastatic growth even in the presence of anti-androgens (Mellado et al. 2009). This switch to an androgen-independent phenotype could be due to the survival and selection for primary tumor cells with mutant AR protein allowing altered binding of antagonist or with altered downstream signaling of AR and positive signaling of anti-androgen-bound AR (Mellado et al. 2009). Another option for the development of androgen independence following anti-androgen therapy is that the prolonged presence of anti-androgens causes *de novo* changes in AR expression or signaling, which allows cells to thrive in the absence of androgen (Mellado et al. 2009).

One of the first described mutations in AR, which results in promiscuous activation, is present in the AR of the LNCaP cell line, derived from human metastatic prostate cancer. These cells express the AR with a T877A mutation, resulting in AR binding to and being activated by progesterone, estrogen and anti-androgens such as flutamide and bicalutamide (Wilding et al. 1989; Hara et al. 2003; Monge et al. 2006). Mutations in samples from patients with prostate cancer show a trend of an increasing presence of mutations as the cancer progresses through anti-androgen treatment and as primary tumors progress to metastatic disease (Taplin et al. 2003; Marques et al. 2005; Bergerat and Ceraline 2009). These mutations may indicate either the mechanism by which androgen independence arises or may result from the development of androgen independence.

In addition to changes in the sequence of the AR expressed by androgen-independent prostate cancer cells, these cells can also overexpress wild-type AR. This overexpression of AR allows cells to respond to much lower levels of androgen than cells expressing a normal level of AR, a condition called AR hypersensitivity. This change in AR expression can either be due to gene amplification or increased protein expression without AR gene amplification (Chen et al. 2004; Holzbeierlein et al. 2004).

A third mechanism that may be involved in the development of androgen independence is local production of androgens. While anti-androgen therapy greatly decreases the levels of circulating androgens, many tissues, including the prostate, are capable of locally producing androgens and thus elevating local androgen levels. Additionally, overexpression of androgen synthesis enzymes such as 5 $\alpha$ -reductase has been observed in prostate cancer samples allowing for increased local production of androgens and escape from anti-androgen-induced decreases in circulating androgen levels (Titus et al. 2005; Titus et al. 2005; Stanbrough et al. 2006; Montgomery et al. 2008).

Finally, as AR is capable of transactivating EGFR and signaling via other rapid signaling pathways, EGFR transactivation is a mechanism by which prostate cancer cells can escape anti-androgen therapy. Overexpression of HER2 results in increased stability and activity of the AR, whereas inhibition of HER2 decreases androgen-stimulated growth in cell lines (Liu et al. 2005; Domingo-Domenech et al. 2008). Activation and crosstalk of AR and Src, EGFR, IGFR and other intracellular signaling pathways has also been shown to occur *in*

*vitro* and may play a role in the development of the androgen-independent phenotype (Mellado et al. 2009).

In addition to its role in female cancers, estrogen also plays a role in prostate cancer. The feedback mechanisms of the various sex steroids, gonadotropins and other hormones are complex and elevated estrogen levels lead to a decrease in circulating testosterone levels via the repression of gonadotropin secretion from the pituitary (Risbridger et al. 2007). This feedback loop was exploited in early androgen ablation therapy by administering diethylstilbestrol (DES), a synthetic estrogen, to males undergoing prostate cancer treatment; however, the downfall of this treatment was that elevated unopposed estrogen in these men led to a variety of negative cardiac side effects (Risbridger et al. 2007). Estrogen exerts paracrine signaling events in prostate tissue, where aromatase, which converts androgens to estrogen, is often overexpressed in prostate cancer epithelium, similar to breast cancers (Ellem et al. 2004). Interestingly, one of the mechanisms for inducing prostate tumors in both mouse and rat models is the administration of exogenous estrogen and testosterone, either ligand alone is not sufficient to induce prostatic lesions (Leav et al. 1989; Ricke et al. 2006). Estrogens can cause the disregulated proliferation of prostate tissue, via ER $\alpha$ , in a tissue recombination model in which androgen application causes the orderly proliferation of prostate tissue; this difference in estrogen regulated proliferation may play a role in cancer initiation (Risbridger et al. 2001). Additionally, ER $\alpha$  mediates an inflammatory response in mice lacking sex steroids (hypogonadal mice, pituitary gonadotropin knockouts); upon



treatment with exogenous estrogen the prostate of these mice fill with inflammatory cells migrating into the lumen of the prostate and filling the lumen with cellular debris (Bianco et al. 2002).

## **1.6 Introduction to estrogen and androgen receptor ligands**

Steroid biosynthesis begins with cholesterol, from which progesterone and pregnenolone are directly synthesized by cleavage of the cholesterol side chain. Androstenedione and dehydroepiandrosterone are produced in the adrenals by a series of enzymatic reactions and converted to testosterone in the testis and other tissues. 5 $\alpha$ -DHT is produced from testosterone by 5 $\alpha$ -reductase. Conversely, testosterone can be converted into estrogen by P450-aromatase and estrogen can be directly made from androstenedione, also by aromatase.

Naturally occurring steroid hormones have varying affinities and activities on the different steroid hormone receptors. The most potent endogenous AR ligand is DHT, although testosterone, estrogen, androstenedione and progesterone all have effects on the AR but at higher concentrations than those required for DHT signaling. The most potent ER ligand is 17 $\beta$ -estradiol. The classical ERs have an affinity for 17 $\beta$ -estradiol of approximately 0.6 nM whereas GPR30 has an affinity for 17 $\beta$ -estradiol of approximately 6 nM (Revankar et al. 2005; Thomas et al. 2005). Thus, endogenously produced steroid hormones can exert their effects via a range of receptors and in a variety of tissues.

Selective estrogen receptor modulators (SERMs) are therapeutic compounds with different pharmacological activities in different tissues. These SERMs often act as agonists in one tissue and antagonists in another.

Tamoxifen is an example of a commonly used SERM that acts as an antagonist of classical ERs in breast and other tissues but as an agonist in bone tissue, which is beneficial for maintenance of bone integrity and density; however, tamoxifen is a GPR30 agonist in all known tissue settings, which significantly clouds its utility as a classical ER antagonist (Filardo et al. 2000; Revankar et al. 2005).

In addition to endogenous AR ligands, a substantial number of synthetic steroidal and non-steroidal AR ligands have been described (Fang et al. 2003). These include steroidal compounds such as methyltrienolone (R1881), a synthetic AR agonist, cyproterone acetate (CPA), a synthetic anti-androgen, and non-steroidal anti-androgens such as BC, flutamide, and nilutamide. Some AR ligands preferentially activate either classical or non-classical AR signaling; for example androstenediol and estren preferentially propagate non-classical signaling, whereas R1881 and nortestosterone preferentially activate classical AR signaling (Kousteni et al. 2001; Gill et al. 2004; Haas et al. 2005). The selective mechanism of these compounds is not known but may provide interesting insights into selective androgen receptor modulators (SARMs) for therapeutic and research purposes.

There are a wide variety of non-steroidal compounds which bind to the AR and ERs, as well as GPR30. These include therapeutic compounds, pesticides, industrial products and byproducts and a range of other molecules and are generally termed endocrine disruptors. Several classes of endocrine disruptors have been described in order to further subdivide this diverse class of molecules.

Xenoestrogens are industrially produced compounds that have estrogenic activity and include both chemicals with known (and often desired) pharmaceutical activity (including ethinyl estradiol and others) as well as compounds with undefined effects where the estrogenic effect is a side effect of the main function of the compound. Additionally, naturally occurring endocrine disruptors can be subdivided into phytoestrogens, or plant-derived estrogens, and mycoestrogens, or fungus-derived estrogens. These endocrine disrupting compounds can act via a variety of mechanisms, including direct agonism/antagonism of steroid hormone receptors, alterations in expression levels of steroid hormone receptors or by interfering with steroid biosynthesis and thus influencing endogenous steroid levels (Soto et al. 2006). Several of the more well-studied endocrine disruptors include bisphenol A (BPA), a plasticizer, as well as a range of isoflavones, naturally occurring molecules found in soy and other legumes. Other well-publicized endocrine disruptors include the pesticide DDT and its metabolites, which have been shown to have xenoestrogenic effects and cause problems with both male and female reproductive function as well as development (Rogan and Ragan 2003; Venners et al. 2005; Aneck-Hahn et al. 2007).

### **1.7 Introduction to high throughput screening (HTS)**

In recent years, HTS technology has greatly improved. As pharmaceutical companies invested increasing resources in the development of combinatorial chemistry to generate large chemical libraries for screening and as genomic methods identified an increasing number of molecular targets these fields

converged and allowed rapid growth in HTS technology (An and Tolliday 2009). Methods for data acquisition and analysis have improved in both their speed and resolution and the technology has become more widely available (An and Tolliday 2009). Among the available methods are those that are biochemical in nature and those that are cell-based. Biochemical assays measure enzyme activity, ligand-receptor interactions and other small-molecule interactions. Cell-based assays are typically used to identify modulators of cellular pathways and can include GPCR signaling, reporter gene assays and other functional assays (An and Tolliday 2009). Both biochemical and cell-based assays have advantages and disadvantages as a result of their basic properties. Whereas biochemical assays are often less costly, easier to miniaturize and investigate defined target interactions, they do not always recapitulate events occurring *in vivo* or even in cell-based systems due to their *in vitro* nature. Additionally, since biochemical assays investigate a very specific event, off target effects of a screened compound are often missed due to a lack of context in cells or whole organisms. Cell-based assays can be more difficult than basic biochemical assays to miniaturize and are often more costly, but also provide a broader knowledge about a given screen. Also, cell based assays typically do not require any *a priori* knowledge of the molecular target to be screened and can be completed in whole organisms (i.e. Zebrafish embryos, *C. elegans* or plants) to give a broader physiological relevance to screening results (An and Tolliday 2009).

A variety of factors should be considered when designing a cell-based HTS assay. The assay must be balanced to deliver an appropriate amount of biological information while still remaining feasible in terms of cost, miniaturization and other practical factors (An and Tolliday 2009). These considerations include the use of cell lines, primary cells or a model organism for screening. The type of assay can be chosen from a broad range of techniques, including functional assays, phenotypic assays or reporter gene assays. Finally, an appropriate readout mechanism must be chosen from either uniform well measurements, including luminescence or spectrophotometric readouts, or from single cell, high-content readouts including high throughput image analysis or flow cytometry. Once these factors have been considered, an assay can be developed while optimizing reagent stability, signal-to-noise, concentrations of cells and reagents and overall reproducibility (An and Tolliday 2009).

Flow cytometry is a powerful method for analysis of a large, often varied, population of cells. This technology uses hydrodynamic focusing of cells into a single-cell stream in order to interrogate each cell individually as it passes through the laser beam. Data collected for each cell, or event, includes information about its light-scattering properties, which give information about cell size and intracellular granularity, and any number of independent fluorescent parameters, which can include fluorescent ligand or antibody binding to the cell, staining with cell viability dyes and DNA content. The power of this valuable tool can be further enhanced by using it in a HTS environment.

Flow cytometry-based assays have the advantage of being multiplexable and acquiring data for different receptors or proteins being investigated at the same time through the use of beads with varying amounts of fluorescence used for each target and read by the cytometer simultaneously (Edwards et al. 2009). Additionally, HTS by flow cytometry has the ability to interrogate single cells, yielding data on each, rather than assays which give the output as an average of all the cells or beads or proteins in a given well. This provides an additional layer of data that can be especially useful in the context of cell-based assays in which cellular responses are not completely homogenous (Edwards et al. 2004).

The HyperCyt® HTS flow cytometry system incorporates all the advantages of screening by flow cytometry and significantly speeds sample reading compared to other flow cytometry-based HTS systems currently available (Ramirez et al. 2003). This system consists of an autosampler capable of reading from a 96- or 384- well plate, a flow cytometer and a software package, which both directs autosampler function and also allows for deconvolution of the complex data set resulting from screening and contains all data for all wells of a plate as a single time-delineated file. Utilizing this system allows analysis of a 96 well plate in less than 3 minutes.

### **1.8 Introduction to *in vivo* tumor imaging**

The ability to follow tumor development and properties, both in clinical and research applications, is critical to increasing our understanding of tumor biology as well as to design therapeutic ligands and to track the efficacy of therapy *in vivo*. These technologies can assist in finding distant metastases, determining

receptor expression in a heterogeneous tumor, and provide many other metabolic and biological clues to the biology of tumors (Chodosh and Cardiff 2006; Mankoff et al. 2008).  $^{18}\text{F}$ -fluorodeoxyglucose positron emission tomography (FDG-PET) is an example of a successfully implemented tool to assess both initial tumor location as well as effects of treatment on tumor size and localization (Coleman 2000). The concept underlying this technique is that tumor cells are typically more metabolically active than other cells in the body and, as such, take up more radiolabeled glucose than other cells and this difference can be detected by a PET scanner. A similar rationale was used in the design and use of  $^{18}\text{F}$ -fluoro-estradiol to detect and monitor tumors expressing ERs, often tumors initiating in the breast, endometrium and ovaries (Van de Wiele et al. 2000).

There are several major types of imaging currently employed for monitoring tumors and receptor imaging, computed tomography (CT), ultrasound, positron emission tomography (PET) and single photon emission computed tomography (SPECT) (Van Den Bossche and Van de Wiele 2004; Chodosh and Cardiff 2006). CT images are generated by a series of radial x-rays processed by a computer to give a three dimensional (3D) image of the body. Ultrasound yields images based on ultrasonic waves reflected back to the sensor to generate the image. PET can be used to monitor biodistribution of positron-emitting isotopes including  $^{18}\text{F}$ ,  $^{11}\text{C}$  and  $^{15}\text{O}$ . SPECT imaging can similarly be used to track the distribution of gamma-emitting isotopes including  $^{111}\text{In}$ ,  $^{99\text{m}}\text{Tc}$  and  $^{123}\text{I}$ . These isotopes can often be integrated into ligands that bind specifically to the receptor

of interest. Ultrasound and CT are not typically used for visualizing interactions of specific receptors and ligands but each have their place in imaging of tumors; ultrasound gives high quality images of liquid (blood, lymph, etc.) flow within tissues and is rapid and inexpensive, CT gives very high quality images of tumors and allows for 3D reconstruction of images (Chodosh and Cardiff 2006).

Technologies for imaging receptors within a tumor each have different mechanisms of image acquisition. SPECT directly monitors gamma emissions from injected isotopes by capturing scintillation flashes generated when the gamma emission interacts with a sodium iodide crystal immediately in front of the photomultiplier tube (PMT) detector. These emissions are collected by PMTs and deconvoluted using software to determine the exact source of the gamma emission within the body. In contrast to SPECT, PET detects an indirect signal from the isotope. As the isotope emits a positron, the particle collides with an electron and this collision creates two photons that travel in opposite directions. These photons are detected by PMTs and computers can determine where in the volume of the patient the photons originated and thus the location of the radiotracer (Van Den Bossche and Van de Wiele 2004).

PET and SPECT each have advantages and disadvantages, which should be taken into account when designing a radiotracer for tumor and receptor imaging. PET radioisotopes have a short half-life (on the order of tens of minutes to hours) and therefore neither the radioisotope nor the radioisotope-ligand complex can be produced off site, which restricts the use of PET radiotracers to facilities with either a generator or a cyclotron. By contrast, SPECT isotopes have



significantly longer half-lives (several hours) that allow them to both be generated off site as well as for longer acquisition times to be used in the SPECT camera, allowing the receptor-ligand binding to come to equilibrium and for receptor density to be determined. Although SPECT images can be acquired for longer times due to the longer half lives of the isotopes, PET cameras are currently of higher resolution, which allows better localization of radioisotope binding (Van Den Bossche and Van de Wiele 2004).

The requirements for a radiopharmaceutical are fairly straightforward. First, the receptor to which the radiopharmaceutical is targeted must have a known ligand. This ligand must have fairly high specificity and must be capable of being labeled with the isotope at a high specific activity so the receptor system is not saturated by unlabeled ligand and so receptor binding can be detected via either PET or SPECT. The high specific activity of a radioligand also allows a lower dose of the ligand to be injected, which prevents the radioligand from excessively activating receptors during imaging. A successful radioligand also must have a low background signal in non-receptor-expressing tissues and must not be metabolized too quickly for binding to successfully occur (Liu 2008).

Thus far, several radiopharmaceuticals have been investigated for tracking classical ERs. For example, estrogen has been brominated at the 16 $\alpha$  position with  $^{77}\text{Br}$  and this was specifically taken up by estrogen-receptor positive tumors in a small number of patients. Estrogen has also been successfully labeled at the 16 $\alpha$  position with  $^{123}\text{I}$  and  $^{18}\text{F}$  with imaging results similar to those obtained for brominated estrogen (Van de Wiele et al. 2000). Additionally,

tamoxifen has been labeled with  $^{123}\text{I}$  for direct imaging of tamoxifen binding to estrogen receptors in tumor tissue *in vivo* (Van Den Bossche and Van de Wiele 2004).

## 1.9 Rationale for project

As the AR is an important therapeutic target for treatment of prostate cancer, a HTS screen was developed and used to identify compounds from a library of potential endocrine disruptors with the aim of identifying novel mediators of transcription. The development and optimization of this screen, as well as the results from the library screen, are described in Chapter 2.

The recent description of GPR30 as an estrogen receptor (Revankar et al. 2005; Thomas et al. 2005) has added significant complexity to the study of estrogen physiology. GPR30 is activated by both antagonists of classical ERs, including ICI182,780 (Filardo et al. 2000), as well as by SERMs such as tamoxifen (Revankar et al. 2005). The lack of a selective antagonist for GPR30 was the driving force behind one part of this project, which utilized the HyperCyt® high-throughput screening platform in an assay optimized for screening in 384-well plates to search for modulators of GPR30, ER $\alpha$  and ER $\beta$ , as detailed in Chapter 3. This search was successful and identified the selective GPR30 antagonist G15, which is characterized in Chapter 4, along with a second-generation GPR30-selective antagonist, G36. Chapter 5 describes the use of GPR30-selective compounds, including G15 and the GPR30 agonist G-1, to investigate the role of GPR30 in a glioma cell line and help elucidate the role of GPR30 in this type of cancer. Finally, Chapter 6 illustrates the biological

characterization of G-15-based radiotracers, which could be useful in characterizing receptor expression in tumors.

# 2 ANDROGEN RECEPTOR SCREENING

## 2.1 Introduction

Androgens are important in normal development and function of males. The canonical pathway for androgen function involves transcription of androgen-responsive genes mediated by the 110 kD soluble protein termed the androgen receptor (AR). In the context of classical androgen signaling, this receptor resides predominantly in the cytoplasm prior to stimulation by androgenic compounds, which bind to the receptor and result in its rapid disassociation from molecular chaperones including hsp90, receptor dimerization and translocation of the ligand-receptor complex to the nucleus (Roy et al. 2001). Once the AR-ligand complex enters the nucleus, it functions predominantly as a transcription factor, driving transcription of androgen-responsive genes via androgen response elements located in the DNA (Gelman 2002). These genes include those with androgen response elements (ARE) such as prostate-specific antigen (PSA), maspin and fibroblast growth factor 1 (Dehm and Tindall 2006) and genes that lack the ARE element including EGFR (Brass et al. 1995; Lange et al. 1998) and *c-fos* (Richer et al. 1998; Church et al. 2005).

The AR can also signal via rapid non-classical signaling pathways, including MAPK, ERK, PLC and Src (Rahman and Christian 2007). These rapid signaling events occur within minutes, whereas transcriptional events require several hours. For example, treatment of patients experiencing myocardial ischaemia (MI) within 30 m of onset reduces the harmful effects of MI and androgen signaling induces vasodilation (Rosano et al. 1999; Webb et al. 1999; Webb et al. 1999). In Sertoli cells, acute application of androgen opens L-type calcium channels and influx of extracellular calcium (Lyng et al. 2000; Loss et al.

2004). Increased intracellular calcium can lead to cytoskeletal rearrangements in Sertoli cells (Loss et al. 2004). In addition to increases in intracellular calcium, AR can transactivate EGFR, activating MAPK and resulting in CREB phosphorylation and downstream gene transcription (Cheng et al. 2007). In addition to roles crucial to male physiology, rapid AR signaling has long been known to play a role in *Xenopus* oocyte maturation and has recently been shown to be important in meiotic division in mice as well (Lutz et al. 2001; Gill et al. 2004; White et al. 2005). In all, rapid AR signaling combined with classical genomic signaling mediated by the AR can regulate a wide range of physiological outcomes, including many aspects of male sexual development and physiological function.

In addition to its important role in normal physiology, signaling through the AR plays a role in pathological states, including prostate cancer. Blockade of AR signaling can be achieved using a variety of AR antagonists, including bicalutamide (BC) and cyproterone acetate (CPA). These compounds function as competitive antagonists of the AR and, when present at appropriate doses, effectively block AR function and impede disease progression (Schaufele et al. 2005; Marcelli et al. 2006). While these therapeutic compounds are effective for a time, most prostate cancers eventually progress to an androgen-independent phenotype characterized by disease progression even in the absence of androgens or in the presence of very low levels of androgens that previously were not sufficient to induce proliferation of tumor cells (Mellado et al. 2009). The molecular basis for this androgen-independent prostate cancer is not known but

several theories exist, including expression of mutant AR with hypersensitivity to low levels of androgen, altered binding to anti-androgenic compounds and/or altered downstream signaling in response to these compounds, as well as dysregulation of cell signaling events that allow proliferation in the absence of androgen (Mellado et al. 2009).

In addition to therapeutic compounds applied to AR signaling, there is also a wide range of environmental compounds that interact with the AR and influence signaling either positively or negatively. These compounds include plant flavinoids and naturally occurring compounds from plants and fungi in addition to industrial byproducts and compounds such as bisphenol A (BPA), a plasticizing compound recently highlighted in the popular press for its ability to interfere with normal endocrine function, as well as the pesticide DDT and its metabolites (Rogan and Ragan 2003; Venners et al. 2005).

The NIH and the Interagency Coordinating Committee on the Validation of Alternative Methods (ICCVAM) have compiled a list of this type of compound that it recommends for extensive follow-up testing for estrogenic, androgenic and other hormone disrupting activity (NIH 2003). This list includes physiologically relevant steroids, including DHT, E2 and their precursor compounds. Also included are plant flavinoids, plasticizing compounds, pesticides and their metabolites and a variety of other compounds with suspected endocrine disrupting activity.

Assays for assessing endocrine disrupting activity of compounds are widely varied, including *in vitro* assays for receptor binding activity, cell-based

assays with a range of endpoint outcomes and *in vivo* assays carried out in animal models (An and Tolliday 2009). These assays possess different advantages and disadvantages. For instance, most animal model experiments are expensive and time consuming but can give a better approximation of systemic endocrine disrupting activity of a compound (O'Rourke et al. 2009). In contrast, fully *in vitro* based assays are fairly inexpensive and rapid to complete but often give insight only into a single facet of endocrine disrupting activity; often receptor binding, which gives no insight into the agonist or antagonist character of the compound, and even then truncated receptor fragments are often used that can have altered binding to compounds. A compromise between these two types of assays is cell-based assays, including transcriptional reporter assays, proliferation assays and cytotoxicity assays (An and Tolliday 2009). These assays often span a timeframe of several days and, if they are well designed, have the ability to produce significant amounts of data in a relevant cell type (Wyler et al. 2009).

Factors to consider when developing a cell-based assay system include the cell type used and the receptor status of those cells, the type of assay to be completed and the method for collecting data at the assay endpoint (Liu et al. 2009). A wide array of cell types exist, coming from mice, monkeys, humans, dogs and many other species. The choice of organism is important since different species express different cofactors and vary in the sequence of the AR itself. Additionally, cell lines can be 'normal' or non-transformed or derived from different pathological sites including primary tumors or metastatic sites. These



cells can also be AR-negative, AR-positive or something in between, such as the DU-145 cell line that expresses an AR although it is non-functional. Assay type can be chosen based on desired outcome; for example, a researcher desiring data on the rapid signaling events of the AR would not chose a transcriptional endpoint and vice-versa (An and Tolliday 2009). Additionally, assays with fluorescent readouts, be they GFP-based or based on another fluorescent probe based on Alexa dyes, fluorescein or Cy dyes, have the advantage of being highly sensitive and compatible with miniaturization (An 2009). Finally, an effective assay for screening an aspect of endocrine disrupting activity should have a fairly rapid mechanism for data collection so a large number of compounds can be screened effectively.

With these considerations in mind, we set out to develop a rapid AR transcriptional assay with the idea of screening the ICCVAM library of compounds to determine their endocrine disrupting potential. That assay development project resulted in the MARS assay, detailed in the following section, as published in *Cytometry*.

## **2.2 A multifunctional androgen receptor screening (MARS) assay using the high-throughput HyperCyt® flow cytometry system**

Megan K. Dennis<sup>4</sup>, Harmony J.C. Bowles<sup>1</sup>, Debra A. MacKenzie<sup>1</sup>, Scott W. Burchiel<sup>1,2,3</sup>, Bruce S. Edwards<sup>2,4</sup>, Larry A. Sklar<sup>2,3,4</sup>, Eric R. Prossnitz<sup>3,5</sup>, and Todd A. Thompson<sup>1,2,3,\*</sup>

College of Pharmacy<sup>1</sup>, Cancer Research and Treatment Center<sup>2</sup>, New Mexico Center for Environmental Health Sciences<sup>3</sup>, Department of Pathology<sup>4</sup>, and Department of Cell Biology and Physiology<sup>5</sup>, University of New Mexico Health Sciences Center, Albuquerque, New Mexico 87131

Grant Sponsor: National Institute of Environmental Health Sciences; Contract Grant: Pilot project to TAT from P30 ES-012072. National Institute of Health; Contract Grant: U54 MH-074425-01.

\* Correspondence to: Todd A. Thompson, University of New Mexico College of Pharmacy, 2703 Frontier, NE, Albuquerque, New Mexico, 87131

E-mail: [tthompson@salud.unm.edu](mailto:tthompson@salud.unm.edu)

Keywords: Androgen receptor assay; androgens; anti-androgens; flow cytometry; HyperCyt®; biomolecular screening

### 2.2.1 ABSTRACT

The androgen receptor (AR) is a steroid hormone receptor which regulates transcription of androgen-sensitive genes and is largely responsible for the development and maintenance of male secondary sexual characteristics. Chemicals that interfere with AR activity may lead to pathological conditions in androgen-sensitive tissues. A variety of reporter systems have been developed, driven by androgen-sensitive promoters, which screen for chemicals that modulate androgenic activity. We have developed a flexible, high-throughput AR transcriptional activation assay, designated the Multifunctional Androgen Receptor Screening (MARS) assay, to facilitate the identification of novel modulators of AR transcriptional activity using flow cytometry. Androgen-independent human prostate cancer-derived PC3 cells were transiently cotransfected with an expression vector for the wild-type human AR and an androgen-sensitive promoter regulating the expression of destabilized enhanced GFP (dsEGFP). The transfected cells were stimulated with established androgenic and anti-androgenic compounds and then assessed for increased or decreased dsEGFP expression. To screen for antagonists of AR transcription, the AR agonist R1881, was coadministered at submaximal concentrations with potential AR antagonists. The assay was formatted for high-throughput screening using the HyperCyt® flow cytometry system. Agents with established androgenic and anti-androgenic activity were used for validation of the MARS assay. AR agonists were found to potently induce dsEGFP. Furthermore, AR antagonists blocked dsEGFP expression when coadministered with low-dose R1881, which

also occurred in a dose-dependent manner. Modulators of AR transcriptional activity can be successfully identified by the MARS assay, utilizing a rapid, flexible, sensitive, and high-throughput format. Dose-response curves can be successfully generated for these compounds, allowing for an assessment of potency. Because of its simplicity and high-throughput compatibility, the MARS assay and HyperCyt® system combined with flow cytometric analysis represents a valuable and novel addition to the current repertoire of AR transcriptional activation screening assays.

## 2.2.2 INTRODUCTION

Endogenous androgens such as testosterone and dihydrotestosterone (DHT) are necessary for the normal development and maintenance of male sex accessory organs, such as the prostate gland (Wilding 1995). Disruption of androgenic activity is of increasing concern as a mediator of disease in males (Lamb et al. 2001; Hess-Wilson and Knudsen 2006). With a growing awareness that endocrine disrupting chemicals influence the activity of steroid hormone receptors, including the AR, it is important to identify and determine the potency of the broad range of compounds that have the ability to modulate AR transcriptional activity (Soto et al. 2006). Assays that screen for endocrine disrupting compounds are proving to be invaluable for identifying and characterizing agents that alter AR activity, which may contribute to endocrinopathies.

The action of androgens is mediated by the androgen receptor (AR), an 110 kD protein residing in the cytoplasm that, upon binding androgen, undergoes a conformational rearrangement and translocates to the nucleus, dimerizes, and alters the transcriptional regulation of androgen-responsive genes (Roy et al. 2001; Gelmann 2002). In addition to endogenous AR ligands, a substantial number of synthetic steroidal and non-steroidal AR ligands have been described (Fang et al. 2003). These include steroidal compounds such as methyltrienolone (R1881), a synthetic AR agonist, cyproterone acetate (CPA), a synthetic anti-androgen, and non-steroidal anti-androgens such as bicalutamide (BC), flutamide, and nilutamide. Antagonists of the AR block AR transcriptional activity

through at least one of two mechanisms. For example, AR antagonists may block the conformational change of the AR which occurs upon agonist binding, preventing nuclear translocation of the AR and dimerization of receptors, thus inhibiting AR-mediated gene transcription (Schaufele et al. 2005). Alternatively, AR antagonists may bind the AR resulting in translocation of the AR into the nucleus; however, a functional AR transcriptional complex does not develop, thus inhibiting AR activation (Marcelli et al. 2006). In either instance, the critical activity is the inhibition of a functional AR complex that modulates transcriptional activity, which is not discerned by *in vitro* assays that screen only for AR competitors or that screen for receptor nuclear translocation without assessing transcriptional activation.

Induction of gene expression by a wide array of transcription factors, including steroid hormone receptors such as the AR, has been studied using a variety of reporter gene assays. These assays are typically comprised of a reporter plasmid that is either transiently or stably transfected into an appropriate cell line either concurrent with a receptor expression vector or into a cell line expressing the receptor of interest. The reporter plasmid contains response elements specific for the receptor of interest regulating a promoter which in turn drives expression of the reporter gene; expression of this reporter gene can be measured by specific assays for the reporter of interest. Commonly used reporter genes in these assays include the enzymes luciferase,  $\beta$ -galactosidase, and chloramphenicol acetyltransferase (CAT) which require analysis based on the entire cell population rather than transcriptional activation on a single cell level

(Arnone et al. 2004). Additionally, in order to measure the activity of luciferase,  $\beta$ -galactosidase, or CAT, an exogenous substrate must be added to the assays to develop the signal. Thus, a reporter gene assays are available that allow some flexibility in the development of assays for gene expression regulation by transcription factors, such as the AR.

Green fluorescent protein (GFP) is an alternative reporter gene which has several distinct advantages; GFP based assays are unique from most other reporter assays in that they allow analysis of intact cells on a single cell basis and they do not require addition of reagents to cells in order to detect assay signal. The commonly used form of GFP, termed enhanced green fluorescent protein (EGFP), is relatively stable when expressed in mammalian cell lines, with a half life of approximately 24 hr. A destabilized form of green fluorescent protein (dsEGFP) has been generated by fusing a PEST sequence to the C-terminus of EGFP, effectively reducing the half life of dsEGFP to 2 hr while retaining the spectral properties of EGFP (Li et al. 1998). The dsEGFP has been shown to be an effective reporter in a range of assays, including those for activation of c-fos (Bi et al. 2002), IL-8 induced transcription (Kiss-Toth et al. 2000), NF- $\kappa$ B activation (Li et al. 1998; Hellweg et al. 2003), proteasome inhibition (Andreatta et al. 2001) and, perhaps most relevant to steroid hormone receptor transcriptional assays, for activation of transcription by glucocorticoid receptor (Necela and Cidlowski 2003). Several of these reports compare EGFP and dsEGFP as transcriptional reporters (Kiss-Toth et al. 2000; Bi et al. 2002;

Hellweg et al. 2003) and demonstrate that dsEGFP is a more dynamic reporter than EGFP which also provides more reproducible results.

In this study, we establish the utility of a multifunctional androgen receptor screening assay (designated the MARS assay) using PC3 prostate cancer cells (Kaighn et al. 1979) transiently cotransfected with expression vectors for the human AR (hAR) and a reporter plasmid consisting of the androgen-responsive MMTV promoter driving expression of dsEGFP. The activities of the potent synthetic androgen R1881 and the therapeutically employed AR antagonist bicalutamide were initially established in the MARS assay system prior to extension of the assay to a small test set of compounds with known abilities to modulate AR transcriptional function. We show the effectiveness of the MARS assay in screening this set of compounds and the dynamic range of the assay, which allows for delineation of dose-response activities for both AR agonists and AR antagonists. Due to the cell based nature of this assay, it was naturally incorporated with the HyperCyt® system allowing for high-throughput flow cytometric analysis of compounds that modulate AR activity.



### 2.2.3 RESULTS

The ability of PC3 cells transiently cotransfected with pDsRedhAR and pMMTVdsEGFP to respond to androgenic stimuli was initially established by microscopic examination of low power fields for dsEGFP positive cells following treatment (**Fig. 2.1A-D**) prior to formatting the assay for HyperCyt high-throughput flow cytometry (**Fig. 2.1E**). To verify AR-dependent dsEGFP expression in response to androgen stimulation, PC3 cells seeded and cotransfected on glass coverslips were stimulated with either vehicle (i.e., DMSO) or 10 pM R1881. The expression of dsEGFP was dependent on androgen stimulation, as dsEGFP expression was induced in R1881-treated cells, while unstimulated cells displayed no background dsEGFP expression (**Fig. 2.1A-B**). Additionally, dsEGFP expression in this system was dependent on expression of the AR, as cells cotransfected with pIRES2-DsRedExpress and MMTVdsEGFP showed no activation of the MMTV promoter upon stimulation with androgen (data not shown). To insure uniform transfection across each well of a 96-well plate, the levels of DsRed expressed from either pIRES2-DsRedExpress or pDsRedAR were assessed by fluorescence microscopy prior to treatment. The dynamic range of the MARS assay was illustrated by stimulation of cells with sub-maximal concentrations of R1881 (e.g., 1 pM), resulting in dsEGFP expression in a lower number of cells (**Fig. 2.1C**) than observed with maximal stimulation. The use of R1881 concentrations in the linear dose-response range allows for the investigation of compounds with AR antagonist activity in that coadministration of low-dose R1881 enables the

identification of potential antagonists. **Figure 2.1D** illustrates the effect of a well-characterized AR antagonist, BC, on low-dose R1881 induction of dsEGFP (**Fig. 2.1C**).

A time-course study was performed using the MARS assay in order to establish the optimal time point after treatment for the screening assay. For both cytometric and microscopic analyses, a time at which maximal dsEGFP expression was induced provides the greatest dynamic range for evaluation of transcription modulation in the MARS assay. PC3 cells in 96-well plates were cotransfected with pDsRedhAR and pMMTVdsEGFP and stimulated with R1881 in the absence or presence of bicalutamide. At 6, 12, 24, 48 and 72 hr after treatment, wells were imaged and the number of dsEGFP expressing cells determined (**Fig. 2.2A**). This microscopic analysis established that 24 hr post treatment was the optimal time for analysis of the MARS assay, as the difference in dsEGFP expression between background and 1 nM R1881 treated cells was found to be maximally induced at this time point. Additionally, dsEGFP expression in wells treated with 1 pM R1881 was maximal at 24 hr after treatment, and this dsEGFP expression could be efficiently inhibited by the presence of 1  $\mu$ M bicalutamide at 24 hr.

To determine the dynamic properties of the MARS assay, an androgen dose-response using PC3 cells cotransfected with pDsRedhAR and pMMTVdsEGFP was performed. Cells stimulated with doses of R1881 ranging from  $10^{-15}$  to  $10^{-9}$  M were analyzed by counting the number of dsEGFP expressing cells in 4 independent wells and the percent of dsEGFP positive cells

were compared to the maximum number of cells expressing dsEGFP in wells treated with 10 nM R1881 (**Fig. 2.2**). A three parameter logistics curve analysis of the R1881 dose-response gives an  $EC_{50}$  for R1881 of  $7.81 \times 10^{-13}$  M (**Fig. 2.2**). Importantly, treatment of cells with varying doses of R1881 in the presence of 1  $\mu$ M of the AR antagonist BC shifted the dose response to the right, with an  $EC_{50}$  of  $4.73 \times 10^{-12}$  M (**Fig. 2.2**).

Various established steroidal ligands for the AR as well as natural and synthetic non-steroidal compounds possess AR modulating activity. To assess the effectiveness of the MARS assay for AR ligands other than R1881 and BC, a test set of compounds with reported androgenic and anti-androgenic activities was selected (**Fig. 2.3**). These compounds were tested at a single dose of 10  $\mu$ M in a high-throughput screening format using the MARS assay (**Fig. 2.4**). PC3 cells cotransfected with pDsRedhAR and pMMTVdsEGFP were seeded in 96-well plates, stimulated with a test compound dose of 10  $\mu$ M and dsEGFP induction was assayed 24 hr later (**Fig. 2.4A**). Cells were collected for flow cytometric analysis of dsEGFP expression after trypsinization. Analysis of dsEGFP positive cells was performed using the HyperCyt rapid autosampling system with a CyAn ADP flow cytometer and data analysis was performed using IDLQuery software.

Activation of the MMTV promoter was assessed by analysis of wells based on percent cells expressing dsEGFP. The gate for distinguishing GFP-positive response was defined by analyzing a 96-well plate of cells and setting the positive response threshold at a level at which 5% of total events in the plate

were above the gate. The percent responding cells in wells containing 10 nM R1881 was defined as 100% and all wells were normalized to this response using the formula:

$$\text{Response relative to R1881} = \frac{\text{Number of gated events per well}}{\text{Number of gated events with 10 nM R1881}} \times 100$$

R1881, DHT, E2, progesterone, BC, nilutamide and androstenedione all induced significant increases in the percent of cells expressing dsEGFP compared to unstimulated wells (**Fig. 2.4A**). The specificity of these compounds in transactivating the MMTV promoter via the AR was confirmed in cells cotransfected with pIRES2DsRedExpress and MMTVdsEGFP; in the absence AR expression, these compounds did not promote transcription or dsEGFP expression via the MMTV promoter (data not shown).

Compounds with putative AR antagonist activity were also screened in the 96-well HyperCyt® format (**Fig. 2.4B**). In this assay, a dose of 1 pM R1881 was used in all wells to induce a low level of dsEGFP expression sufficient to allow detection of compounds with AR antagonist activity. Similar to the AR agonist assay, a gate was set such that 5% of total events in the plate were in the GFP positive region, and the percent of GFP positive cells in each well was determined. The percent of GFP positive cells in wells treated with 1 pM R1881 alone was defined as 100% and normalization of each well was completed using the formula:

$$\text{Response relative to 1 pM R1881} = \frac{\text{Number of gated events per well} \times 100}{\text{Number of gated events with 1 pM R1881}}$$

Compounds with significant antagonist activity at 10  $\mu\text{M}$  in this assay included DES, progesterone, BC, CPA, nilutamide, and flutamide (**Fig. 2.4B**). Treatment of wells with 10  $\mu\text{M}$  of the potent AR agonists R1881 and androstenedione resulted in significant increases in dsEGFP positive cells compared to 1 pM R1881 controls (**Fig. 2.4B**).

In addition to distinguishing AR agonists and antagonists, a viable AR transcriptional assay should address the question of ligand potency. To assess the activity of several AR transcriptional agonists and antagonists identified in single-point assays, dose-responses for the various compounds were completed (**Fig. 2.5**). Dose response curves were performed for AR agonists including the synthetic androgen agonist R1881 (presented in the analysis of each agonist to facilitate comparison of potency between agonists), as well as naturally occurring hormones including DHT, E2, progesterone and androstenedione (**Fig. 2.5A-D**). Analysis of agonist potency using percent cells responding was completed in a similar manner to the single-point agonist screen. R1881 was the most potent transcriptional agonist of the AR agonists tested, with an  $\text{EC}_{50}$  value of  $1.34 \times 10^{-12}$  M (**Fig. 2.5A and Table 2.1**). DHT, an endogenous AR ligand, was found to be the second most potent agonist of AR-mediated transcription (**Fig. 2.5A**). Androstenedione, a biosynthetic precursor of DHT and E2, displayed an activity significantly lower than the endogenous AR ligands but slightly better than the ligands of other steroid receptors (**Fig. 2.5B**). Ligands for other steroid hormone

receptors, progesterone and estrogen, were found to induce AR-mediated transcription only at much higher concentrations compared to DHT or R1881 (Figs. 2.5C-D).

In addition to determining the agonist activity of AR ligands, the anti-androgenic activity of several steroidal and non-steroidal anti-androgens was assessed (Fig. 2.6A-D). This assay was conducted in a manner similar to the AR agonist dose-responses, except varying concentrations of potential antagonists were determined in the presence of 1 pM R1881 and the inhibition of dsEGFP expression relative to the induction of dsEGFP by 1 pM R1881 was assessed. The dose-response curve for the well-established anti-androgen bicalutamide was included with each antagonist analysis to allow for comparison between antagonists (Fig. 2.6A-D). Flutamide was found to be the most effective AR antagonist in this assay, with a calculated  $IC_{50}$  of  $1.51 \times 10^{-10}$  M (Fig. 2.6B and Table 2.1). The nonsteroidal anti-androgen nilutamide was found to be a potent inhibitor of the AR (Fig. 2.6C). Interestingly, the well-established synthetic estrogen DES was found to be an inhibitor of AR activity using the MARS assay (Figure 2.6D). Table 1 shows  $EC_{50}$  and  $IC_{50}$  values determined using the MARS assay for AR agonists and AR antagonists, respectively.

## 2.2.4 DISCUSSION

In this study, an assay is presented for the assessment of AR transcriptional activity using destabilized EGFP in prostate cells, the HyperCyt® high-throughput screening system, and flow cytometry, which was designated the MARS assay. The utility of the MARS assay was examined using microscopy-based methods prior to scaling up the assay for high-throughput capabilities using HyperCyt and flow cytometry. Here, we have validated the MARS assay using a representative set of established natural and synthetic AR agonists and antagonists to determine AR transcriptional modulating activity at a single dose as well as in a dose-response, which demonstrated the sensitivity of the MARS assay and its ability to detect a dynamic range of dsEGFP expression in response to various AR ligands.

The use of dsEGFP as the reporter in this assay was practical for several reasons. GFP-based systems are simpler to perform than most other reporter methods, such as luciferase or CAT based reporter assay methods, because addition of exogenous reagents are not required for development of the reporter signal. Additionally, GFP expression can be verified by microscopic methods as a very rapid assessment of assay performance. The use of dsEGFP rather than the more stable EGFP confers several additional benefits on the MARS assay. Prolonged EGFP expression can be toxic to cells (Liu et al. 1999) and this has the potential to significantly influence results. Additionally, the decreased stability of dsEGFP, which has a half-life in living cells of 2 hr, allows for increased dynamic range of GFP fluorescence as the rapid turnover of dsEGFP prevents

buildup of basally expressed intracellular EGFP which potentially results in a higher level of baseline fluorescence (Li et al. 1998). Following initial assay validation by microscopy, we chose to use flow cytometry in later assays for a number of reasons. Microscopic methods allow for analysis of single cells in relatively small numbers, which can be time and resource intensive. Cell homogenization assays such as luciferase- and CAT-based assays allow only for analysis of response on a population level, potentially missing more subtle effects of stimulation on the single cell level. Flow cytometry allows rapid analysis of samples on a single cell basis and provides a convenient method for assaying fluorescence intensity of a population of cells. Additionally, the HyperCyt autosampling system allows for rapid sampling of treated wells from either a 96- or 384-well plate, further increasing the throughput of the MARS assay by allowing collection of numerous samples in only a few minutes (Ramirez et al. 2003).

The ability of the MARS assay to distinguish AR transcriptional agonists from antagonists was demonstrated in this study. For example, the AR agonists R1881, DHT, E2, progesterone and androstenedione all induced significant increases in the percent of dsEGFP positive cells following 24 hr stimulation compared to unstimulated control cells. This same set of AR agonists also significantly increased the level of dsEGFP expression within the cells expressing dsEGFP, as evidenced by an increase in mean fluorescence intensity within this cell population. Note that although 24 hr was determined as the optimal time point for MARS assay sensitivity, dsEGFP expression by AR agonists could be



detected as soon as 6 hr after treatment (**Fig. 2.2A**). In the single-dose antagonist assay, the known AR antagonists BC, CPA, nilutamide, and flutamide all significantly reduced the percent of cells expressing dsEGFP stimulated by 1 pM R1881. Interestingly, DES, a potent estrogen receptor agonist, was found to act as an AR antagonist, which we speculate may account for some of its therapeutic action in prostate cancer treatment. Although not pursued in the current study, the MARS assay was also capable of detecting AR agonists, such as R1881, DHT, E2 and androstendione, in the antagonist assay, as these agents were found to significantly increase transcriptional responses when compared to 1 pM R1881-stimulated wells. Thus, the MARS assay may prove to have even greater utility as a simultaneous screen for AR agonists and antagonists.

An important facet of the MARS assay is the ability to generate dose-response curves for AR transcriptional agonists as well as antagonists. Our results show the sensitivity of the MARS assay in response to stimulation by a variety of compounds. The  $EC_{50}$  values as determined by the MARS assay are, on the whole, lower than those reported in the literature, demonstrating the high sensitivity of the MARS assay. For example, the calculated  $EC_{50}$  for R1881 of  $1.34 \times 10^{-12}$  M determined in this study is lower than typically seen in the literature, but is in agreement with the  $EC_{50}$  value calculated in our initial microscopic analysis of  $0.88 \times 10^{-12}$  M. Values obtained for DHT, E2 and progesterone typically fall into the low end of reported  $EC_{50}$  values for these compounds in AR transcriptional assays. A notable exception to this trend is androstenedione, for

which there are few reported  $EC_{50}$  values for AR activation. Our  $EC_{50}$  value for androstenedione is  $1.82 \times 10^{-7}$  M, while others (Araki et al. 2005; Roy et al. 2006) have reported  $EC_{50}$  values from 1 to 10 nM. There are several significant differences between the MARS assay and many of the other assay systems that have been used which may account for these differences. Notably, the MARS assay uses PC3 cells, a prostate adenocarcinoma-derived cell line which although not natively androgen responsive, is well-characterized for androgen responsiveness upon forced AR expression (Terouanne et al. 2000; Kizu et al. 2004; Fuse et al. 2007). Other assay systems use cell types which do not express AR and which are not otherwise androgen responsive, including a variety of primate kidney cell lines (Cos7, CV-1) and human cell lines including hepatic (HepG2), cervical (HeLa), breast (T47D) and kidney (HEK293). In fact, reporter assays in cell lines such as 22Rv-1, a human prostatic cancer cell line that is androgen responsive, have been shown to be more sensitive to androgen-mediated transcription activation than parallel reporter assays in cell lines such as HepG2 that are not natively androgen responsive (Simon and Mueller 2006). The use of dsEGFP as a reporter system used may also influence assay sensitivity. Thus, we show that the MARS assay is exquisitely sensitive for analyzing AR activity and is in general agreement with other assay systems for measurements of AR agonist activity.

In addition to determining  $EC_{50}$  values for AR agonists, the MARS assay can also be used to assess the potency of AR antagonists and to calculate  $IC_{50}$  values for these compounds. Similar to the AR agonists tested in this study, the

MARS assay appears to be more sensitive to the effects of antagonists on dsEGFP expression than prior assays, with  $IC_{50}$  values generally lower than those reported in other assays. Notably, several compounds typically considered anti-androgens show partial agonist characteristics when administered at high doses in the MARS assay. All AR antagonists tested except DES and flutamide showed some agonist character at concentrations of 1  $\mu$ M or 10  $\mu$ M, consistent with previously reported observations (e.g., BC (Berno et al. 2006; Fuse et al. 2007), CPA (Simon and Mueller 2006), nilutamide (Chang et al. 2006)). DES and flutamide did not have background agonist activity and significantly inhibited AR stimulation by androgen and thus appear to be complete antagonists of AR-mediated transcription in this assay, consistent with previous reports (Araki et al. 2005).

Analysis of data generated from the HyperCyt® system in the MARS assay using different analytical methods may give subtly different results. For example, analysis on the basis of percent cells expressing dsEGFP over a fixed point allows investigation of how many cells are transcriptionally activated by AR stimulation of the MMTV-controlled reporter dsEGFP, whereas the analysis of responding cells on the basis of mean fluorescence allows some delineation of the variable level of gene expression induced by different stimuli. By determining the product of percent cells expressing dsEGFP and the mean fluorescent intensity of these cells, an estimation of total fluorescence allows for concurrent assessment of the number of cells actively transcribing via the MMTV promoter as well as the level of transcriptional activity in these cells. For single high-dose

assays as well as agonist dose-response assays, the three different analysis methods give similar results; however, the subtle differences in these analyses are particularly interesting in the context of dose-response curves for antagonistic compounds. Generally, the AR antagonists tested in this assay decrease the percent responding cells at low doses, while a higher dose of antagonist is required to decrease dsEGFP expression levels in the remaining responding cells. As a product of percent responding cells and mean fluorescence, the total fluorescence of wells treated with AR antagonists also tends to decrease at lower levels of antagonist. Interestingly, treatment with AR agonists such as progesterone, DHT and E2 at 10  $\mu$ M induced expression of dsEGFP in a lower number of cells than R1881; however, in the cells expressing dsEGFP the level of expression was similar to that induced by R1881, as evidenced by the similarity in mean fluorescence of responding cells.

There are many possible applications and extensions of the MARS assay for future use. Because transient transfection is used in the MARS assay, the cell type, receptor under forced expression, and the promoter modulated by the receptor under forced expression could be customized for the interests of the assay. This may prove useful for comparing the functionality of the AR between species (e.g., rat to hAR), comparing polymorphic variants of the hAR, or in evaluating the activity of other nuclear hormone receptors. Furthermore, the rapid, flexible, and sensitive nature of the assay will make it useful for assessing a variety of compounds with the potential to modulate AR transcriptional activity, including environmental contaminants, pesticides and other potential endocrine

disrupting substances. The high-throughput design of the MARS assay will allow for the screening of large libraries of compounds for AR transcriptional activity with the potential of discovering novel AR agonists and antagonists. Such agents may prove useful for research and therapeutic purposes. In addition to direct extensions of the MARS assay, the validation of this method, particularly in tandem with the description of a glucocorticoid receptor dsEGFP-based reporter assay (Necela and Cidlowski 2003), suggests the utility of similar reporter gene assays utilizing dsEGFP for other steroid hormone receptors which function as transcription factors upon agonist stimulation. Therefore, we speculate that the HyperCyt® system can be used with many different cell types, receptors, and receptor reporters in combination with diverse chemical libraries, providing for numerous high-throughput screening assay options.

In summary, we have developed an AR transcriptional reporter assay that has the benefits of being rapid, sensitive and amenable to high-throughput screening, utilizing transiently transfected PC3 prostate cells expressing a dsEGFP reporter plasmid in tandem with an expression vector for the wild-type hAR. In the experiments presented, the MARS assay was shown to be dependent on AR expression in order to drive dsEGFP expression in response to agonist stimulation. AR transcriptional antagonists are capable of inhibiting this dsEGFP expression when coadministered with agonists of AR activity. Additionally, AR-driven dsEGFP expression in the MARS assay occurs in a dose-dependent manner, showing the dynamic range of the assay. The use of flow cytometry allows for rapid analysis of dsEGFP expression on a cell-by-cell basis

and, in concert with the use of dsEGFP as the reporter, allows for analysis of cells without the need for exogenous reagents to develop the reporter signal. This assay should be useful for a wide variety of future endeavors, including high throughput screening of a variety of potential modulators of AR transcription and extension to other transcriptional reporter assays including those involving other steroid hormone receptors.

## 2.2.5 MATERIALS & METHODS

**2.2.5.1 Chemicals** All chemicals were obtained from Sigma-Aldrich (St. Louis, MO) unless otherwise stated. R1881 (i.e., methyltrienolone) was from PerkinElmer (Waltham, MA). Bicalutamide was from ZereneX Molecular (Manchester, UK). Cyproterone acetate and 4-androstenedione were from Steraloids (Newport, RI).

**2.2.5.2 Expression vectors** The pIRES2-DsRedExpress plasmid was obtained from Clontech (Mountain View, CA). The human AR was PCR amplified using *Pfu* DNA polymerase (Stratagene, La Jolla, CA) and directionally subcloned into the XhoI/SacII sites of pIRES2-DsRedExpress to construct pDsRedhAR. The pMMTVdsEGFP plasmid was constructed by replacing the luciferase gene from pMMTVlux (Thompson et al. 1993) as an XhoI/NotI fragment and with the destabilized EGFP from pd2EGFP-1 (Clontech).

**2.2.5.3 Cell culture & transfection** PC3 human prostate carcinoma cells (ATCC, Manassas, VA) were maintained in Dulbecco's modified Eagle's medium (DMEM) + 5% fetal bovine serum (FBS, Invitrogen, Carlsbad, CA). For the MARS assay, PC3 cells were plated 72 hr prior to transfection in 96-well flat-bottomed tissue culture plates at 4,000 cells per well in DMEM containing 4% charcoal-stripped FBS (CSS) and 1% FBS. Cells were transfected with pDsRedhAR and pMMTVdsEGFP at a ratio of 1:20 using Fugene 6 according to the manufacturers' directions (Roche Diagnostics, Indianapolis, IN). In addition, to test for non-specific MMTV promoter activation (i.e., not mediated by the AR), cells were transfected with pCMV $\beta$  in place of pDsRedhAR and pMMTVdsEGFP

at a ratio of 1:20 using Fugene 6, as described above. For confocal microscopic analysis, cells were seeded at a concentration of  $2 \times 10^4$  cells per well onto 12 mm glass coverslips 72 hr prior to transfection.

**2.2.5.4 Transcriptional activation assays** Twenty-four hours after transfection, test compounds or vehicle were added to cells in DMEM containing 4% CSS and 1% FBS. For antagonist assays, potential AR antagonist compounds or vehicle were added to cells in DMEM containing 1 pM R1881, 4% CSS and 1% FBS. To control for non-specific activation of the MMTV promoter, cells cotransfected with the pIRES2-DsRedExpress and pMMTVdsEGFP vectors were treated identically to plates in the agonist assay as described above and induction of dsEGFP expression in the absence of the AR was noted. Cells were incubated for 24 hr following transfection before analysis by microscopy or using the HyperCyt® system.

**2.2.5.5 Microscopic analysis** For confocal microscopic analysis of dsEGFP fluorescence, treated coverslips were fixed overnight in 2% paraformaldehyde (Electron Microscopy Sciences, Hatfield, PA) in phosphate-buffered saline (PBS) at 4°C. Coverslips were washed 3× with PBS and mounted using VECTASHIELD Mounting Medium (Vector Laboratories, Burlingame, CA) containing 6 μM 4',6-diamidino-2-phenylindole (DAPI, Sigma-Aldrich, St. Louis, MO). Confocal images were collected using a Zeiss LSM 510 microscope and a 20× objective. For fluorescence microscopy, the number of dsEGFP positive cells per treatment was determined using an Olympus IX70 inverted microscope at 40× magnification. Images from each well were captured using an Olympus



Digital Camera with MagnaFire 2.1A Digital Microimaging software as 8-bit TIFF images and the number of dsEGFP positive cells per an image were counted using ImageJ software (Rasband 2007). Four wells were examined for each treatment and each experiment was performed in duplicate. Consistency of transfection over a 96-well plate was established by examining for equivalence of DsRed expression between wells from either pIRES2-DsRedExpress or pDsRedhAR using fluorescence microscopy prior to sample treatment.

**2.2.5.6 HyperCyt® analysis** Twenty-four hours after treatment, medium was removed from each well cells in 96-well plates were trypsinized with 25  $\mu$ L 0.25% trypsin-EDTA (Sigma-Aldrich, St. Louis, MO) for 3 min. Trypsin was neutralized by addition of 75  $\mu$ L DMEM containing 5% FBS and cells were transferred to 96-well V bottom PCR plates. Cells were pelleted by centrifugation at 1,200 $\times$ g and gently resuspended in 25  $\mu$ L DMEM. Plates were rotated at approximately 12 rpm at 4°C for up to 30 min prior to analysis. The HyperCyt® autosampling system (Kuckuck et al. 2001; Ramirez et al. 2003) was used to sample individual wells for 1.2 sec per well (approximately 2.5  $\mu$ L sample pickup). Samples were acquired using a CyAn™ ADP flow cytometer (Dako, Inc., Fort Collins, CO). Data analysis was completed using IDLQuery software written by Dr. Bruce Edwards (Edwards et al. 2007).

## 2.2.6 FIGURE LEGENDS

**2.2.6.1 Figure 2.1. Methods of analysis using the MARS assay** For either analysis method, PC3 cells are transfected with pDsRedAR and pMMTVdsEGFP at a ratio of 1:20. After 24 hr, cells were treated with test compounds and dsEGFP expression was assessed following an additional 24 hr incubation. Representative photomicrographs showing AR agonist and antagonist activity by confocal microscopy in the MARS assay (A-D). Cells seeded on glass coverslips and treated with vehicle (A), 1 nM R1881 (B), 1 pM R1881 (C), or 1 pM R1881 + 10  $\mu$ M bicalutamide (D). Coverslips were fixed following 24 hr stimulation and stained with DAPI. Images are representative 20x fields. MARS assay by HyperCyt® (E). PC3 cells are seeded in a 96-well tissue culture plate, treated with test compound and allowed 24 hr to respond to treatment. After 24 hr, cells are removed from each well by trypsinization and sampled using the HyperCyt® high throughput flow cytometry. The percent of events in each well above a set gate was used to determine the androgenicity or anti-androgenicity of test compounds.

**2.2.6.2 Figure 2.2. MARS assay analyzed by microscopy** Time course data (A) for dsEGFP expression in PC3 cells seeded in 24-well tissue culture plates and cotransfected with pDsRedhAR and pMMTVdsEGFP. Cells were treated with R1881 with or without bicalutamide and dsEGFP expression was quantified by microscopy at 6, 12, 24, 48 and 72 hr post-treatment. Each time point represents the number of dsEGFP-positive cells per low power field in three independent wells. Dose-response data (B) for the MARS assay. PC3 cells

seeded in 24-well tissue culture plates and cotransfected with pDsRedhAR and pMMTVdsEGFP were treated with varying concentrations of R1881 in the absence or presence of 1  $\mu$ M bicalutamide. Each point represents 4 independent wells and experiments were performed in duplicate. Three parameter dose-response curves were analyzed using Graph Pad Prism software.

**2.2.6.3 Figure 2.3. Chemical structures of the test set of compounds used for MARS assay validation** Representative agonists (A) and antagonists (B) of AR mediated transcription including the steroidal compounds R1881 and DHT (AR agonists), CPA (AR antagonist), E2 (ER agonist), progesterone (PR agonist) and androstenedione (DHT and E2 precursor). Also shown are the nonsteroidal anti-androgenic compounds bicalutamide, flutamide and nilutamide (AR antagonists) and DES (ER agonist).

**2.2.6.4 Figure 2.4. Androgenic activity of compounds in a single-dose MARS assay** The androgenic (A) and anti-androgenic (B) activity of a test set of compounds was assessed using the MARS assay and HyperCyt®. Cells were seeded in 96-well tissue culture plates, cotransfected with pDsRedAR and MMTVdsEGFP at a ratio of 1:20, and stimulated 24 hr later with compounds as indicated. Following a 24 hr induction of dsEGFP expression, wells were trypsinized and cells analyzed by HyperCyt® high throughput flow cytometry. The percent of GFP<sup>+</sup> cells in each well was normalized to 1 nM R1881 treatment in the agonist assay (A) or to vehicle + 1 pM R1881 in the antagonist assay (B). \*\* p<0.0001, \* p<0.05, compared to unstimulated and vehicle (+1 pM R1881) in panels (A) and (B), respectively. Bars represent at least four wells from three

independent experiments in (A) and at least ten wells from three independent experiments in (B).

**2.2.6.5 Figure 2.5. Dose-response curves for AR agonists in the MARS assay** The potency of select compounds with observed androgenic (A-D) activity in the single-dose MARS assay was assessed using serial dilutions of the indicated compound to stimulate cells in the MARS assay (A-D). Each point is representative of at least four wells in each of two independent experiments.

**2.2.6.6 Figure 2.6. Dose-response curves for AR antagonists in the MARS assay** The potency of select compounds with observed anti-androgenic (A-D) activity in the single-dose MARS assay was assessed using serial dilutions of the indicated compound to stimulate cells in the MARS assay in the presence (A-D) of 1 pM R1881. Each point is representative of at least four wells in each of two independent experiments.

**2.2.6.7 Table 2.1. EC<sub>50</sub> and IC<sub>50</sub> Values for MARS**

**Figure 2.1 Methods of analysis using the MARS Assay**

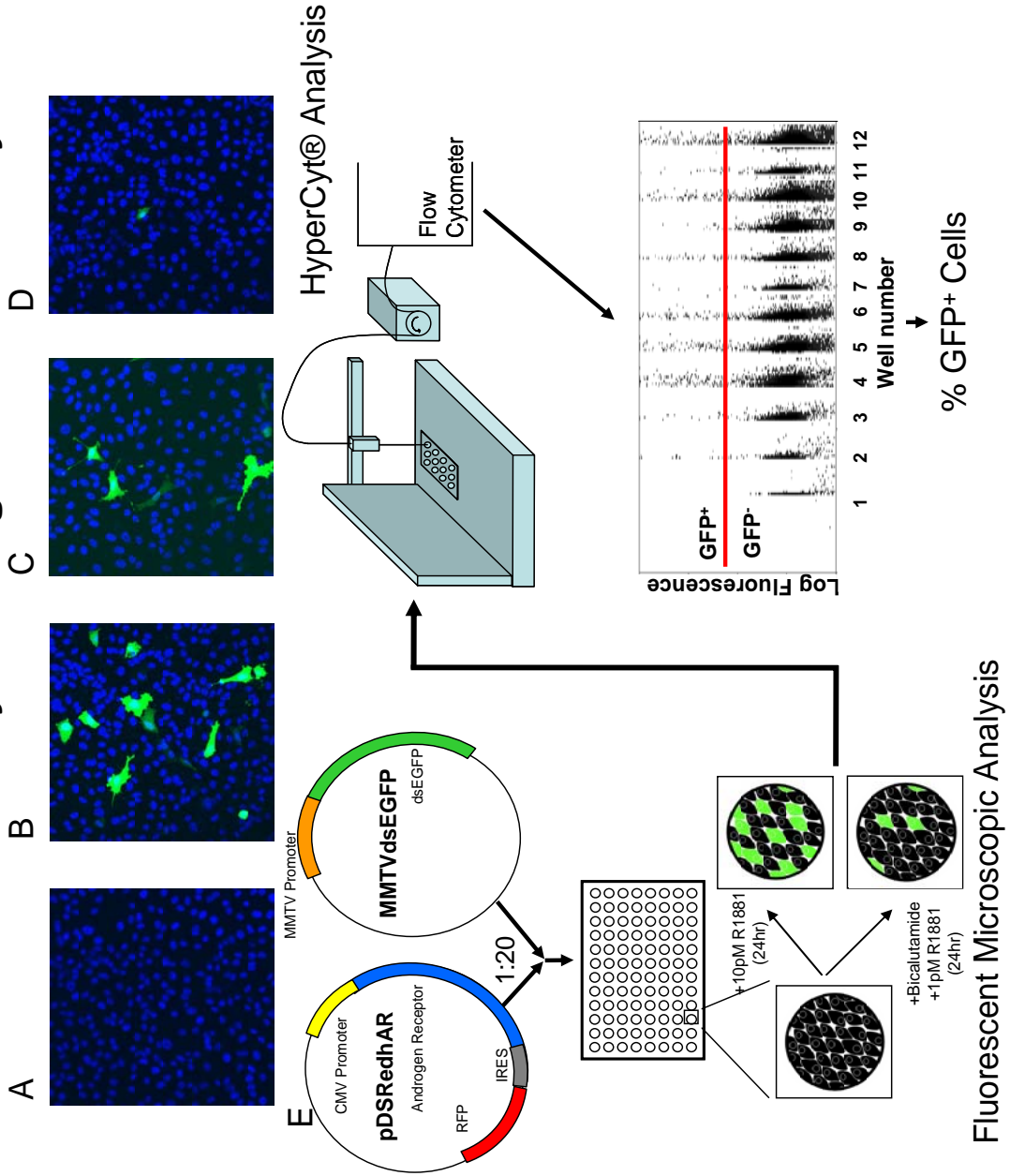


**Figure 2.2 MARS assay analyzed by microscopy**

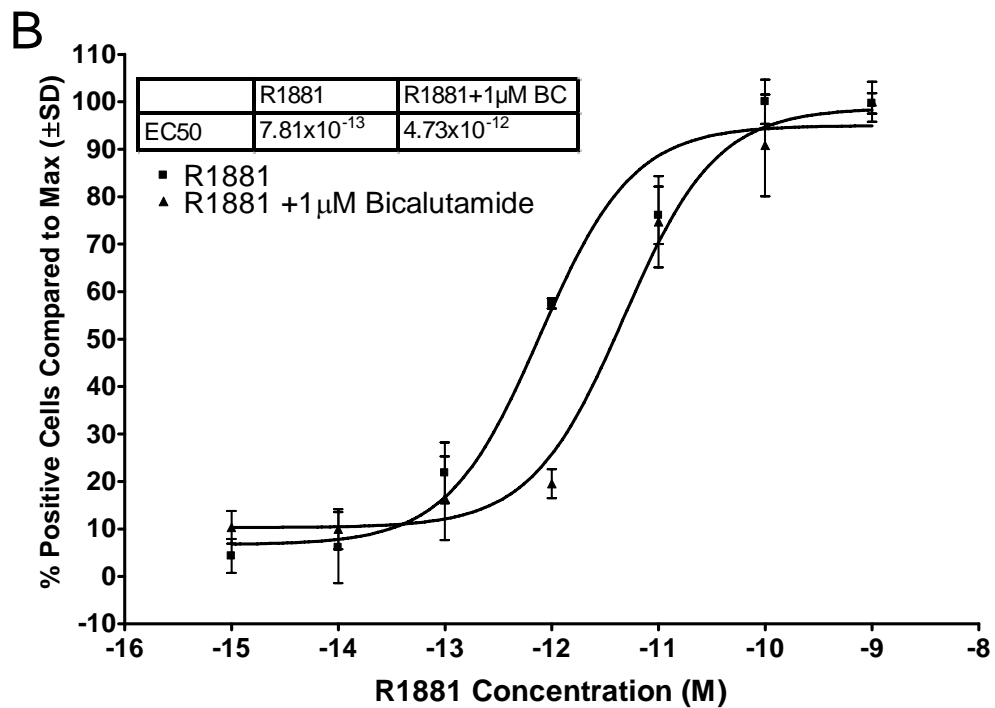
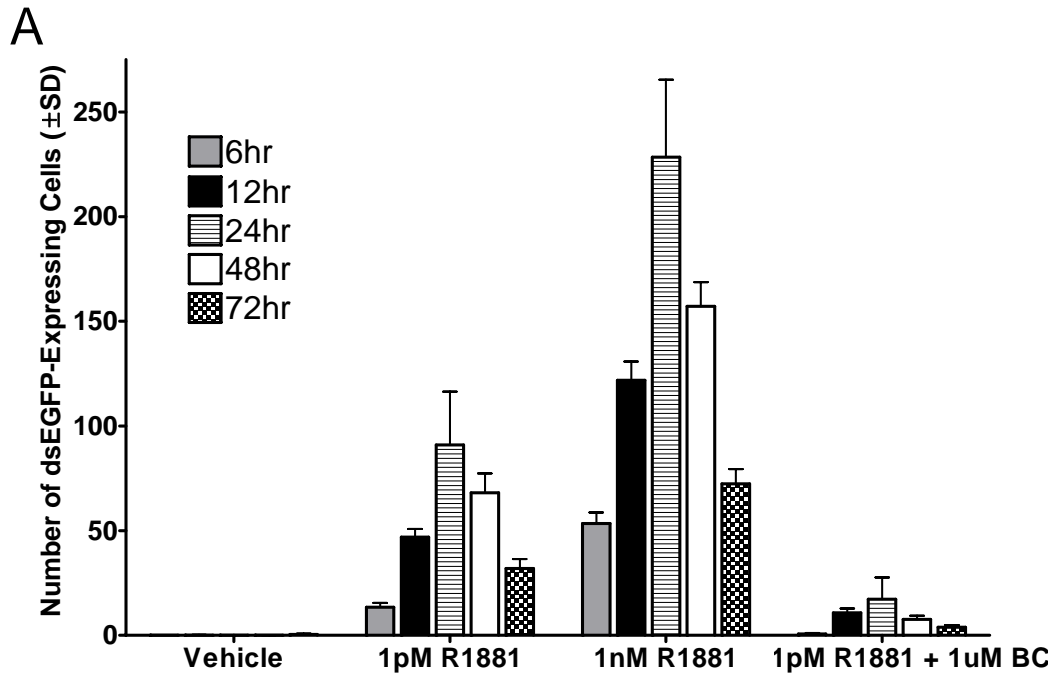
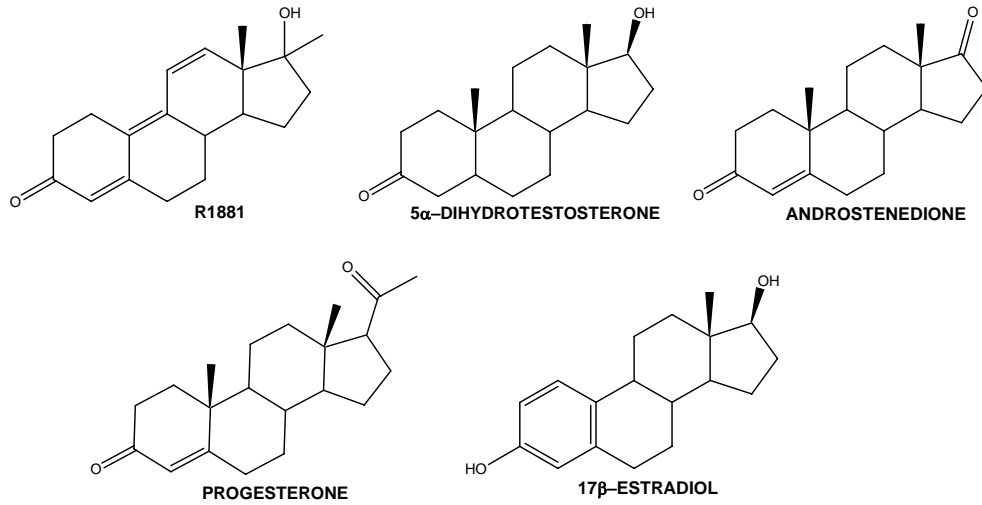


**Figure 2.3 Chemical structures of the test set of compounds used for MARS assay validation**

**A**



**B**

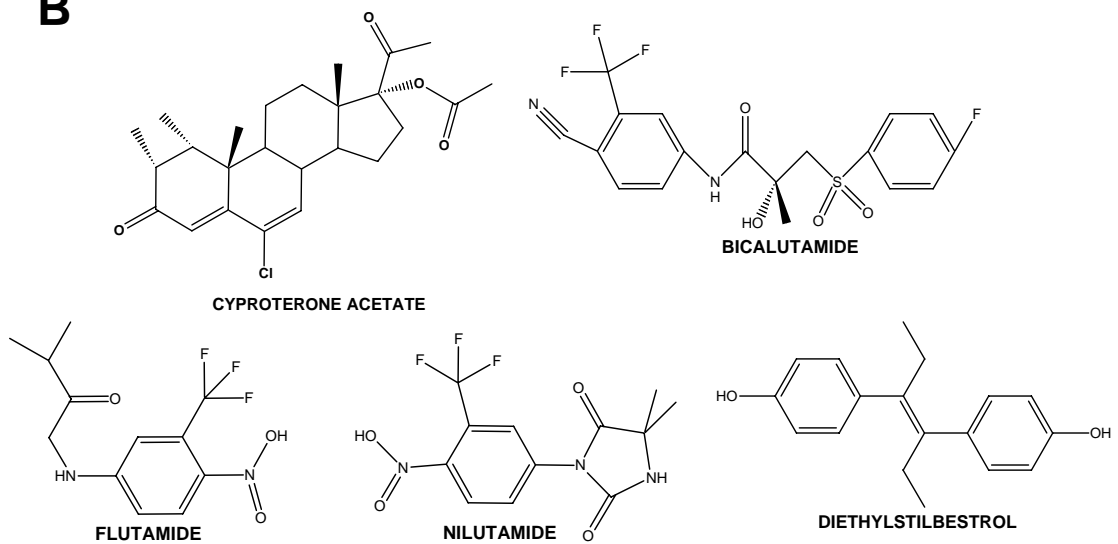


**Figure 2.4 Androgenic activity of compounds in a single-dose MARS assay**

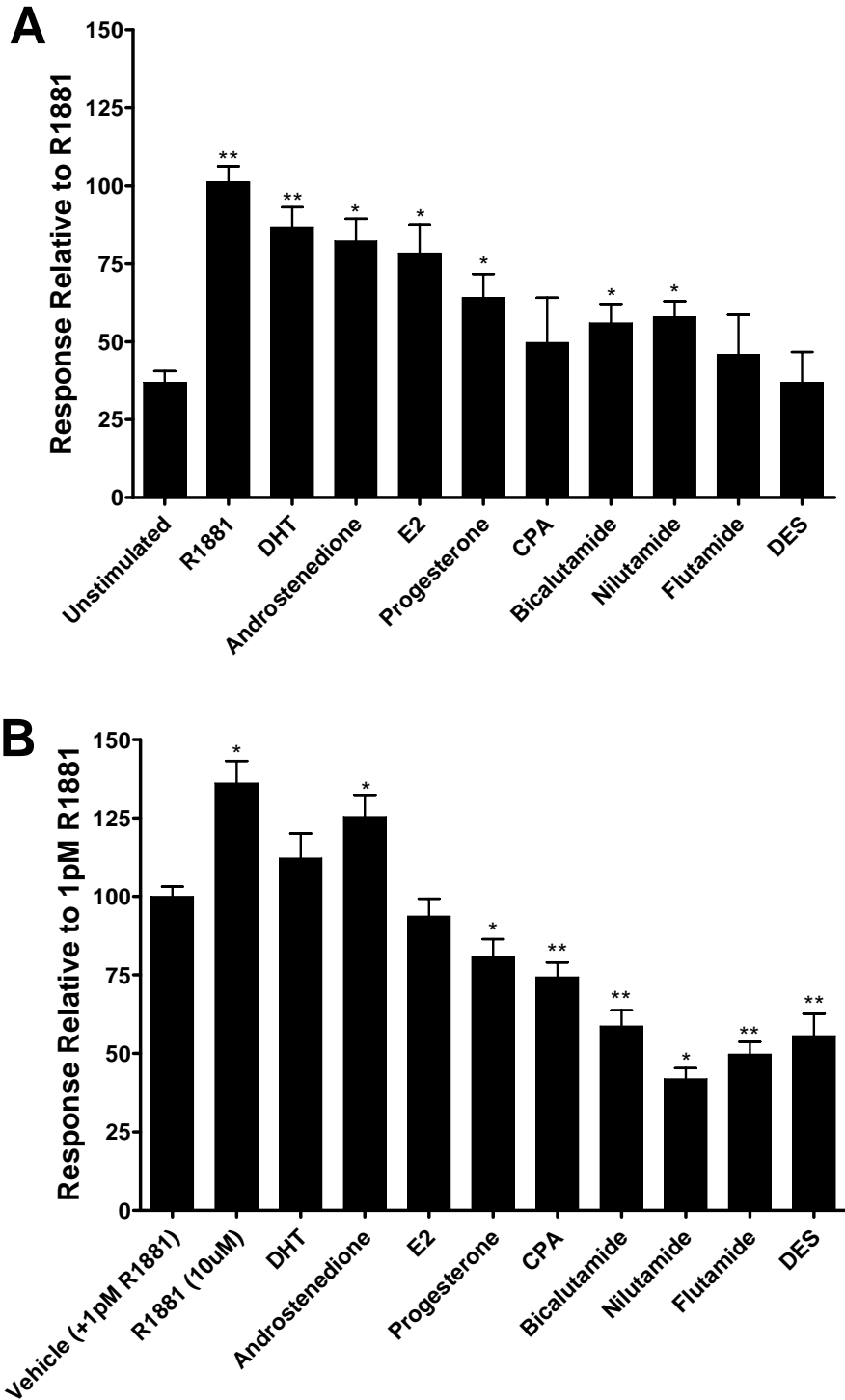




**Figure 2.5 Dose-response curves for AR agonists in the MARS assay**

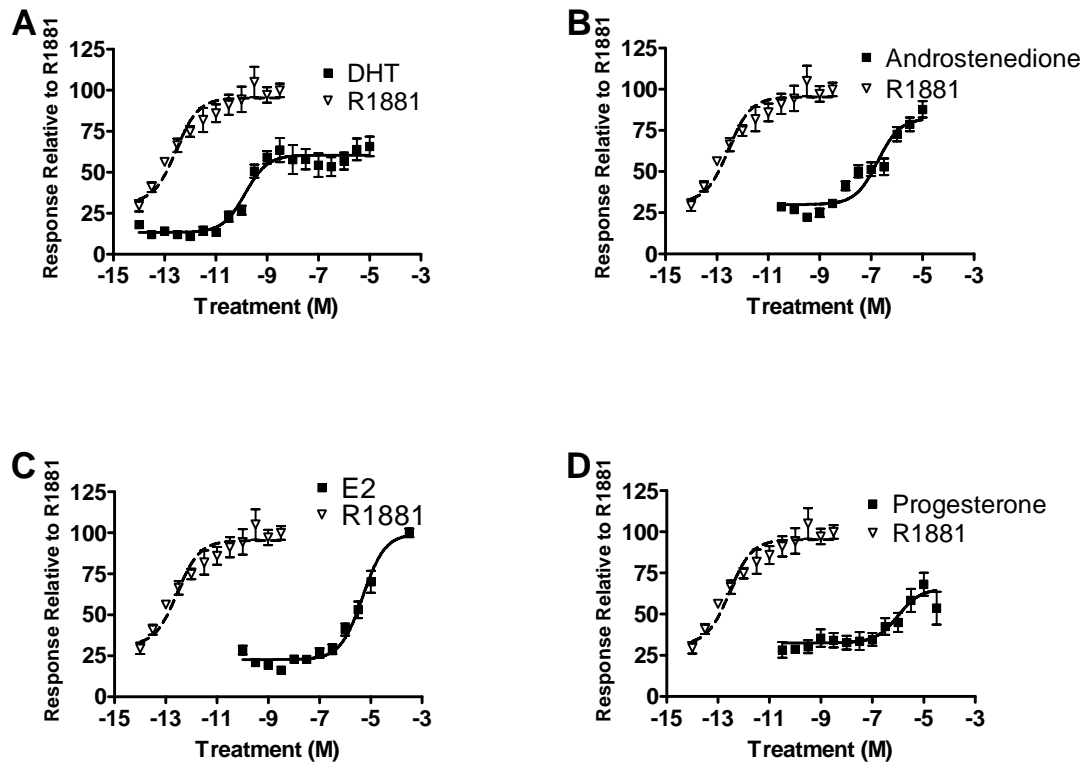


**Figure 2.6 Dose-response curves for AR antagonists in the MARS assay**

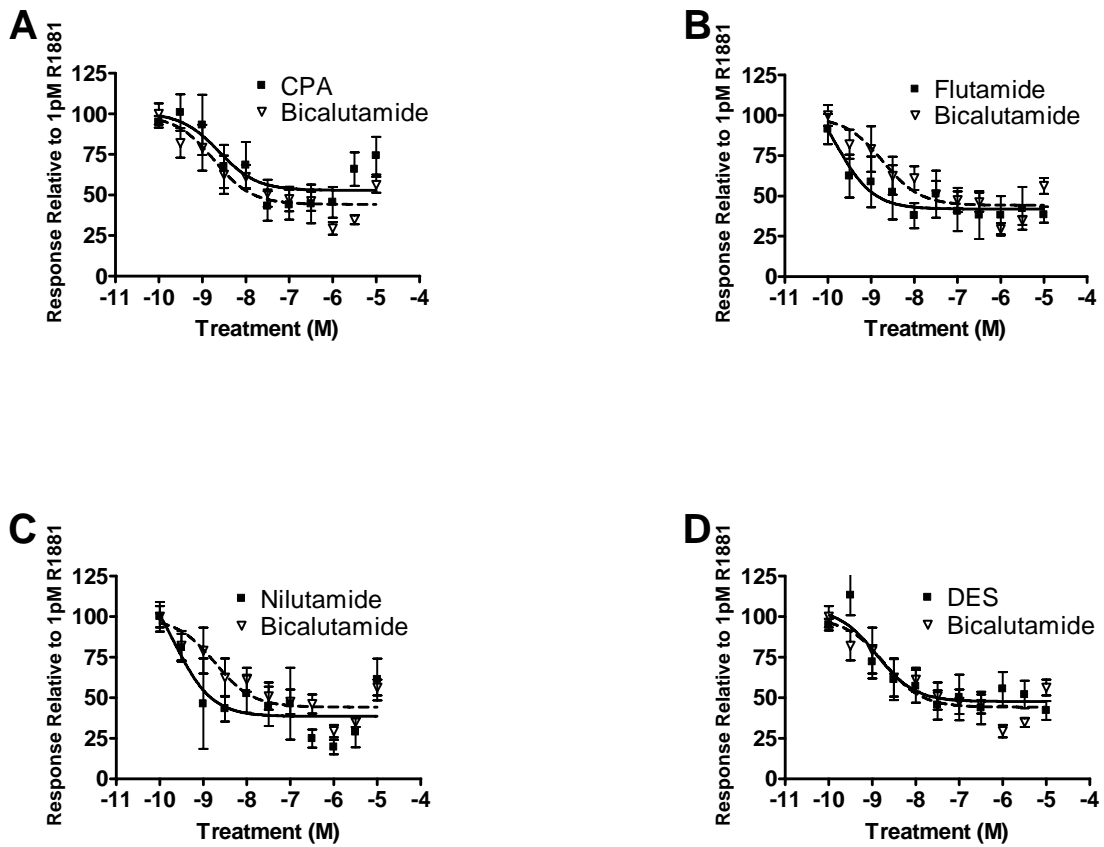


**Table 2.1 EC<sub>50</sub> and IC<sub>50</sub> values for MARS**

	EC50 (M)	IC50 (M)
R1881	$1.34 \times 10^{-12}$	-
DHT	$1.38 \times 10^{-10}$	-
Androstenedione	$1.08 \times 10^{-07}$	-
Progesterone	$1.01 \times 10^{-06}$	-
Estrogen	$4.88 \times 10^{-06}$	-
Flutamide	-	$1.51 \times 10^{-10}$
Nilutamide	-	$2.77 \times 10^{-10}$
DES	-	$1.27 \times 10^{-09}$
Bicalutamide	-	$1.85 \times 10^{-09}$
CPA	-	$2.41 \times 10^{-09}$

### 2.3 Segue

The development of the MARS assay resulted in a rapid assay for AR function that could be applied to a much larger set of compounds than those chosen for the initial validation of the assay. With this capability, screening of the full ICCVAM set was undertaken, with the goal of identifying both androgenic and anti-androgenic effects of these compounds. The following section discusses the preliminary screening results from the first full set of endocrine disrupting compounds screened by the MARS assay as well as brief follow-up experiments intended to further elucidate the anti-androgenic character of a selected subset of compounds.

## 2.4 AR / ICCVAM Screening Section

### 2.4.1 ABSTRACT

The AR is important in a range of physiological processes in males, including development of secondary sexual characteristics and maintenance of sexual organs throughout life. In addition to its normal role in male physiology, the AR is important in prostate cancer. Initial treatment for most advanced prostate cancers involves androgen blockade, as removal of androgen signaling prevents tumor growth. Eventually, prostate cancer becomes androgen-independent or castration resistant and tumor cells become capable of proliferating in the absence of androgen, leading to a much more difficult-to-treat form of cancer. Compounds other than androgen are also capable of mediating AR signaling, both positively and negatively. We screened a library of potential endocrine disrupting chemicals, to identify small molecules with novel activity against the AR, including compounds that could act as AR antagonists with possible therapeutic value. We used the MARS assay to screen compounds for AR transcriptional activity and a nuclear translocation assay of AR from the cytosol to the nucleus, as nuclear translocation is a required step in the induction of transcription. We found that apigenin, a flavone, is an effective antagonist of AR-mediated transcription and also prevents nuclear translocation of AR.

## 2.4.2 INTRODUCTION

Endocrine disruptors are a large class of chemicals that bind to AR and ER and modulate receptor function. Included among endocrine disruptors are xenoestrogens, which are industrial byproducts that have estrogenic or androgenic activity, either by design such as ethinyl estradiol or which have inadvertent off target effects on ER or AR, such as pesticides like DDT and its metabolites (Rogan and Ragan 2003; Venners et al. 2005; Aneck-Hahn et al. 2007). In addition to xenoestrogens are naturally derived compounds such as phytoestrogens and mycoestrogens, derived from plants and fungi, respectively. Endocrine disruptors can act in several ways, including altering expression levels of steroid hormone receptors themselves, interfering with steroid biosynthetic pathways and direct signaling through steroid receptors (Soto et al. 2006).

The AR is a member of the steroid hormone superfamily of nuclear receptors, a 110 kD protein that resides in the cytosol prior to androgen stimulation, at which point it translocates to the nucleus, dimerizes and mediates transcription of androgen responsive genes (Roy et al. 1999; Gelmann 2002). The physiological ligands for AR include 5 $\alpha$ -DHT and related androgens, synthetic ligands such as R1881, a more stable androgen mimetic, and BC, an anti-androgen used therapeutically for the treatment of prostate cancer. Following ligand binding, AR can also mediate rapid signaling events in addition to genomic signaling; these rapid signaling pathways can result in activation of PI3K, Src and phosphorylation of CREB, which results in genomic signaling via an indirect mechanism (Migliaccio et al. 2000; Cheng et al. 2007).

The effects of endocrine disruptors on AR function are beginning to be defined, with pesticides such as DDT and its metabolites being shown to cause problems with both male and female reproductive function as well as development (Rogan and Ragan 2003; Venners et al. 2005; Aneck-Hahn et al. 2007). Description of the endocrine-disrupting effects of the full ICCVAM library would greatly add to our knowledge of androgen disrupting chemicals and may lead to the discovery of new anti-androgens for the treatment of prostate cancer. With that in mind, we utilized the MARS assay to screen the full ICCVAM library for effects on AR-mediated transcription as well as for the ability of compounds to translocate the AR from the cytoplasm to the nucleus.

## 2.4.3 RESULTS AND DISCUSSION

### 2.4.3.1 The MARS assay identifies AR transcriptional agonists and antagonists

The MARS assay was used to screen the ICCVAM library of 119 potentially endocrine-disrupting compounds. Screening for agonists of AR-mediated transcription resulted in the identification of a number of compounds with transcriptional agonist activity at 10  $\mu$ M (**Fig 2.8A, Figure with SEM, compound names in Appendix as S1**). Compounds identified as transcriptional agonists included those identified in the preliminary MARS screening (Dennis et al. 2008) and known transcriptional agonists including 5 $\alpha$ -DHT, androstenedione, and methyltestosterone. Additionally, compounds included as negative controls that should not have induced transcription such as the protein translation inhibitor Actinomycin D did not enhance AR-mediated transcription, verifying that the MARS assay was functioning as expected in this expanded screening format. Similar results for reproducibility were seen in the antagonist screen (**Fig. 2.8B, expanded Figure in Appendix as S2**), wherein antagonists such as bicalutamide, cyproterone acetate and finasteride acted as antagonists of AR-mediated transcription, as expected.

In addition to known antagonists of AR-mediated transcription, several compounds were able to inhibit transcription as well or better than known antagonists. These compounds include 4-hydroxytamoxifen (TAM), bisphenols A (BPA) and B but not the closely related bisphenol C2, as well as apigenin.



### 2.4.3.2 Translocation of AR-GFP

In addition to investigating the transcription-modulating abilities of compounds contained in the ICCVAM library, we also investigated the ability of compounds to translocate the AR from the cytoplasm to the nucleus. The translocation of the AR to the nucleus is a critical step in the initiation of transcription following AR activation although some AR antagonists also induce translocation. The assay for AR translocation is based on either PC3 cells or Cos7 cells transfected with an AR-GFP expression vector, treating these cells with androgen, and assessing AR-GFP translocation to the nucleus. Both PC3 cells and Cos7 cells efficiently translocate AR-GFP to the nucleus upon androgen stimulation, and this effect is maximal after 30 min (**Fig 2.9A**). Cos7 cells were used for AR-GFP translocation experiments with the ICCVAM compounds as they show similar androgen-mediated AR-GFP translocation, transfect at a higher efficiency than PC3 cells and adhere more efficiently to the glass coverslips, facilitating imaging of AR-GFP localization (data not shown). Results for AR-GFP translocation after stimulation with 1  $\mu$ M of ICCVAM compounds are summarized in **Table 2.2**.

One compound that had intriguing effects on AR transcription was apigenin, a plant-derived flavone. This compound did not induce transcription via the AR (**Fig 2.9B**) and blocked androgen stimulated transcription more effectively than bicalutamide (**Fig 2.9C**). In AR-GFP translocation assays, 1  $\mu$ M bicalutamide promotes the translocation of AR-GFP, even though it acts as a transcriptional antagonist at this concentration (Dennis et al. 2008). Conversely,

apigenin is also a transcriptional antagonist of AR-mediated transcription at this concentration yet treatment of cells expressing AR-GFP with 1  $\mu$ M apigenin does not result in the nuclear translocation of AR-GFP (**Fig. 2.9D**).

To further investigate the antagonist properties of apigenin and other anti-androgens, the AR-GFP translocation assay was used again. In this setup, a sub-maximal concentration of R1881 was used to induce nearly complete translocation of AR-GFP and newly identified antagonists were co-administered with R1881 in order to determine if the antagonists can effectively block R1881-induced AR-GFP translocation. This assay had no positive control, as previously known AR antagonists all induce the translocation of AR-GFP into the nucleus and no compounds were previously known that do not translocate AR-GFP. We found that TAM effectively blocks the R1881-induced translocation of AR-GFP (**Fig. 2E**). Interestingly, apigenin was unable to block the AR-GFP translocation induced by R1881 although it is an efficient antagonist of R1881-mediated transcription in the MARS assay. Additionally, BPA shows an intermediate phenotype in this assay, partially blocking R1881-mediated translocation of AR-GFP. These results suggest that there are several subclasses of anti-androgens, all of which block R1881-mediated transcription in the MARS assay. Some antagonists of the AR, including bicalutamide and cyproterone acetate, induce translocation of AR-GFP on their own, in the absence of AR agonist. Other antagonists do not induce AR-GFP translocation on their own but also fail to block R1881-induced AR-GFP translocation. Finally, a third group of antagonists is able to block both transcription and AR-GFP translocation induced by R1881.

The differences in biological properties of these antagonists will be interesting to investigate in the future with regard to their ability to mediate proliferation of prostate cancer cells and to influence other relevant processes to tumorigenesis and tumor growth.

## 2.4.4 MATERIALS & METHODS

**2.4.4.1 Chemicals** All chemicals were obtained from Sigma-Aldrich (St. Louis, MO) unless otherwise stated. R1881 (i.e., methyltrienolone) was from PerkinElmer (Waltham, MA). BC and letrozole were from Zerenex Molecular (Manchester, UK). Other compounds in the ICCVAM library were from Sigma, except: 4-androstenedione, corticosterone, CPA, dexamethasone, finasteride, fluoxymestron, meso-hexestrol, medroxyprogesterone, 17beta-trenbolone, cortisol, 4-hydroxyandrostenedione, 17alpha-hydroxyprogesterone, levonorgestrel, melengestrol acetate, mestranol, and pregnenolone from Steraloids, Apomorphine from Tocris. Hydroxyflutamide and formononetin from Axxora. 32% paraformaldehyde (PFA) was from Electron Microscopy Sciences. Vectashield was from Vector Labs.

**2.4.4.2 Expression vectors** The pIRES2-DsRedExpress plasmid was obtained from Clontech (Mountain View, CA). The human AR was PCR amplified using *Pfu* DNA polymerase (Stratagene, La Jolla, CA) and directionally subcloned into the XhoI/SacII sites of pIRES2-DsRedExpress to construct pDsRedhAR. The pMMTVdsEGFP plasmid was constructed by replacing the luciferase gene from pMMTVlux (Thompson et al. 1993) as an XhoI/NotI fragment and with the destabilized EGFP from pd2EGFP-1 (Clontech). The AR-GFP expression vector was a kind gift from Tad H. Koch, Ph.D.

**2.4.4.3 Cell culture & transfection** PC3 human prostate carcinoma cells (ATCC, Manassas, VA) were maintained in Dulbecco's modified Eagle's medium (DMEM) + 5% fetal bovine serum (FBS, Invitrogen, Carlsbad, CA). Cos7

monkey kidney cells (ATCC, Manassas, VA) were maintained in DMEM containing 10% FBS with 100 units/mL penicillin and 100 µg/mL streptomycin. Cells were grown as a monolayer at 37°C, in a humidified atmosphere of 5% CO<sub>2</sub> and 95% air.

For the MARS assay, PC3 cells were plated 72 hr prior to transfection in 96-well flat-bottomed tissue culture plates at 4,000 cells per well in DMEM containing 4% charcoal-stripped FBS (CSS) and 1% FBS. Cells were transfected with pDsRedhAR and pMMTVdsEGFP at a ratio of 1:20 using Fugene 6 according to the manufacturers' directions (Roche Diagnostics, Indianapolis, IN). In addition, to test for non-specific MMTV promoter activation (i.e., not mediated by the AR), cells were transfected with pCMVβ in place of pDsRedhAR and pMMTVdsEGFP at a ratio of 1:20 using Fugene 6, as described above. For confocal microscopic analysis, cells were seeded at a concentration of 2×10<sup>4</sup> cells per well onto 12 mm glass coverslips 72 hr prior to transfection.

For AR-GFP translocation assays, PC3 or Cos7 cells in 6-well plates were transfected using Lipofectamine 2000 (Invitrogen) per manufacturer's directions. Cells were trypsinized 6 hr following transfection and 10,000 cells were seeded onto 12 mm glass coverslips in phenol red free DMEM/F-12 containing 10% charcoal stripped FBS. Cells were allowed to adhere for 24 hr prior to translocation assays.

**2.4.4.4 Transcriptional activation assays** Twenty-four hours after transfection, test compounds or vehicle were added to cells in DMEM containing 4% CSS and 1% FBS. For antagonist assays, potential AR antagonist

compounds or vehicle were added to cells in DMEM containing 1 pM R1881, 4% CSS and 1% FBS. To control for non-specific activation of the MMTV promoter, cells cotransfected with the pIRES2-DsRedExpress and pMMTVdsEGFP vectors were treated identically to plates in the agonist assay as described above and induction of dsEGFP expression in the absence of the AR was noted. Cells were incubated for 24 hr following transfection before analysis by microscopy or using the HyperCyt® system.

**2.4.4.5 HyperCyt® analysis** Twenty-four h after treatment, medium was removed from each well cells in 96-well plates were trypsinized with 25 µL 0.25% trypsin-EDTA (Sigma-Aldrich, St. Louis, MO) for 3 min. Trypsin was neutralized by addition of 75 µL DMEM containing 5% FBS and cells were transferred to 96-well V bottom PCR plates. Cells were pelleted by centrifugation at 1,200×g and gently resuspended in 25 µL DMEM. Plates were rotated at approximately 12 rpm at 4°C for up to 30 min prior to analysis. The HyperCyt® autosampling system (Kuckuck et al. 2001; Ramirez et al. 2003) was used to sample individual wells for 1.2 sec per well (approximately 2.5 µL sample pickup). Samples were acquired using a CyAn™ ADP flow cytometer (Dako, Inc., Fort Collins, CO). Data analysis was completed using IDLQuery software written by Dr. Bruce Edwards (Edwards et al. 2007).

**2.4.4.6 AR translocation assays** For AR-GFP translocation assays, PC3 or Cos7 cells transfected with AR-GFP and seeded onto 12 mm glass coverslips were serum starved for 24 hr prior to analysis. Cells were stimulated with compounds as indicated in figure legends and fixed with 2% PFA

in PBS for 15 m at 37°C. Coverslips were then washed three times with PBS and mounted in Vectashield containing DAPI. Confocal images were collected on a Zeiss LSM 510 system.

## 2.4.5 FIGURE LEGENDS

### 2.4.5.1 Figure 2.8. AR transcriptional activity of ICCVAM compounds

For either analysis method, PC3 cells are transfected with pDsRedAR and pMMTVdsEGFP at a ratio of 1:20. After 24 hr, cells were treated with test compounds and dsEGFP expression was assessed following an additional 24 hr incubation using the HyperCyt® system as previously described (Dennis et al. 2008). **A)** Agonist activity of ICCVAM compounds on AR-mediated transcription. Wells were treated with 10  $\mu$ M compound and expression was compared to GFP expression induced by 10 pM R1881. **B)** Antagonist activity of ICCVAM compounds on AR-mediated transcription. Wells were treated with 1 pM R1881 and 10  $\mu$ M compound and inhibition of AR-mediated transcription was assessed.

### 2.4.5.2 Figure 2.9. AR-GFP Translocation assay

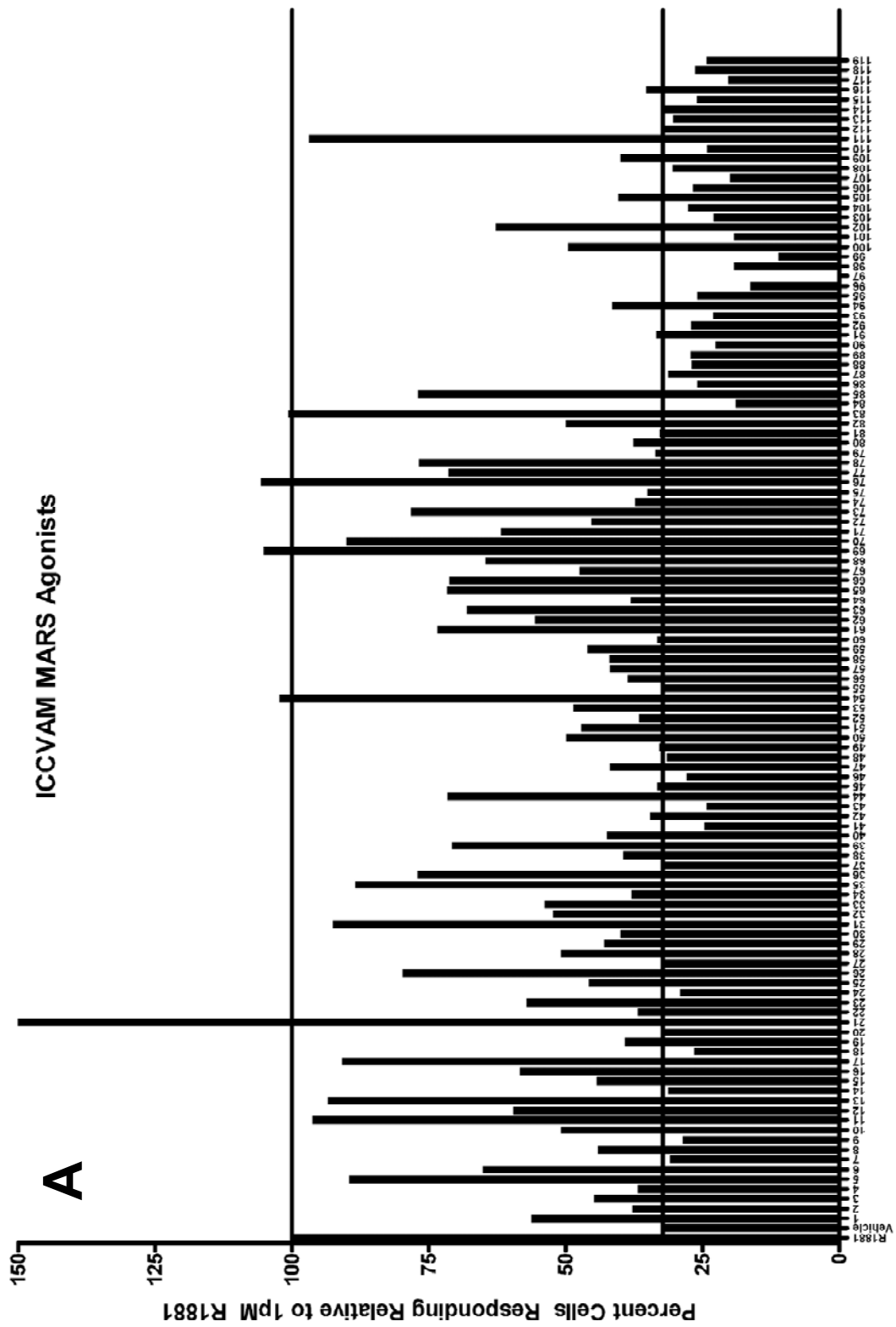
PC3 or Cos7 cells were transiently transfected with the AR-GFP reporter plasmid, treated with compound(s) as indicated and fixed with 2% PFA prior to imaging by confocal microscopy. **A)** Time course of AR-GFP translocation in PC3 (left) and Cos7 (right) cells. Cells were treated for indicated times with 10 nM R1881 to determine the time course of R1881-induced AR-GFP translocation. **B)** Apigenin agonist activity as measured by the MARS assay compared to R1881 and DMSO controls. **C)** Apigenin as an antagonist of R1881-induced AR-mediated translocation, compared to DMSO and bicalutamide controls. **D)** AR-GFP translocation induced by bicalutamide and apigenin. Cells were treated with 1  $\mu$ M bicalutamide or apigenin. **E)** R1881-mediated AR-GFP translocation blocked by



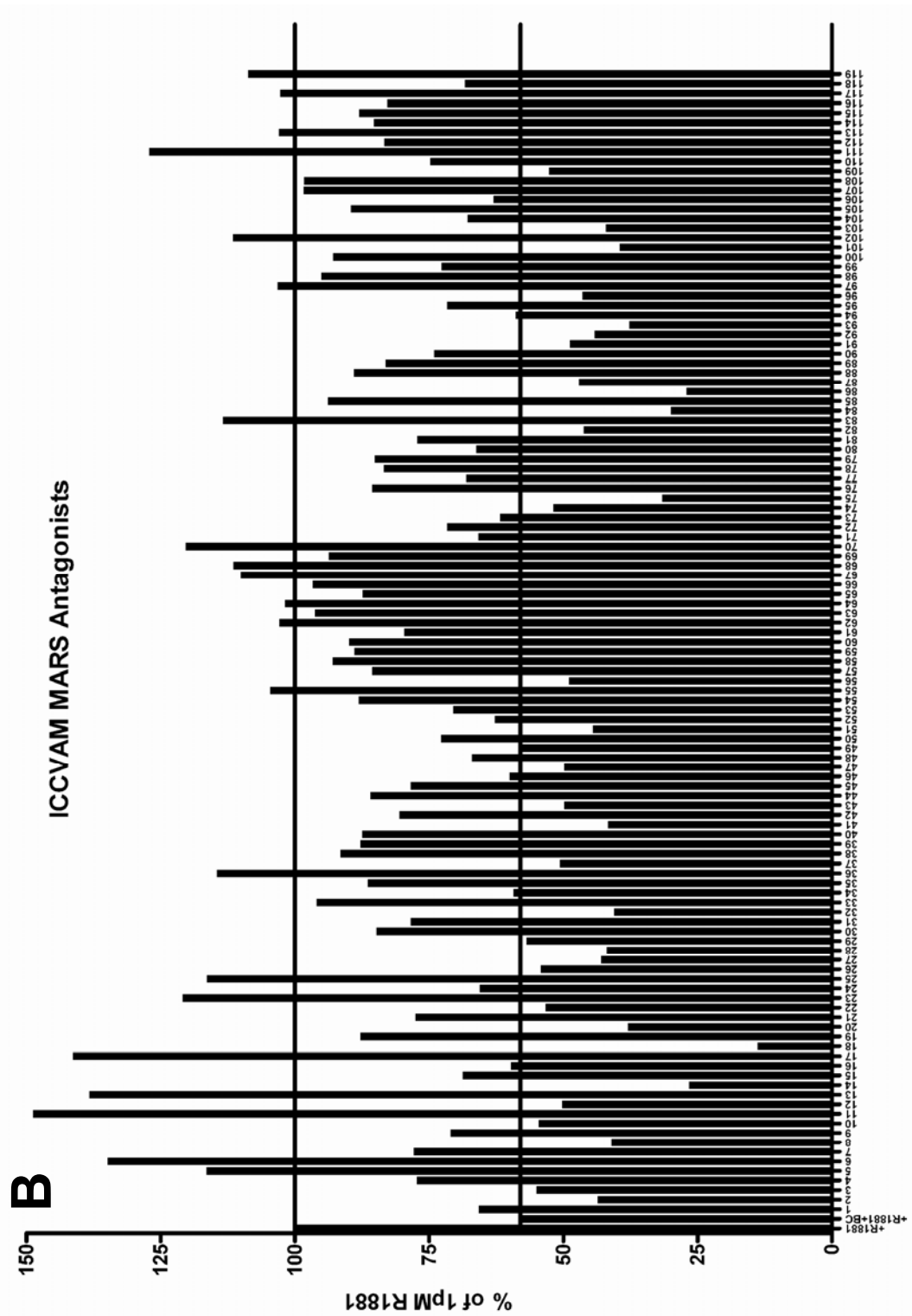
compounds. Cells were incubated with 100 pM R1881 and 1  $\mu$ M compound for 30 min.

**2.4.5.3 Table 2.2. Summary of AR-GFP translocation induced by ICCVAM compounds**

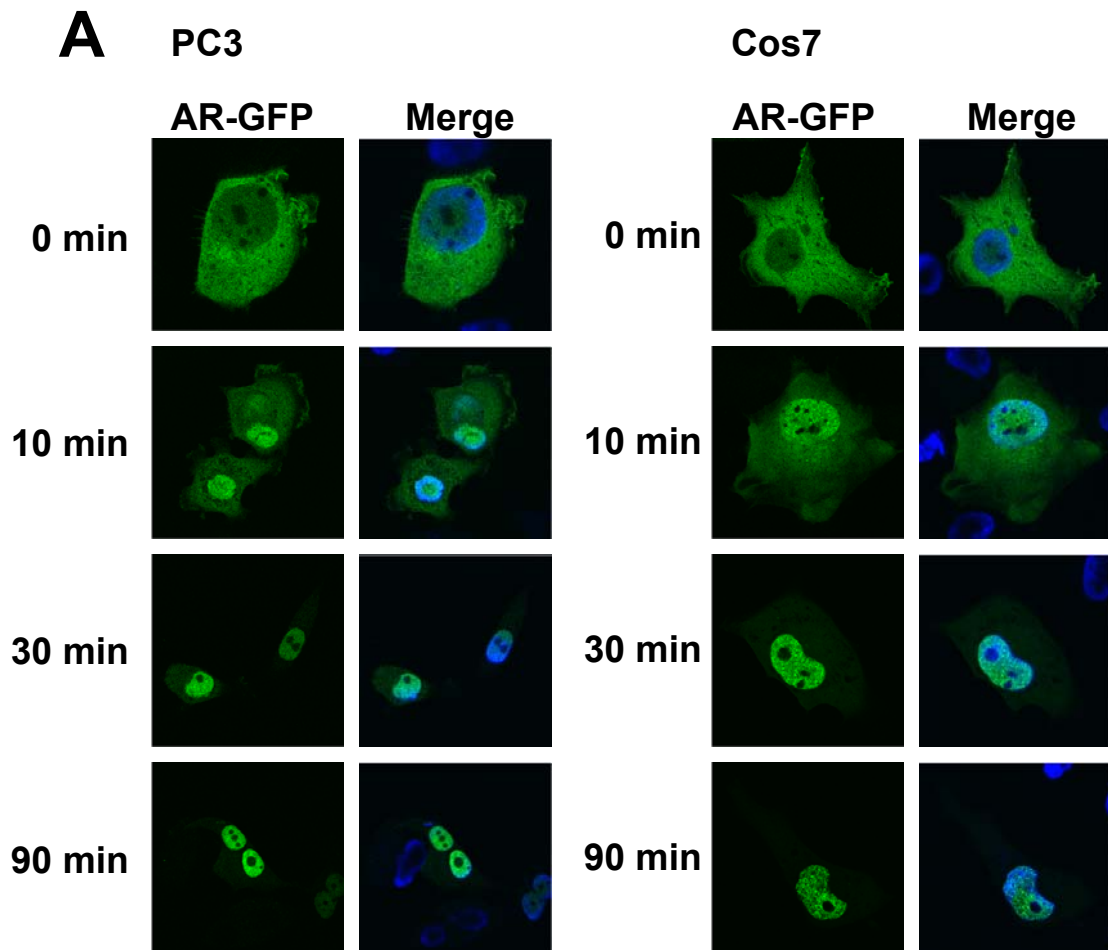
2.4.5.1 FIGURE 2.8



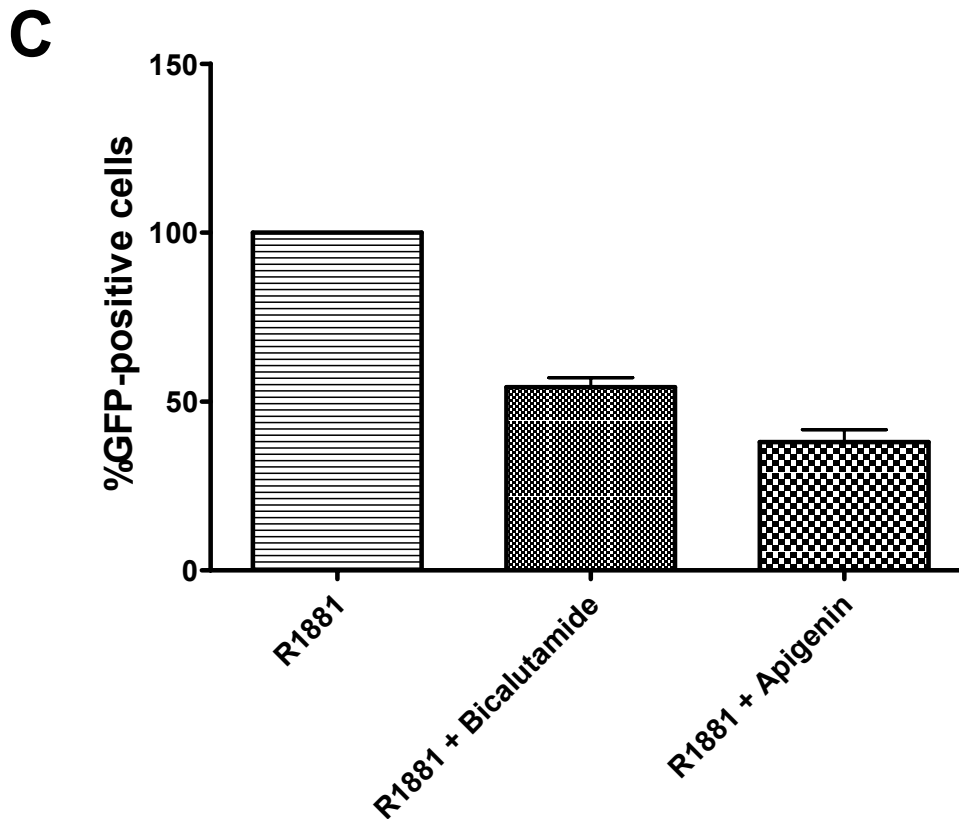
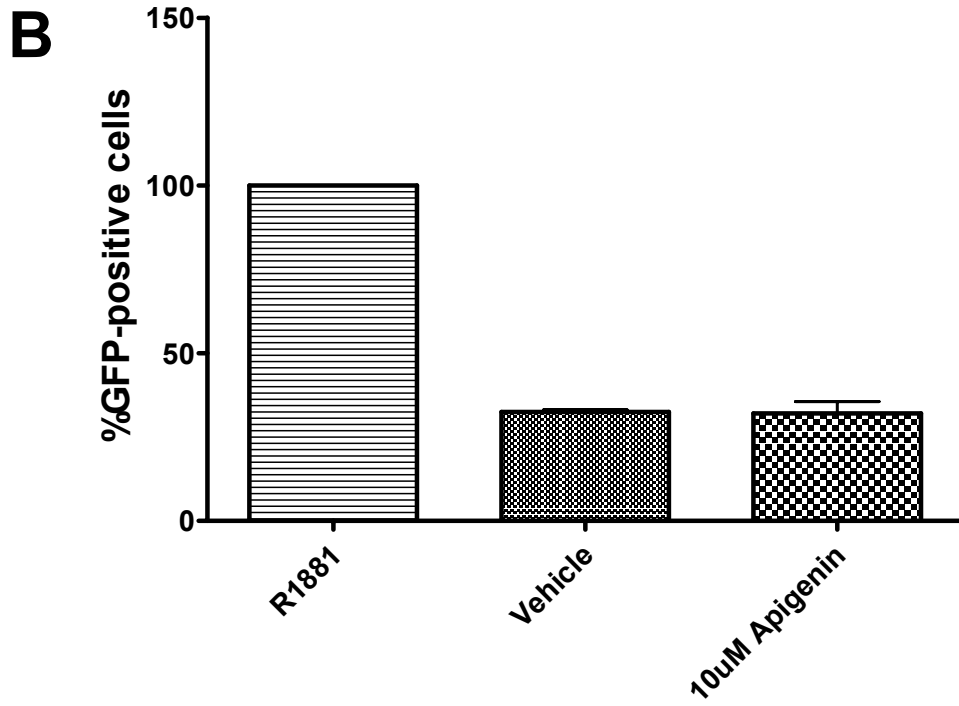
### 2.4.5.1 FIGURE 2.8



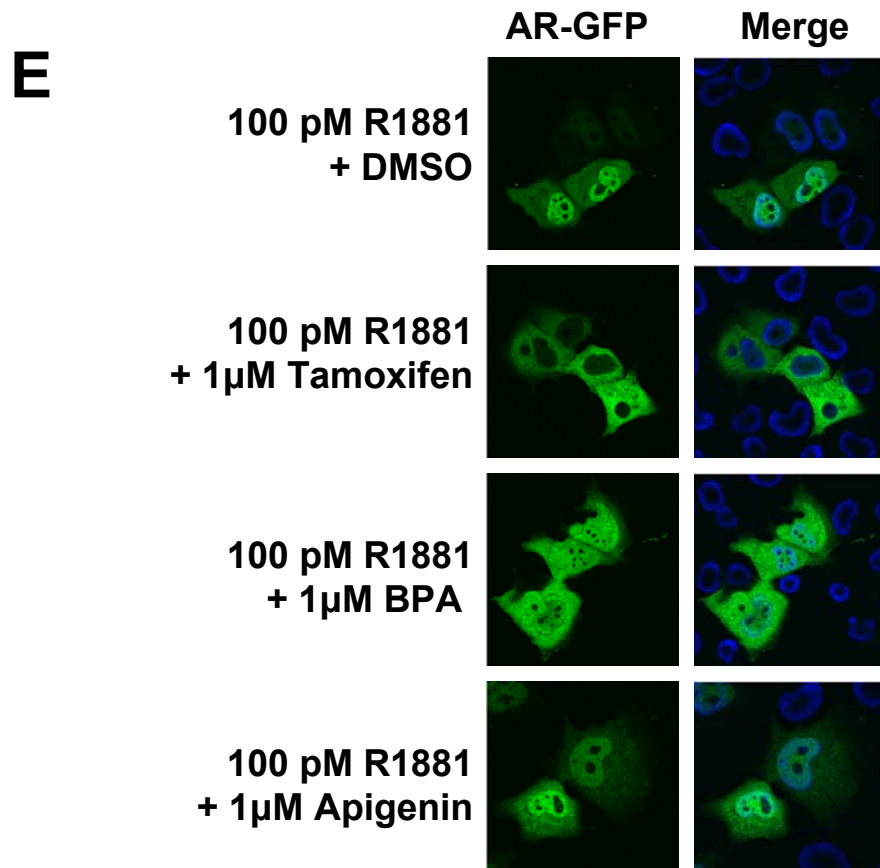
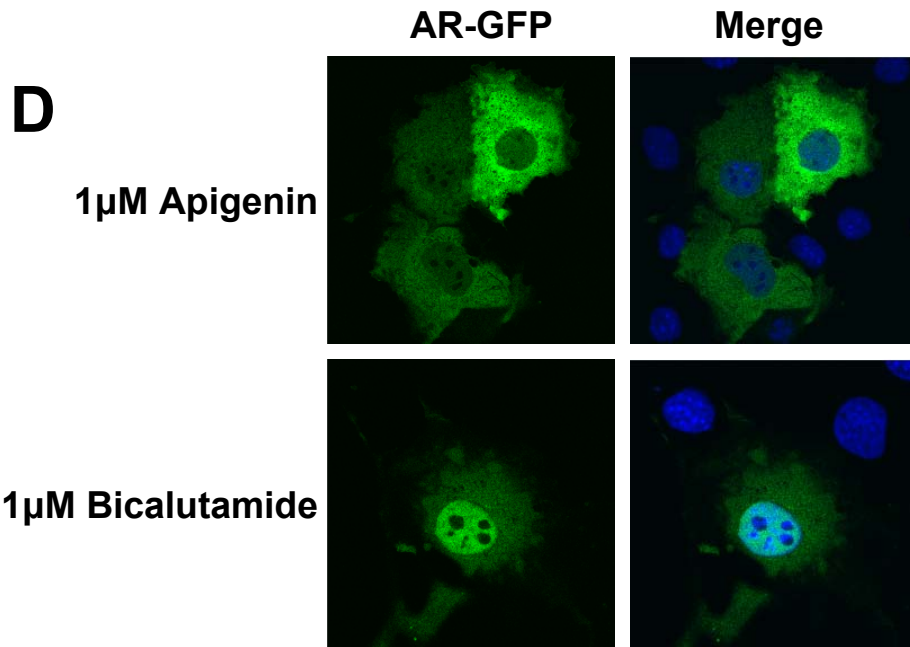
## 2.4.5.2 FIGURE 2.9



## 2.4.5.2 FIGURE 2.9



## 2.4.5.2 FIGURE 2.9



## 2.4.5.2 Table 2.2

Plate/ well #	Compound	AR-GFP Translocation
1C2	Actinomycin D	-
1C5	Apigenin	-
1C6	Apomorphine	-
1C8	Atrazine	-
1D2	Bisphenol A	-
1D3	Bisphenol B	-
1D6	Butylbenzyl phthalate	-
1B2	2-sec-butylphenol	-
1D9	Clomiphene citrate	-
1B6	4-cumylphenol	-
1E5	Daidzein	-
2B2	o,p'-DDT	-
1E6	Dexamethazone	-
1E7	Dibenzo[a,h]anthracene	-
1A3	17 $\alpha$ -estradiol	-
1A4	17 $\alpha$ -ethinyl estradiol	-
1F6	Fenarimol	-
1F8	Finasteride	-
1F9	Flavone	-
1G2	Flutamide	-
1G4	Genistein	-
1G5	Haloperidol	-
1H10	meso-hexestrol	-
1B8	4-hydroxytamoxifen	-
1G8	ICI 182,780	-
1G10	Kaempferol	-
1G11	Kepone	-
1H2	Ketoconazole	-
1H6	Linuron	-
2A10	Nilutamide	-
2A8	p-n-nonylphenol	-
1B3	4-tert-octylphenol	-
2B7	Phenolphthalin	-
2B9	Pimozide	-
2C3	Propylthiouracil	-

Plate/w ell #	Compound	AR-GFP Translocation
2C5	Reserpine	-
2C7	Sodium azide	-
2C9	Tamoxifen	-
1A2	12-o-tetradecanoylphorbol-13-acetate	-
1H7	L-thyroxine	-
1A10	2,4,5-trichlorophenoxyacetic acid	-
2D2	Vinclozolin	-
2D3	Zearalenone	-
1C3	Ammonium perchlorate	+
1B4	4-androsenedione	+
1C11	Bicalutamide	+
1D10	Corticosterone	+
1E4	Cyproterone acetate	+
2B4	p,p'-DDE	+
1E11	Di-n-butyl phthalate	+
1E9	Diethylhexyl phthalate	+
1E10	Diethylstilbestrol	+
1B11	5 $\alpha$ -dihydrotestosterone	+
1A6	17 $\beta$ -estradiol	+
1F4	Estrone	+
1F10	Fluoranthene	+
1F11	Fluoxymestrone	+
1G7	Hydroxyflutamide	+
1H8	Medroxyprogesterone acetate	+
2A4	Methyltestosterone	+
R1881	Methyltrienolone (R1881)	+
2A5	Mifepristone	+
2A11	Norethynodrel	+
2B3	Oxazepam	+
2B6	Phenobarbital	+
2B11	Procymidone	+
2C2	Progesterone	+
2C8	Spirolactone	+
1A7	17 $\beta$ -trenbolone	+
2A2	p,p'-methoxychlor	n/d
2A7	Morin	n/d

## 2.5 Overall Conclusions

The development of the MARS assay and extension of this assay into a primary screen of the ICCVAM library demonstrates the utility of the HyperCyt® system to screen a whole cell reporter assay using adherent cells. This assay was optimized to provide information about the ability of a range of compounds to modulate transcription via the AR as well as to analyze wells quickly and effectively. The initial characterization of the MARS assay illustrates that a cell-based reporter assay utilizing destabilized eGFP can effectively and efficiently be miniaturized and run via high throughput screening. These experiments also demonstrate that the MARS assay has sufficient dynamic range and sensitivity to generate time-based and concentration-based measurements, resulting in dose-response curves for an array of AR-interacting compounds. The follow-up experiments illustrate that the MARS assay can be utilized to screen a larger library of compounds with equal sensitivity and reliability. These follow-up experiments also illustrate an efficient microscopy-based secondary assay for AR nuclear translocation utilizing the expression of an AR-GFP construct and monitoring these cells for nuclear translocation of AR-GFP following stimulation with an array of ligands. These final assays also identify an AR antagonist that, unlike bicalutamide and cyproterone acetate, does not induce translocation of AR-GFP and may represent a new class of anti-androgenic molecules.



# 3 ESTROGEN RECEPTOR SCREENING

### 3.1 ABSTRACT

Estrogen signaling is mediated by at least three receptors, ER $\alpha$ , ER $\beta$  and GPR30. Each of these receptors mediates different downstream signaling events, depending on the tissue and other contextual factors. Although untangling estrogenic signaling is complex. Animal and cell culture models, knockout and siRNA technology have proven useful for determining the role of a single estrogen receptor. Nevertheless, identification of selective ligands for each receptor would greatly benefit estrogen receptor research. One such ligand, G-1, is a selective agonist of GPR30 function, with no substantial activity on ER $\alpha$  or ER $\beta$ . Additional ligands for ER $\alpha$ , ER $\beta$  and GPR30 would be of great use. To this end, we set out to screen the NIH Roadmap library of compounds for selective mediators of ER $\alpha$ , ER $\beta$  or GPR30 function. Initially, competition binding was used to find ER $\alpha$ /ER $\beta$  interacting compounds and this screening was followed with a series of functional assays to determine the activity of hit compounds. This screening led to the identification of a GPR30-selective antagonist, G15, to compliment the GPR30-selective agonist G-1.

### 3.2 INTRODUCTION

The NIH-funded Molecular Libraries Roadmap Initiative, including the University of New Mexico Center for Molecular Discovery, is charged with identifying small molecule probes for the investigation of any number of biological processes within the realm of academic science. These probes should have several characteristics, including specific binding to the target of interest and a higher affinity than any previously described small molecules directed at that target. The Roadmap Initiative aims to discover these small molecules using HTS of different targets via a range of systems, including an array of whole cell assays, using yeast, mammalian cells and bacteria, as well as systems that are more classically *in vitro* in character, such as protein-protein interactions. One of the assays chosen for screening at UNM was an estrogen receptor binding assay, utilizing whole cells expressing ER $\alpha$  or ER $\beta$ , with follow-up assays carried out in cells expressing GPR30 in order to rule out compounds with cross-reactivity between receptors.

Estrogen exerts its myriad effects on the human body via three major receptors, the classical ERs, ER $\alpha$  and ER $\beta$  (Kuiper et al. 1996), and the recently described G protein-coupled estrogen receptor GPR30 (Revankar et al. 2005). The classical ERs, ER $\alpha$  and ER $\beta$ , are relatively similar in size and structure, as well as in cellular localization. ER $\alpha$ /ER $\beta$  are members of the steroid hormone receptor superfamily of soluble receptors (approximately 67 kD soluble proteins) that are almost exclusively localized to the nucleus, regardless of the presence of ligand. ER $\alpha$  and ER $\beta$  also share significant sequence homology, particularly in

the ligand binding and DNA-binding domains (Hewitt et al. 2005). While ER $\alpha$  and ER $\beta$  share 60% sequence homology in their ligand binding domains, there is enough disparity between the receptors that the ligand binding pocket is altered, with ER $\beta$  having a more restricted binding pocket (Zeng et al. 2008). GPR30, as a GPCR, has a very different sequence and structure than the classical ERs and, as membrane proteins are difficult to crystallize in order to generate x-ray structures, the binding pocket for estrogen and related ligands in GPR30 is not specifically known.

In addition to estrogen, the classical ERs, as well as GPR30, bind to an array of related and unrelated compounds. For example, all three receptors bind tamoxifen, a selective estrogen receptor modulator (SERM), although the functionality of this binding is different for the receptors, with tamoxifen acting as an antagonist of ER $\alpha$  and ER $\beta$  but an agonist of GPR30 (Revankar et al. 2005). Other compounds with cross reactivity to all three receptors include ICI182,780, an antagonist of classical ERs but agonist of GPR30 (Filardo et al. 2000), and raloxifene, also an antagonist of classical ERs but agonist of GPR30 (Chapter 5). This trend towards classical ER antagonists acting as agonists of GPR30 is intriguing but, to this point, not thoroughly investigated. Two small molecules, PPT and DPN, have been described as selective mediators of ER $\alpha$  and ER $\beta$  function, respectively (Traupe et al. 2007); however, we have seen that PPT is also an agonist of GPR30, whereas DPN has no functional activity against GPR30 (Chapter 5). The one compound that has been identified as a selective mediator of estrogen receptor function is G-1, a GPR30-selective agonist that

has no significant ability to bind to or mediate function of ER $\alpha$  or ER $\beta$  (Bologa et al. 2006). Identification of additional selective ligands for ER $\alpha$ , ER $\beta$  and GPR30 would greatly enhance the ability of investigators to untangle the web of estrogenic signaling, both *in vitro* and *in vivo*.

As there was a lack of selective molecules for ER $\alpha$ , ER $\beta$  and GPR30, we undertook a HTS-based screen of a selected library of compounds from the NIH Roadmap Initiative library with the aim of identifying compounds with selectivity towards one or more estrogen receptor. In order to accomplish this, we modified an existing assay in order to utilize the 384-well plate screening capacity and to optimize this fluorescence-based ligand binding assay to this format.

### 3.3 RESULTS & DISCUSSION

#### 3.3.1 ER $\alpha$ and ER $\beta$ primary screen assay development

This screen aimed to take a preexisting fluorescence-based competitive binding assay and miniaturize it to be more efficient. Briefly, the assay involves transiently transfected Cos7 cells expressing either ER $\alpha$ -GFP or ER $\beta$ -GFP. The cells are harvested, resuspended and incubated with E2-Alexa633 (E2-Alexa) and compounds for screening in a saponin containing buffer to allow the E2-Alexa entry into the cells. Following a wash step, cells are analyzed on a flow cytometer with 488 and 633 nm lasers. Alexa-633 mean channel fluorescence (MCF) of GFP-expressing cells incubated with screened compounds is compared to Alexa-633 MCF in the absence or presence of excess unlabeled competitor to determine the extent of competition of compounds with E2-Alexa for binding to ERs. In order to more efficiently screen compounds for binding to ER $\alpha$  and ER $\beta$ , the existing E2-Alexa based assay needed to be miniaturized in order to run the assay in 384-well plates instead of the existing 96-well plate based assay (Revankar et al. 2005; Bologna et al. 2006). This miniaturization would reduce the amount of reagents needed, including transiently transfected Cos7 cells, and allow for better integration of liquid handling tools available for 384-well plate setup. Additionally, this miniaturization allowed for a better interface with the Roadmap compound library that is provided in 384-well plates and would require reformatting for use in a 96-well plate based assay.

Initially, untransfected cells at different concentrations were dispensed in 384-well plates and analyzed by the HyperCyt® system as they would be in the

final assay. These results indicated a positive correlation between cell concentration and the number of cells read from each well, as expected (**Fig. 3.1A**). Subsequently, a longer sip time (1800 ms versus 900 ms in the initial assay) was used in order to acquire data from more transfected cells and improve assay reliability. In order to ensure that cells would remain in suspension in wells for the duration of the assay when read at 1800 ms per well, transfected cells were placed in rows A and P of a 384-well plate, with untransfected cells in rows B-O and the entire plate was read with 1800 ms sips. These assays indicated that regardless of the cell concentrations in the wells, a similar number of GFP-positive (i.e. transfected and ER $\alpha$ /ER $\beta$ -expressing) cells were picked up in rows A and P and that cells would remain in suspension for the entire 384-well plate with longer sip times (**Fig. 3.1B**).

In addition to finding an optimal cell number for each well, the optimal concentration of E2-Alexa needed to be determined. These variables are not necessarily completely independent of one another, so an assay was performed with both varying concentrations of cells as well as a range of E2-Alexa concentrations from 1.875 nM to 60 nM (**Fig. 3.1C**). Results from this assay indicated that a concentration of E2-Alexa between 3.75 nM and 7.5 nM with 50,000 cells per well would yield an optimal inhibition of E2-Alexa.

One final consideration in formatting the assay for 384-well plates was the requirement for retaining the initial dynamic range of the assay. In order to test this parameter, varying concentrations of cells were incubated with 5 nM E2-Alexa and a range of unlabeled E2 concentrations in order to generate a series

of binding curves with different cell concentrations (**Fig. 3.1D**). These assays indicated that, while all but the most concentrated cells gave similar  $IC_{50}$  values for E2, the optimal number of cells per well was in the 50,000 cells/well range, as concentrations significantly above or below this number were less effective at inhibiting E2-Alexa binding and resulted in a smaller dynamic range in which to find competitive inhibitors of E2 binding.

Finally, to verify results observed with unlabeled E2 blocking E2-Alexa binding were consistent with previously tested compounds, the GPR30-selective agonist G-1 and the SERM raloxifene, which are known to not bind  $ER\alpha$  and to bind  $ER\alpha$ , respectively, were tested in this format. Results indicate that, as expected, G-1 does not significantly displace E2-Alexa binding from  $ER\alpha$ -transfected Cos7 cells whereas raloxifene does block E2-Alexa binding significantly (**Fig. 3.1E**).

### **3.3.2 Primary $ER\alpha$ and $ER\beta$ screening**

Compounds from the Roadmap library were initially screened for binding to  $ER\alpha$  and  $ER\beta$  using the optimized 384-well E2-Alexa based binding assay. The optimized conditions for this screen included 50,000 cells per well and 5 nM E2-Alexa with an 1800 ms sip time for sampling wells and obtaining a sufficient number of GFP-positive,  $ER\alpha$  or  $ER\beta$  expressing cells. Data was analyzed by gating on the cell population in forward/side scatter dot plots, then by gating a histogram of GFP-expression on only the high-GFP (i.e. receptor) expressing cells, these cells were then binned into single wells using IDLQuery software and each well was analyzed on the basis of mean channel fluorescence in FL-8/APC



(**Fig. 3.2A**). Plates were configured such that columns 2 and 24 contained untransfected cells and would thus appear as blank bins when plates were analyzed; this setup allowed for clear identification of individual rows and faster binning of wells than in plates configured without empty columns (**Fig. 3.2B**). Additionally, control compounds (DMSO vehicle or E2 block) were placed in columns 1 and 23, respectively, which also allowed for delineation of rows within the data file containing all 384 wells (**Fig. 3.2B**). Compounds that significantly blocked E2-Alexa binding resulted in a decrease in mean channel fluorescence that can be visualized in **Figure 3.2B**.

Upon analysis of the initial primary screening results, a very large number of compounds were identified as preliminary 'hits,' on the basis of their ability to block binding of E2-Alexa to either ER $\alpha$ , ER $\beta$  or both. This number of compounds was too large to follow up all compounds with dose-response binding curves, so a second round of primary screening was undertaken, with all compounds used at 100 nM rather than the initial 10  $\mu$ M concentration (**Full results as Fig. S3 in Appendix**). The 100 nM screen produced a much more manageable number of preliminary hits and included lead compounds with potential differential binding to ER $\alpha$  and ER $\beta$ . This 100 nM screen was also effective in this assay since there are many compounds with low-nanomolar affinities for ER $\alpha$  and ER $\beta$  already known and the identification of compounds with only micromolar affinities would likely not lead to good probes.

### 3.3.3 Secondary screening of ER $\alpha$ /ER $\beta$ hits

Following the preliminary screens of the Roadmap compounds against ER $\alpha$  and ER $\beta$ , 48 of these compounds were chosen based on their ability to block E2-Alexa binding to either ER $\alpha$ , ER $\beta$  or both classical ERs. These 48 compounds were then screened in a 7-point dose-response assay in order to determine their affinities for ER $\alpha$  and ER $\beta$  and identify any with differential binding to the two receptors or any compounds with very high affinity binding to both receptors (**Fig. 3.3** for examples or **Fig. S4** in Appendix for full data). This screening led to the identification of a number of compounds with minimal ER $\alpha$  or ER $\beta$  binding (**Fig. 3.3A**), as well as some which completely disagreed with preliminary screening results and were not confirmed as hits in this follow-up screen (**Fig. 3.3B**). Some compounds were identified with differential binding to ER $\alpha$  and ER $\beta$  (**Fig. 3.3C**).

### 3.3.4 GPR30 preliminary screening and counter screen of ER $\alpha$ , ER $\beta$ hits

Preliminary screening of 34 compounds with a structural scaffold similar to the known GPR30-selective agonist G-1 was accomplished using a calcium mobilization screen in SKBr3 cells, which endogenously express GPR30. Additionally, compounds of interest identified in ER $\alpha$ /ER $\beta$  preliminary screening and verified by ER $\alpha$ /ER $\beta$  dose-response assays were screened for activity against GPR30 in this assay. SKBr3 cells loaded with Indo-1AM and placed in a fluorimeter with appropriate excitation and emission filters and monochrometers were stimulated with E2, which causes a rapid increase in calcium mobilization, as visualized by the changes in emission of Indo-1 at 400 and 490 nm.

Compounds that function as agonists of GPR30, including the GPR30-selective agonist G-1, also elicit this increase in intracellular calcium, and compounds with antagonist activity against GPR30 would be expected to block the rapid increase in intracellular calcium caused by E2 addition. With these outcomes in mind, we screened the compounds of interest in this assay (**Appendix Fig. S5**). As expected, there were a number of compounds with no activity against GPR30 as well as several compounds with agonist activity against GPR30 (**Fig. 3.4**). Interestingly, we also identified compounds with antagonist activity against GPR30 in this screen (**Fig. 3.4**).

### **3.3.5 Identification of GPR30/ER $\alpha$ /ER $\beta$ selective compounds**

Results from the GPR30 counter screen were compared to results from ER $\alpha$  and ER $\beta$  binding assays in order to initially identify compounds with differential binding or activity against the three estrogen receptors. This comparison identified a number of compounds that appeared to activate a single receptor. As a follow-up assay to determine compound selectivity, a PI3K activation assay was used. When cells expressing either ER $\alpha$ , ER $\beta$  or GPR30 and a RFP-tagged pleckstrin homology (PH) domain from Akt (PH-RFP), which selectively binds to PIP3, are treated with E2, the PH-RFP reporter translocates from a cytoplasmic location to a nuclear and peri-nuclear location. This translocation is also observed when treating cells with other known agonists (i.e. GPR30-expressing cells treated with tamoxifen) and can be blocked using inhibitors of EGFR or PI3K. The compounds identified by comparison of primary screening and GPR30 counter-screening data were analyzed using the PI3K

activation assay to determine their agonist and antagonist characteristics in the context of expression of a single estrogen receptor expressed with a GFP tag in Cos7 cells. Additionally, Cos7 cells transfected with PH-RFP alone were treated with the compounds to ensure that effects seen in cells were not due to non-receptor mediated events. A summary of this data can be seen in **Figure 3.5**. While compounds with selective activity against ER $\alpha$  and ER $\beta$  were discovered, the most interesting compound found in these screens may be MLS555771, a selective antagonist of GPR30 function, which would complete the set of GPR30-selective compounds along with the selective agonist G-1.

### 3.4 MATERIALS & METHODS

**3.4.1 Cell culture and transfection** Cos7 cells (ATCC, Manassas, VA) were maintained in DMEM containing 10% fetal bovine serum (FBS), 100 units/mL penicillin and 100 µg/mL streptomycin. SKBr3 cells (ATCC, Manassas, VA) were maintained in RPMI-1640 containing 10% FBS, 100 units/mL penicillin and 100 µg/mL streptomycin. Cells were grown as a monolayer at 37°C, in a humidified atmosphere of 5% CO<sub>2</sub> and 95% air. Transient transfection of Cos7 cells with ER $\alpha$ -GFP, ER $\beta$ -GFP, GPR30-GFP or PH-RFP was done using Lipofectamine 2000 (Invitrogen) according to manufacturer's instructions. ER $\alpha$ -GFP and ER $\beta$ -GFP constructs have been described elsewhere (Matsuda et al. 2002). PH-mRFP1 and GPR30-GFP constructs have been described elsewhere (Revankar et al. 2005).

**3.4.2 ER $\alpha$  and ER $\beta$  ligand binding assays** Cos7 cells expressing ER $\alpha$ -GFP or ER $\beta$ -GFP were serum starved in serum-free, phenol red-free DMEM/F-12 for 24 hr before the experiment. Cells were gently removed from tissue culture plates by scraping, washed once in PBS and resuspended at concentrations as indicated (5,000,000 cells/ml for final screening assay). 10 µL cells were plated into 384-well plates, preincubated with test compounds for 10 m prior to addition of 10 µL of 10 nM E2-Alexa633 diluted in permeabilization buffer (0.025 % saponin, 5 mM EGTA, 100mM NaCl and 1 mM MgCl<sub>2</sub> in 80 mM piperazine-N-N'-bis(2-ethane sulfonic acid)-KOH (pH 6.8)) and incubated for 10 min at 37°C. The saponin was neutralized by addition of 150 µL PBS containing 2% BSA, cells were pelleted for 5 min at 1000 rpm and the supernatant removed before cells were resuspended

in 20  $\mu$ L PBS containing 2% BSA. Samples were analyzed using the HyperCyt® high throughput flow cytometry system using 1800 ms sip time per well. Files were analyzed on the basis of mean channel fluorescence in channel 8 (Log APC) using IDLquery software written by Dr. Bruce Edwards.

**3.4.3 Intracellular calcium mobilization** SKBr3 cells ( $1 \times 10^7$ /mL) were incubated in HBSS containing 3  $\mu$ M Indo1-AM (Invitrogen) and 0.05% pluronic acid F-127 for 1 hr at RT. Cells were then washed twice with HBSS, incubated at RT for 20 min, washed again with HBSS, resuspended in HBSS at a density of  $10^8$  cells/mL and kept on ice until assay, performed at a density of  $2 \times 10^6$  cells/mL.  $Ca^{++}$  mobilization was determined ratiometrically using  $\lambda_{ex}$  340 nm and  $\lambda_{em}$  400/490 nm at 37°C in a spectrofluorometer (QM-2000-2, Photon Technology International) equipped with a magnetic stirrer. The relative 490 nm / 400 nm ratio was plotted as a function of time.

**3.4.4 PI3K activation** The PIP3 binding domain of Akt fused to mRFP1 (PH-RFP) was used to localize cellular PIP3. Cos7 cells (cotransfected with GPR30-GFP, ER $\alpha$ -GFP or ER $\beta$ -GFP and PH-RFP) were plated on coverslips and serum starved for 24 hr followed by stimulation with ligands as indicated. The cells were fixed with 2% PFA in PBS, washed, mounted in Vectashield containing DAPI (Vector Labs) and analyzed by confocal microscopy using a Zeiss LSM510 confocal fluorescent microscope.

### 3.5 FIGURE LEGENDS

#### 3.5.1 Figure 3.1. Optimization of ER $\alpha$ /ER $\beta$ ligand binding assay

**A)** Untransfected Cos7 cells of varying concentrations were placed 20  $\mu$ L volume of PBS containing 2% BSA in a 384 well plate and sampled using HyperCyt $\text{\textcircled{R}}$  to determine how many cells were picked up using a 900 ms sip time. **B)** Cos7 cells transfected with ER $\alpha$ -GFP were placed in rows A and P of a 384 well plate at the indicated concentrations with the same concentrations of untransfected cells in rows B-O and the entire plate sampled for 1800 ms to determine the number of GFP-positive events acquired per well and verify that cells would remain in suspension for the acquisition time required for an entire plate. **C)** The role of cell concentration and E2-Alexa concentration was investigated to determine appropriate cell concentrations and corresponding appropriate E2-Alexa concentrations. Varying cell concentrations were placed in wells containing the indicated concentrations of E2-Alexa with or without unlabeled E2 block and the ability of unlabeled E2 to block E2-Alexa binding at different cell concentrations was determined. **D)** The dynamic range of 5 nM E2-Alexa blocking unlabeled E2 was determined in wells with different concentrations of cells. **E)** Relevant compounds raloxifene and G-1 in addition to E2 were tested to verify that the binding assay worked as expected in the 384-well format with non-estrogen blocking of E2-Alexa.

**3.5.2 Figure 3.2. Preliminary ER $\alpha$ /ER $\beta$  binding screen** **A)** Top panel: Gating of data to identify GFP-expressing cells. Lower panel: Gated cells from top panel. Data from screening of a 384-well plate containing ER $\alpha$ -GFP expressing Cos7

cells and one plate of Roadmap library compounds. **B)** Blowup of red region from **Fig. 3.2A**. Red regions represent individual wells or 'timebins.' **1** represents an unblocked control well containing transfected cells, E2-Alexa and DMSO vehicle. **2 and 6** represent wells containing untransfected cells which appear as empty wells in this analysis since cells not expressing ER $\alpha$ -GFP were not included in the analysis gate. **3** represents a compound which does not interfere with ER $\alpha$  binding to E2-Alexa. **4** represents a compound which blocks E2-Alexa binding to ER $\alpha$ , as indicated by the decrease in mean channel fluorescence. **5** represents a positive control well containing transfected cells, E2-Alexa and unlabeled E2 block.

**3.5.3 Figure 3.3. Examples of results from ER $\alpha$ /ER $\beta$  dose-response screening** **A)** Dose-response data from a compound identified in 10  $\mu$ M screening of ER $\alpha$  and ER $\beta$  but with no significant binding to either receptor below the primary screening concentration. **B)** Dose-response data from a compound preliminarily classified as a hit but with no apparent binding activity to ER $\alpha$  or ER $\beta$  in dose response screening. **C)** Dose-response data from a compound with some ER $\alpha$  binding selectivity.

**3.5.4 Figure 3.4. Example data from GPR30 calcium mobilization primary and counter screens** Traces from three Roadmap compounds as well as the E2 control showing the three potential outcomes from GPR30 calcium mobilization screens. **(a)** represents addition of Roadmap compound or vehicle control, **(b)** represents addition of E2. **Red trace:** DMSO vehicle added at **(a)**, E2 added at **(b)**. **Green trace:** identification of compound with no apparent ability to modulate

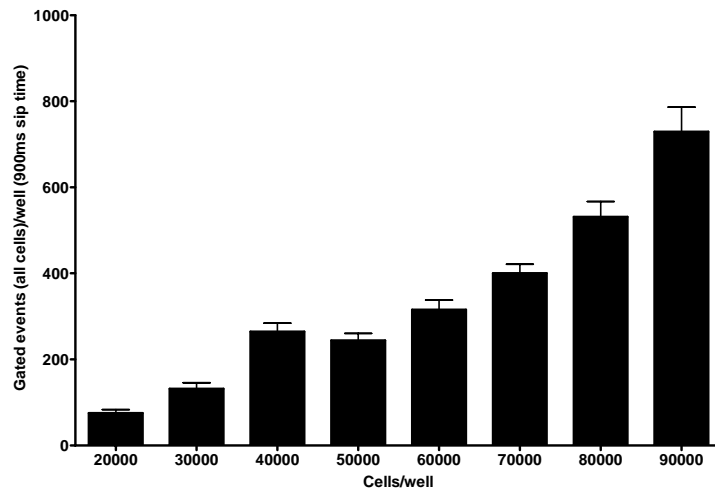


GPR30 calcium modulation. **Blue trace:** identification of compound with agonist activity towards GPR30. **Yellow trace:** identification of compound with antagonist activity towards GPR30, evidenced by the prevention of E2 mediated calcium mobilization at **(b)**.

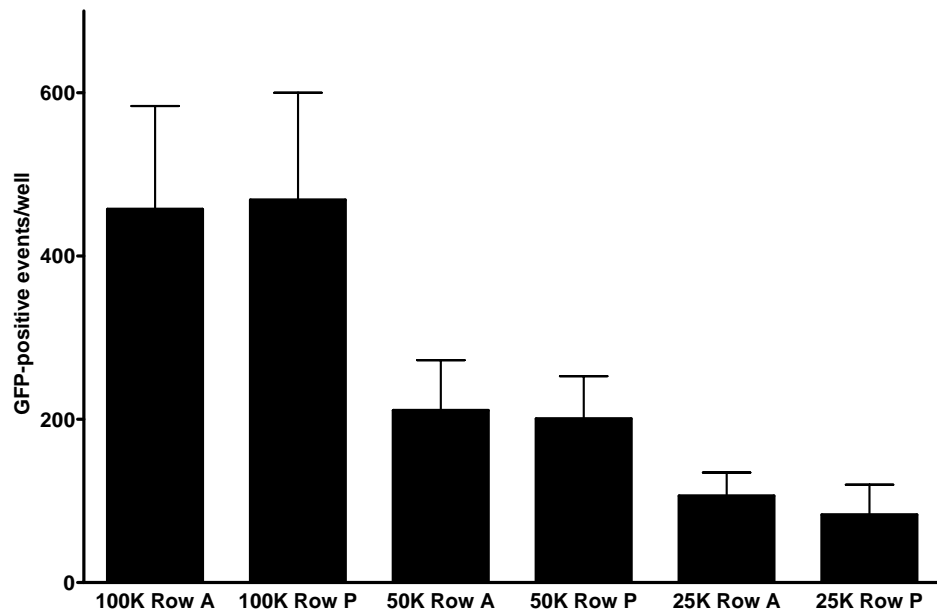
**3.5.5 Figure 3.5. Venn diagram of selective compounds identified in roadmap screening of ER $\alpha$ , ER $\beta$  and GPR30** Red compounds are antagonists, green compounds are agonists and red/green mixed compounds show mixed agonist/antagonist activity depending on the receptor expressed. Numbers represent plate and well numbers.

### 3.6.1 Figure 3.1

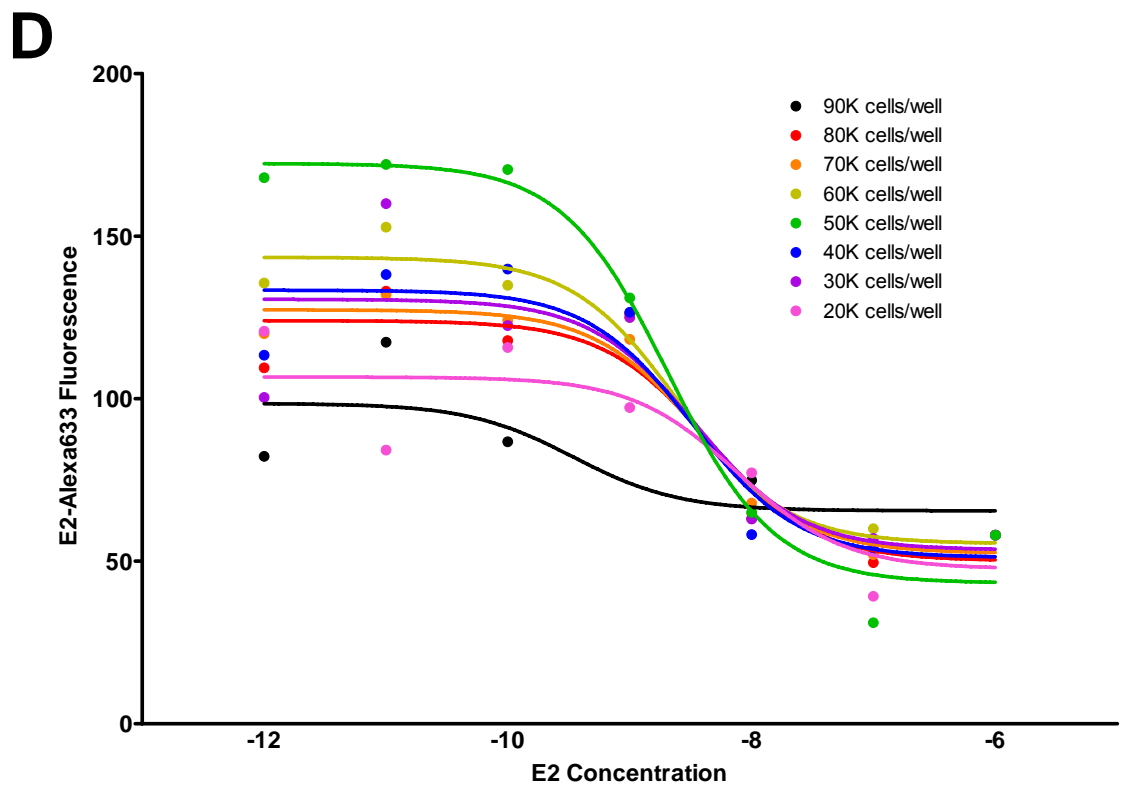
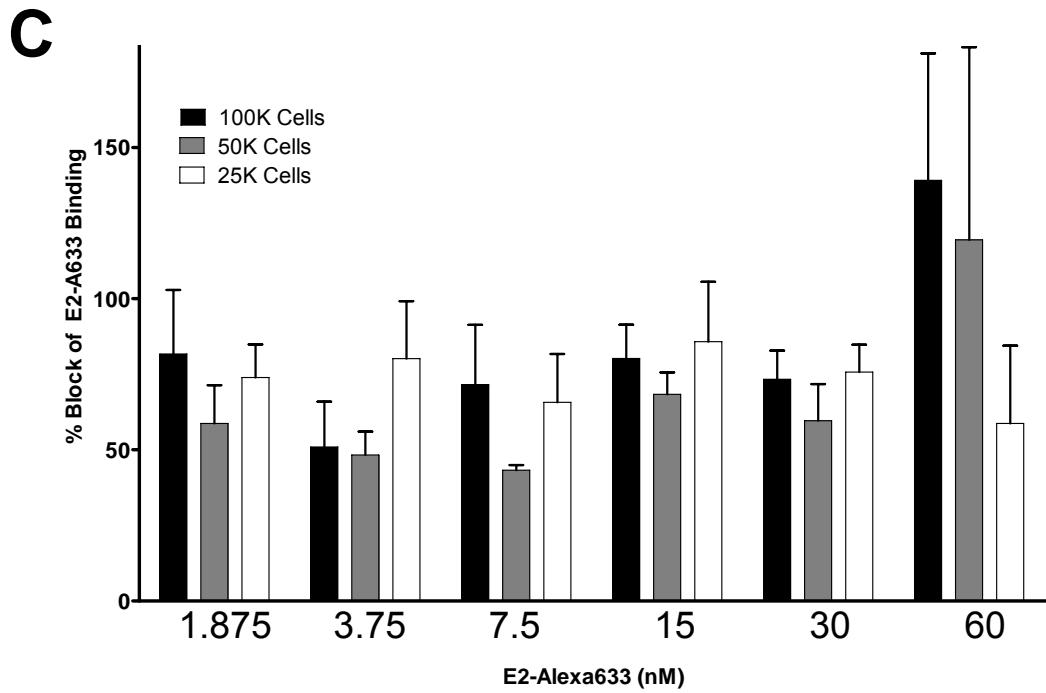
**A**



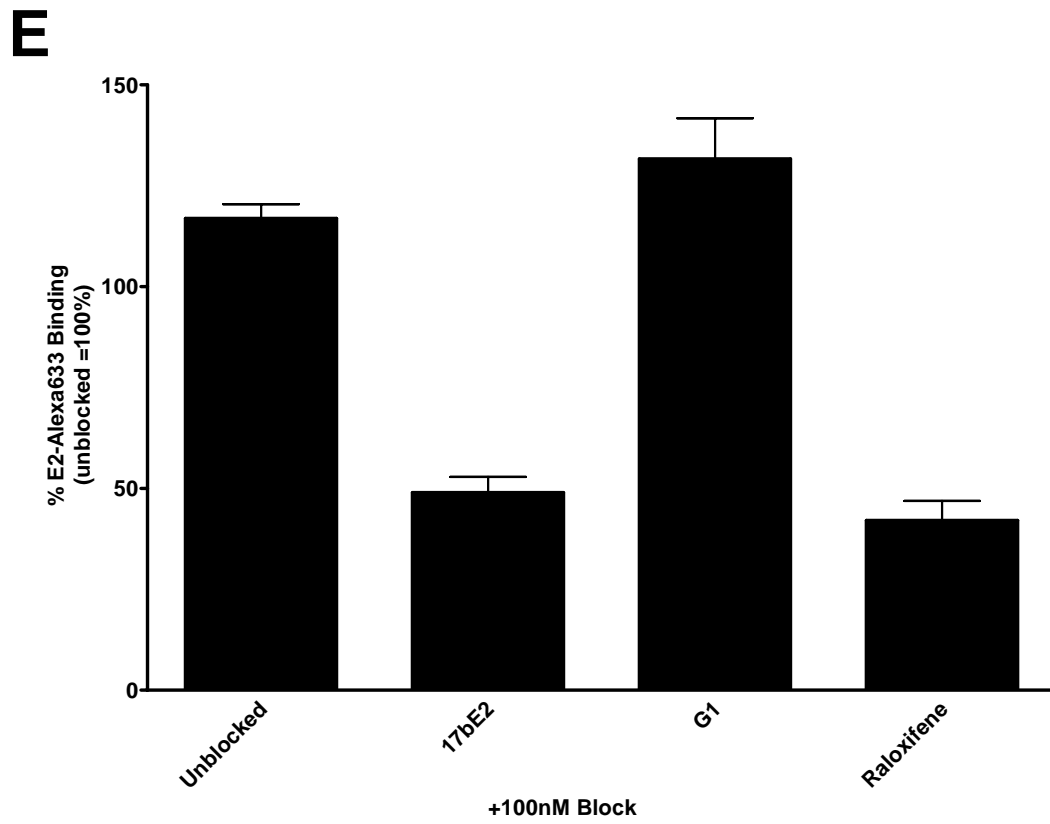
**B**



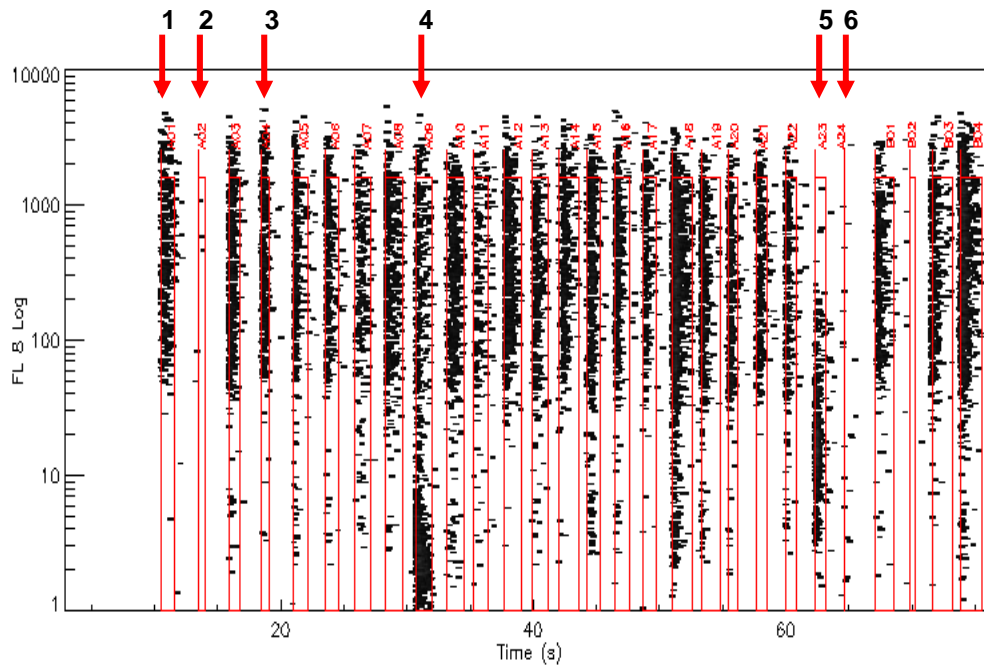
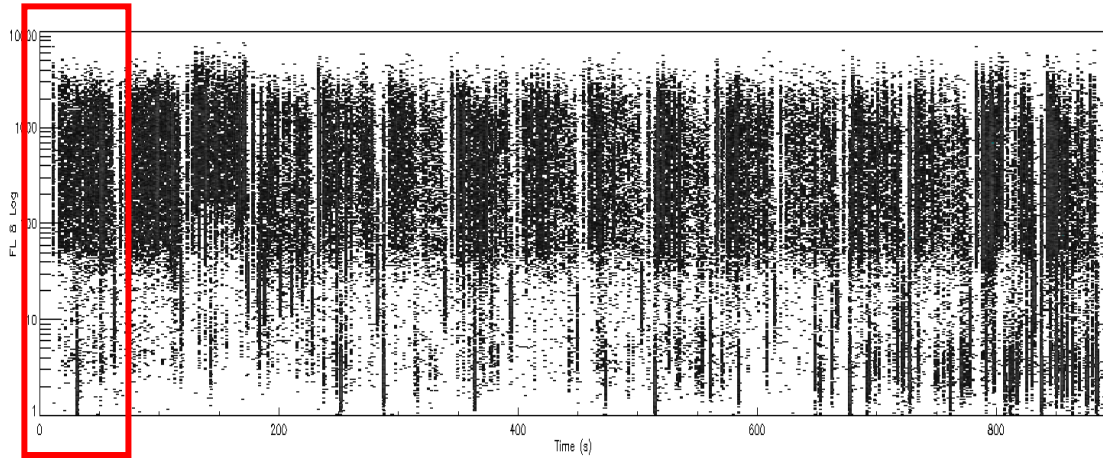
### 3.6.1 Figure 3.1



### 3.6.1 Figure 3.1

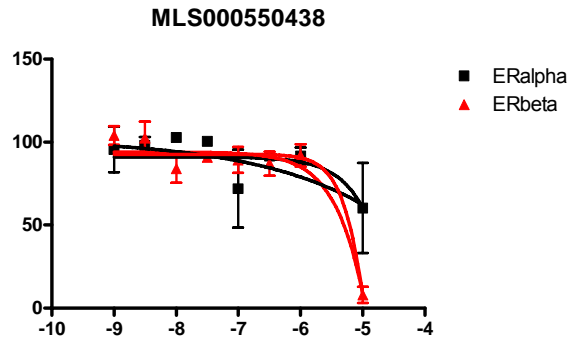


### 3.6.2 Figure 3.2

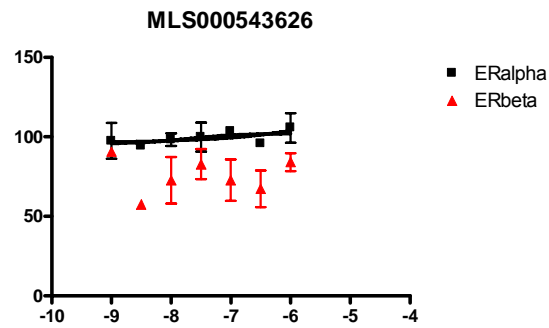


### 3.6.3 Figure 3.3

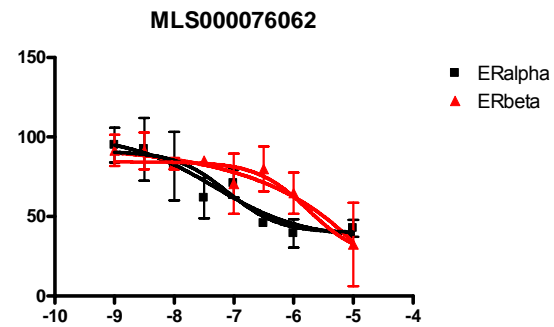
**A**



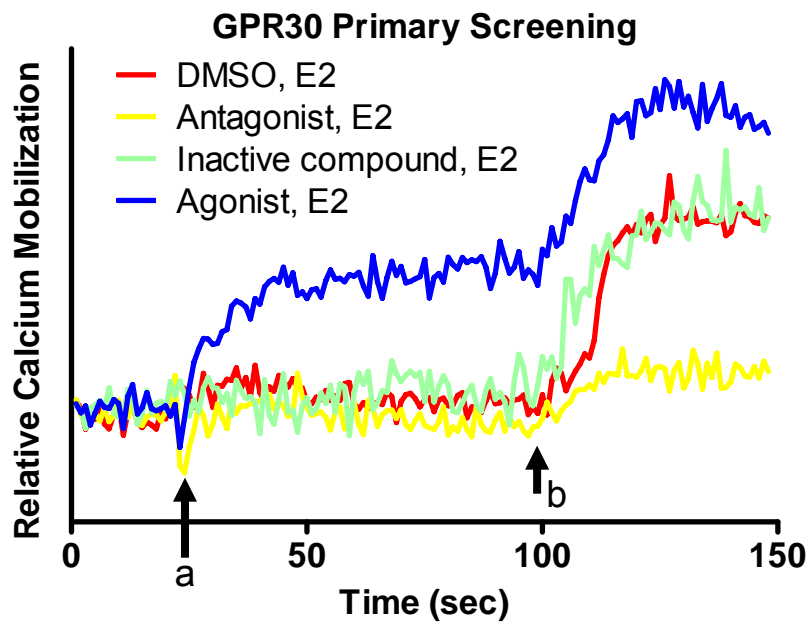
**B**



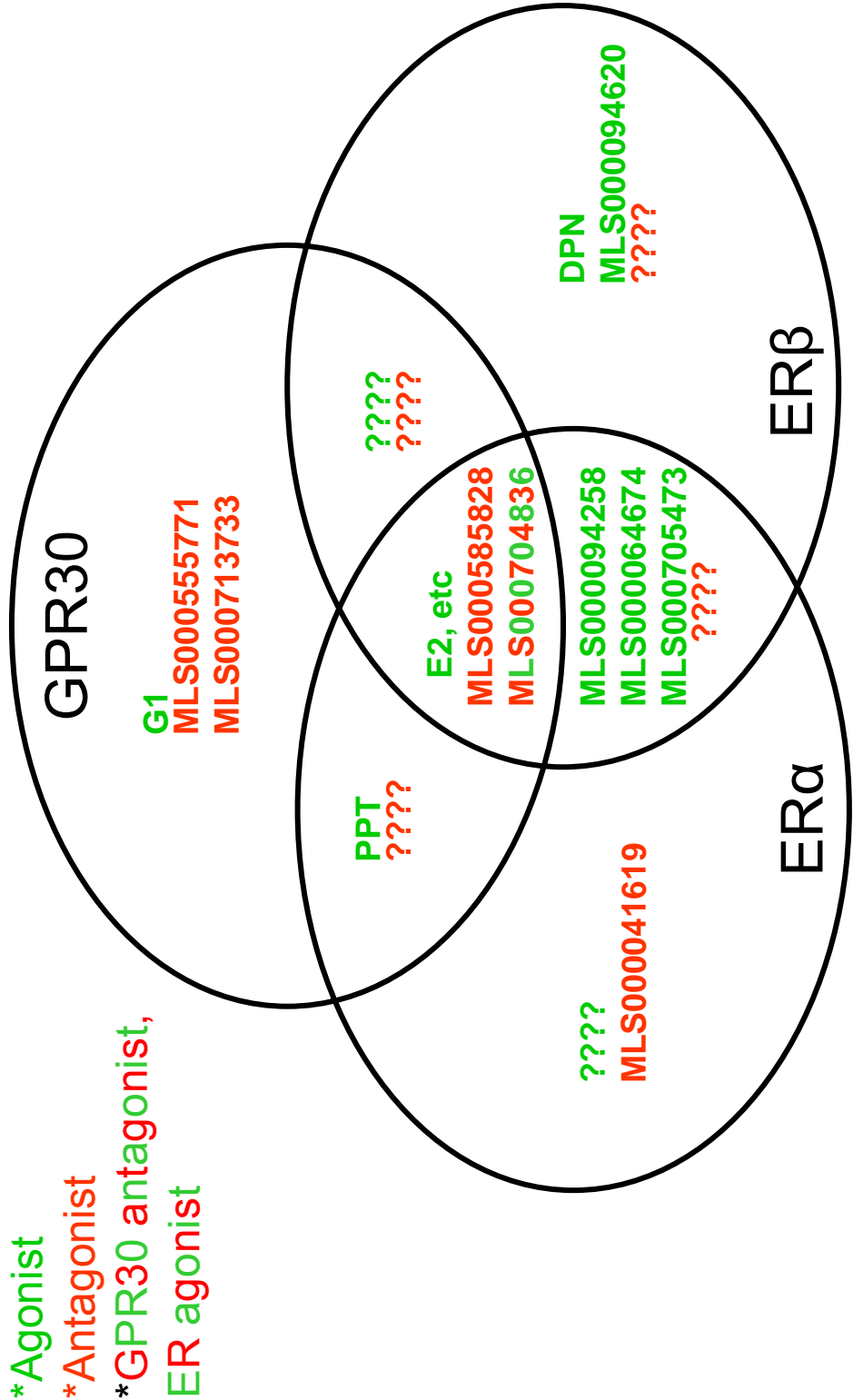
**C**



### 3.6.4 Figure 3.4



3.6.5 Figure 3.5





# 4 CHARACTERIZATION OF GPR30 ANTAGONISTS

#### 4.1 Introduction

The ability to study GPR30 function was greatly enhanced by the discovery and characterization of G-1, the first GPR30-selective agonist. The elucidation of this compound's biologic activity and its ability to stimulate GPR30 both in cell-based systems as well as *in vivo* assays has allowed a variety of laboratories around the world to begin probing GPR30 function independent of classical ER function. The companion compound to G-1, a selective antagonist of GPR30, was discovered during the Roadmap Initiative screening of compounds against the classical ERs and GPR30 and this compound was named G15. Initial screening and secondary follow-up screening from the roadmap initiative demonstrated that G15 had no significant effect on classical estrogen receptor function at concentrations up to 10  $\mu\text{M}$ , whereas it effectively blocked G-1 or E2-mediated GPR30 function at doses below the threshold for classical ER activity.

Additional characterization of G15 was required to delineate its biological activity and to verify that it functioned as a GPR30 antagonist *in vivo*. The efforts to define the activity of G15 are described in the following section, as published in *Nature Chemical Biology*.

## 4.2 *In vivo* Effects of a GPR30 Antagonist

Megan K. Dennis<sup>1</sup>, Ritwik Burai<sup>2</sup>, Chinnasamy Ramesh<sup>2</sup>, Whitney K. Petrie<sup>1</sup>, Sara N. Alcon<sup>1</sup>, Tapan K. Nayak<sup>1</sup>, Cristian G. Bologa<sup>3</sup>, Andrei Leitao<sup>3</sup>, Eugen Brailoiu<sup>6</sup>, Elena Deliu<sup>6</sup>, Nae J. Dun<sup>6</sup>, Larry A. Sklar<sup>4,5</sup>, Helen J. Hathaway<sup>1,4</sup>, Jeffrey B. Arterburn<sup>2,4\*</sup>, Tudor I. Oprea<sup>3,4\*</sup> and Eric R. Prossnitz<sup>1,4\*</sup>

<sup>1</sup> Department of Cell Biology & Physiology, <sup>3</sup> Division of Biocomputing, Department of Biochemistry & Molecular Biology, <sup>4</sup> UNM Cancer Center, and <sup>5</sup> Department of Pathology, University of New Mexico Health Sciences Center, Albuquerque, NM 87131; <sup>2</sup> Department of Chemistry and Biochemistry, New Mexico State University, Las Cruces, NM 88003 and <sup>6</sup> Department of Pharmacology, Temple University School of Medicine, Philadelphia, PA 19140

One sentence summary: Using a potent selective GPR30 antagonist, we investigate the physiological effects of GPR30 activity on uterine and neurological responses.

\* Correspondence should be addressed to E.R.P. ([eprossnitz@salud.unm.edu](mailto:eprossnitz@salud.unm.edu)), T.I.O. ([toprea@salud.unm.edu](mailto:toprea@salud.unm.edu)) or J.B.A. ([jarterbu@nmsu.edu](mailto:jarterbu@nmsu.edu)).

#### 4.2.1 ABSTRACT

Estrogen is central to many physiological processes throughout the human body. We have previously shown that the G protein-coupled receptor GPR30/GPER, in addition to classical nuclear estrogen receptors (ER $\alpha$ / $\beta$ ), activates cellular signaling pathways in response to estrogen. In order to distinguish between the actions of classical estrogen receptors and GPR30, we have previously characterized a selective agonist of GPR30, G-1 (1). To complement the pharmacological properties of G-1, we sought to identify an antagonist of GPR30 that displays similar selectivity against the classical estrogen receptors. Here we describe the identification and characterization of a G-1 analog, G15 (2) that binds to GPR30 with high affinity and acts as an antagonist of estrogen signaling through GPR30. *In vivo* administration of G15 reveals that GPR30 contributes to both uterine and neurological responses initiated by estrogen. The identification of this antagonist will accelerate the evaluation of the roles of GPR30 in human physiology.

#### 4.2.2 INTRODUCTION

Estrogens play an important role in many areas of human physiology (including reproduction and the immune, vascular and nervous systems) as well as disease states such as cancer, depression and reproductive disorders (Edwards 2005; Lange et al. 2007). Estrogen has long been known to act through soluble nuclear receptors that function as ligand-activated transcription factors. However, in addition to gene regulation, estrogen also mediates rapid signaling events, more commonly associated with growth factor and G protein-coupled receptors (Fu and Simoncini 2008). Recent studies reveal that GPR30 (International Union of Basic and Clinical Pharmacology designation: GPER), an intracellular transmembrane G protein-coupled estrogen receptor, mediates numerous aspects of cellular signaling ranging from calcium mobilization to EGFR transactivation to gene regulation (Prossnitz et al. 2008). The classical nuclear estrogen receptors (ER $\alpha$ / $\beta$ ) appear to overlap with GPR30 not only in many of their cellular and physiological responses (Prossnitz et al. 2008) but also in their ligand specificity (Prossnitz et al. 2008), making pharmacologic resolution of individual receptor functions challenging. For example, 17 $\beta$ -estradiol (**3**), 4-hydroxytamoxifen (**4**) and ICI182,780 (**5**) each bind to GPR30 in addition to classical estrogen receptors, though with different outcomes with respect to agonism and antagonism (Filardo et al. 2000; Revankar et al. 2005; Thomas et al. 2005). Whereas 17 $\beta$ -estradiol, 4-hydroxytamoxifen and ICI182,780 all activate GPR30, 17 $\beta$ -estradiol is an ER $\alpha$ /ER $\beta$  agonist, 4-hydroxytamoxifen is a selective estrogen receptor modulator (SERM) and ICI182,780 is a pure ER $\alpha$ /ER $\beta$

antagonist (Ariazi et al. 2006). Interestingly, until recently, GPR30-specific ligands were unknown.

In 2006, we described a highly selective GPR30 agonist named G-1 that shows no detectable activity towards the classical estrogen receptors (Bologa et al. 2006). This compound activates multiple cellular signaling pathways via GPR30 and has been used to examine the cellular and physiological actions of GPR30. Cellular effects include activation of calcium mobilization in cancer cells (Bologa et al. 2006), luteinizing hormone-releasing hormone (LHRH) neurons (Noel et al. 2009) and hypothalamic neurons (Brailoiu et al. 2007), spinal neuron depolarization (Dun et al. 2009), protein kinase C activation (Kuhn et al. 2008) and phosphatidylinositol-3-kinase (PI3K) activation (Bologa et al. 2006), gene expression (Albanito et al. 2007; Prakash Pandey et al. 2009), proliferation (Albanito et al. 2007; Teng et al. 2008), oocyte meiotic arrest (Pang et al. 2008) and primordial follicle formation (Wang et al. 2008). G-1 has also been used to probe the role of GPR30 in vivo with reported effects including estrogen-induced thymic atrophy (Wang et al. 2008), experimental autoimmune encephalomyelitis (Wang et al. 2009) and vascular regulation (Haas et al. 2009). In each of these animal models, the G-1-mediated effects were absent in GPR30 knockout mice, establishing the selectivity of this compound for GPR30. Thus, the availability of a selective GPR30 agonist has, in a very brief time, greatly advanced our understanding of the biological functions of GPR30.

Unfortunately, to date, antagonists of GPR30 have not been identified. To better understand the actions of GPR30, we identified a selective GPR30

antagonist using a combination of virtual and biomolecular screening. The compound is related in structure to the agonist G-1 and binds to GPR30 but not ER $\alpha$  or ER $\beta$ . Cellular assays demonstrate that this antagonist prevents both estrogen- and G-1-mediated mobilization of intracellular calcium in ER-negative breast cancer cells. Furthermore, estrogen-mediated GPR30-dependent PI3K activation is blocked, whereas no effect on either ER $\alpha$  or ER $\beta$ -mediated PI3K activation in response to estrogen is observed. *In vivo* studies utilizing both the agonist and antagonist reveal that GPR30 contributes to estrogen-mediated proliferation of the uterine epithelium and plays an important role in the anti-depressive effects of estrogen. The introduction of this first GPR30-selective antagonist should provide additional avenues for characterizing the physiological functions of GPR30.

## 4.2.3 RESULTS

### 4.2.3.1 Virtual & biomolecular screening and chemical synthesis

We recently employed a combination of virtual and biomolecular screening to identify the first GPR30-specific ligand, a substituted dihydroquinoline, named G-1 (Bologa et al. 2006) (**Fig. 4.1A**). To identify potentially novel GPR30-specific ligands, we again employed virtual screening to identify G-1-like structures of interest from the NIH Molecular Libraries Small Molecule Repository (MLSMR). We performed a SMARTS substructure search (Daylight Theory Manual, Daylight Chemical Information Systems Inc., <http://www.daylight.com/dayhtml/doc/theory/theory.smarts.html>) of the MLSMR (consisting of 144,457 molecules at the time of the search, March 2007) for compounds containing the core scaffold of G-1 (**Fig. 4.1B**) using a custom JAVA program built using the OpenEye OEJava toolkit (OEChem - Java Theory Manual, OpenEye Scientific Software Inc., <http://www.eyesopen.com/docs/html/javaproq/>). The search identified 64 molecules, of which 57 were obtained from the MLSMR.

To accomplish the primary biomolecular screen for GPR30 antagonism, we utilized calcium mobilization in GPR30-expressing SKBr3 cells and tested for the ability of the compound to block cellular activation by estrogen. Primary screening of the 57 G-scaffold containing compounds from the MLSMR yielded 8 that showed some inhibition of estrogen-mediated calcium mobilization in cells expressing GPR30. Of particular interest was one compound (designated G15) that closely resembled G-1 but lacked the ethanone moiety of the molecule (**Fig.**



**4.1C).** Based on the structural overlap of G-1 with estrogen and in particular the similar, though not identical spacing of oxygen atoms at the extremes of the molecules, we speculated that the ketone functionality of G-1 might play an important role as a hydrogen bond acceptor by inducing conformational changes that activate GPR30. For this reason, in parallel to the virtual screening efforts, G15 was also chemically synthesized as a possible antagonist candidate.

The tetrahydro-3H-cyclopenta[c]quinoline scaffold of G-1 is synthetically accessible via the versatile three-component Povarov cyclization. We evaluated a series of reaction conditions employing protic and Lewis acid catalysts to optimize reaction rate, yield, and diastereoselectivity for the construction of G-1-like derivatives. Our optimized one-step procedure employing the catalyst  $\text{Sc}(\text{OTf})_3$  in acetonitrile (Kobayashi et al. 1995) resulted in rapid reaction times, high product yield and enhanced selectivity favoring the syn diastereomeric products. The synthesis of G15 from aniline, 6-bromopiperonal and cyclopentadiene is illustrated in **Fig. 4.1D**. Precipitation from dichloromethane/methanol gave analytically pure G15 in yields exceeding 85% as a racemic mixture of syn diastereomers. The syn diastereomer is distinguished by the  $^1\text{H-NMR}$  coupling pattern of H-4 (4.65 ppm) with a coupling constant of 3.25 Hz that is characteristic for the syn orientation of the cyclopentene ring and phenyl group. The product was fully characterized by NMR spectroscopy, and HPLC-MS with positive ion detection (showing the correct molecular ion ( $\text{MH}^+$ )) as well as UV detection ( $\text{PDA}/\lambda_{\text{max}} = 294 \text{ nm}$ ), yielding a single peak.

#### 4.2.3.2 G15 inhibits cellular signaling through GPR30

Chemically synthesized G15 was subjected to multiple cellular and physiological assays in order to characterize its biological effects. Competitive binding assays using endogenous GPR30 and a novel iodinated GPR30-selective G-1 analog (manuscript in preparation), demonstrated that G15 binds to GPR30 with an affinity of approximately 20 nM (**Fig. 4.2A**). This compares to an affinity for G-1, utilizing the same assay, of approximately 7 nM, similar to our previously reported affinity of G-1 for recombinant GPR30 of 11 nM (Bologa et al. 2006) and reported affinities for 17 $\beta$ -estradiol between 3-6 nM (Revankar et al. 2005; Thomas et al. 2005). Thus removal of the ethanone moiety resulted in a decrease in relative binding affinity of approximately 3 fold. Additional competitive binding studies to assess interactions with ER $\alpha$  and ER $\beta$  revealed that similar to G-1, G15 displays little binding to ER $\alpha$  and ER $\beta$  at concentrations up to 10  $\mu$ M, where estrogen competes with a  $K_i$  of approximately 0.3-0.5 nM (**Figs. 4.2B and C**). These results reveal that G15, like G-1, displays high affinity for GPR30 with minimal binding to ER $\alpha$  and ER $\beta$  ( $K_i > 10 \mu$ M).

Evaluation of the functional capabilities of G15 with respect to the rapid mobilization of intracellular calcium demonstrated that G15 alone was incapable of inducing a response in SKBr3 breast cancer cells, which are ER $\alpha$  and ER $\beta$  negative but express GPR30, whereas stimulation by either estrogen or G-1 induced a response (**Fig. 4.3A**). In contrast, stimulation of the cells with G-1 or estrogen subsequent to G15 exposure substantially reduced the response to G-1 or estrogen (**Fig. 4.3B**). There was however no inhibition of the calcium response

mediated by ATP through endogenous purinergic receptors, indicating the antagonistic effect is specific to GPR30. Inhibition of G-1-mediated calcium mobilization in SKBr3 cells by G15 was dose-dependent, yielding an  $IC_{50}$  of approximately 185 nM (**Fig. 4.3B**), whereas inhibition of E2-mediated calcium mobilization yielded a similar  $IC_{50}$  of approximately 190 nM (**Fig. 4.3C**).

In addition to intracellular calcium mobilization, we have demonstrated that estrogen stimulation of  $ER\alpha$  or  $ER\beta$  or GPR30 results in the nuclear accumulation of PIP3 as a result of PI3K activation (Revankar et al. 2005), revealed by the translocation of an Akt PH domain-fluorescent protein fusion protein reporter (Balla and Varnai 2002). To determine whether G15 similarly inhibits GPR30-mediated PI3K activation, we examined the activation of PI3K in receptor-transfected Cos7 cells, where estrogen stimulates the nuclear accumulation of PIP3 through all three receptors and G-1 selectively activates GPR30 but not  $ER\alpha$  or  $ER\beta$ . Not only was G15 capable of inhibiting the G-1-mediated activation of PI3K in GPR30-transfected cells, it also effectively blocked the estrogen-mediated response in GPR30-transfected cells (**Fig. 4.4A**) but had no effect on the estrogen-mediated response in  $ER\alpha$  or  $ER\beta$ -transfected cells, even at concentrations 100-fold greater than that required to inhibit GPR30 (**Fig. 4.4B**). To determine whether G15 inhibits PI3K activation in cells endogenously expressing GPR30, we examined PI3K activation in SKBr3 breast cancer cells. As in GPR30-transfected cells, G15 was able to inhibit both estrogen and G-1 stimulation of PI3K (**Fig. 4.4C**). In total, these results demonstrate that G15 can selectively inhibit GPR30.

#### 4.2.3.3 G15 inhibits GPR30-mediated function in vivo

One goal of developing GPR30-specific agonists and antagonists is the elucidation of the roles of GPR30 in normal and disease physiology. One of the best characterized assays for estrogenic activity is the uterine response in the mouse, where uterine water content (i.e. imbibition) and epithelial cell proliferation are highly responsive to estrogen treatment, particularly following ovariectomy (Owens and Ashby 2002). In the ovariectomized mouse model, a single injection of estrogen (E2) led to a 17-fold increase in the proliferative index of uterine epithelia relative to control, as measured by immunodetection of Ki-67 protein (**Fig. 4.5A**). Here we show that the GPR30 agonist G-1 also increases proliferation, by 3-4 fold over sham (**Fig. 4.5B**), and that there is little difference in proliferation rates across a 25-fold dose range, suggesting a maximal response was achieved. In contrast, treatment with the GPR30 antagonist G15 alone did not alter proliferation relative to sham injections (**Fig. 4.5B**). When mice were treated with G15 plus E2 (**Fig. 4.5A**), proliferation was reduced by approximately 50% in a dose-dependent manner, being maximal at a 10-fold molar excess of G15. G15 treatment also blocked G-1-induced proliferation in a dose-dependent manner (**Fig. 4.5B**), being maximal at a 15-fold molar excess of G15. These results suggest that GPR30 contributes to a specific estrogenic response, proliferation. Neither G-1 nor G15 had any effect on uterine wet weight or imbibition, evaluated by measuring uterine weight and by microscopic evaluation of histologic sections (not shown). In conclusion, GPR30 appears to

contribute to the proliferative response in the uterus, while another response, inhibition, appears to be solely mediated by ER $\alpha$  (Hewitt et al. 2005).

Clinical observations suggest that vulnerability to depression in the female population is associated with hormonal fluctuations, in which estrogens may play an important role. For example, chronic treatment of women with E2 or conjugated equine estrogens attenuated depressive symptoms during perimenopausal and postpartum periods (Epperson et al. 1999; Genazzani et al. 1999). Several animal models have been developed to evaluate putative antidepressants (Porsolt et al. 1978; Willner 1990) and have demonstrated the antidepressive effects of estrogenic compounds (Estrada-Camarena et al. 2003). Among these, the tail suspension test (Steru et al. 1985; Steru et al. 1987) is a convenient model in which many antidepressants reduce the duration of immobility, suggesting this parameter is an index of antidepressant activity (Cryan et al. 2005). Since GPR30 expression has been demonstrated in the male (as well as female) brain (Brailoiu et al. 2007), male mice were used to evaluate the potential neurological effects of G-1 and G15, given that behavioral and neurochemical depression studies are carried out almost exclusively in male mice (Cryan et al. 2005). The antidepressant action of G-1 was compared to that of E2 and the tricyclic antidepressant desipramine, which markedly reduced immobility time, when compared to control vehicle-injected animals (**Fig. 4.5C**). G-1 dose-dependently decreased immobility time, whereas pretreatment of the mice with G15, which alone had no significant effect on immobility time, significantly attenuated the effects of both G-1 and E2. Pretreatment of the mice

with G15 did not influence the immobility time of subsequent desipramine treatment. Together, these results suggest a neurological role for GPR30 in the regulation of depression.

#### 4.2.4 DISCUSSION

In this paper, we described the synthesis and characterization of the first GPR30 antagonist, G15. Binding studies demonstrated that G15 exhibited only moderately reduced binding to GPR30 (about 3-fold) compared to G-1, and yet no significant binding to either ER $\alpha$  or ER $\beta$  at concentrations as high as 1-10  $\mu$ M. Functional assays revealed that G15 blocked both estrogen- and G-1-mediated mobilization of intracellular calcium in ER-negative SKBr3 breast cancer cells. In addition, GPR30-dependent PI3K activation by either estrogen or G-1 was blocked by prior incubation with G15. However, G15 was unable to prevent estrogen-mediated PI3K activation through either ER $\alpha$  or ER $\beta$ . *In vivo* studies demonstrated that G15 completely blocked uterine epithelial cell proliferation mediated by GPR30 in response to G-1 but only partially inhibited the estrogen-mediated response (presumably occurring through activation of all estrogen receptors). Finally, we established that the anti-depressive effects of estrogen appear to be mediated through GPR30, in that G-1 recapitulated the effects of estrogen and that G15 inhibited the anti-depressive effects of both G-1 and estrogen.

The selectivity of G15 towards GPR30 in cellular assays is consistent with the selectivity of G-1 for GPR30 in cells expressing both GPR30 and classical estrogen receptors as well as the stimulatory effects of estrogen in cells expressing only GPR30. Given the similarity in structure between G15 and G-1, with the difference being the lack of an ethanone moiety in G15, we suggest that G-1 activates GPR30 in a similar manner to the way in which estrogen activates

classical estrogen receptors and presumably GPR30. Crystal structures of estrogen-bound ER $\alpha$  reveal extensive hydrogen bonding networks between the hydroxyl groups of the estrogen and receptor hydrogen bond donors and acceptors (Tanenbaum et al. 1998). Assuming that G-1 activates GPR30 through similar networks of hydrogen bonds at the distal ends of the molecule, removal of one hydrogen bond acceptor could allow binding to occur without the agonist-induced receptor conformational changes required for activation.

Although estrogen mediates effects on most physiological systems, including the nervous, immune and vascular systems, its most appreciated role is in reproduction. In the uterus, a variety of cellular and molecular responses, including inhibition, proliferation, and induction of gene expression, are mediated by estrogen. Whereas ER $\alpha$  plays a major role in these responses (Hewitt et al. 2005), ER $\beta$  appears to play no role in inhibition, although it plays a role in the suppression of uterine epithelial proliferation (Wada-Hiraike et al. 2006). Here, we have demonstrated that the GPR30-specific antagonist G15 is capable of partially inhibiting estrogen-dependent uterine epithelial proliferation, but not inhibition (wet weight increase), suggesting that GPR30, in addition to ER $\alpha$ , plays a role in promoting uterine epithelial proliferation. Our results are in contrast to a recent paper that reported no effect of G-1 on proliferation in the uterus (Otto et al. 2008); however in that report, G-1 effects on uterine epithelial proliferation were not quantitated. It is possible that a 3-fold difference in proliferation was not detected by visual inspection alone, particularly when compared to the massive response to estrogen. In contrast to the restricted role



of GPR30 in uterine responses to estrogen, GPR30 appears to contribute in a significant way to the anti-depressive effects of estrogen with G-1 fully recapitulating the estrogen-mediated effects, and G15 equally inhibiting both estrogen- and G-1-mediated responses.

Although estrogen mediates the full range of uterine responses, including proliferation, imbibition, immune responses and gene expression, other estrogenic compounds have been observed to regulate these responses differentially. For example, DES (6) is weaker than estrogen in inducing uterine eosinophilia, imbibition and proliferation, equal to estrogen in mediating epithelial hypertrophy and stronger than estrogen in inducing the reduction of epithelial cell height and myometrial cell hypertrophy (Grunert et al. 1986). In addition, genistein (7) has only a limited ability to induce proliferation whereas estrogen-regulated genes are fully induced (Diel et al. 2004). Finally, the ER $\alpha$ -selective compound PPT (8) is less effective in stimulating imbibition and the expression of complement component 3 and glucose-6-phosphate dehydrogenase but is as effective as estrogen in regulating lactoferrin, androgen receptor, and progesterone receptor expression (Frasor et al. 2003). Since genistein has been shown to bind and activate GPR30 (Thomas and Dong 2006), it is unclear whether the varying effects of genistein and other compounds on distinct aspects of uterine physiology are due to either differential activation of classical estrogen receptor(s) or complex combinatorial effects on multiple estrogen receptors, including GPR30.

In conclusion, we report the identification and preliminary characterization

of the first selective GPR30 antagonist. The discovery of this high affinity GPR30-selective antagonist that does not bind significantly to classical nuclear estrogen receptors has yielded novel insights into the physiological roles of GPR30 in the reproductive and nervous systems. Future studies utilizing GPR30-selective agonists and antagonists will further define the role of GPR30 *in vivo* and open the door to the generation of diagnostics and therapeutics directed at individual estrogen receptors.

## 4.2.5 METHODS

**4.2.5.1 Chemical synthesis and characterization of G15.** The compound G15 (4-(6-Bromo-benzo[1,3]dioxol-5-yl)-3a,4,5,9b-tetrahydro-3H-cyclopenta[c]quinoline) was synthesized using an optimized one-step procedure similar to Kobayashi et. al. (Kobayashi et al. 1995).

**4.2.5.2 Ligand binding assays** Binding assays for ER $\alpha$  and ER $\beta$  were performed as previously described (Revankar et al. 2005). Briefly, Cos7 cells were transiently transfected with either ER $\alpha$ -GFP or ER $\beta$ -GFP). Following serum starvation for 24 h, cells ( $\sim 5 \times 10^4$ ) were incubated with G-15 for 20 min in a final volume of 10  $\mu$ L prior to addition of 10  $\mu$ L of 20 nM E2-Alexa633 in saponin-based permeabilization buffer. Following 10 min at RT, cells were washed once with 200  $\mu$ L PBS/2%BSA, resuspended in 20  $\mu$ L and 2  $\mu$ L samples were analyzed on a DAKO Cyan flow cytometers using HyperCyt™ as described (Ramirez et al. 2003). For GPR30 binding, a radioiodinated derivative of G-1, was used. Briefly, Hec50 cells were cultured in phenol-red free DMEM/F-12 containing 10% charcoal-stripped FBS, plated in 24-well tissue culture plates and grown to 80% confluence. Wells were rinsed with PBS and cells were incubated with competitor (G-1 or G15) for 30 min prior to addition of approximately 0.5-1  $\mu$ Ci of radioligand. The  $^{125}$ I radiolabeled ligand was prepared from the corresponding tributylstannane using Iodo-gen beads (Pierce) following the manufacturer's recommended protocol. Complete details of the synthesis and radiolabeling are described elsewhere (Ramesh et al. 2009). Wells were incubated at 37°C for 1 hr, rinsed with PBS and radioactivity collected by ethanol

extraction and counted in a Wallac Wizard 1480 gamma counter (Perkin Elmer, Gaithersburg, MD).

**4.2.5.3 Intracellular calcium mobilization** SKBr3 cells ( $1 \times 10^7$ ) were incubated in HBSS containing 3  $\mu$ M indo1-AM (Invitrogen) and 0.05% pluronic acid for 1 hr at RT. Cells were then washed twice with HBSS, incubated at RT for 20 min, washed again with HBSS, resuspended in HBSS at a density of  $10^8$  cells/mL and kept on ice until assay, performed at a density of  $2 \times 10^6$  cells/mL.  $Ca^{++}$  mobilization was determined ratiometrically using  $\lambda_{ex}$  340 nm and  $\lambda_{em}$  400/490 nm at 37°C in a spectrofluorometer (QM-2000-2, Photon Technology International) equipped with a magnetic stirrer. The relative 490 nm/400 nm ratio was plotted as a function of time.

**4.2.5.4 PI3K activation** The PIP3 binding domain of Akt fused to mRFP1 (PH-mRFP1) was used to localize cellular PIP3. Cos7 cells (cotransfected with GPR30-GFP or ER $\alpha$ -GFP and PH-mRFP1) or SKBr3 (transfected with PH-mRFP1) cells were plated on coverslips and serum starved for 24 hr followed by stimulation with ligands as indicated. The cells were fixed with 2% PFA in PBS, washed, mounted in Vectashield and analyzed by confocal microscopy using a Zeiss LSM510 confocal fluorescent microscope.

**4.2.5.5 Mouse uterine estrogenicity assay** C57Bl6 female mice (Harlan) were ovariectomized at 10 weeks of age. E2, G-1, and G15 were dissolved in absolute ethanol at 1 mg/mL (E2 and G-1 were diluted to 10  $\mu$ g/mL in ethanol, G15 was diluted to 50  $\mu$ g/mL in ethanol). For treatment with all three compounds, 10  $\mu$ L was added to 90  $\mu$ L aqueous vehicle (0.9% NaCl with 0.1% albumin and

0.1% Tween-20). Ethanol alone (10  $\mu$ L) was added to 90  $\mu$ L aqueous vehicle as control (sham). At 12 days post-ovariectomy, mice were injected subcutaneously at 5:00 pm with 100  $\mu$ L consisting of 1) sham; 2) 200 ng E2 (0.74 nmol); 3) 40, 200, or 1000 ng G-1 (0.1, 0.5, or 2.4 nmol, respectively); 4) 272, 900, 2725, or 10000 ng G15 (2.4, 7.4, or 27 nmol, respectively) or 5) G15 combined with E2 or G-1 (at the same concentrations as used individually: G-1 was used at 200 ng (0.5 nmol) in all G-1 + G15 combination experiments). The doses of G15 were chosen to represent an approximately 1:1, 1:3.3, 1:10, and 1:35-fold molar excess relative to E2. Eighteen hr after injection, mice were sacrificed and uteri were dissected, fixed in 4% paraformaldehyde, and embedded in paraffin. Five-micron sections were placed on slides, and proliferation in uterine epithelia was quantitated by immunofluorescence using anti-Ki-67 antibody (LabVision) followed by goat anti-mouse IgG conjugated to Alexa488 (Invitrogen). Nuclei were counterstained with 4',6-diamidino-2-phenylindole (DAPI). At least 4 animals per treatment were analyzed, and the Ki-67 immunodetection was repeated three times per mouse.

**4.2.5.6 Mouse depression assay** Adult male ICR mice, weighing 20-25 g, were used. Animals were maintained at room temperature, with free access to tap water and standard diet, under a 10:14 light/dark cycle (lights on 8:00h) and were housed 5/cage. Mice were acclimated to the laboratory for at least one hour before testing and used only once. All experiments were conducted during the light phase, between 8:30 and 14:30 h. Procedures used in this study were performed in accordance with the NIH Guide for the Care and Use of Laboratory

Animals and approved by the Institutional Animal Care and Use Committee. The procedure was similar to that described by Steru *et al.* (Steru *et al.* 1985). Mice were isolated and suspended 35 cm above the floor by an adhesive tape placed 1 cm from the tip of the tail. The mouse was 15 cm away from the nearest object. The total amount of time each animal remained immobile (mice were considered immobile only when they hung passively and completely motionless) during a 6-min period was recorded (in seconds) as immobility time. Each animal received two successive injections (0.1 mL/mouse) in order to eliminate any possible bias comparing single-compound treatments to dual-compound treatments. G1 and G15 were first dissolved in DMSO and diluted with saline; the final concentration in DMSO was 1 mM. Desipramine and E2 (cyclodextrin-encapsulated, 4-5.5% E2) were dissolved in saline solution and DMSO was added to a final concentration of 1 mM. An appropriate vehicle-treated group (saline with 1 mM DMSO) was included as a control (sham). All solutions were freshly prepared before each experimental series. Independent groups of mice (n=12-16) were treated with two consecutive intraperitoneal injections as follows: vehicle solution + vehicle solution (sham group); vehicle + G-1 (indicated amount in nmol); vehicle + desipramine (10mg/kg); G15 (10nmol/mouse) + desipramine (10mg/kg); G15 (10nmol/mouse) + G-1 (1nmol/mouse); vehicle + G15 (10nmol/mouse); vehicle + soluble E2 (5 mg/kg); G15 (25nmol/mouse) + soluble E2 (5 mg/kg). The second compound was injected 15 min (7 min for E2) after the first injection and the tail suspension test performed 30 min after the second injection.

#### 4.2.6 ACKNOWLEDGEMENTS

This work was supported by NIH grants CA118743 and CA127731, and grants from the Oxnard and Stranahan Foundations to ERP, by the New Mexico Molecular Libraries Screening Center (NIH MH074425) to LAS, the New Mexico Tobacco Settlement fund to TIO, the New Mexico Cowboys for Cancer Research to JBA and NIH grants R37 NS18710 to NJD and HL90804 to EB. Flow cytometry data and confocal images in this study were generated in the Flow Cytometry and Fluorescence Microscopy Facilities, which received support from the University of New Mexico Health Sciences Center and the University of New Mexico Cancer Center as detailed: <http://hsc.unm.edu/crtc/microscopy/Facility.html>. In vivo data were generated with the support by the UNM Cancer Center Animal Models & Imaging Core.

## 4.2.7 FIGURE LEGENDS

**4.2.7.1 Figure 4.1. Structures of G-1 and G15 (A)**, the substructure utilized for virtual screening of the MLSMR (where “A” means any atom (except hydrogen) and “Any” means any type of bond) **(B)** and G15 **(C)**.

**4.2.7.2 Figure 4.2. Ligand binding properties of G15** Ligand binding affinities of 17 $\beta$ -estradiol, G-1 and G15 for GPR30, ER $\alpha$  and ER $\beta$ . For GPR30 **(A)**, Hec50 cells, which endogenously express GPR30 but neither ER $\alpha$  and ER $\beta$ . were incubated with trace quantities of an iodinated G-1 derivative and the indicated concentration of either G-1 ( $\mu$ ) or G15 ( $\tau$ ) as competitor. For ER $\alpha$  and ER $\beta$ . Cos7 cells were transfected with either ER $\alpha$ -GFP **(B)** or ER $\beta$ -GFP **(C)**. For the latter, competitive ligand binding assays were performed using 10 nM E2-Alexa633 and the indicated concentration of either 17 $\beta$ -estradiol ( $\mu$ ) or G15 ( $\tau$ ). Data indicate the mean  $\pm$  s.e.m. of at least three separate experiments.

**4.2.7.3 Figure 4.3. G15 antagonism of intracellular calcium mobilization by GPR30 (A)** The effect of G15 on the subsequent mobilization of calcium by G1, E2 or ATP was evaluated using indo1-AM-loaded SKBr3 cells. G15 (1  $\mu$ M, red line) or vehicle (ethanol, black line) was added at 20 sec (first arrow). G-1 (200 nM), 17 $\beta$ -estradiol (E2, 100 nM) or ATP (1  $\mu$ M, a purinergic receptor control) was added at 80 sec (second arrow). **(B)** Dose response profile of G-1-stimulated SKBr3 cells to increasing concentrations of G15. **(C)** Dose response profile of 17 $\beta$ -estradiol-stimulated SKBr3 cells to increasing concentrations of G15. In panels **B** and **C**, G-1 and 17 $\beta$ -estradiol were used at 100 nM and 30 nM, respectively, concentrations that yield approximately the half-



maximal calcium response for each ligand (approximately 25% that of the full ATP response). Data in panel **A** are representative of at least three independent experiments. Data in panels **B** and **C** represent the mean  $\pm$  s.e.m. from at least three separate experiments.

**4.2.7.4 Figure 4.4. G15 antagonism of PI3K activation by GPR30** The activity of G15 was evaluated using Cos7 cells transfected with Akt-PH-mRFP1 and either GPR30-GFP (**A**), ER $\alpha$  or ER $\beta$  (**B**) or SKBr3 cells transfected with Akt-PH-mRFP1 (**C**). 17 $\beta$ -estradiol, G-1 and G15 were used at the indicated concentrations. The white bar in upper panel of (**A-C**) denotes 10  $\mu$ m for all images. Data are representative of three independent experiments.

**4.2.7.5 Figure 4.5. Effects of G15 on physiological responses mediated by GPR30** Epithelial uterine cell proliferation was assessed in the presence of E2 or E2 + G15 (**A**) or in the presence of G-1, G15, or G-1 + G15 (**B**) in ovariectomized female C57Bl6 mice. Compounds (amount in parentheses indicates nmol/mouse). Proliferation of uterine epithelium was quantitated by immunofluorescence using anti-Ki-67 antibody. (**C**) Immobility in adult male ICR mice was assessed as an indicator of depression. Mice were suspended from the tip of the tail and the total amount of time each animal remained immobile during a 6-min period was recorded. Compounds (amount in parentheses indicates nmol/mouse; desipramine and soluble E2 were used at 10 mg/kg and 5 mg/kg respectively) were administered intraperitoneally. Each group consisted of 10-12 animals. For all panels, results are expressed as mean  $\pm$  s.e.m., and statistical

significance ( $P<0.05$ ) was assessed by student's  $t$  test: \*, significantly different than sham; \*\*, significantly different than E2 or G-1, respectively.

Fig. 4.1 Structures of G-1 and G15

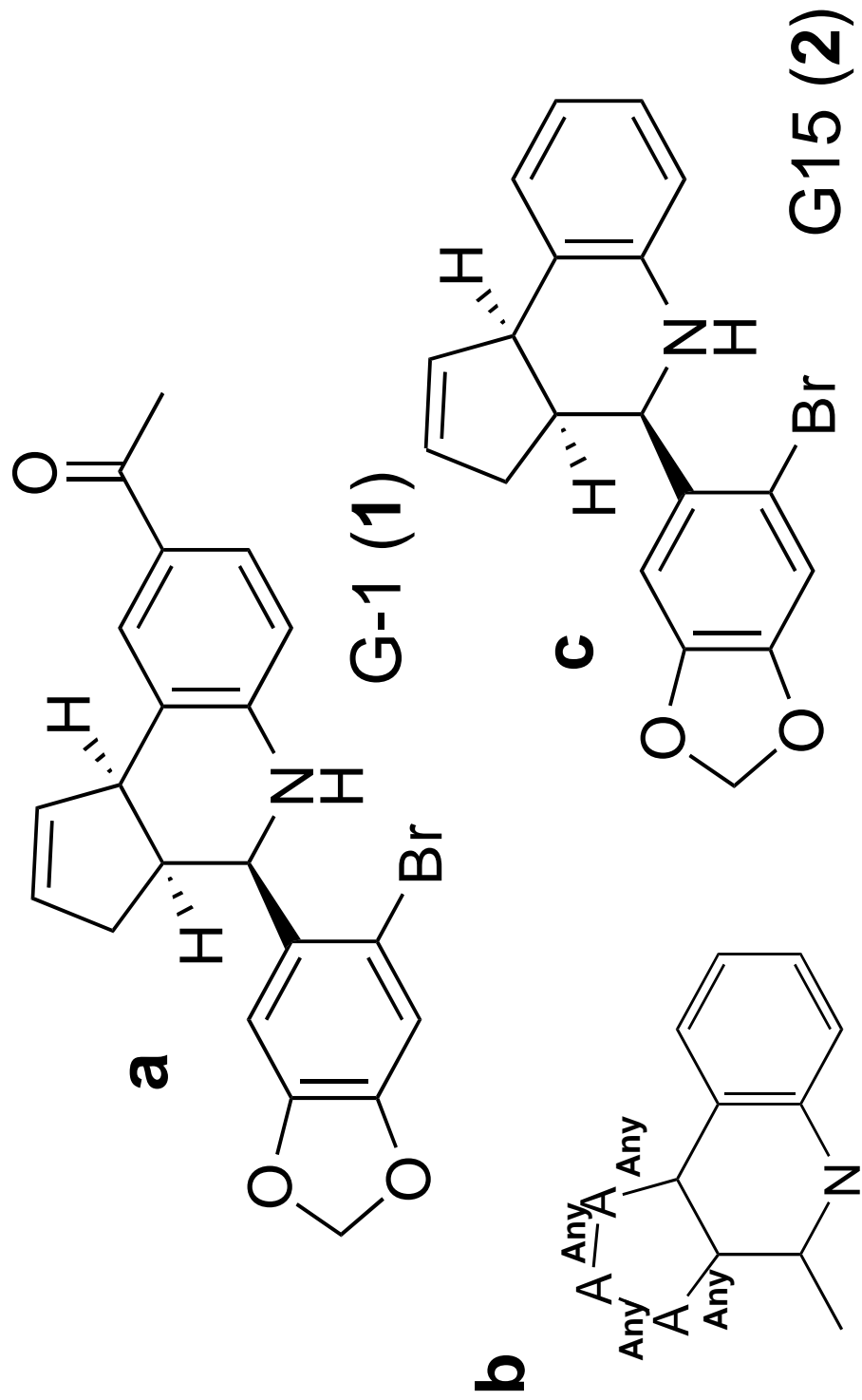
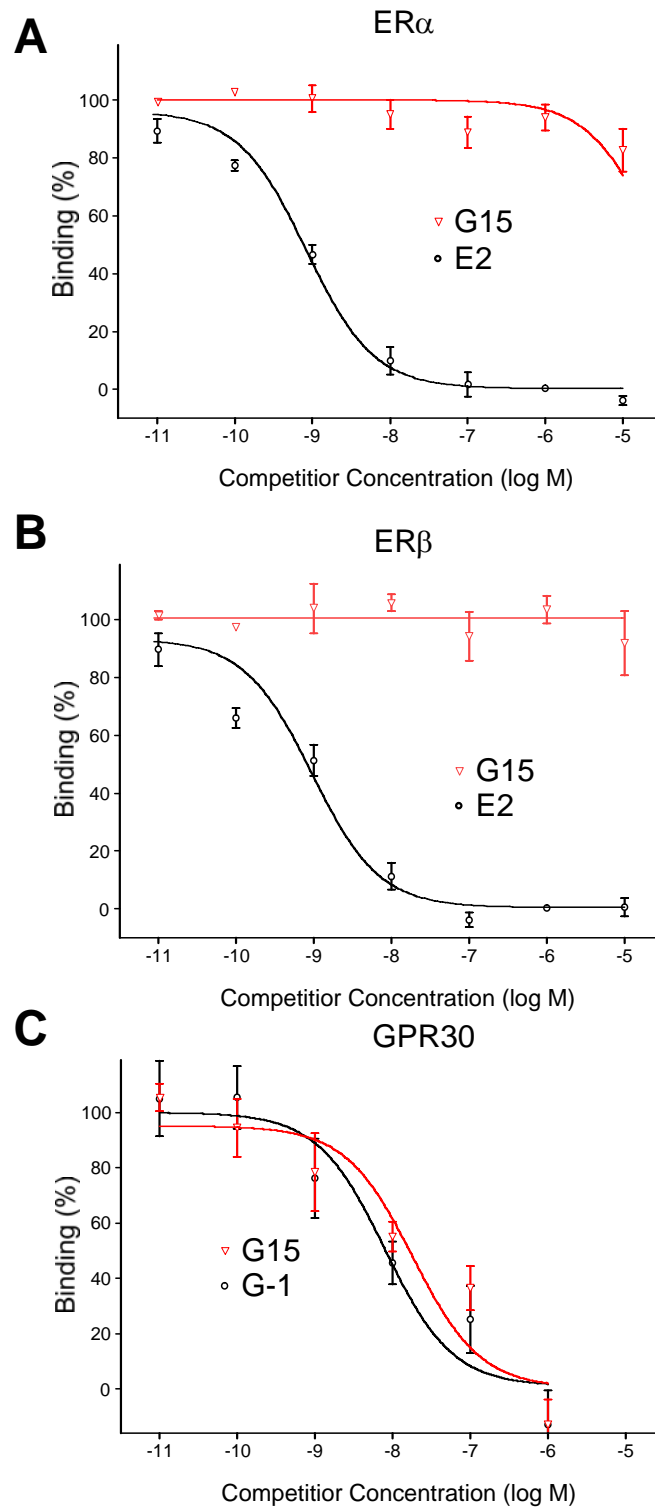


Fig. 4.2 Ligand binding properties of G15



**Fig. 4.3 G15 antagonism of intracellular calcium mobilization by GPR30**

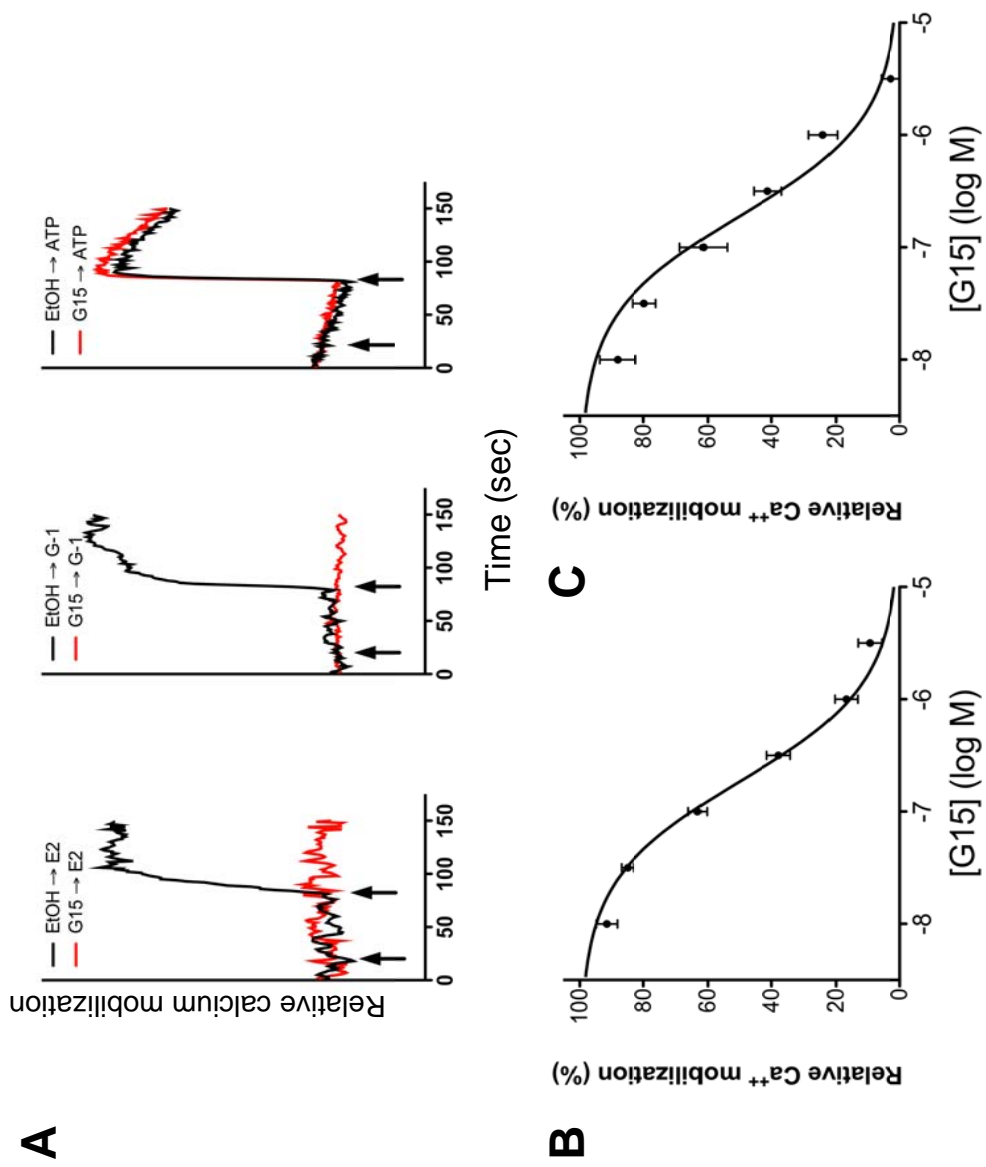


Fig. 4.4A G15 antagonism of PI3K activation by GPR30

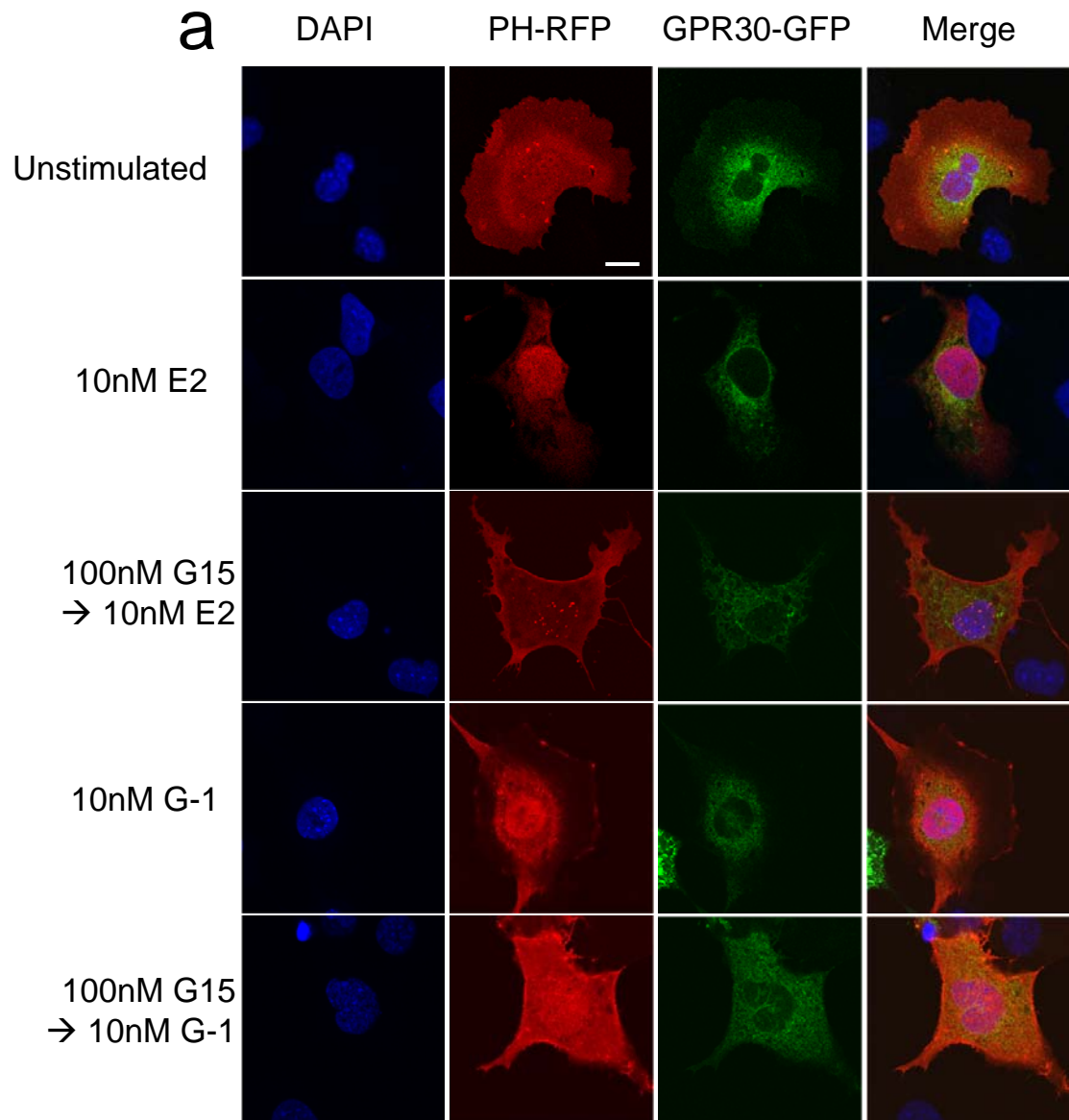


Fig. 4.4B G15 antagonism of PI3K activation by GPR30

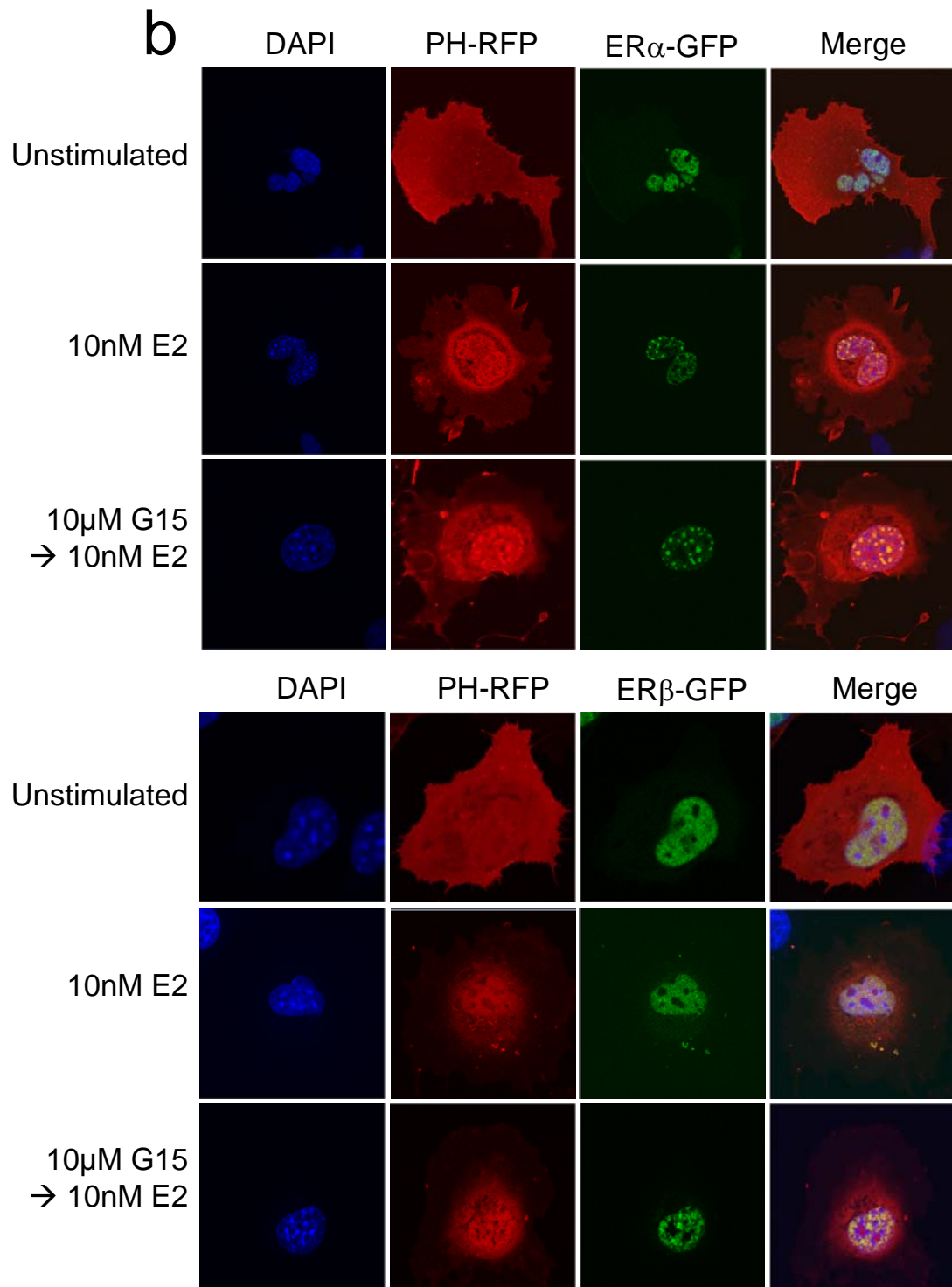


Fig. 4.4C G15 antagonism of PI3K activation by GPR30

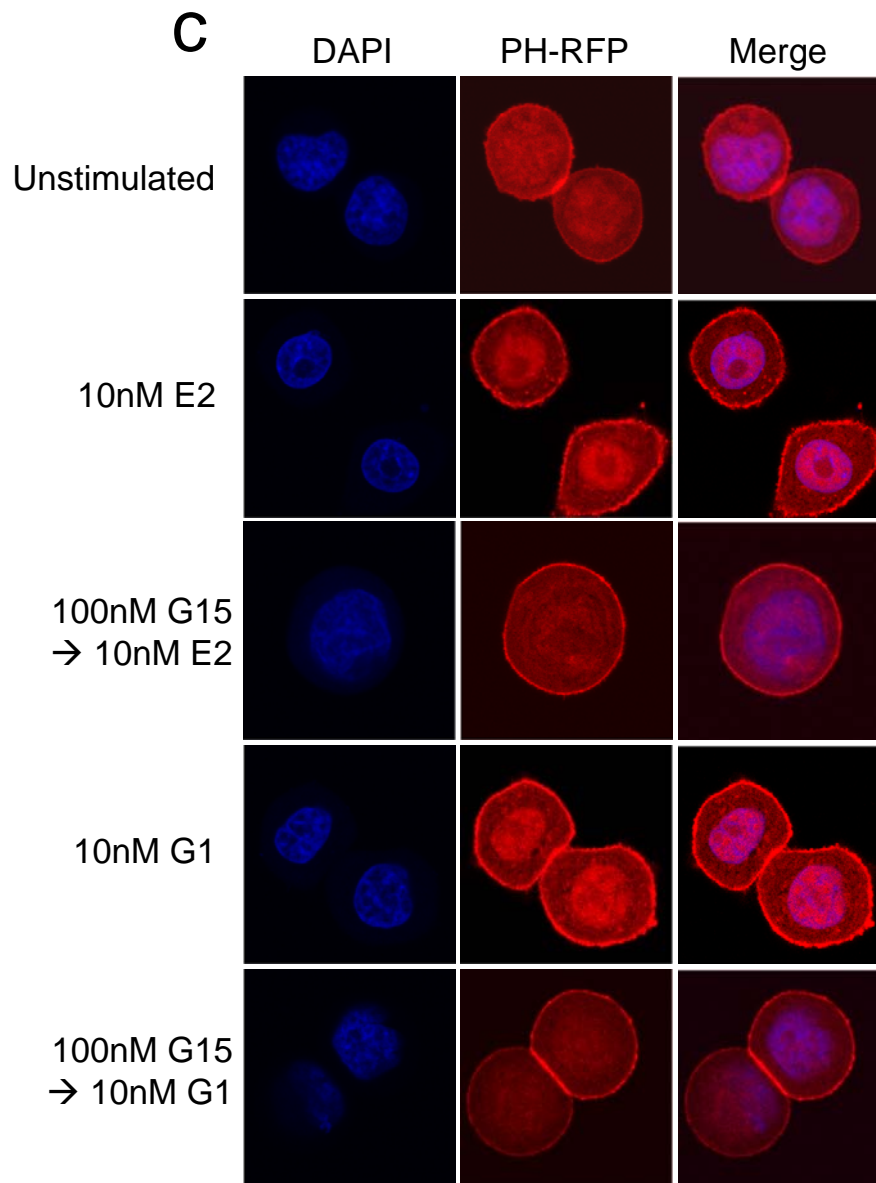
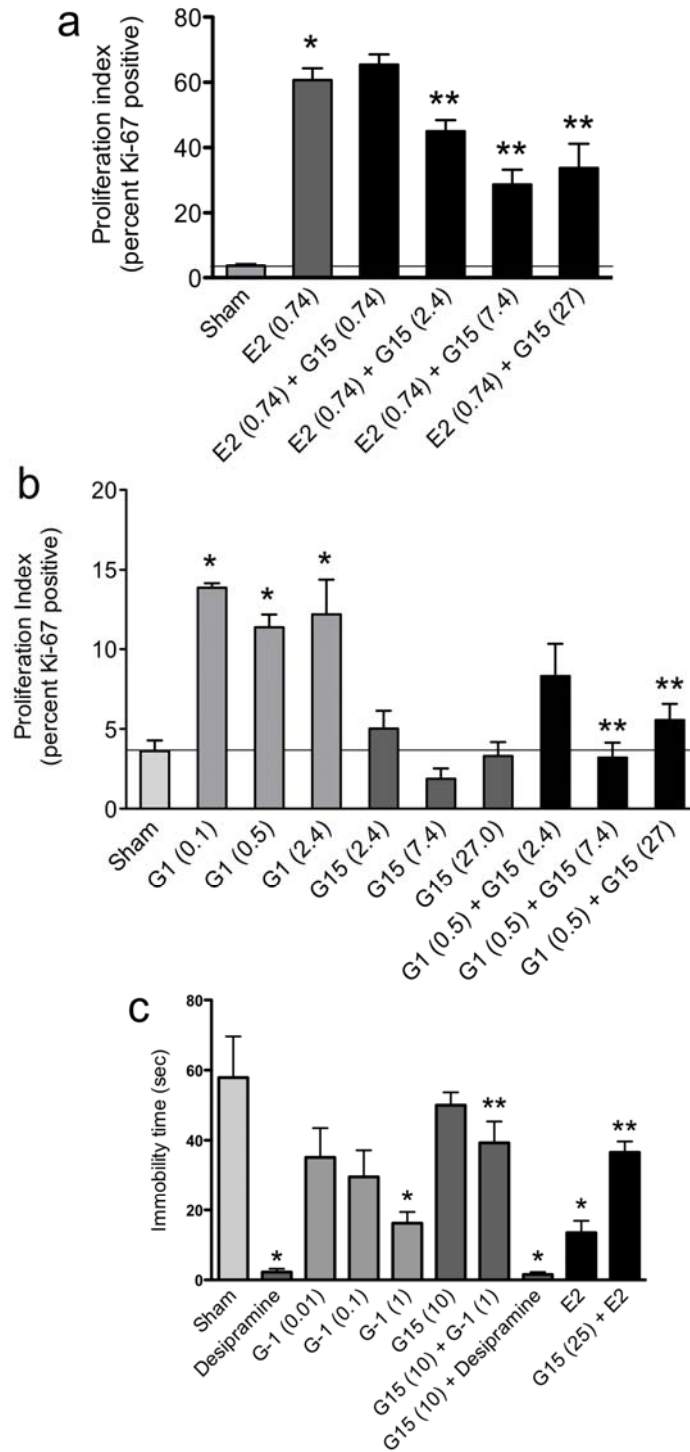




Fig. 4.5 Effects of G15 on physiological responses mediated by GPR30



### 4.3 Segue

With the successful identification of a GPR30-selective antagonist with similar structure to the GPR30-selective agonist G-1, further characterization of this compound as well as this class of GPR30-selective compounds was undertaken. The structural similarities between G-1 and G15 led to the synthesis of a wide variety of so-called G-scaffold compounds, with one or two changes on each molecule to investigate the structure-activity relationship between GPR30 and its ligands. The characterization of the second-generation GPR30-antagonist, G-36, is detailed in the following section.

## 4.4 G36 Manuscript

### 4.4.1 ABSTRACT

Selective ligands for estrogen receptors are beginning to contribute to the study of different receptor function in biological systems. With the identification and characterization of G15 as a selective antagonist of GPR30 function both *in vitro* as well as *in vivo*, the repertoire of selective estrogen receptor ligands is increased. As G-1, the selective agonist of GPR30, and G15 have a similar structure, we created a series of structurally similar compounds to try to identify an antagonist of GPR30 with increased specificity and selectivity compared to G15, which was discovered to have weak off target effects on classical ER-mediated transcription at high concentrations in follow up experiments. These efforts led to the identification of G36, a second GPR30-selective antagonist. Using binding assays to rule out ER $\alpha$ /ER $\beta$  interactions, we investigated the antagonist properties of G36 using PI3K activation assays and calcium mobilization assays. We found that G36 is equally effective to G15 as an antagonist of GPR30 and that G36 exhibits fewer off-target effects than G15.

#### 4.4.2 INTRODUCTION

Selective antagonists of receptor function have been useful in identifying biological function of many receptors. One of the key features central to all small molecule selective ligands is that they have minimal off-target effects in *in vitro* systems and, more importantly, in *in vivo* systems so effects seen from a given small molecule can be attributed solely to the receptor of interest.

Estrogen receptors ER $\alpha$ , ER $\beta$  and GPR30 mediate a range of physiological functions in both normal and diseased pathology. GPR30 is the most recently described of the three ERs and its contributions to overall E2 biology are still not well characterized (Revankar et al. 2005). The identification of a selective agonist for GPR30, G-1, has led to great advances in characterizing GPR30 function in just a few years (Bologa et al. 2006). Recently, a GPR30-selective antagonist, G15, was described and this small molecule should greatly assist in further elucidation of GPR30 function versus ER $\alpha$  and ER $\beta$  function (Dennis et al. 2009).

In follow-up characterization of G15, we found that high doses (10  $\mu$ M) of G15 can stimulate limited transcription via ERE (less than 15% of transcription promoted by physiological levels of E2, unpublished data). These doses of G15 are beyond what is required to block the effects of physiological levels of estrogen; however, administration of too high of doses of G15 with the assumption that more of an antagonist will better antagonize GPR30 could lead to off target effects. With this knowledge, along with the observation that G-1 and G15 share a similar chemical structure, a series of so-called 'G-scaffold'

compounds were synthesized to find a more selective antagonist of GPR30. These efforts led to the identification of G36, a structurally similar compound to G-1 and G15, which also functions as an antagonist of GPR30 function. G36 was characterized in a similar fashion to G15, utilizing it to block various E2-mediated functions in cells expressing GPR30 and illustrating a lack of binding to ER $\alpha$  and ER $\beta$  along with decreased off-target effects via the classical ERs.

### 4.4.3 RESULTS & DISCUSSION

#### 4.4.3.1 Identification of G36

In order to screen the range of G-scaffold compounds synthesized by Dr. Jeff Arteburn's group at New Mexico State University (**structures in Appendix, Fig. S6**), we employed the calcium mobilization assay with SKBr3 cells expressing endogenous GPR30 but lacking ER $\alpha$ /ER $\beta$  expression. This assay is amenable to screening a large number of compounds relatively quickly and can be used to identify agonists and antagonists of GPR30-mediated calcium mobilization in the same assay. Screening of the set of G-scaffold compounds resulted in the identification of several that appeared to block E2-induced calcium mobilization in SKBr3 cells, including G36, which had a very similar structure to G-1 and G15 (**Fig. 4.6**) and was selected for follow-up assays based on this similarity.

#### 4.4.3.2 G36 exhibits decreased binding to ER $\alpha$ and ER $\beta$ at high doses compared to G15

We first verified that G36 did not bind to ER $\alpha$  or ER $\beta$  using the fluorescent-estrogen competition binding assay. This assay utilizes flow cytometry to monitor compound binding in transiently transfected Cos7 cells expressing either ER $\alpha$ -GFP or ER $\beta$ -GFP and unlabeled compounds to competitively inhibit E2-Alexa binding to receptors in permeabilized whole cells (Revankar et al. 2005). This assay verified that G36 does not bind significantly to either ER $\alpha$  or ER $\beta$  at concentrations up to 10  $\mu$ M, whereas G15 begins to show low levels of binding at concentrations higher than 1  $\mu$ M (**Fig. 4.7**). This finding

that G36 has decreased binding to classical ERs compared to G15 suggested that G36 may be more specific for GPR30 than G15 with regard to cross reactivity to ER $\alpha$ /ER $\beta$ . This finding was verified by an ERE-luciferase transcription assay, that demonstrated G36 exhibits decreased off-target transcription through the ERE than does G15 at high doses (data not shown).

#### **4.4.3.3 G36 effectively blocks E2-induced PI3K activation in GPR30 expressing cells**

We next investigated the potency of G36 with respect to inhibiting GPR30 function and compared its activity to that of G15. First, we utilized the PI3K activation assay in which cells are transiently transfected with either ER $\alpha$  or GPR30 and a reporter of PIP3 localization, the pleckstrin homology (PH) domain of Akt (which preferentially binds to PIP3 versus other phosphoinositides) fused to RFP (PH-RFP). These cells can then be stimulated with E2 or other receptor agonists leading to the translocation of PH-RFP from a cytoplasmic location into the nucleus and peri-nuclear region. This PH-RFP translocation can be blocked by inhibitors of PI3K function and inhibitors of receptor function, including G15 (Dennis et al. 2009). We treated Cos7 cells expressing PH-RFP and either ER $\alpha$  or GPR30 fused to GFP with E2 and either G15 or G36 to determine the antagonist activity of G36. We have previously shown that, in cells expressing ER $\alpha$  only, treatment with E2 and G15 leads to activation of PI3K and nuclear translocation of PH-RFP, as G15 does not block E2 function through ER $\alpha$ . Conversely, treatment of GPR30 expressing cells with E2 and G15 does not lead to the activation of PI3K, as G15 can effectively block E2-mediated activation of

PI3K in GPR30-expressing cells. Similarly, we find that G36, when used at a 10-fold molar excess like G15, can fully block E2-induced PI3K activity in GPR30 expressing cells but not in cells expressing ER $\alpha$  (**Fig. 4.8A**). Additionally, G36 can fully block PI3K activation induced by E2 in SKBr3 cells expressing only endogenous GPR30 and transfected with PH-RFP and G-1 mediated PH-RFP translocation in these cells (**Fig. 4.8B**). These results indicate that G36, like G15, is an antagonist of GPR30-mediated PI3K activation.

#### **4.4.3.4 G36 blocks E2-induced calcium mobilization**

As we used the calcium mobilization assay with SKBr3 cells expressing endogenous GPR30 to screen for initial activity of G36, we were aware that G36 blocked E2-induced calcium mobilization in these cells; however, the initial screen did not address the potency of G36 in a dose-dependent manner. We therefore investigated the potency of G36 in this assay as another comparison to G15 to verify that G36 is at least as active against GPR30 function as G15. Using Indo-1AM-loaded SKBr3 cells, we blocked E2-induced calcium mobilization with increasing doses of G36 and plotted this data as a function of G36 concentration to determine an IC<sub>50</sub> value for G36 (**Fig. 4.9**). This data shows that G36 has very similar efficacy to G15 in this assay, as the IC<sub>50</sub> for G15 is  $1.91 \times 10^{-7}$  (Dennis et al. 2009), and the IC<sub>50</sub> determined for G36 in this assay is  $1.45 \times 10^{-7}$ . This similarity is not surprising, since G15 and G36 share significant structural similarity.



#### 4.4.4 MATERIALS & METHODS

**4.4.4.1 Ligand binding assays** Binding assays for ER $\alpha$  and ER $\beta$  were performed as previously described (Revankar et al. 2005). Briefly, Cos7 cells were transiently transfected with either ER $\alpha$ -GFP or ER $\beta$ -GFP). Following serum starvation for 24 hr, cells ( $\sim 5 \times 10^4$ ) were incubated with G-15 for 20 min in a final volume of 10  $\mu$ L prior to addition of 10  $\mu$ L of 20 nM E2-Alexa633 in saponin-based permeabilization buffer. Following 10 min at RT, cells were washed once with 200  $\mu$ L PBS/2%BSA, resuspended in 20  $\mu$ L and 2  $\mu$ L samples were analyzed on a DAKO Cyan flow cytometers using HyperCyt™ as described (Ramirez et al. 2003).

**4.4.4.2 Intracellular calcium mobilization** SKBr3 cells ( $1 \times 10^7$ ) were incubated in HBSS containing 3  $\mu$ M indo1-AM (Invitrogen) and 0.05% pluronic acid for 1 hr at RT. Cells were then washed twice with HBSS, incubated at RT for 20 min, washed again with HBSS, resuspended in HBSS at a density of  $10^8$  cells/mL and kept on ice until assay, performed at a density of  $2 \times 10^6$  cells/mL. Ca<sup>++</sup> mobilization was determined ratiometrically using  $\lambda_{ex}$  340 nm and  $\lambda_{em}$  400/490 nm at 37°C in a spectrofluorometer (QM-2000-2, Photon Technology International) equipped with a magnetic stirrer. The relative 490/400 nm ratio was plotted as a function of time.

**4.4.4.3 PI3K activation** The PIP3 binding domain of Akt fused to mRFP1 (PH-mRFP1) was used to localize cellular PIP3. Cos7 cells (cotransfected with GPR30-GFP or ER $\alpha/\beta$ -GFP and PH-mRFP1) or SKBr3 (transfected with PH-mRFP1) cells were plated on coverslips and serum starved for 24 hr followed by

stimulation with ligands as indicated. The cells were fixed with 2% PFA in PBS, washed, mounted in Vectashield and analyzed by confocal microscopy using a Zeiss LSM510 confocal fluorescent microscope.

#### 4.4.5 FIGURE LEGENDS

##### 4.4.5.1 Figure 4.6. Structures of G-1, G15 and G36

4.4.5.2 Figure 4.7. G36 Binding to ER $\alpha$ / $\beta$  Cos7 cells transiently transfected with either ER $\alpha$ -GFP or ER $\beta$ -GFP were used to determine inhibition of E2-Alexa binding by 10  $\mu$ M G15 and G36 to classical ERs. 100% represents binding of E2-Alexa in cells lacking unlabeled block. E2 block is blocking of E2-Alexa binding by 100 nM E2 and represents fully blocked E2-Alexa binding, E2-Alexa which binds under this condition is non-specific background binding.

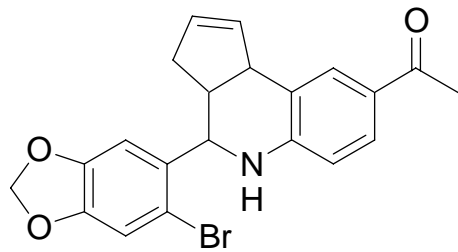
##### 4.4.5.3 Figure 4.8. G36 Blocks PI3K activity mediated by GPR30 A)

Cos7 cells were transfected with PH-RFP and either ER $\alpha$ -GFP or GPR30-GFP. Cells were treated for 15 min with inhibitors (G15 or G36) or DMSO vehicle as indicated and then stimulated for 15 min with 10 nM E2 prior to fixation with 2% PFA and confocal imaging. B) SKBr3 cells expressing endogenous GPR30 were transfected with PH-RFP. Cells were treated as in A with compounds as indicated.

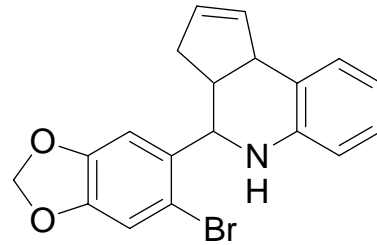
##### 4.4.5.4 Figure 4.9. G36 Blocks E2-induced calcium mobilization in cells expressing GPR30

SKBr3 cells expressing endogenous GPR30 and neither ER $\alpha$  or ER $\beta$  were loaded with Indo-1AM for calcium mobilization experiments. The effects of G36 on subsequent calcium mobilization induced by E2 were evaluated using a range of G36 doses. Data were as plotted as percent of E2-induced calcium mobilization versus G36 dose and an IC<sub>50</sub> for the inhibition curve was determined.

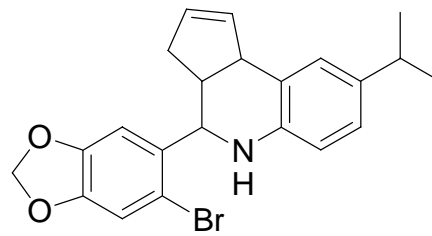
#### 4.4.5.1 Figure 4.6



**G-1**

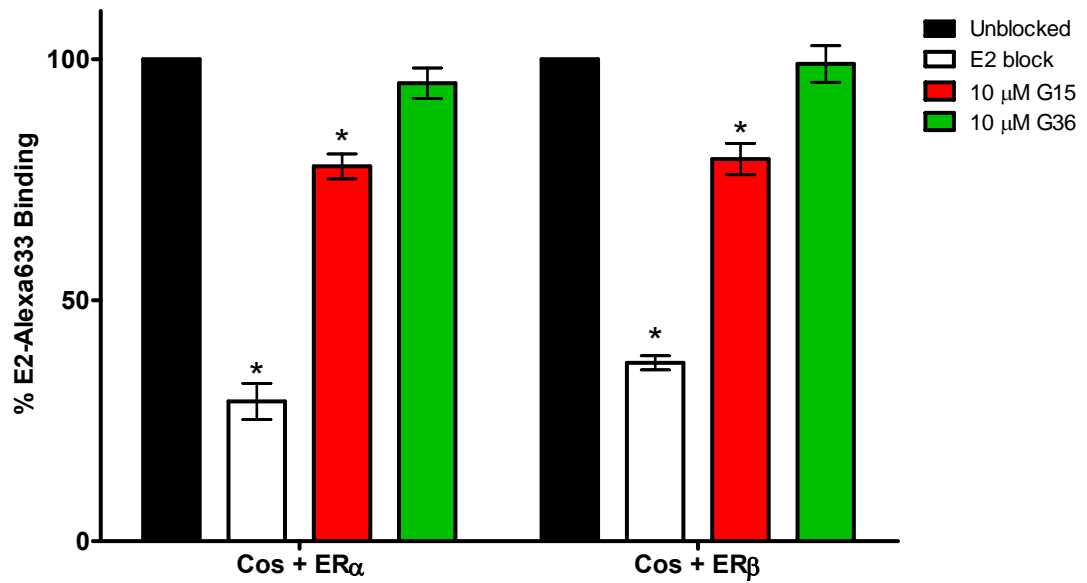


**G15**

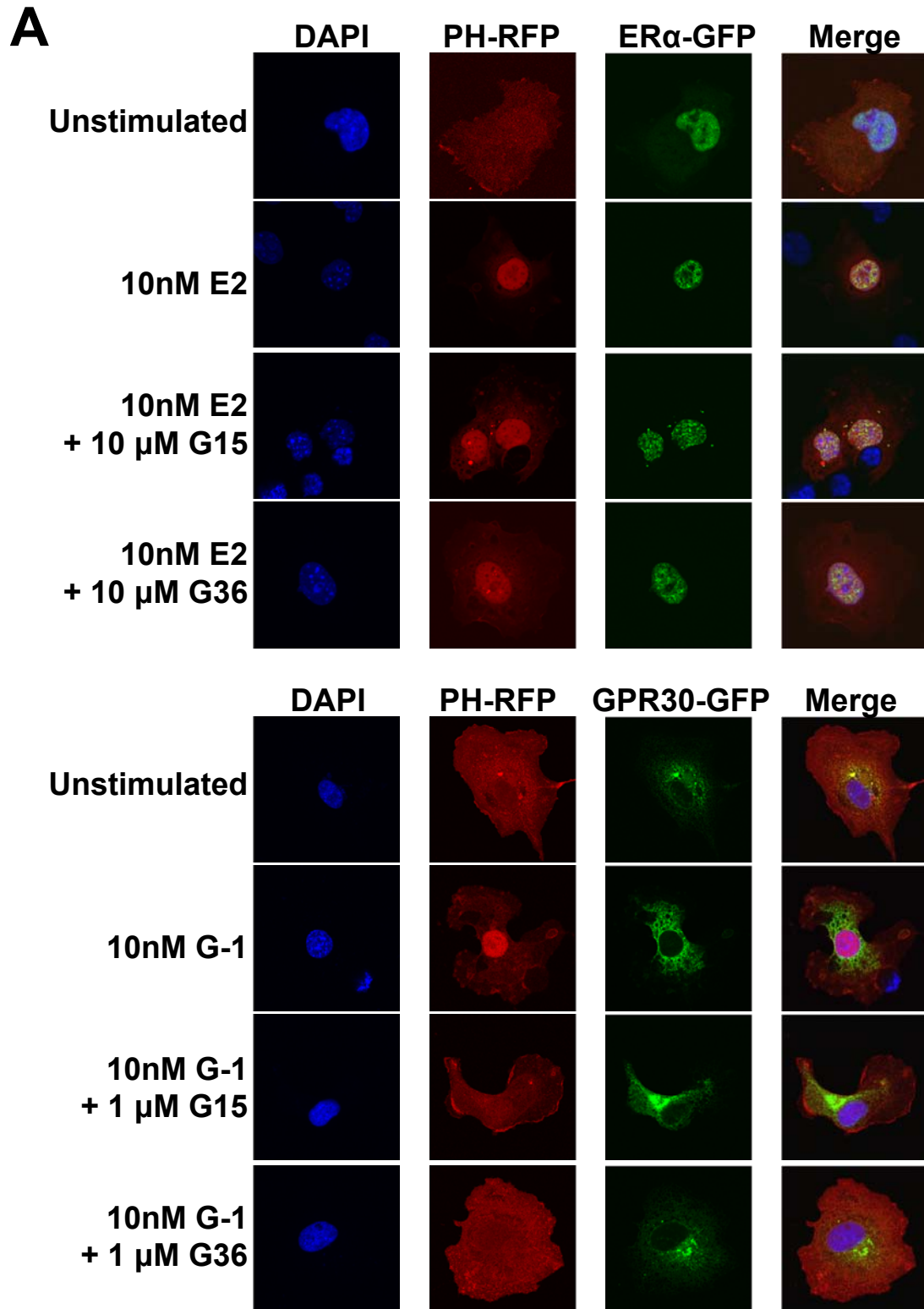


**G36**

#### 4.4.5.2 Figure 4.7

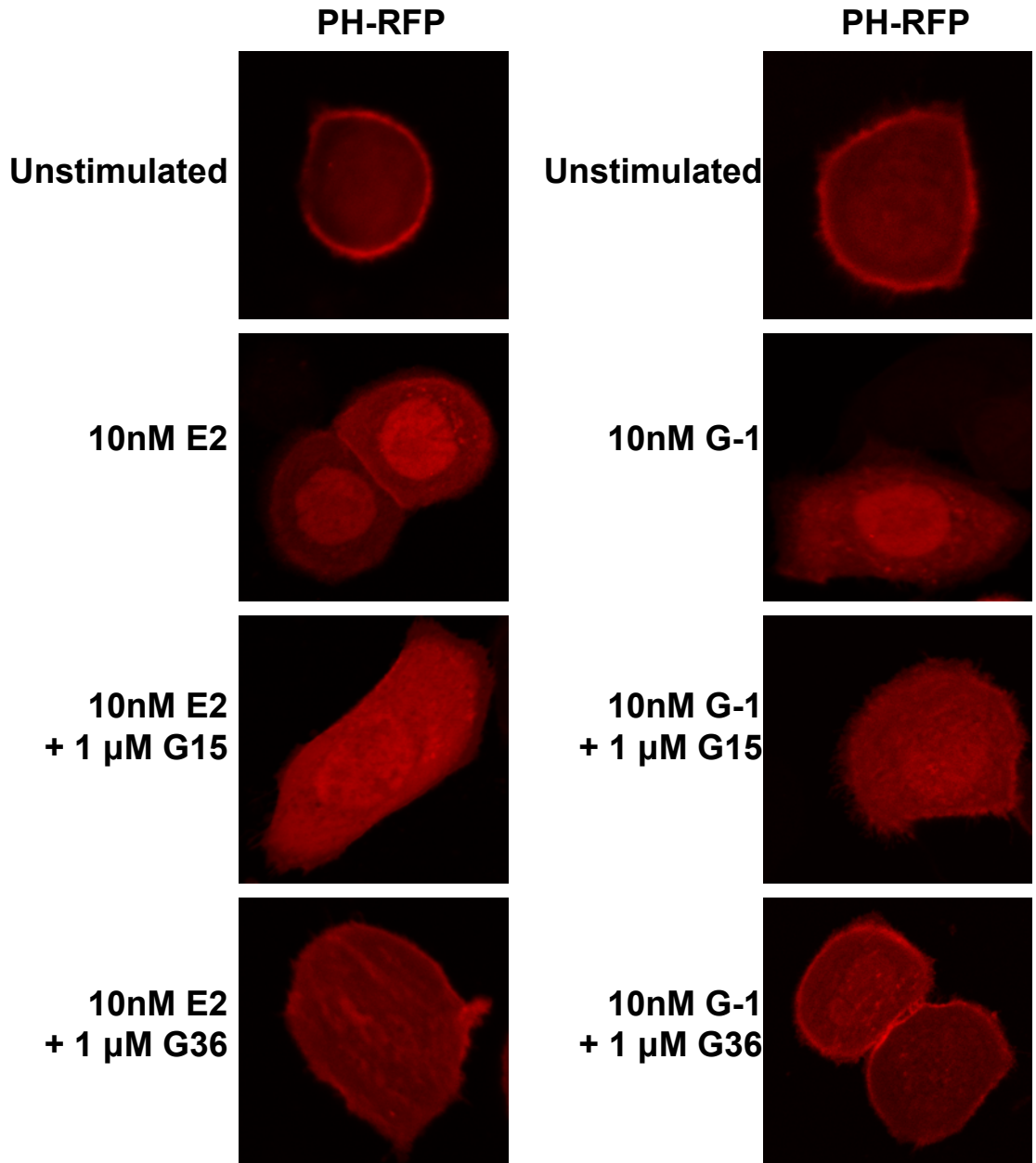


### 4.4.5.3 Figure 4.8

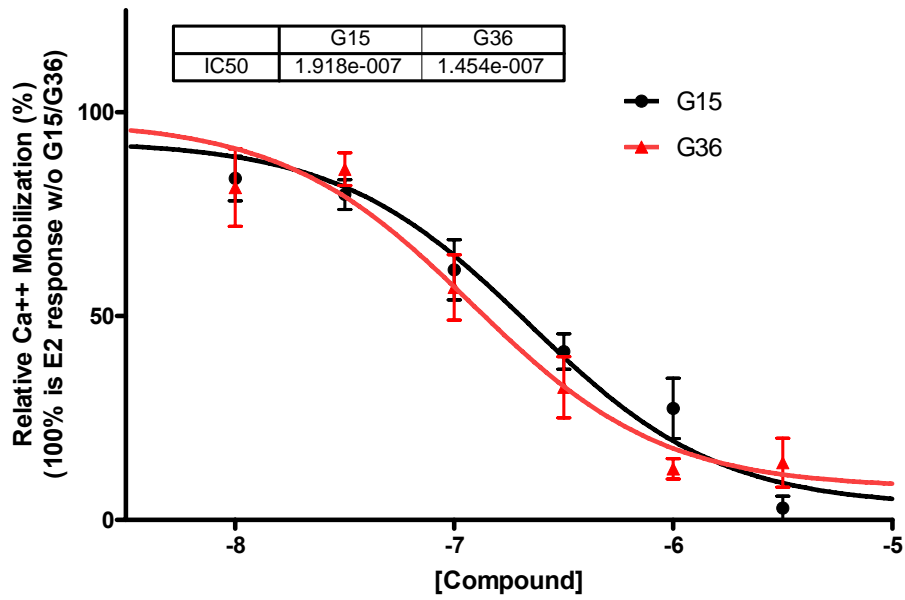


### 4.4.5.3 Figure 4.8

**B**



#### 4.4.5.4 Figure 4.9





## 4.5 Summary

In this chapter, we described the characterization of two GPR30 antagonists, G15 and G36. G15 was identified by the NIH Roadmap Initiative-funded screen of ER $\alpha$ /ER $\beta$ /GPR30 as described in Chapter 3. G36 was identified from a set of compounds synthesized by our collaborators at New Mexico State University based on the structural similarities between G-1 and G15. This compound was selected from the series of compounds based on its ability to inhibit E2-induced calcium mobilization in GPR30-expressing cells and further characterization revealed that it is as effective an antagonist of GPR30 function as G15, but with fewer off-target effects. Thus, G36 may represent a superior antagonist for GPR30 in follow-up studies, both *in vitro* as well as *in vivo*. Hopefully these GPR30 antagonists, coupled with the GPR30 agonist G-1 previously described by our group, can greatly advance the study of GPR30 function and begin to unravel estrogen signaling through GPR30 compared to ER $\alpha$  and ER $\beta$ .

# 5 GPR30 SIGNALING IN CANCER

## 5.1 Introduction

Cancers typically thought of as involving estrogen include cancers of the breast, uterus and other female reproductive organs; however, estrogen also appears to be involved in glioma. Significantly more men than women are diagnosed with glioma (Velema and Percy 1987; Preston-Martin 1996), suggesting a link between sex steroids or another difference between men and women as a predisposing factor. Additionally, women who have taken exogenous estrogens appear to be protected from glioma (Huang et al. 2004; Hatch et al. 2005). Interestingly, in animal models of glioma, tumor progression is slowed when estrogen is present in rats, either in intact females or in ovariectomized females supplemented with exogenous estrogen (Plunkett et al. 1999; Barone et al. 2009).

There are several types of glioma: astrocytomas are of astrocyte origin and have histological characteristics consistent with astrocyte over-proliferation; oligodendrogliomas arise from oligodendrocytes; mixed oligoastrocytomas have cells from both populations within the tumor (Louis 2006). Glioblastomas are the most malignant form of astrocytoma and have one of the poorest median survivals after diagnosis of any type of malignancy (Lino and Merlo 2009). Treatment of glioblastoma typically includes surgical resection of as much tumor as possible and follow-up treatment with external radiation and/or cytotoxic agents (Lino and Merlo 2009). Interestingly, tamoxifen was shown to be effective in a series of clinical trials (Vertosick et al. 1992; Couldwell et al. 1996; Cloughesy et al. 1997; Mastronardi et al. 1998; Brandes et al. 1999), as well as

several *in vitro* studies showing that tamoxifen inhibits growth of glioma cell lines (Pollack et al. 1990; Zhang et al. 2000).

Glioblastoma typically does not express classical ERs, although there are reports of ER $\alpha$ - and ER $\beta$ -expressing tumors (Fujimoto et al. 1984; Leslie et al. 1994). Glioblastoma cell lines also tend not to express classical ERs (Plunkett et al. 1999; Hui et al. 2004), although there are differing reports on ER status of some cell lines (Barone et al. 2009). The expression of GPR30 in glioblastoma cells or tumors has not been characterized to this point, although GPR30 is known to be expressed in some brain tissue (Funakoshi et al. 2006; Brailoiu et al. 2007).

With this background knowledge, it seems relevant to investigate the expression and function of GPR30 in glioblastoma and glioma cell lines. To this end, we examined GPR30 expression in a malignant glioblastoma cell line, U87-MG. As we found GPR30 expressed in these cells, functional characterization of GPR30 in this context was completed. We used PI3K activation as an assessment of rapid signaling and the localization of the PI3K product PIP3 as a readout for signaling initiated by a wide range of stimuli. Additionally, knockdown of GPR30 and inhibitors of GPR30 signaling were used to further define GPR30 signaling in these cells. Finally, in order to add physiological relevance to data collected in the U87-MG cell line, we stained tissue from a patient who had undergone surgical resection of their tumor and demonstrated expression of GPR30 in astrocytes and a dramatic increase in astrocyte density within the tumor.

## 5.2A Role for GPR30 in Glioblastoma

Megan K. Dennis<sup>1</sup>, Hugo Arias-Pulido<sup>2</sup>, and Eric R. Prossnitz<sup>1,3 \*</sup>

<sup>1</sup> Department of Cell Biology & Physiology, <sup>2</sup> Translational Therapeutics Laboratory,

<sup>3</sup> UNM Cancer Center, The University of New Mexico Cancer Center, Albuquerque, NM, USA

One sentence summary: We identify a role for GPR30 in glioblastoma using the human neoplastic cell line U87 and patient tissue samples.

### 5.2.1 ABSTRACT

Gliomas are the most common type of brain tumor and occur more commonly in males than in females. The most malignant of these, glioblastoma, has an extremely short median survival following diagnosis of less than one year. Recently, estrogen and tamoxifen treatment of glioblastomas in animal models as well as in clinical trials has been shown to improve survival; however, most glioblastomas do not express either of the classical estrogen receptors, ER $\alpha$  or ER $\beta$ . The recently described estrogen receptor, GPR30, has not been characterized in glioma and thus we set out to determine the relevance of GPR30 to estrogen and tamoxifen signaling in gliomas. Using the glioblastoma cell line U87-MG, we first demonstrate GPR30 expression. GPR30 is also shown to be functionally active in U87-MG and can be activated by a range of ligands, including estrogen, tamoxifen and the GPR30-selective agonist G-1. This signaling can also be inhibited by knockdown of GPR30 or use of the GPR30-selective antagonist G15. Furthermore, ER $\alpha$  or ER $\beta$  are not shown to be functionally relevant by the complete abrogation of estrogen stimulation by the GPR30-selective antagonist G15 or in cells in which GPR30 expression has been knocked down using siRNA. Finally, we demonstrate expression of GPR30 in GFAP-positive astrocytes, both in normal brain tissue from a tumor patient, as well as within the tumor margins, where GPR30-GFAP double positive cells are abundant. These findings reveal that GPR30 is the functional estrogen receptor in a glioma cell line and that these findings are relevant to human tumor tissue, suggesting modulation of GPR30 activity may represent a novel therapeutic avenue for glioblastoma.

## 5.2.2 INTRODUCTION

Glial cell tumors can be subdivided into astrocytomas and oligodendrogliomas, depending on the cell type contained in the tumor (Louis 2006). Glioblastoma is the most malignant form of astrocytoma, with very poor treatment prognoses and survival rates; the median survival after diagnosis is less than one year (Jukich et al. 2001; Newton 2004). The incidence of glioblastoma, and of all glial tumors, is significantly higher in males than in females (Velema and Percy 1987; Preston-Martin 1996) and the use of exogenous estrogens by women is associated with lower risk of developing glioma (Huang et al. 2004; Hatch et al. 2005). Additionally, several *in vivo* studies in rats bearing human glioblastoma tumors have shown that female rats have a survival advantage, which is dependent on circulating estrogen (Plunkett et al. 1999; Barone et al. 2009).

There are three major estrogen receptors, each with different expression patterns in the brain. The two classical estrogen receptors (ERs), ER $\alpha$  and ER $\beta$ , stimulate rapid, non-genomic signaling in addition to their historically defined role as ligand activated transcription factors. In the brain, ER $\alpha$  is expressed in many regions including the septum, the diagonal band of Broca, the bed nucleus of the stria terminalis, the organum vasculosum of the lamina terminalis, the medial preoptic area, periventricular nucleus, arcuate nucleus, amygdale and ventromedial nucleus (Kuiper et al. 1998). Reports of ER $\alpha$  expression in malignant gliomas are mixed and sporadic (Fujimoto et al. 1984; Leslie et al. 1994) and reports of ER $\alpha$  expression in U87-MG cells are inconsistent (Plunkett

et al. 1999; Barone et al. 2009). ER $\beta$  is more widely expressed in the brain, with expression in the cerebral cortex, the hippocampus, medial septum, diagonal band of Broca, the organum vasculosum of the lamina terminalis, the nucleus of the stria terminalis, the medial preoptic area, periventricular nucleus, suprachiasmatic nucleus, supraoptic nucleus, paraventricular nucleus and amygdala (Kuiper et al. 1998). ER $\beta$  expression in glioblastoma is not well characterized, and reports of ER $\beta$  expression in glioblastoma cell lines are also mixed, with the majority of lines tested being negative for ER $\beta$  expression (Plunkett et al. 1999; Barone et al. 2009). A third estrogen receptor, GPR30, has recently been described (Revankar et al. 2005; Thomas et al. 2005). Unlike the classical ERs, GPR30 is a member of the 7 transmembrane G protein-coupled receptor family. GPR30 signals through rapid signaling pathways including Akt and ERK and can mediate downstream transcription events including *c-fos* transcription (Filardo et al. 2000; Filardo et al. 2002; Maggiolini et al. 2004). In the brain, GPR30 is expressed in the cortex, striatum, hippocampus, brainstem autonomic nuclei and the hypothalamic-pituitary axis (Funakoshi et al. 2006; Brailoiu et al. 2007) although expression in glioblastoma has not been reported.

There is evidence for estrogen influencing glioblastoma tumors: tumor incidence is lower in women and estrogen has been shown to be protective in an animal model of glioblastoma. Previous studies have not identified a mechanism for these effects and reports on expression of estrogen receptors in glioblastoma are varied. The present study investigates the role of the estrogen receptor



GPR30 in glioblastoma; both in the U87-MG human cell line as well as expression of GPR30 in samples from human tumors.

## 5.2.3 RESULTS

### 5.2.3.1 Expression of GPR30 in U87-MG cells

To determine the endogenous expression of GPR30 in U87-MG cells, cells were stained with an antibody to the C-terminus of GPR30 (**Fig. 5.1A**). The cells stained positive for GPR30 expression and the pattern of this staining was appropriate for GPR30 expression, with a strong reticular staining pattern consistent with the expression of GPR30 in the endoplasmic reticulum. Knockdown of endogenous GPR30 with siRNA also decreased staining of receptor (**Fig. 5.1B**). These experiments demonstrate that U87-MG cells express GPR30.

### 5.2.3.2 Functional characterization of GPR30 in U87-MG cells

To assess the functionality of GPR30 in U87-MG cells, a series of PI3K activation assays were carried out. Stimulation of GPR30 with E2 and other GPR30 agonists, including the GPR30-selective agonist G-1, the selective estrogen receptor modulator (SERM) 4-hydroxytamoxifen (TAM) and the classical ER antagonist ICI182,780, results in the rapid translocation of PIP3 from the cytoplasm to the nucleus (Revankar et al. 2005). This translocation can be tracked by using the fluorescent reporter PH-RFP, containing the PIP3-binding pleckstrin homology (PH) domain of Akt fused to mRFP. Cells can then be stimulated with a range of GPR30 agonists in the absence and presence of GPR30-selective antagonists and the involvement of signaling pathways investigated using signaling inhibitors. Additionally, knockdown of endogenous GPR30 in cells can be used to verify involvement of GPR30.

Stimulation of PH-RFP expressing U87-MG cells with estrogen resulted in a rapid accumulation of PIP3 to the nucleus, consistent with estrogen receptor activation. Additionally, treatment of these cells with the GPR30 selective agonist G-1 resulted in rapid accumulation of PIP3 to the nucleus, supporting a role for GPR30 as an estrogen receptor in these cells. Treatment with other known GPR30 agonists, including tamoxifen and ICI182,780 also caused activation of PI3K. Interestingly, PI3K was also activated by raloxifene (a SERM used for the prevention of osteoporosis in postmenopausal women that inhibits classical ER activity in the breast but activates classical ER in the bone), Genistein (a plant-derived isoflavone), and PPT (a compound previously thought to be a selective ER $\alpha$  agonist). DPN, a compound used for the selective activation of ER $\beta$ , did not activate PI3K in this assay and thus probably has no activity against GPR30. (Fig. 5.2A)

Knockdown of GPR30 in PH-RFP expressing cells abrogated the response to E2 and G-1, indicating that the activation of PI3K by estrogen in these cells requires GPR30 (Fig. 5.2B). This also supports the published observation (Plunkett et al. 1999; Hui et al. 2004) that U87-MG cells do not express either classical estrogen receptor and supports the idea that GPR30 is the functionally active estrogen receptor in these cells.

In addition to knockdown of GPR30 to confirm GPR30 as the active estrogen receptor in these cells, a series of inhibitors were also used. Transactivation of EGFR is involved downstream of estrogen activation of GPR30 and upstream of the activation of PI3K, thus the EGFR inhibitor AG1478,

as well as the PI3K inhibitor LY294002, have been previously shown to inhibit GPR30-mediated PI3K activation in Cos7 cells expressing only GPR30 and neither classical ER (Revankar et al. 2005). In the current study, both of these inhibitors prevented E2 and G-1 mediated activation of PI3K, consistent with a role for GPR30. Additionally, the GPR30-selective antagonists G15 and G36 also blocked PI3K activation by either E2 or G-1 (**Fig. 5.2C**).

### **5.2.3.3 Expression of GPR30 in patient tumor samples**

In order to assess the expression of GPR30 in glioblastoma cells *in vivo*, cryosections from patients undergoing resection of glioblastoma were costained for GPR30 and GFAP. In sections from non-tumor sections of the brain, GPR30, GFAP double-positive cells were sparsely found throughout the section and all GPR30-positive cells were positive for GFAP and vice-versa (**Fig. 5.3A**). The expression of GFAP and GPR30 in these cells also colocalized at a subcellular level. In tumor tissue, the number of GFAP-GPR30 double positive cells greatly increased, as did the overall density of cells (as indicated by nuclear staining with DAPI, which also indicated more abnormal nuclei in tumor sections), and the tissue appeared less organized (**Fig. 5.3B**). The subcellular localization of GPR30 and GFAP also appeared less colocalized in tumor sections.

#### 5.2.4 DISCUSSION

A connection between sex steroids, particularly estrogen, and the incidence of gliomas is beginning to emerge. Evidence for a link exists in epidemiological data that clearly shows a higher incidence of glioma tumors in males (Velema and Percy 1987; Preston-Martin 1996). Additional studies using glioma tumor models in rats has demonstrated that female rats have increased survival following inoculation with tumor cells and that this survival is estrogen-dependent, as ovariectomized females lost this survival advantage and supplementing ovariectomized females with physiological levels of estrogen, but not progesterone, restored the survival advantage (Plunkett et al. 1999; Barone et al. 2009).

While the link between glioma and estrogen has been established, the mechanism for this interaction is poorly defined. Most reports indicate that the majority of human tumors do not express ER $\alpha$  or ER $\beta$  (Fujimoto et al. 1984; Leslie et al. 1994), and most glioma cell lines used in modeling human disease are also ER $\alpha$ , ER $\beta$  negative (Plunkett et al. 1999; Hui et al. 2004). Further observations that tamoxifen can inhibit growth of glioma cell lines (Pollack et al. 1990; Zhang et al. 2000) and that high-dose tamoxifen treatment can slow progression of human gliomas (Vertosick et al. 1992; Couldwell et al. 1996; Cloughesy et al. 1997; Mastronardi et al. 1998; Brandes et al. 1999) add to the mystery surrounding the role of estrogen and SERM signaling in glioma.

With the discovery and characterization of GPR30 as an alternate estrogen receptor (Revankar et al. 2005; Thomas et al. 2005) that is activated by

tamoxifen, we were interested in the role of GPR30 signaling in glioma. We show by antibody staining that U87-MG glioblastoma cells express GPR30 and that GPR30 expression in these cells can be effectively knocked down using GPR30 siRNA. Since U87-MG cells do not express either classical ER, the expression of GPR30 in these cells could represent an alternate pathway for estrogen signaling. This may also suggest that other glioma cell lines and human tumor samples express GPR30 and therefore are capable of signaling via an estrogen receptor.

After establishing that U87-MG cells express GPR30, we set out to characterize the functional relevance of this receptor. Activation of GPR30 by estrogen, tamoxifen, or specific GPR30 ligands, such as G-1, results in the rapid activation of PI3K in U87-MG cells and this activation can be abrogated using GPR30 siRNA or the GPR30-selective antagonist G15. Our findings support a role for GPR30 as the functional estrogen receptor in these cells, consistent with earlier reports which do not observe expression of either ER $\alpha$  or ER $\beta$  (Plunkett et al. 1999; Hui et al. 2004). Barone, et al demonstrate that U87-MG cells used in their study do express ER $\alpha$  and ER $\beta$ ; however, they do not directly demonstrate the functional importance of these receptors in their study, only showing that the presence of estradiol (either endogenous or exogenously administered) slowed tumor progression. This data does not rule out GPR30 as the relevant functional estrogen receptor in these cells.

The finding that tamoxifen is effective at inhibiting growth in glioma cell lines as well as effective in clinical trials of patients with gliomas is particularly

intriguing in light of GPR30 expression in these tumors. Previously, the effects of tamoxifen in glioma have been described as estrogen receptor-independent and instead attributed to the ability of tamoxifen to inhibit protein kinase C (PKC) (Pollack et al. 1990; Zhang et al. 2000) and further shown to be dependent on NF- $\kappa$ B (Hui et al. 2004), as the cell lines used to investigate tamoxifen's role in glioma have been negative for expression of ER $\alpha$  and ER $\beta$ . In this study, we demonstrate that one of these ER $\alpha$ , ER $\beta$  negative cell lines, U87-MG, do express a third estrogen receptor, GPR30, and that GPR30 is functionally active in these cells to mediate signaling of both estrogen and tamoxifen. This finding could suggest another pathway for the role of tamoxifen in the inhibition of glioma growth that is independent of the classical estrogen receptors but is GPR30-dependent. Investigation of the involvement of GPR30 in preventing glioma could be undertaken using GPR30-knockout mice bearing U87-MG tumors and determining if estrogen or tamoxifen is capable of slowing tumor growth and extending survival in these mice lacking GPR30.

The data presented here support the importance of estrogen signaling in glioma and posit that this signaling is via GPR30. We suggest a role for GPR30 in the therapeutic effects of tamoxifen against gliomas and illustrate that GPR30 is a functional estrogen receptor in these cells. Finally, we present data showing the expression of GPR30 in human glioblastoma tissue and the co-expression of GPR30 and GFAP in tumor astrocytes.

## 5.2.5 MATERIALS & METHODS

**5.2.5.1 Reagents** E2, 4-hydroxytamoxifen, raloxifene, genistein and LY294002 were from Sigma. AG1478 was from Calbiochem. DPN, PPT and ICI182,780 were from Tocris Chemicals. G-1, G15 and G36 were synthesized by Dr. Jeff Arteburn at New Mexico State University. Goat anti rabbit Alexa488-conjugated, goat anti rabbit Alexa-568 and donkey anti mouse Alexa568-conjugated secondary antibodies were from Invitrogen. Rabbit antiGPR30 C-terminal antibody was made by New England Peptide, Inc. Mouse anti-human GFAP antibody (catalog #M0761) was obtained from DakoCytomation. Earle's MEM media and RPMI 1640 were obtained from Fisher Sciences. 32% paraformaldehyde (PFA) was obtained from Electron Microscopy Sciences.

**5.2.5.2 Cell culture and transfection** U87MG cells were cultured in Earle's MEM containing nonessential amino acids (Gibco), 1mM sodium pyruvate, 10% fetal bovine serum, 2 mM L-glutamine, 100 units/mL penicillin and 100 µg/mL streptomycin. Cells were grown as a monolayer at 37°C, in a humidified atmosphere of 5% CO<sub>2</sub> and 95% air. For microscopy experiments, cells were seeded onto 12 mm glass coverslips and allowed to adhere for at least 24 hr prior to antibody staining or 12 hr prior to transfection. 24 hr before PI3K experiments were completed, media was replaced with serum-free, phenol-red free RPMI 1640. For experiments requiring GPR30 knockdown or transient transfection of PH-mRFP, Lipofectamine2000 (Invitrogen) was used according to manufacturers instruction. PH-mRFP vector was transfected at ¼ the recommended amount to achieve appropriate expression levels and in



experiments requiring both GPR30 knockdown and PH-mRFP transfection, PH-mRFP was transfected into cells 24 hr following GPR30 knockdown transfection in 6-well plates and cells were reseeded onto 12 mm glass coverslips for staining. siRNA was transfected into cells 72 hr prior to antibody staining or use in functional assays.

**5.2.5.3 Immunofluorescence staining** Cells were plated on 12 mm glass coverslips and fixed with 2% PFA in PBS for 15 min at 37°C. Coverslips were washed three times with PBS and blocked/permeabilized for 1 hr with 0.05% Triton X-100 and 3% bovine serum albumen in PBS. Primary antibody was diluted in 3% normal goat serum and coverslips were incubated for 4 hr at room temperature. Coverslips were washed three times with PBS and incubated with secondary antibody diluted in 3% normal goat serum. Coverslips were washed three times and mounted with Vectashield containing DAPI (Vector Labs). Confocal images were collected on a Zeiss LSM 510 confocal microscope. Staining of tissue sections followed a similar protocol with the following changes; cryosections (8-10  $\mu$ M) were fixed for 30 min in 2% PFA at 37°C and primary antibody was incubated overnight at 4°C.

**5.2.5.4 PI3K Activation** The PIP3 binding domain of Akt fused to mRFP1 (PH-RFP) was used to assess production and localization of PIP3 by PI3K activation as previously described (Revankar et al. 2005). Briefly, cells were transfected with PH-RFP (and GPR30 siRNA, as appropriate), plated on 12 mm glass coverslips and serum starved for 24 hr. Cells were treated with inhibitors and stimulated as indicated. Following 15 min stimulation, cells were fixed with

2% PFA in PBS for 15 min at 37°C, washed three times with PBS and mounted using Vectashield with DAPI. Confocal images were collected on a Zeiss LSM 510 confocal microscope.

**5.2.5.5 Inhibitors** Inhibitors were used as follows (concentration, preincubation time): AG1478 (25  $\mu$ M, 60 min), LY294002 (10 $\mu$ M, 20 min), G15 (1 $\mu$ M, 20 min), G36 (1 $\mu$ M, 20 min). All inhibitors were present during ligand stimulation.

## 5.2.6 ACKNOWLEDGEMENTS

This work was supported by NIH R01 CA127731 (to ERP). Confocal images in this study were generated in the Fluorescence Microscopy Facility, which received support from the University of New Mexico Health Sciences Center and the University of New Mexico Cancer Center as detailed: <http://hsc.unm.edu/crtc/microscopy/Facility.html>.

## 5.2.7 FIGURE LEGENDS

**5.2.7.1 Figure 5.1. Expression of GPR30 in U87-MG cells** U87-MG cells were stained with DAPI and antibody to GPR30. **A)** Staining of endogenous GPR30 in U87-MG. Top panel, preimmune rabbit serum control. Middle panel, staining of GPR30 at 40x magnification. Lower panel; higher magnification staining of GPR30 to better show sub-cellular localization, DAPI not shown for better visualization of GPR30 staining. **B)** Staining of GPR30 in U87-MG treated with GPR30 siRNA. Top panel, preimmune rabbit serum. Middle panel, control siRNA transfection with scrambled siRNA. Lower panel, transfection with anti-GPR30 siRNA. Data are representative of three independent experiments.

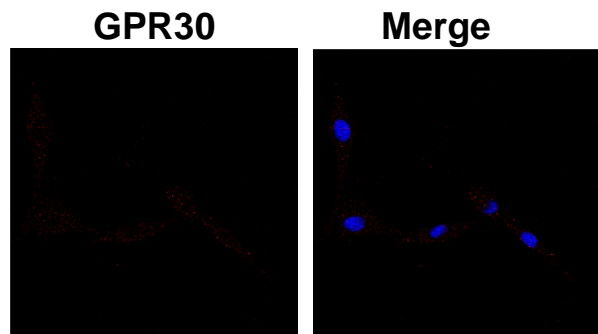
**5.2.7.2 Figure 5.2. GPR30 activates PI3K in U87-MG cells** U87-MG cells were transfected with Akt-PH-mRFP1 to assess PIP3 localization. Nuclear PIP3 accumulation indicates GPR30 activation. **A)** Cells treated for 15 min with compounds as indicated. **B)** Cells transfected with control siRNA or GPR30 siRNA were treated as indicated. **C)** Cells treated with estrogen or G-1 and inhibitors of GPR30 signaling as indicated. Data are representative of three independent experiments.

**5.2.7.3 Figure 5.3. GPR30 is expressed in astrocytes in human glioblastoma** Cryosections from a glioblastoma and from normal tissue outside of tumor margins were costained for GPR30 and GFAP expression. **A)** Confocal images at 63x. **B)** Confocal images at 40x.

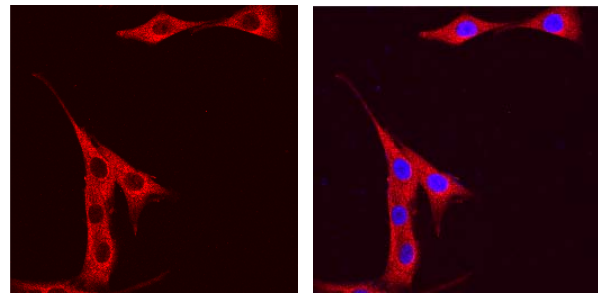
### 5.2.7.1 Figure 5.1

**A**

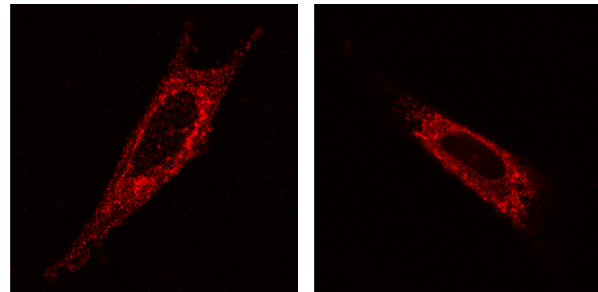
Preimmune serum  
40x



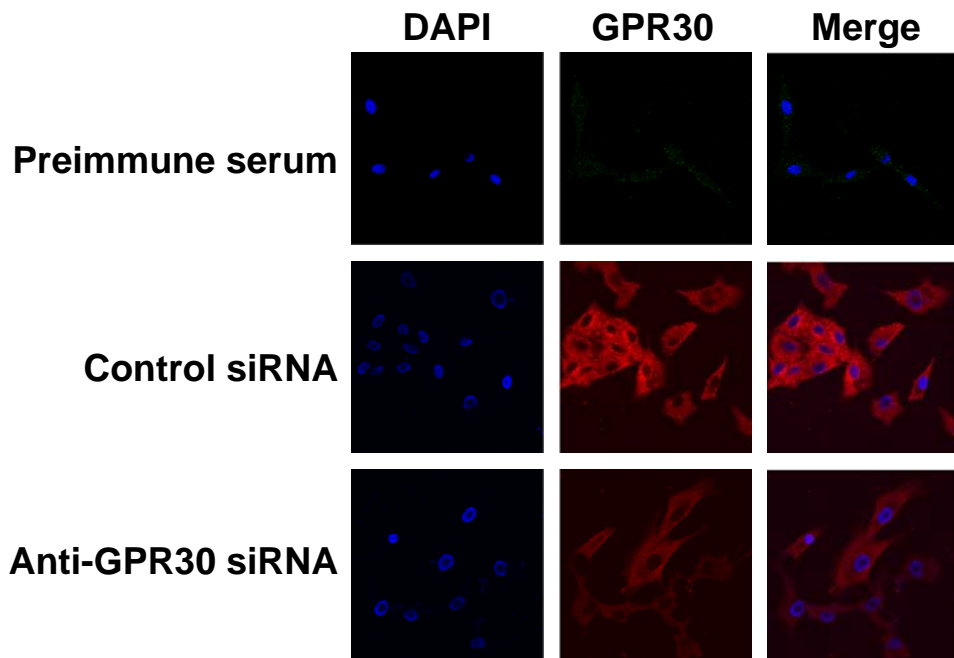
GPR30  
40x



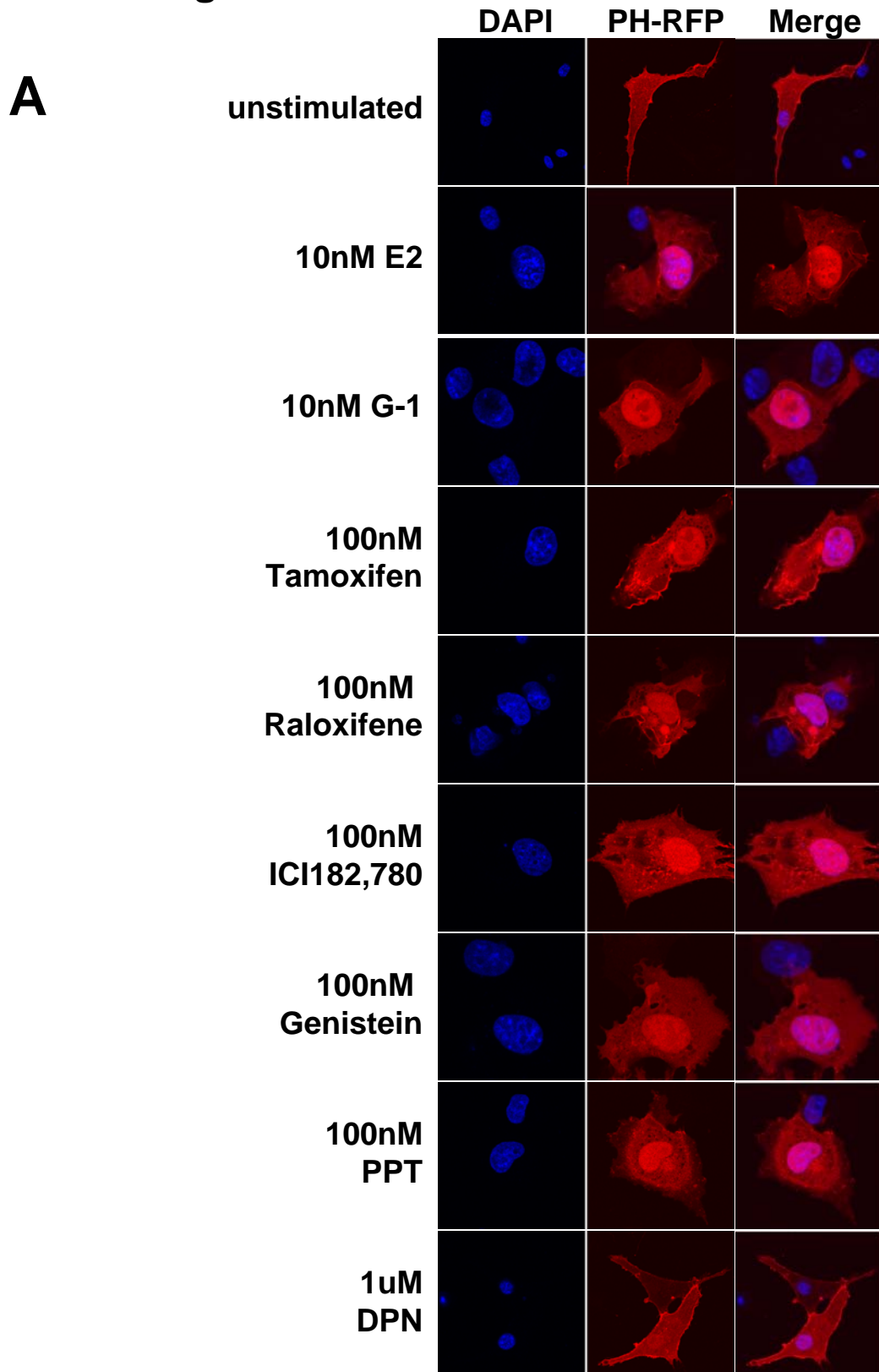
GPR30  
63x



**B**

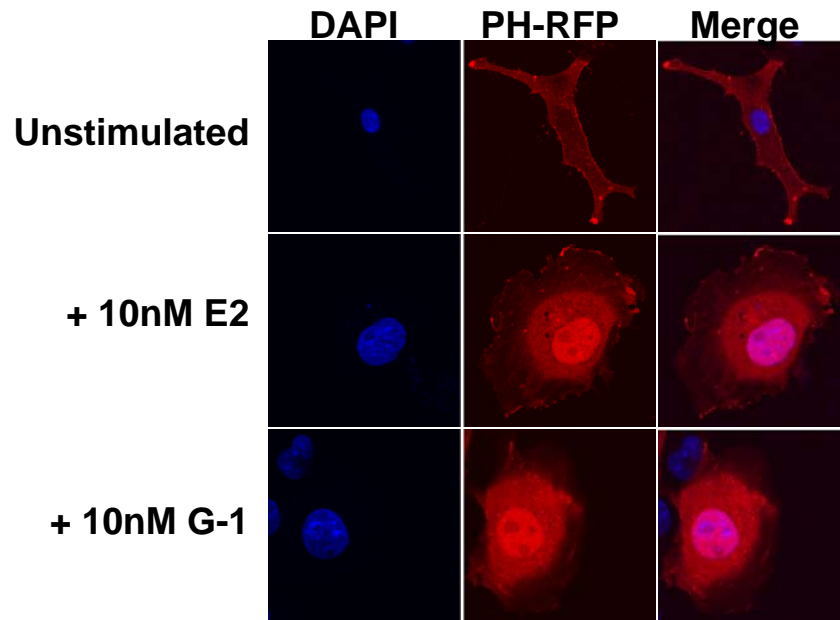


### 5.2.7.2 Figure 5.2

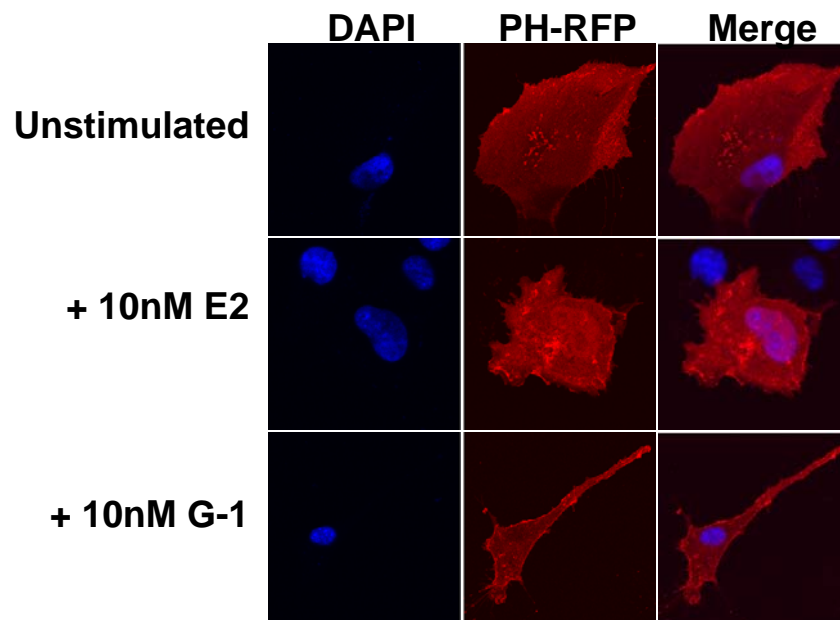


### 5.2.7.2 Figure 5.2

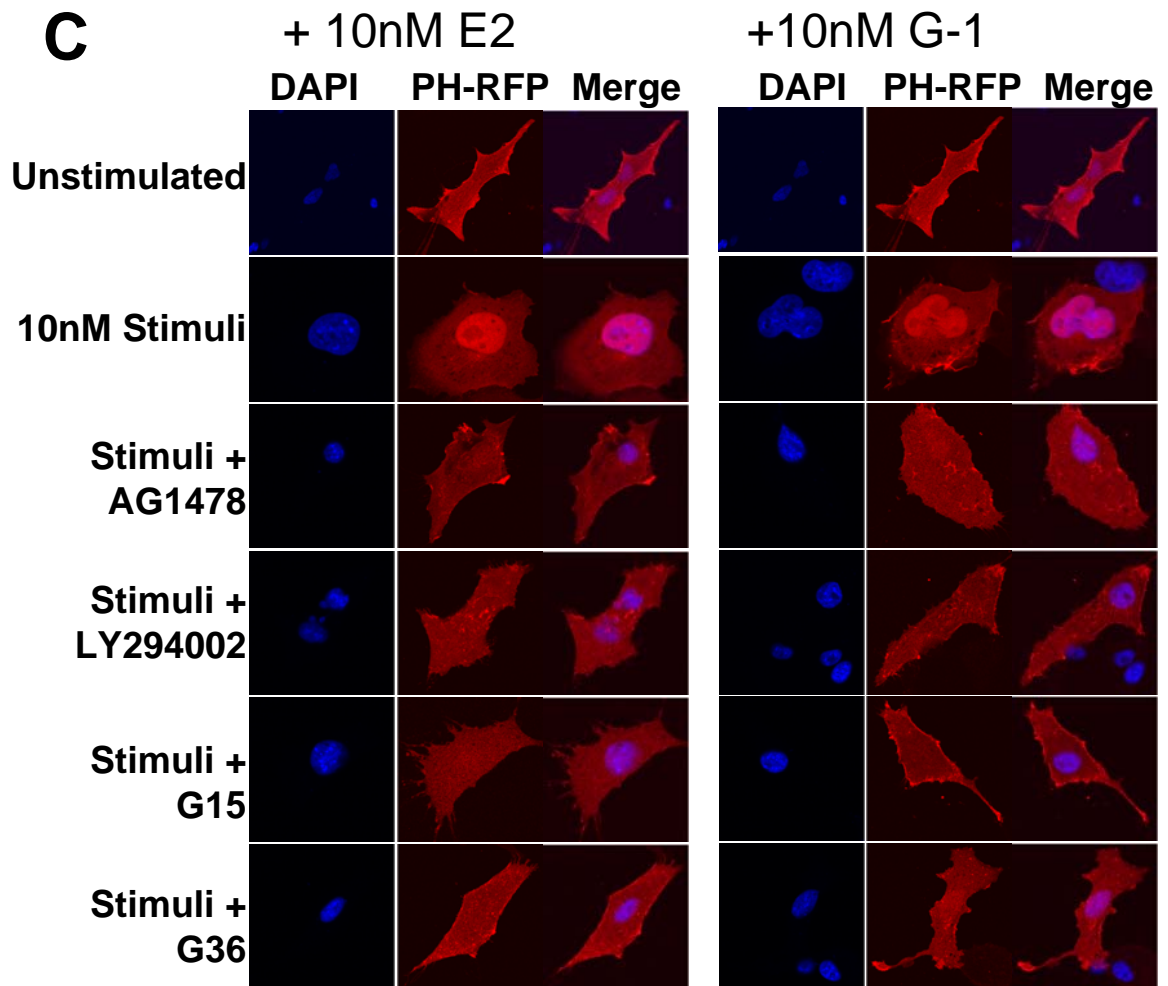
#### **B** Control siRNA transfected



#### Anti-GPR30 siRNA



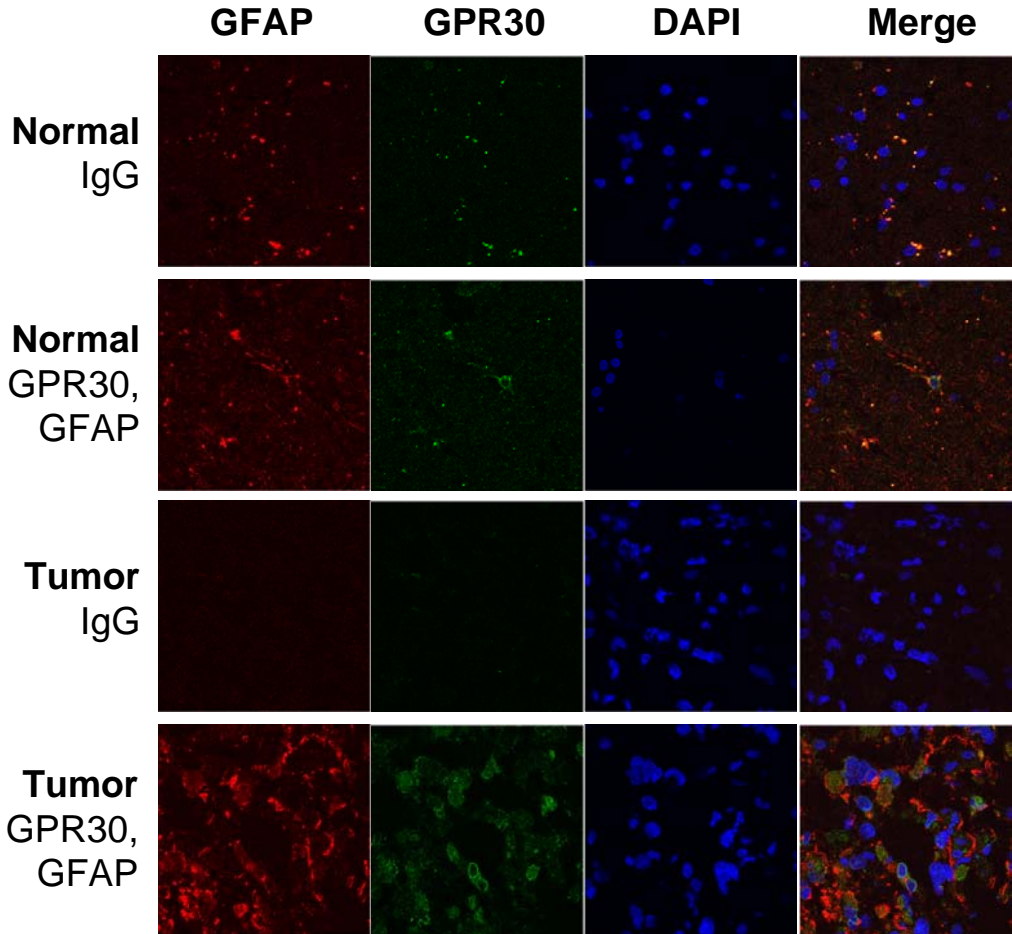
### 5.2.7.2 Figure 5.2





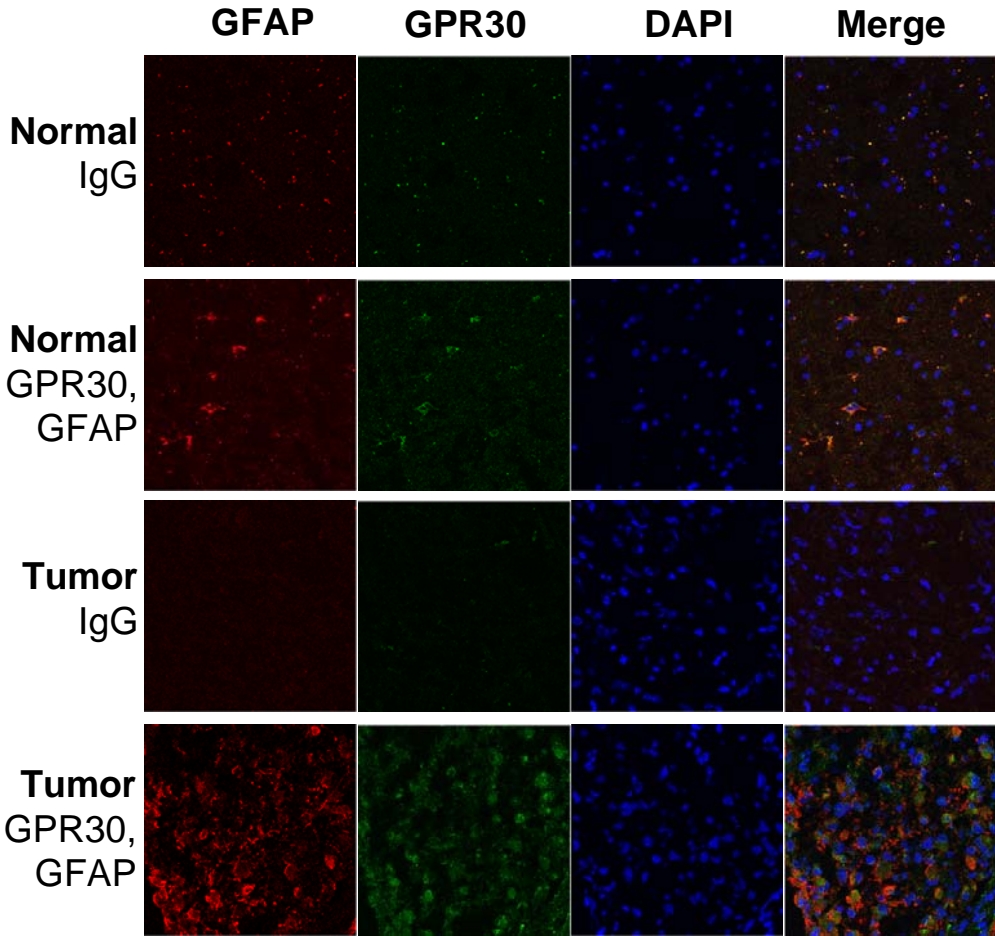
5.2.7.3 Figure 5.3

**A**



5.2.7.3 Figure 5.3

**B**



## 5.2.6 CONCLUSION

This work demonstrates the functional expression of GPR30 in a glioblastoma cell line and further complicates the web of effects that estrogen and tamoxifen have in this cancer, which does not typically express either classical ER. While malignant gliomas still carry a very poor survival prognosis, tamoxifen treatment of some patients has led to increased survival in a few small trials and the molecular basis of this therapy has never been fully explored. It would be intriguing to determine the GPR30 status of tumors that respond to tamoxifen treatment and further investigate the potential role of GPR30 in mediating this response. Additionally, the findings in rat models of human glioma that estrogen increases survival have not been followed up on a molecular level: one study shows that U87 cells in the xenograft express both ER $\alpha$  and ER $\beta$  (Barone et al. 2009), while two additional studies show that those cells do not express classical ERs (Plunkett et al. 1999; Hui et al. 2004) but that estrogen is still capable of extending survival. These results point to a classical ER-independent role for estrogen in this tumor model and, again, GPR30 may play a role since it is expressed and functionally active in U87 cells as shown in this chapter. The work in this chapter also builds upon the previous chapter wherein two GPR30-selective antagonists were identified and characterized and further illustrates the utility of these antagonists in a cell system to demonstrate a lack of classical ER functionality when all effects of E2 on PI3K signaling are blocked using either GPR30 selective antagonist.

# 6 GPR30 *in vivo* IMAGING AGENTS

## 6.1 Introduction

Tumor imaging is a field that has greatly advanced in recent years. Advances in radiolabeled ligands for specific targets overexpressed in tumor tissue have allowed the tracking of a specific type of tumor and can enable the analysis of receptor expression in tumors without requiring invasive procedures such as biopsy (Chodosh and Cardiff 2006; Mankoff et al. 2008). One of the first widely employed tumor imaging modalities utilized  $^{18}\text{F}$ -fluorodeoxyglucose (FDG) and positron emission scanning (PET) to detect cells with increased metabolic activity, which typically corresponds to tumor cells both in the primary tumor as well as in distant metastases (Coleman 2000). FDG-PET can also be used to monitor the effects of different treatments on tumor size and growth, by comparing scans of tumors prior to treatment with those taken after treatment (Coleman 2000). As an advance from FDG, ligands for specific receptors have been labeled with  $^{18}\text{F}$  in order to visualize tumors based on receptor overexpression and ectopic expression of receptors in tissue not typically known to express a certain receptor. One example of this is  $16\alpha\text{-}^{18}\text{F}\text{-}17\beta\text{-estradiol}$  (FES), which has been successfully used to image estrogen receptor expression in tumors, both for tumor detection as well as to determine the efficacy of different treatment modalities (Van de Wiele et al. 2000). In addition to FES, other ligands have also been investigated in pre-clinical models and small clinical studies for ER imaging *in vivo*. These include  $16\alpha\text{-}^{77}\text{Br}\text{-E2}$  and  $16\alpha\text{-}^{123}\text{I}\text{-E2}$ , both of which are taken up specifically in ER-positive tumors as seen in small patient studies (Van de Wiele et al. 2000). Additionally, labeling of tamoxifen with  $^{123}\text{I}$

has also allowed for tumor imaging *in vivo* (Van Den Bossche and Van de Wiele 2004).

Tumor imaging can be accomplished by a variety of modalities, including CT, ultrasound, PET and SPECT (Van Den Bossche and Van de Wiele 2004; Chodosh and Cardiff 2006). PET and SPECT can be used to image distribution of radioligands, whereas CT and ultrasound are used to image tumor mass, reconstruct 3D images of tumors and image fluid flow within and around tumors (Chodosh and Cardiff 2006). PET images are generated by tracing positron-emitting isotopes, including  $^{18}\text{F}$ ,  $^{11}\text{C}$  and  $^{15}\text{O}$ . SPECT images are generated by imaging gamma-emitting isotopes including  $^{111}\text{In}$ ,  $^{99\text{m}}\text{Tc}$  and  $^{123}\text{I}$ . Both SPECT and PET imaging isotopes can be integrated into selective ligands for a given receptor, as in FES, for tumor imaging.

Radioligands have similar requirements to pharmacological compounds. First, the ligand must bind specifically to the receptor of interest with high affinity and the radioligand must have a high specific activity such that sub-physiologic doses of the radioligand can image receptors without activating the receptor. Additionally, this prevents saturation of the receptor with excess unlabeled or poorly labeled ligand and allows PET/SPECT detectors to successfully image the tumor tissue. Also, the radioligand must have a low signal-to-noise ratio so that background binding is low and does not interfere with tumor visualization, and metabolism of the radioligand must be slow enough that imaging can be completed prior to metabolism of the injected compound (Liu 2008).

With the description of the GPR30-selective ligand G-1 (Bologa et al. 2006), as well as the observation that GPR30 expression in ovarian (Smith et al. 2009), endometrial (Smith et al. 2007) and inflammatory breast cancers (Arias-Pulido et al. 2009) is often of prognostic value, we undertook two studies to characterize ligands for *in vivo* imaging based on the G-1 scaffold. One study looks at the development of <sup>125</sup>I-labeled G-1 derivatives for SPECT/CT imaging while the other investigates <sup>111</sup>In-labeled derivatives also used in SPECT/CT small animal imaging studies.

## 6.2 Characterization of Iodinated GPR30 Imaging Agents

### 6.2.1 ABSTRACT

A series of iodo-substituted molecules based on the G-1 structure was synthesized as potential targeted imaging agents for the G protein-coupled estrogen receptor GPR30. The affinity and specificity of binding to GPR30 versus the classical estrogen receptors ER $\alpha$ / $\beta$  and functional responses associated with ligand-binding were determined. Selected iodo-substituted G-1 derivatives exhibited IC<sub>50</sub> values lower than 20 nM in competitive binding studies with GPR30-expressing human endometrial cancer cells. These compounds functioned as antagonists of GPR30 and blocked estrogen-induced PI3K activation and calcium mobilization. The tributylstannyl precursors of selected compounds were radiolabeled with <sup>125</sup>I using the iodogen method. *In vivo* biodistribution studies in female ovariectomized athymic (NCr) nu/nu mice bearing GPR30-expressing human endometrial tumors revealed GPR30-mediated uptake of the radiotracer ligands in tumor, adrenal and reproductive organs. Quantitative SPECT/CT studies revealed significant differences in the pharmacokinetic profiles, and *in vivo* characteristics of these radioligands, suggesting possible modifications to improve targeting characteristics.



## 6.2.2 INTRODUCTION

Estrogen is a critical hormone that regulates a multitude of biological processes. The nuclear estrogen hormone receptors ( $ER\alpha$  and  $ER\beta$ ) are best characterized for their regulation of gene expression and consequently are important targets in many disease states that include cancer (Deroo and Korach 2006), cardiovascular disease (Friedrich et al. 2006), skeletal (Termine and Wong 1998), neurological (Hurn and Macrae 2000) and immunological conditions (Dai et al. 2009). The identification of GPR30, a GPCR estrogen receptor (GPER/GPR30; Filardo et al. 2000; Revankar et al. 2005; Thomas et al. 2005), has introduced additional complexity to the web of estrogen signaling through both genomic and non-genomic mechanisms. Thus far, GPR30 function overlaps that of  $ER\alpha$  and  $ER\beta$  in many cases, although in some systems one or more of the three estrogen receptors has been demonstrated to be crucial for function (Prossnitz et al. 2008). Additionally, the ligand specificity beyond E2 is different for the three receptors, with compounds such as the selective estrogen receptor mediator tamoxifen and the anti-estrogen ICI182,780 acting as antagonists of  $ER\alpha/ER\beta$  function but as an agonists of GPR30 (Filardo et al. 2000; Revankar et al. 2005). Studies with breast, ovarian and endometrial cancers indicate roles for both  $ER\alpha/\beta$  and GPR30 in tumorigenesis and suggest the potential for clinical diagnostic and prognostic applications based on receptor expression (Filardo et al. 2006; Smith et al. 2007; Arias-Pulido et al. 2009; Smith et al. 2009). Determining the unique signaling pathways and resultant physiological changes downstream of each estrogen receptor will lead to a greater understanding of

disease as well as of normal physiology and may lead to the development of drugs targeting a single receptor which could be useful therapeutics for treating various estrogen related diseases.

The first GPR30-selective ligand, an agonist named G-1, was identified using virtual and biomolecular screening approaches (Bologa et al. 2006). G-1 has been shown to signal specifically via GPR30 and has been extensively used to probe GPR30 function both *in vivo* and *in vitro* (Albanito et al. 2007; Brailoiu et al. 2007; Albanito et al. 2008; Alyea et al. 2008; Kamanga-Sollo et al. 2008; Madak-Erdogan et al. 2008; Otto et al. 2008; Pang et al. 2008; Sirianni et al. 2008; Teng et al. 2008; Wang et al. 2008; Dun et al. 2009). Recently, we have described the identification and characterization of a GPR30-selective antagonist, G15, discovered through a combined effort including synthetic chemistry, virtual and biomolecular screening through the New Mexico Molecular Libraries Screening Center (Dennis et al. 2009). G15 effectively blocks GPR30 function in cells expressing GPR30 but has no effect on ER $\alpha$  or ER $\beta$  mediated signaling via either PI3K or by interfering with E2-induced intracellular calcium release. This intriguing pair of compounds, which share a similar structural scaffold, have the potential to greatly enhance future studies of GPR30 by allowing investigators to probe the function of GPR30 using a selective agonist as well as an antagonist to investigate the physiological roles of GPR30 in normal and disease states.

The use of radiolabeled ligands to investigate estrogen receptor function would allow for characterization and identification of GPR30 in live animals and in

tumor models. The commercial availability of [ $^3\text{H}$ ]-17 $\beta$ -estradiol has facilitated the characterization of receptor distribution and ligand binding of the classical estrogen receptors using cellular extracts, cell culture and *in vivo* models. The increased use of PET and SPECT to image positron- and gamma-emitting isotopes, respectively, has greatly advanced the field of tumor imaging and the use of radiolabeled estrogen derivatives in particular has advanced the field of *in vivo* estrogen receptor imaging, both in small animal models as well as in the clinic (Hochberg and Rosner 1980; Katzenellenbogen et al. 1980; Cummins 1993; Hanson 2000; Van de Wiele et al. 2000). [ $^{18}\text{F}$ ]-FES has been used in the clinic to visualize both primary tumors as well as distant metastases, as well as to determine receptor expression to predict tumor response to therapy and visualize tumor response following therapy (McGuire et al. 1991; Yoo et al. 2005; Linden et al. 2006; Yoshida et al. 2007). Additionally,  $^{123}\text{I}$ -labeled 11 $\beta$ -methoxy-iodovinylestradiol has been used to image estrogen receptor status in breast cancer (Rijks et al. 1997).  $^{125}\text{I}$ -based radioligands possess high specific activity and can be detected with great sensitivity which allows for a range of experimental studies including receptor binding studies, and allows efficient determination of receptor content in tissues and convenient detection and quantification of images. The development of GPR30-selective radiotracers would have significant value for characterizing receptor binding properties and investigations of imaging applications based on targeting this receptor.

Herein we report the synthesis of a series of iodo-substituted quinoline derivatives **1-7** as selective ligands and potential targeted imaging agents for

GPR30. These compounds were evaluated against a panel of functional and competitive ligand binding assays using GPR30 and ER $\alpha$ / $\beta$  transfected Cos7 as well as Hec50 and SKBr3 cells, which endogenously express only GPR30, to evaluate receptor selectivity and potential cross-reactivity. Selected derivatives **6** and **7** were demonstrated to be GPR30-selective antagonists. The corresponding tributylstannane derivatives were radiolabeled with  $^{125}\text{I}$  and used to determine GPR30 receptor binding affinity in cell culture, and to evaluate biodistribution and *in vivo* imaging in a mouse tumor model.

### 6.2.3 RESULTS AND DISCUSSION

The iodinated compounds **1-7** were evaluated in cell-based binding and functional assays to determine the potency and type of signaling response (agonism or antagonism) associated with ligand-induced GPR30- and ER $\alpha/\beta$ -mediated signaling as shown in **Tables 6.1 and 6.2**. These compounds were profiled using transfected Cos7 cells expressing GPR30, ER $\alpha$  or ER $\beta$ , in addition to Hec50 and SKBr3 cells, which endogenously express only GPR30. Functional characterization of the compounds using either the extent (or inhibition of E2-mediated increase) in intracellular calcium or the activation of PI3K as measured by production of PIP3 in the nucleus, as previously described (Revankar et al. 2005; Bologna et al. 2006; Dennis et al. 2009). The specificity of the response in these assays was demonstrated in control Cos7 cells that do not endogenously express GPR30 or ER $\alpha/\beta$ . The comparison of the observed ligand-induced responses across cells expressing individual receptors in comparison to estrogen-induced responses, in addition to comparison of differential binding to receptors, provides a profile of the selectivity/cross-reactivity of the compounds.

We have previously shown the specificity of binding of the GPR30-selective ligand **G-1** to GPR30 versus the classical estrogen receptors ER $\alpha/\beta$  using cell-based competitive binding assays (Bologna et al. 2006). In order to characterize the selectivity of iodinated compounds **1-7**, the same cell based assay employing transfected Cos7 cells was used to evaluate binding of these compounds to the classical estrogen receptors. These assays confirmed that compounds **1, 3** and **6**, like **G-1**, do not exhibit binding to either of the classical

estrogen receptors ER $\alpha$ / $\beta$ . Compounds **2**, **4** and **5** exhibited minimal binding to ER $\alpha$  at high concentrations (blocking less than 35% of E2-Alexa633 binding when present at 10  $\mu$ M). Hydrazone **7** was the only iodinated derivative to show any detectable binding to ER $\beta$ , which was also minimal. These low levels of competition at 10  $\mu$ M compare to an IC<sub>50</sub> for estrogen in the same assay of approximately 0.4 nM (Bologa et al. 2006).

Cell-based functional assays for compounds **1-7** were carried out in parallel to binding studies in order to assess the functional characteristics of this series of compounds. Stimulation of cells expressing ER $\alpha$  or GPR30 results in the receptor-dependent activation of PI3K which can be visualized using the pleckstrin homology (PH)-domain of Akt fused to RFP (PH-RFP), which serves as a reporter of PIP3 localization. Receptor activation leads to the translocation of this reporter from a cytoplasmic or plasma membrane-associated localization to the nucleus (Revankar et al. 2005; Bologa et al. 2006; Dennis et al. 2009). We evaluated the ability of compounds **1-7** alone to induce PI3K activation or the ability of these compounds to block estrogen-stimulated PI3K activation to determine the agonist and antagonist properties of each compound in transfected Cos7 cells expressing ER $\alpha$  or GPR30; additionally Cos7 cells transfected with PH-RFP reporter alone were treated with all compounds to confirm that the results in receptor-transfected cells were receptor-dependent. As expected due to their lack of binding to ER $\alpha$ , compounds **1-6** were unable to induce either activation of PI3K or inhibit estrogen-induced PI3K activation in ER $\alpha$  transfected Cos7 cells. Compound **7**, which exhibited very weak binding to ER $\alpha$  was also

unable to influence PI3K activity in ER $\alpha$ -transfected Cos7 cells. Additionally, none of compounds **1-7** was able to activate PI3K in Cos7 cells lacking estrogen receptor expression. Thus, none of the seven iodinated derivatives shows any functional activity mediated through ER $\alpha$  or any ability to activate PI3K via other mechanisms. Compound **1** showed strong GPR30-dependent activation of PI3K as expected for an isostructural analog of **G-1**. A regioisomeric dependence of iodide substitution on GPR30-mediated PI3K activation was observed for compounds **2-5**. Compounds **2** and **5** exhibited partial agonist properties on PI3K, acting as agonists when applied to cells in the absence of estrogen but also demonstrating the ability to inhibit the full activation of PI3K by estrogen. Compound **3** was a weaker agonist of PI3K than **1**, and compound **4** had no functional effect. Compounds **6** and **7** were able to block the estrogen-induced PI3K activation via GPR30 and thus appear to function as antagonists of GPR30 function in this context.

As rapid signaling via GPR30 results in increased intracellular calcium levels (Revankar et al. 2005), we investigated whether compounds **1-7** had similar agonist and antagonist properties in a cell-based calcium assay using SKBr3 cells, which endogenously express only GPR30. In these cells, stimulation with GPR30 agonists, including estrogen and **G-1**, elicits a rapid increase in intracellular calcium levels that can be easily monitored using the cell-permeant fluorescent calcium indicator Indo-1. Consistent with the PI3K activation profiles, compounds **6** and **7** blocked estrogen-induced calcium mobilization and thus functioned as antagonists of estrogen-mediated GPR30 function. Additionally,

compound **2** appears to weakly antagonize estrogen-mediated calcium mobilization. Compounds **1, 3, 4 & 5** can all be characterized as partial agonists in the context of this assay, as all compounds mobilize calcium when applied alone and all four compounds display some degree of inhibition of estrogen-mediated calcium mobilization. However, as in the PI3K assay, compound **1** is a potent agonist of calcium mobilization similar to **G-1**.

Some variability in compound profiles exists between the two GPR30 functional assays (i.e. compound **4** was inactive in the PI3K assay but a partial agonist of GPR30 in the calcium assay and compound **1** is a potent agonist in the PI3K assay and a partial, though still potent, agonist in the calcium assay). This is potentially due to the different cellular systems used in the assays and also may be related to assay sensitivity and the differing time courses of the assays. The PI3K assay employs ectopically expressed receptors in cells that may lack required cofactors for full compound activity; thus some compounds may elicit weaker or no responses in this system compared to a system in which cells with endogenous receptor are used, such as the calcium assay used to profile the compounds. Additionally, the PI3K assay is a phenotypic assay in which many fields of cells must be analyzed and an average response determined relative to control stimulated cells, whereas the calcium assay is a more quantitative assay in which smaller changes in signaling are more likely to be observed. Importantly, compounds **6** and **7** displayed consistent activity as antagonists of GPR30 function in both functional assays.



## 6.2.4 CONCLUSIONS

In this study, we developed a series of iodinated compounds that exhibit high affinity and selectivity towards GPR30 versus the classical estrogen receptors. The synthetic compounds were characterized using cell-based competitive binding and functional assays to identify binding affinity, specificity and agonist or antagonist response associated with receptor-mediated signaling pathways. Two compounds incorporating either conjugated phenylurea or hydrazone linkages, respectively, were selected for radiolabeling with  $^{125}\text{I}$  to provide **6\*** and **7\***. These compounds functioned as antagonists of GPR30-mediated calcium mobilization, and were used for competitive ligand binding assays in cell culture. Comparative *in vivo* studies were used to evaluate the biodistribution, pharmacokinetics and the potential for GPR30-targeted tumor imaging in an animal model. Although both radiotracers **6\*** and **7\*** exhibited receptor-mediated uptake in tumor, adrenal and reproductive organs, neither was effective for tumor imaging due to poor targeting characteristics, high background and issues with plasma protein binding and rapid metabolism. Both compound classes were significantly more lipophilic than either estradiol or the GPR30-selective probes **G-1** and **G15**, which likely contributes towards the observed non-target tissue uptake. The *in vivo* data obtained from this study provide valuable insight for the design of the next generation of GPR30-targeted radiotracers. We have previously described  $^{99\text{m}}\text{Tc}$ -labeled  $17\beta$ -estradiol derivatives that incorporate pyridin-2-yl-hydrazine chelates for SPECT imaging applications (Ramesh et al. 2006; Nayak et al. 2008). These studies suggest that

incorporating this  $^{99m}\text{Tc}$ -imaging modality into the tetrahydro-cyclopenta[c]quinoline scaffold could result in GPR30-selective agents with decreased lipophilicity, increased chemical and metabolic stability, reduced plasma-protein binding, and overall improvements in targeting characteristics for *in vivo* imaging applications.

## 6.2.5 MATERIALS & METHODS

**6.2.5.1 Intracellular calcium mobilization** SKBr3 cells ( $1 \times 10^7$ /mL) were incubated in HBSS containing 3  $\mu$ M Indo1-AM (Invitrogen) and 0.05% pluronic acid F-127 for 1 hr at RT. Cells were then washed twice with HBSS, incubated at RT for 20 min, washed again with HBSS, resuspended in HBSS at a density of  $10^8$  cells/mL and kept on ice until assay, performed at a density of  $2 \times 10^6$  cells/mL.  $\text{Ca}^{++}$  mobilization was determined ratiometrically using  $\lambda_{\text{ex}}$  340 nm and  $\lambda_{\text{em}}$  400/490 nm at 37°C in a spectrofluorometer (QM-2000-2, Photon Technology International) equipped with a magnetic stirrer. The relative 490/400 nm ratio was plotted as a function of time.

**6.2.5.2 PI3K activation.** The PIP3 binding domain of Akt fused to mRFP1 (PH-RFP) was used to localize cellular PIP3. Cos7 cells (cotransfected with GPR30-GFP or ER $\alpha$ -GFP and PH-RFP) or SKBr3 (transfected with PH-RFP) were plated on coverslips and serum starved for 24 hr followed by stimulation with ligands as indicated. The cells were fixed with 2% PFA in PBS, washed, mounted in Vectashield containing DAPI (Vector Labs) and analyzed by confocal microscopy using a Zeiss LSM510 confocal fluorescent microscope.

**6.2.5.3 Ligand binding assays** Binding assays for ER $\alpha$  and ER $\beta$  were performed as previously described (Revankar et al. 2005). Briefly, Cos7 cells were transiently transfected with either ER $\alpha$ -GFP or ER $\beta$ -GFP. Following serum starvation for 24 hr, cells ( $\sim 5 \times 10^4$ ) were incubated with compounds **1-7** for 10 min in a final volume of 10  $\mu$ L prior to addition of 10  $\mu$ L of 20 nM E2-Alexa633 in saponin-based permeabilization buffer. Following 5 min at RT, cells were

washed once with 1 mL PBS/2%BSA, resuspended in 200  $\mu$ L and analyzed on a FACS Caliber flow cytometer (BD Biosciences).

**6.2.5.4 Cell culture** ER $\alpha$ / $\beta$ -negative and GPR30-negative Cos7 cells and ER $\alpha$ / $\beta$ -negative and GPR30-expressing human endometrial carcinoma Hec50 cells were cultured in DMEM medium, fetal bovine serum (10%), 100 units/mL penicillin and 100  $\mu$ g/mL streptomycin. ER $\alpha$ / $\beta$ -negative and GPR30-expressing SKBr3 cells were cultured in RPMI-1640 medium, fetal bovine serum (10%), 100 units/mL penicillin and 100  $\mu$ g/mL streptomycin. Cells were grown as a monolayer at 37°C, in a humidified atmosphere of 5% CO<sub>2</sub> and 95% air.

**6.2.5.5 Statistical analysis** All numerical data were expressed as the mean of the values  $\pm$  the standard error of mean (S.E.M). Graphpad Prism version 4 (San Diego, CA, USA) was used for statistical analysis and a P value less than 0.05 was considered statistically significant.

## 6.2.6 ACKNOWLEDGEMENTS

This work was supported by NIH grants R01 CA127731 (JBA, ERP), CA116662 (ERP), U54MH074425 and U54084690 (LAS), the University of New Mexico Cancer Research and Treatment Center (NIH P30 CA118100), the New Mexico Cowboys for Cancer Research Foundation (JBA), Oxnard Foundation (ERP) and the Stranahan Foundation (ERP). Images in this paper were generated in the University of New Mexico Cancer Center Fluorescence Microscopy Facility, supported as detailed on the webpage: <http://hsc.unm.edu/crtc/microscopy/Facility.html>. Flow cytometry data was generated in the Flow Cytometry Shared Resource Center supported by the University of New Mexico Health Sciences Center and the University of New Mexico Cancer Center.

## **6.2.7 FIGURE LEGENDS**

**6.2.7.1 Figure 6.1. Structures of 17 $\beta$ -estradiol (E2), GPR30-selective agonist (G-1) and antagonist (G-15)**

**6.2.7.2 Figure 6.2. Structure of direct and pendant iodo-substituted tetrahydro-cyclopenta[c]quinoline derivatives.**

**6.2.7.3 Table 6.1. Binding and functional characterization of GPR30-targeted compounds (summary)**

**6.2.7.4 Table 6.2. Binding and functional characterization of GPR30-targeted compounds (raw data)**

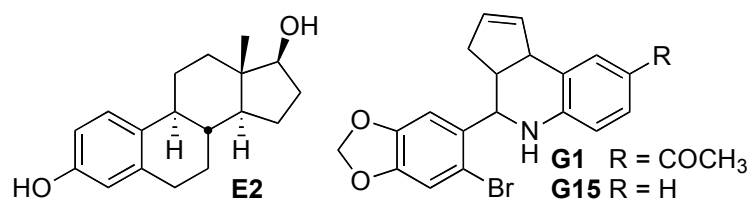


**Figure 6.1. Structures of 17β-estradiol (E2), GPR30-selective agonist (G-1) and antagonist (G-15)**

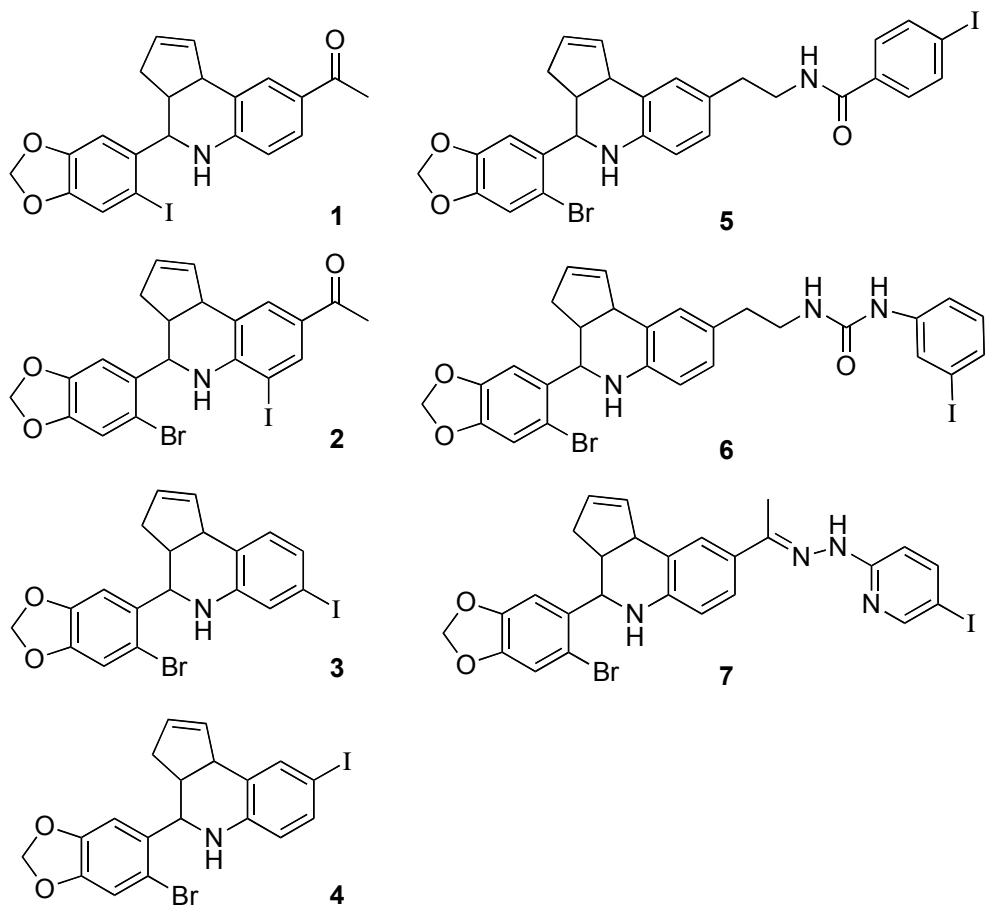


**Figure 6.2. Structure of direct and pendant iodo-substituted tetrahydro-cyclopenta[*c*]quinoline derivatives**



Compound	CLog P	ER $\alpha$ binding <sub>1</sub>	ER $\beta$ binding <sub>1</sub>	GPR30 binding (IC <sub>50</sub> )	GPR30 agonism (Calcium) <sub>2</sub>	GPR30 antagonism (Calcium) <sub>3</sub>	ER $\alpha$ agonism (PI3K) <sub>4</sub>	ER $\alpha$ antagonism (PI3K) <sub>5</sub>	GPR30 agonism (PI3K) <sub>4</sub>	GPR30 antagonism (PI3K) <sub>5</sub>
<b>E2</b>	3.37	+++	+++	3-6nM	+++	-	+++	-	+++	-
<b>G-1</b>	4.55	-	-	7nM	+++	-	-	-	+++	-
<b>1</b>	4.94	-	-	ND	+++	+/-	-	-	+++	-
<b>2</b>	5.82	-	+/-	ND	-	+	-	-	+/-	+/-
<b>3</b>	6.00	-	-	ND	+	+/-	-	-	+/-	-
<b>4</b>	6.00	-	+/-	1.7nM	+	+/-	-	-	-	-
<b>5</b>	6.71	-	+/-	16.2nM	+	+/-	-	-	++	+/-
<b>6</b>	7.00	-	-	8.4nM	-	++	-	-	-	+++
<b>7</b>	6.35	+/-	-	1.7nM	-	+	-	-	-	+

**Table 6.1 Binding and functional characterization of GPR30-targeted compounds (summary)**

<sup>1</sup> +/- denotes that 10 $\mu$ M compound blocks ~25% of 10nM E2-Alexa binding, - denotes <10% inhibition of E2 binding.

<sup>2</sup> +++ denotes calcium mobilization in response to 10  $\mu$ M compound is 80-100% of reference compound (E2), + denotes calcium mobilization in response to 10 $\mu$ M compound is 20-40% of reference compound

<sup>3</sup> ++ denotes 10 $\mu$ M compound blocks 80-100% of E2-induced calcium mobilization, + denotes 10 $\mu$ M compound blocks 50-60% of E2-induced calcium mobilization, +/- denotes 10 $\mu$ M compound blocks less than 50% of E2-induced calcium mobilization

<sup>4</sup> +++ denotes activation of PI3K similar by 10 $\mu$ M compound similar to activation induced by 10nM reference compound (E2), ++ and +/- denote decreased activation of PI3K (qualitative assay)

<sup>5</sup> +++ denotes complete antagonism of 10nM E2-induced PI3K activation by 10 $\mu$ M compound, + and +/- denote lesser degrees of antagonism of 10nM E2-mediated PI3K activation by 10 $\mu$ M compound

Compound	CL <sub>og</sub> P	ER $\alpha$ binding <sup>1</sup>	ER $\beta$ binding <sup>1</sup>	GPR30 binding (IC <sub>50</sub> )	GPR30 agonism (Calcium) <sup>2</sup>	GPR30 antagonism (Calcium) <sup>3</sup>	ER $\alpha$ agonism (PI3K) <sup>4</sup>	ER $\alpha$ antagonism (PI3K) <sup>5</sup>	GPR30 agonism (PI3K) <sup>4</sup>	GPR30 antagonism (PI3K) <sup>5</sup>
<b>E2</b>	3.37	78.2 $\pm$ 3.4 %	75.9 $\pm$ 6.2 %	3-6nM <sup>6</sup>	100 %	n/a	+++	-	+++	-
<b>1</b>	4.55	9.5 $\pm$ 4.1 %	11.2 $\pm$ 5.1 %	7.1nM <sup>7</sup> (2.5-20nM)	81.3 $\pm$ 2.4 %	n/a	-	-	+++	-
<b>3</b>	4.94	-9.6 $\pm$ 15.1 %	-4.6 $\pm$ 7.0 %	ND	89.2 $\pm$ 2.9 %	44.4 $\pm$ 2.4%	-	-	+++	-
<b>4</b>	5.82	11.5 $\pm$ 10.5 %	28.3 $\pm$ 3.9 %	ND	7.2 $\pm$ 0.8 %	62.8 $\pm$ 1.9 %	-	-	+/-	+/-
<b>5</b>	6.00	-4.1 $\pm$ 3.3 %	6.5 $\pm$ 2.7 %	ND	22.3 $\pm$ 3.1 %	41.8 $\pm$ 4.6 %	-	-	+/-	-
<b>6</b>	6.00	-2.9 $\pm$ 3.4 %	24.8 $\pm$ 2.0 %	1.7nM (0.6-4.5nM)	22.0 $\pm$ 7.7 %	49.3 $\pm$ 4.8 %	-	-	-	-
<b>7</b>	6.71	1.5 $\pm$ 5.2 %	25.9 $\pm$ 5.5 %	12.8nM (4.7-34nM)	24.5 $\pm$ 4.9 %	46.5 $\pm$ 2.8 %	-	-	++	+/-
<b>8</b>	7.00	6.8 $\pm$ 5.0 %	10.0 $\pm$ 3.0 %	8.4nM (3.4-20nM)	5.9 $\pm$ 3.0 %	80.1 $\pm$ 2.2 %	-	-	-	+++
<b>9</b>	6.35	30.5 $\pm$ 3.8 %	3.8 $\pm$ 6.7 %	1.7nM (0.7-4.4nM)	7.6 $\pm$ 3.7 %	67.7 $\pm$ 4.8 %	-	-	-	+

**Table 6.1 Binding and functional characterization of GPR30-targeted compounds (data)**

- <sup>1</sup> denotes % inhibition of 10nM E2-Alexa binding by 10 $\mu$ M compound.
- <sup>2</sup> calcium mobilization in response to 10  $\mu$ M compound normalized to 200 nM E2 (100%).
- <sup>3</sup> denotes inhibition of 200 nM E2-induced calcium mobilization by 10 $\mu$ M compound.
- <sup>4</sup> +++ denotes activation of PI3K by 10 $\mu$ M compound similar to activation induced by 10nM reference compound (E2), ++ and +/- denote decreased activation of PI3K (qualitative assay).
- <sup>5</sup> +++ denotes complete antagonism of 10nM E2-induced PI3K activation by 10 $\mu$ M compound, + and +/- denote lesser degrees of antagonism of 10nM E2-mediated PI3K activation by 10 $\mu$ M compound.
- <sup>6</sup> from refs. 5-6.
- <sup>7</sup> values in parentheses represent 90% confidence intervals.

### 6.3 Segue

The biological characterization of the GPR30-selective molecules **1-7** in the series of iodo-substituted GPR30 ligands was used to identify two lead molecules for radiolabeling and *in vivo* tumor imaging studies. The *in vivo* characteristics of these two compounds were not optimal for radioimaging agents, with relatively high background uptake and rapid metabolism of the compounds, which did not allow sufficient time for effective tumor imaging. However, these compounds, along with previously described  $^{99m}\text{Tc}$ -labeled  $17\beta$ -estradiol derivatives (Ramesh et al. 2006; Nayak et al. 2008), add to our knowledge of radioligand design for GPR30-targeted compounds. With this knowledge in mind, we set out to biologically characterize a small set of G-1 related compounds that could be radiolabeled with  $^{111}\text{In}$  for SPECT imaging.

## 6.4 Synthesis and Characterization of Indium Labeled GPR30 Imaging Agents

### 6.4.1 ABSTRACT

Estrogen is an important signaling molecule in a wide range of normal and disease states. Estrogenic signaling is propagated through three receptors, the classical estrogen receptors ER $\alpha$  and ER $\beta$ , as well as the recently described G protein-coupled estrogen receptor GPR30. The development of the GPR30-selective ligands G-1 and G15 has led to the desire for GPR30-selective radiotracers for use in imaging GPR30 expression in tumors. The overexpression of GPR30 in breast, ovarian and endometrial cancers correlates with poor prognosis suggesting that imaging of GPR30 in tumors could be of prognostic value and generation of GPR30-targeted ligands may be of therapeutic use. We describe the biologic characterization of a set of charged and neutral G-1-based ligands and the use of these ligands for *in vivo* small animal SPECT imaging and demonstrate that GPR30-targeted ligands must have a neutral charge in order to effectively bind GPR30. Tumor imaging studies suggest that, as with previously described GPR30-targeted radiotracers, there is high background in non-tumor tissue and the compounds are rapidly metabolized and, as such, are not optimal for GPR30-targeted imaging; however, the indium-labeled compounds described herein exhibit better targeting characteristics and lower background than previously described iodine-labeled GPR30-targeted radiotracers.

## 6.4.2 INTRODUCTION

Estrogen plays an important role in variety of normal physiological and pathological processes. Estrogen exerts its effects mainly via the two known nuclear estrogen receptors (ERs), ER $\alpha$  and ER $\beta$  (Nilsson et al. 2001) . In 2000, GPR30, an orphan classical seven transmembrane G-protein coupled receptor (GPCR) was shown to be involved in estrogen-mediated activation of ERK1/2 in cells lacking ER $\alpha$  and ER $\beta$  but expressing GPR30, implicating the role of GPR30 in estrogen-mediated cellular responses (Filardo et al. 2000). In 2005, two studies reported the mechanistic relationship between GPR30 expression and rapid estrogen-mediated signaling events (Revankar et al. 2005; Thomas et al. 2005). Novel fluorescent estrogen derivatives (E2-Alexa) were used to study the cellular and sub-cellular localization of GPR30 using confocal microscopy (Revankar et al. 2005). The microscopy studies revealed that E2-Alexa detected ER $\alpha$  and ER $\beta$  in the nucleus of the cells, whereas GPR30 was predominantly located in the endoplasmic reticulum with no detectable signal at the plasma membrane. Most GPCRs are localized in the plasma membrane, therefore to further investigate this contradictory observation, we developed a new class of charged estrogen derivatives exhibiting differential cell permeability (Revankar et al. 2007). This new class of estrogen derivatives revealed that positively-charged cell-impermeable molecules did not activate rapid GPR30 signaling, whereas the neutral cell permeable molecules rapidly activated ER and GPR30 in cell-based functional assays (Revankar et al. 2007). These results confirmed the predominantly intracellular location of functional GPR30 in the endoplasmic

reticulum, as indicated by previous confocal microscopy studies (Revankar et al. 2005). However, other studies have reported the presence of GPR30 on the cell surface (Thomas et al. 2005; Filardo et al. 2007).

Recently, we had described a GPR30-selective agonist, G-1 and a GPR30-selective antagonist G15 (Bologa et al. 2006; Dennis et al. 2009). The biological role of GPR30 in physiological and pathological processes was further revealed with this use of these GPR30-selective ligands (Teng et al. 2008; Blasko et al. 2009; Haas et al. 2009; Hazell et al. 2009). Recent clinical studies indicate that GPR30 is expressed and associated with highly aggressive forms of breast, endometrial and ovarian cancer with low survival rates (Filardo et al. 2006; Smith et al. 2007; Arias-Pulido et al. 2009; Smith et al. 2009).

Estrogen has been a widely studied radiopharmaceutical target over the past 35 years. The most successful radiolabeled estrogen derivative,  $16\alpha$ - $^{18}\text{F}$ - $17\beta$ -estradiol (FES) is well characterized in patients with breast, uterine, ovarian and endometrial cancer (Mortimer et al. 1996; Yoshida et al. 2007; Tsujikawa et al. 2008; Yoshida et al. 2009). FES has been used clinically with promising results in imaging ER-expressing tumors and to evaluate responsiveness of tumors to anti-estrogen drugs (Mortimer et al. 1996; Linden et al. 2006; Dehdashti et al. 2009). To study the *in vivo* distribution and role of GPR30, we developed GPR30-selective radioiodinated derivatives (Ramesh et al., submitted). However, these radioiodinated derivatives were unsuitable for *in vivo* use due to rapid metabolism, high lipophilicity and poor *in vivo* targeting characteristics.

ER-targeted imaging agents based on macrocyclic and acyclic polyamino-polycarboxylate chelate designs such as DOTA and DTPA have been previously reported (Delpassand et al. 1996; Lashley et al. 2002; Banerjee et al. 2005; Gunanathan et al. 2007). The 4-hydroxytamoxifen-DTPA ligand demonstrated receptor-specificity; however the binding affinity was 10-fold lower than that of tamoxifen (Lashley et al. 2002). A DTPA-tamoxifen analogue was evaluated for imaging ER-positive lesions (Delpassand et al. 1996). The DTPA-tamoxifen conjugate demonstrated an  $IC_{50}$  of 1  $\mu$ M compared to 2  $\mu$ M for tamoxifen. Biodistribution, autoradiography, and radionuclide imaging demonstrated *in vivo* receptor specificity of  $^{111}\text{In}$ -labeled DTPA-tamoxifen conjugate and tumors could be clearly visualized even after 48 hr (Delpassand et al. 1996). In another report, estradiol was labeled with  $^{177}\text{Lu}$  using *p*-SCN-DOTA as a chelator and *in vitro* cell binding studies demonstrated receptor-specificity (Banerjee et al. 2005). In spite of the success of polyamino-polycarboxylate chelate designs for ER-targeting, the major concern is the possibility of a net charge that can hinder cell binding kinetics by decreasing cell permeability. We have previously shown that a net positive charge can hinder cell permeability but that the ligand still retains receptor-specificity and activates cell signaling (Revankar et al. 2007). One of our goals was to understand the influence of charge on cell binding and permeability. Therefore, we decided to conjugate the GPR30 agonist G-1 with *p*-SCN-DTPA, DOTA and *p*-SCN-DOTA, label it with  $^{111/113}\text{In}$  and perform biological evaluations to understand the role of negatively charged molecules on cell binding. Another goal of this study was to utilize  $^{111}\text{In}$ -labeled GPR30-targeted analogues to study

GPR30 *in vivo* using SPECT imaging modalities. In this report, we describe radiochemistry experiments studying the role of pH and incubation times on labeling efficiency, cell permeability and GPR30 functional assays and *in vivo* biodistribution and imaging studies on GPR30-expressing human endometrial cancer bearing female mice.



### 6.4.3 RESULTS AND DISCUSSION

In this study, we developed GPR30-selective neutral and negatively charged Indium-labeled polyamino-polycarboxylate derivatives for *in vivo* targeting of GPR30, for potential use as cancer diagnostic and therapeutic agents as well as to demonstrate the intracellular localization of GPR30 (**Fig. 6.3**).

In order to investigate the functional properties of the  $^{113}\text{In}$ -labeled derivatives, mobilization of intracellular calcium in GPR30-expressing, ER $\alpha$ / $\beta$ -negative SKBr3 cells was assessed. The  $^{113}\text{In}$ -labeled derivatives carrying a net negative charge,  $^{113}\text{In}$ -G-p-SCN-Bz-DOTA and  $^{113}\text{In}$ -G-p-SCN-Bz-DTPA, were unable to significantly mobilize calcium in these cells within a timeframe consistent with rapid signaling whereas the neutral  $^{113}\text{In}$ -G-DOTA compound was capable of mobilizing calcium in these cells (**Fig. 6.4**). This result suggests that, even applied at a higher concentration than their neutral counterparts, the net negative charge associated with these compounds prevents their rapid entry into the cell and thus their rapid signaling via GPR30.

Additionally, the  $^{113}\text{In}$ -labeled derivatives were used in a PI3-kinase activation assay utilizing the PIP3-binding pleckstrin homology (PH) domain of AKT fused to mRFP (PH-RFP) to localize PI3K activation in SKBr3 cells. Consistent with our findings in the calcium mobilization assay, stimulation of cells with  $^{113}\text{In}$ -G-DOTA resulted in the accumulation of the PH-RFP reporter in the nucleus, indicative of GPR30-mediated PI3K activation (**Fig. 6.5A**). Interestingly, the  $^{113}\text{In}$  derivatives with net negative charges,  $^{113}\text{In}$ -G-p-SCN-Bz-DOTA and

<sup>113</sup>In-G-p-SCN-Bz-DTPA, were able to elicit a weak PI3K activation when administered to cells at higher doses but no PI3K activation was detected when cells were stimulated with low doses of these compounds (**Fig. 6.5B**). This result is consistent with our previous finding that charged compounds at high concentrations can activate PI3K via GPR30 when the cells are stimulated for longer timeframes than in the calcium mobilization assay (3 min vs 15 min) (Revankar, 2007). This may be due to either the slow entry of a low concentration of compound into the cytoplasm, where it can stimulate GPR30, or due to a small fraction of GPR30 present at the cell surface at some time during cell stimulation, although this is less likely due to the lack of calcium mobilization in these same cells over a 180 sec time course.

## 6.4.4 MATERIALS & METHODS

**6.4.4.1 Cell culture** ER  $\alpha/\beta$ -negative and GPR30-expressing human endometrial carcinoma Hec50 cells, ER  $\alpha/\beta$ -negative and GPR30-expressing human breast carcinoma SkBr3 and ER  $\alpha/\beta$  and GPR30-negative monkey kidney Cos-7 cells were cultured in DMEM tissue media (Hec50, Cos7) or RPMI-1640 tissue media (SKBr3), with fetal bovine serum (10%) and 100 units/mL penicillin and 100  $\mu$ g/mL streptomycin. Cells were grown as a monolayer at 37°C, in a humidified atmosphere of 5% CO<sub>2</sub> and 95% air. Lipofectamine2000 was used according to manufacturer's directions for all transfections.

**6.4.4.2 Intracellular calcium mobilization** SKBr3 cells ( $1 \times 10^7$ /mL) were incubated in HBSS containing 3  $\mu$ M Indo1-AM (Invitrogen) and 0.05% pluronic acid F-127 for 1 hr at RT. Cells were then washed twice with HBSS, incubated at RT for 20 min, washed again with HBSS, resuspended in HBSS at a density of  $10^8$  cells/mL and kept on ice until assay, performed at a density of  $2 \times 10^6$  cells/mL. Ca<sup>++</sup> mobilization was determined ratiometrically using  $\lambda_{ex}$  340 nm and  $\lambda_{em}$  400/490 nm at 37°C in a spectrofluorometer (QM-2000-2, Photon Technology International) equipped with a magnetic stirrer.

**6.4.4.3 PI3K activation** The PIP3 binding domain of Akt fused to mRFP1 (PH-RFP) was used to localize cellular PIP3. SKBr3 (transfected with PH-RFP) were plated on coverslips and serum starved for 24 hr followed by stimulation with ligands as indicated. The cells were fixed with 2% PFA in PBS, washed, mounted in Vectashield containing DAPI (Vector Labs) and analyzed by confocal microscopy using a Zeiss LSM510 confocal fluorescent microscope.

**6.4.4.4 Receptor binding** Binding assays for ER $\alpha$  were performed as previously described (Revankar, 2005). Briefly, Cos7 cells were transiently transfected with ER $\alpha$ -GFP. Following serum starvation for 24 hr, cells ( $\sim 5 \times 10^4$ ) were incubated with  $^{113}\text{In}$  labeled derivatives for 10 min in a final volume of 10  $\mu\text{L}$  prior to addition of 10  $\mu\text{L}$  of 20 nM E2-Alexa633 in saponin-based permeabilization buffer. Following 5 min at RT, cells were washed once with 1 mL PBS/2%BSA, resuspended in 200  $\mu\text{L}$  and analyzed on a FACS Calibur flow cytometer (BD Biosciences).

**6.4.4.5 Statistical analysis** All numerical data were expressed as the mean of the values  $\pm$  the standard error of mean (S.E.M). GraphPad Prism version 5 (San Diego, CA, USA) was used for statistical analysis and a *P* value less than 0.05 was considered statistically significant.

#### 6.4.5 CONCLUSION

In conclusion, we have successfully synthesized and evaluated the first generation of non-steroidal  $^{111}\text{In}$  labeled GPR30-targeted analogues for cancer imaging. The  $^{113}\text{In}$  labeled analogues demonstrated the intracellular functionality of GPR30 in whole cell-based assays. The radiochemistry experiments provided valuable information on metal incorporation in acyclic and macrocyclic derivatives of a hydrophobic small molecule. The biodistribution and imaging studies revealed unfavorable *in vivo* targeting characteristics. Further structural modifications are warranted for development of future generations of GPR30 targeted imaging agents.

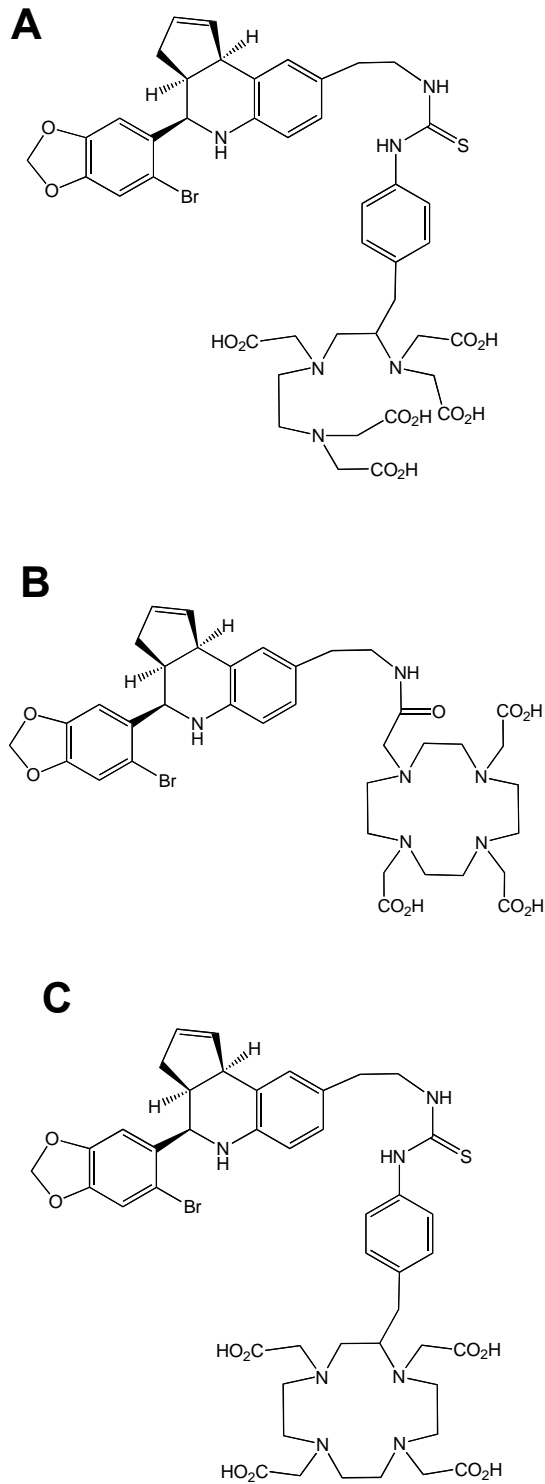
## 6.4.6 FIGURE LEGENDS

**6.4.6.1 Figure 6.3. Structure of G-1 based Indium labeled polyamino-polycarboxylate derivatives** **A)** Structure of  $^{113}\text{In-G-p-SCN-Bz-DTPA}$ , the compound with a (-2) charge. **B)** Structure of  $^{113}\text{In-G-p-SCN-Bz-DOTA}$ , the compound with a (-1) charge. **C)** Structure of  $^{113}\text{In-G-DOTA}$ , the neutral compound.

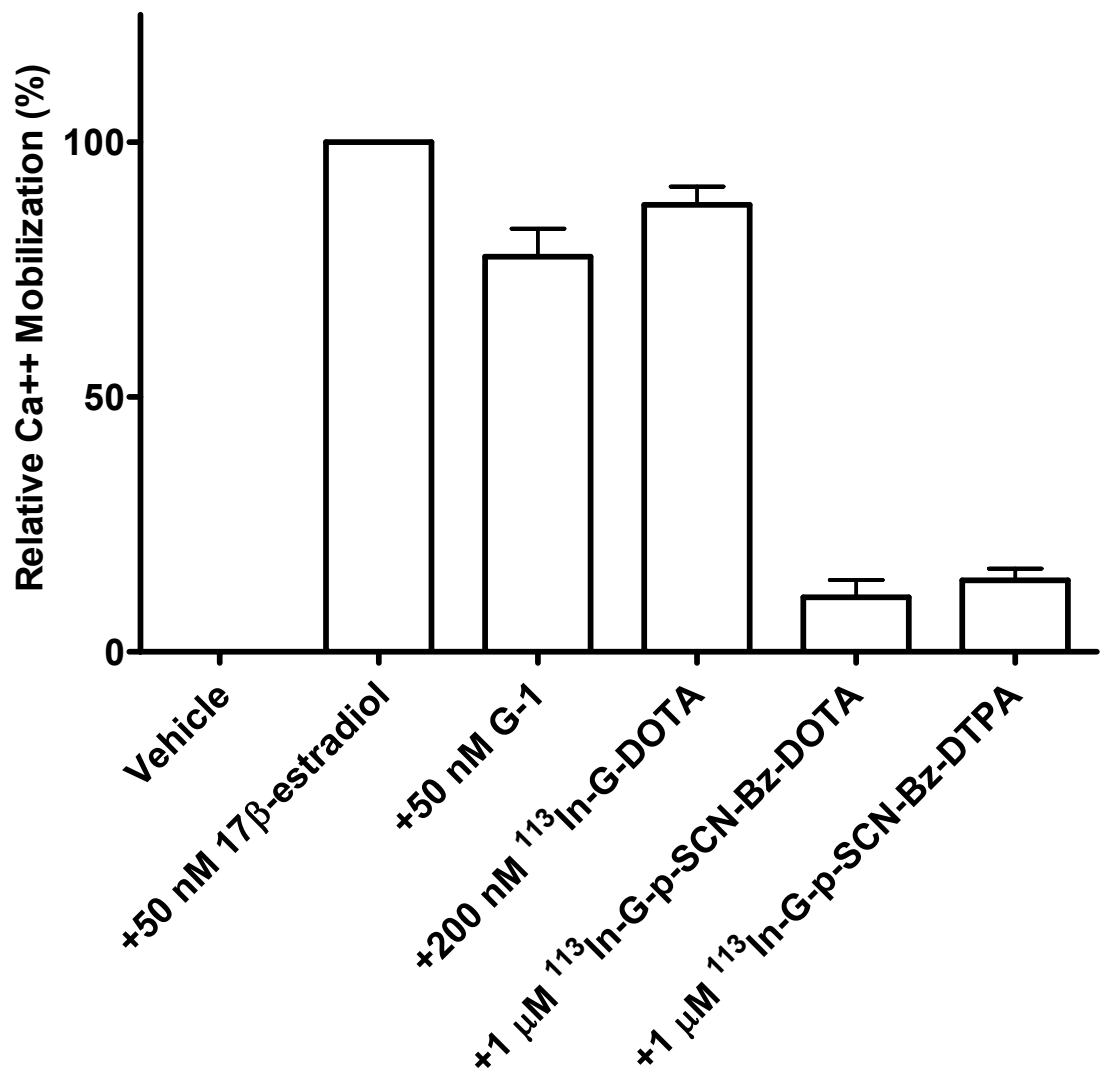
**6.4.6.2 Figure 6.4. Mobilization of intracellular calcium by  $^{113}\text{In}$  labeled derivatives** The effect of  $^{113}\text{In}$  labeled derivatives and known GPR30 agonists was evaluated in indo1-AM-loaded SKBr3 cells. Calcium mobilized by 50 nM  $17\beta$ -estradiol was defined as 100% calcium mobilization and the effects of other ligands compared to this response. All data represent the mean  $\pm$  s.e.m. from three independent experiments.

**6.4.6.3 Figure 6.5. Activation of PI3K via GPR30 by  $^{113}\text{In}$  labeled derivatives** (a, b) The activity of  $^{113}\text{In}$  labeled derivatives was evaluated using GPR30-expressing SKBr3 cells transfected with Akt-PH-mRFP1. E2,  $^{113}\text{In-G-DOTA}$ ,  $^{113}\text{In-G-p-SCN-Bz-DOTA}$  and  $^{113}\text{In-G-p-SCN-Bz-DTPA}$  were used at the indicated concentrations. Data are representative of three independent experiments.

### 6.4.6.1 Figure 6.3

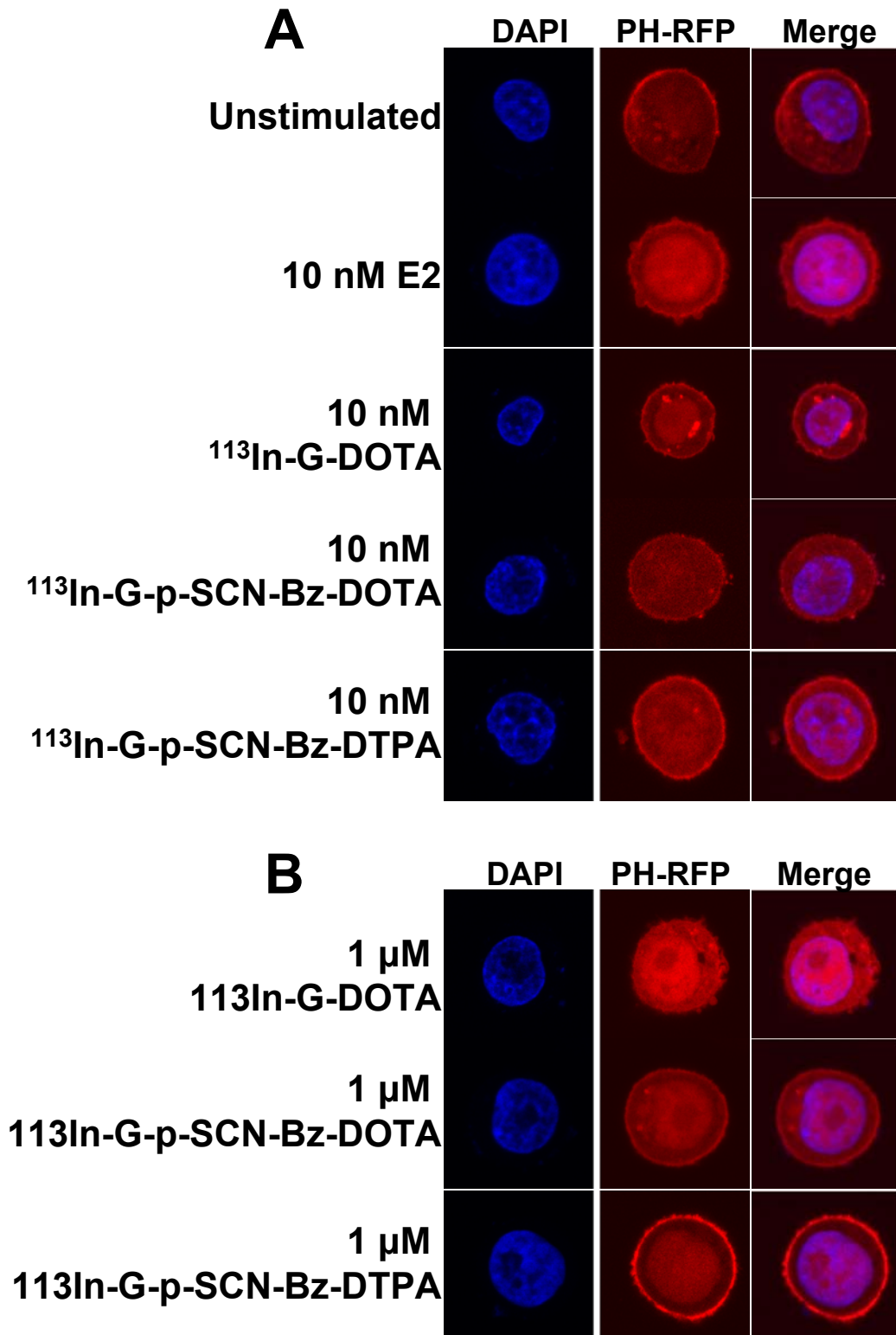


### 6.4.6.2 Figure 6.4





### 6.4.6.3 Figure 6.5



## 6.5 Conclusions

We have developed two series of GPR30-targeted radioligands based on the GPR30-selective agonist G-1. The first set of compounds includes 7 iodinated G-1 analogs. Following biological characterization of these compounds, two of them, **6** and **7** were chosen for further radiolabeling and *in vivo* imaging of Hec50 xenograft tumors.

While these compounds exhibited minimal ER $\alpha$ /ER $\beta$  binding in cell-based binding assays and were specific to GPR30 in PI3K activation assays, the two radioligands exhibited high background activity, possibly due to their high lipophilicity compared to that of their parent compound G-1 (Fig. 6.6).

Uptake of radioligands was seen in intestine and liver and both radioligands were

rapidly metabolized and excreted.

Following characterization of the  $^{125}\text{I}$ -labeled radiotracers, a second series of GPR30-targeted radioligands were characterized. These radiotracers were

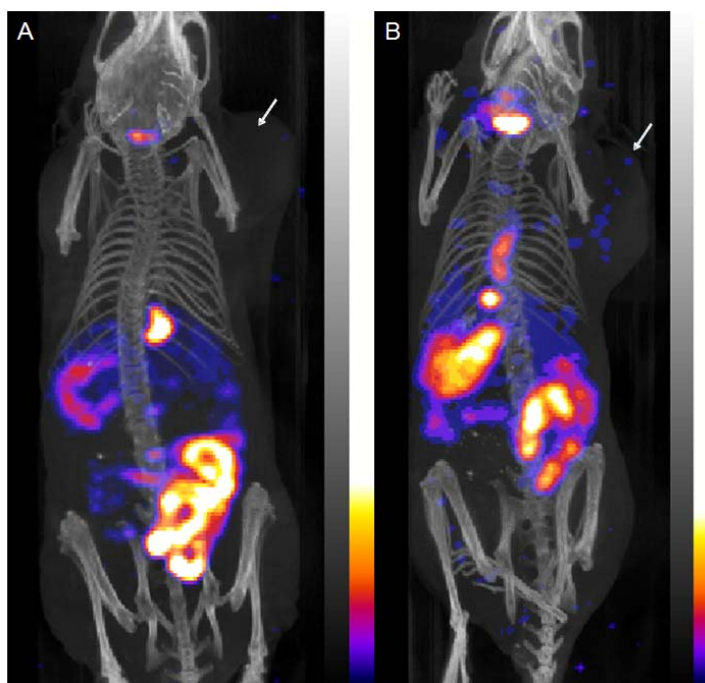


**Figure 6.6** (A) Reconstructed co-registered maximum intensity projection (MIP) SPECT/CT image of radioiodinated **6\***. (B) Reconstructed co-registered maximum intensity projection (MIP) SPECT/CT image of radioiodinated **7\***. The whole body images were acquired 1 hr PI of radioiodinated GPR30-targeted agent via tail vein of an ovariectomized female athymic (NCR) nu/nu human endometrial Hec50 tumor bearing mice (Courtesy of T. Nayak)

chemically similar to one another; however, they carried different charges, ranging from neutral to (-2). We have previously shown that estrogen-derivatives carrying charges do not stimulate GPR30 function to the same extent that uncharged ligands do, demonstrating the intracellular localization of GPR30 (Revankar et al. 2007). The biological activity of these G-1 based compounds was similar to that seen with the charged estrogen derivatives; the neutral compound elicited rapid responses at low doses, whereas the (-1) and (-2) compounds did not elicit rapid calcium mobilization at any concentration and only activated PI3K at much higher concentrations than the neutral compound. When used for *in vivo* imaging (Fig. 6.7), the neutral compound behaved similarly to the iodinated G-1 derivatives,

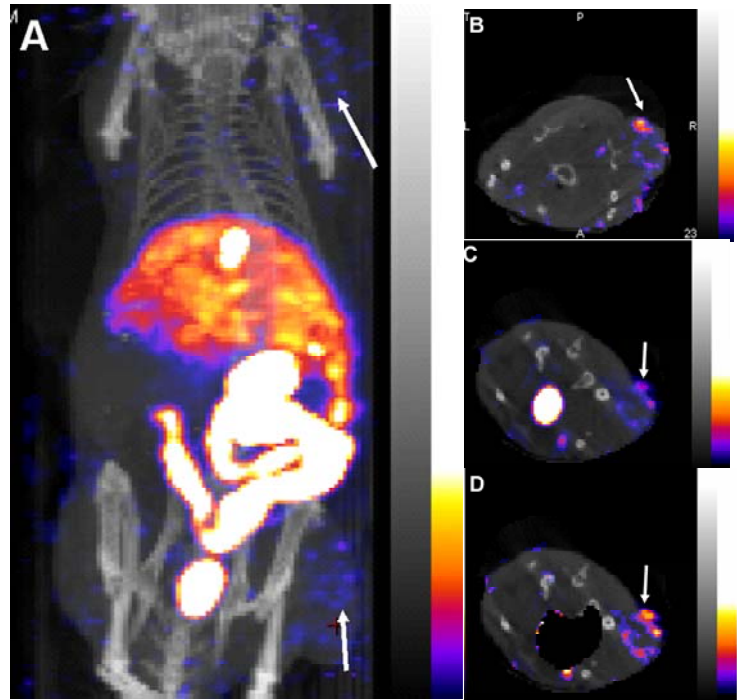


**Figure 6.7** Imaging of Hec50 tumor bearing mice with  $^{111}\text{In}$ -labeled G-1. **A)** Image of a mouse with shoulder and flank tumors showing high intestinal and stomach uptake of tracer with lower uptake in tumors (arrows). **B)** Transverse section through shoulder tumor. **C)** Transverse section through flank tumor. **D)** Transverse section through flank tumor with bladder cropped from image. All images were taken 1h following injection of radiotracer. (Courtesy T. Nayak)

with high background uptake in the intestine and bladder (**Fig. 6.7a**). Transverse image slices of flank (**Fig. 6.7b**) and shoulder tumors (**Fig. 6.7c**) allow for tumor visualization, and when the bladder is cropped from the flank tumor image visualization improves (**Fig. 6.7d**).

The shoulder tumors in these mice could be better visualized by focusing SPECT/CT imaging on the shoulder tumor and obtaining focused images (**Fig. 6.8a-c**).

These studies illustrate that the  $^{111}\text{In}$ -labeled G-1 derivatives are not suitable for *in vivo* imaging;

however, the lessons learned using these compounds may lead to generation of better second- and third- generation GPR30-targeted

radioligands. In the future, GPR30-targeted radiotracers should have lower lipophilicity and linkers to the metal-chelating group which are more stable *in vivo* than the linkers used herein, which may contribute to the rapid metabolism of these compounds and their rapid clearance from the tumors.

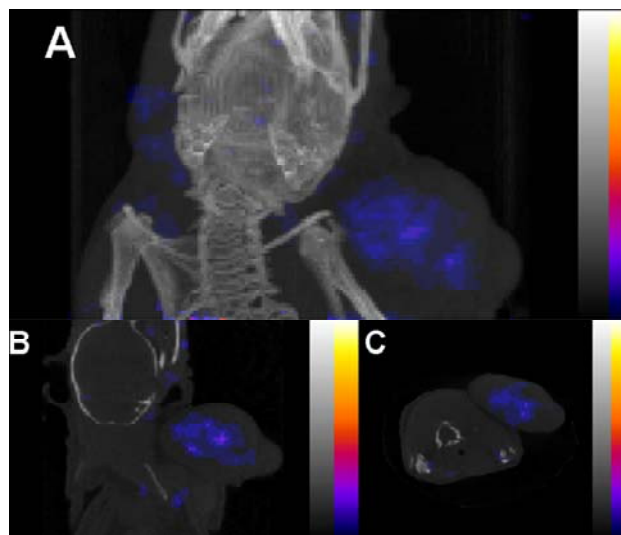


**Figure 6.8 Focused imaging of  $^{111}\text{In}$  GPR30 Radiotracer.** Focused SPECT/CT imaging of a mouse bearing a Hec50 shoulder tumor. **A)** Whole mouse view. **B)** Coronal section. **C)** Transverse view. Images taken 1h following radiotracer injection. (Courtesy T. Nayak)

# **7 SUMMARY, IMPLICATIONS AND FUTURE DIRECTIONS**

## 7.1 SUMMARY

In this work, we aimed to develop assays suitable for HTS that could be used to identify small molecules that interact with a range of steroid receptors, including the AR as well as ER $\alpha$ , ER $\beta$  and GPR30. These assays were utilized to identify several interesting molecules, including a GPR30-selective antagonist that was further characterized in subsequent chapters. This antagonist, as well as the GPR30-selective agonist G-1, was then used to characterize the role of GPR30 signaling in glioma, a type of cancer in which estrogen and tamoxifen have previously been shown to play a role through an undefined mechanism, which we suggest may involve GPR30. Finally, two series of radiolabeled G-1 derivatives were characterized in several cell-based assays to select the best options for a GPR30-specific ligand for *in vivo* imaging.

### 7.1.1 Chapter 2

Previous systems for characterization of AR-mediated transcription have been developed using a wide array of different reporter systems, mostly luciferase or GFP based. Induction of transcription by androgenic compounds is a hallmark of AR activation and, as such, has been used as an endpoint in many assays searching for androgenic and anti-androgenic chemicals. We aimed to develop a HTS assay using dsEGFP as a reporter for AR-mediated transcription and the resultant assay was named the Multifunctional Androgen Receptor Screen (MARS).

The MARS assay utilizes PC3 cells, derived from a metastatic prostate cancer metastasis to bone, which express a non-functional AR but become

androgen-sensitive upon transfection with AR (Terouanne et al. 2000). Importantly, these cells have the correct context for AR-mediated transcription and express the required transcription factors and other cofactors that a non-prostatic cell line may lack, which may allow them to be more sensitive to androgenic compounds and yield more consistent results. The choice of dsEGFP as a reporter is also key (as this reporter has a half life of approximately 2 hr compared to EGFP's half life of 24 hr) and buildup of excessive EGFP in cells has been shown to be toxic (Li et al. 1998). This shorter half-life also allowed us to detect a greater dynamic range of expression, as dsEGFP buildup from compounds that induced a lower level of transcription was discernable from those which caused high levels of transcription; in a system using regular EGFP, the EGFP would build up in both scenarios and reduce the dynamic range of the assay.

We first optimized the time course for dsEGFP expression and used the anti-androgen bicalutamide to show that dsEGFP expression induced by R1881, a synthetic androgen, could be blocked using an anti-androgenic molecule. Next, we verified that a small test series of compounds with known activity against the AR functioned as expected. This test set included 5 $\alpha$ -DHT, the most potent endogenous ligand for the AR, R1881, and bicalutamide, among other compounds. This initial screening verified that the MARS assay functioned as expected, with known AR transcriptional agonists including 5 $\alpha$ -DHT, R1881 and androstenedione inducing AR-mediated transcription. Additionally, at the high dose (10  $\mu$ M) used in the screen, E2 and progesterone, ligands for other steroid

hormone receptors, as well as the anti-androgens bicalutamide and nilutamide all induced transcription through the AR, albeit at lower levels than DHT. The results from the anti-androgens, particularly bicalutamide, were not unexpected; bicalutamide has been previously reported to have a biphasic effect on AR-mediated transcription, with agonist properties at high doses of bicalutamide and antagonist effects when lower doses of BC are used (Wilding et al. 1989; Berno et al. 2006; Fuse et al. 2007).

In addition to the MARS assay's ability to identify agonists of AR-mediated transcription, we also used the MARS assay to identify antagonists of AR-mediated transcription induced by R1881. In this version of the assay, all wells were treated with a low level of R1881 which induced sub-maximal transcription that could be inhibited by the presence of established anti-androgens, including CPA, nilutamide, bicalutamide and flutamide. In this assay setup, E2 and progesterone also acted as anti-androgens, indicating that these two compounds at high doses act as partial agonists of AR-mediated transcription in this assay, as they also induce AR-mediated transcription when applied to wells without R1881. Interestingly, the synthetic estrogen DES also acts as an antagonist of AR-mediated transcription in the MARS assay, with no agonist activity seen in the agonist version of the MARS assay.

These results were extended to include dose-response curves for the small set of compounds screened and results indicated that the MARS assay is sensitive and reproducible, allowing the generation of dose-response curves for both agonists and antagonists of AR-mediated transcription. Dose-response



assays run via the MARS assay indicated that for all of the agonists and antagonists screened, our observed  $EC_{50}$  and  $IC_{50}$  values were lower than previously published results for transcriptional reporter assays, suggesting that the MARS assay may be more sensitive than previous assays and may be able to identify new compounds with androgen disrupting activity.

To this end, we used the MARS assay to screen a library of 119 compounds with potential endocrine disrupting activity suggested by the ICCVAM for future investigation as endocrine disruptors. Included in this library were compounds with known AR activity, including R1881, 5 $\alpha$ -DHT, CPA and BC as positive controls, as well as translation inhibitors such as Actinomycin D as negative controls. In the MARS screen of the ICCVAM library, these control compounds behaved as expected, consistent with the MARS assay being fully functional in this context.

The secondary screen we established for verification of ICCVAM hits used the AR-GFP expression vector. This assay relies on the translocation of the AR from the cytosol to the nucleus following agonist binding and exploits fluorescent protein technology to quickly assay this translocation. We show that some AR antagonists, including BC, cyproterone acetate actually induce translocation of AR-GFP, similarly to R1881 and other AR agonists. Since translocation can only occur if AR translocates to the nucleus, an antagonist which prevents this translocation might be more effective than BC and also may not promote the androgen-independent tumor phenotype almost always seen following androgen ablation therapies. Screening the ICCVAM library for AR-GFP translocation

provides a third large data set which, combined with the primary translational screening data sets generated via the MARS assay can be a powerful tool for identifying new mediators of AR function.

One of these compounds which arose from comparison of MARS agonist and antagonist screening plus the translocation screen was apigenin, a plant-derived flavone. This compound showed no ability to induce transcription via the AR, even at 10  $\mu$ M and was a more effective antagonist of AR-mediated transcription than BC. Interestingly, whereas BC induced translocation of AR-GFP to the nucleus, apigenin did not induce the translocation of AR-GFP from the cytoplasm to the nucleus, indicating that it may be an anti-androgenic compound with fewer detrimental effects than BC and other anti-androgens which promote AR-GFP translocation. However, apigenin treatment was unable to block the nuclear translocation of AR-GFP induced by low doses of R1881, whereas pretreatment with either tamoxifen or BPA did prevent this R1881-mediated AR-GFP translocation, further delineating different classes of anti-androgens.

### **7.1.2 Chapter 3**

Estrogen signaling is a complex network of events, involving at least three receptors and a wide array of downstream targets, including direct transcriptional events as well as rapid signaling events involving Src, MAPK, Akt and many other pathways. Deconvolution of these signaling pathways and identifying the contributions of each estrogen receptor is a difficult process which would be made easier by the identification of selective ligands for each receptor. To date, a

few of these selective ligands have been identified, although some, such as PPT which was previously assumed to only target ER $\alpha$ , have not fully been investigated in light of the discovery of GPR30, and in fact PPT is a GPR30 agonist as well (Chapter 5). The ER $\beta$  selective compound, DPN, does not appear to interact with GPR30 and represents, along with the GPR30-selective agonist G-1 (Bologa et al. 2006), the only specific estrogen receptor ligands. This dearth of selective estrogen receptor ligands led us to screen a computationally-selected subset of the NIH Roadmap small molecule library in search of new probes for estrogen receptor research.

Initially, an existing fluorescence-based ER $\alpha$ /ER $\beta$  binding assay was modified to be amenable to 384-well format HTS using the HyperCyt® system. This assay utilizes E2 labeled with Alexa633 (E2-Alexa) in order to probe the ability unknown compounds to block the E2-Alexa binding in Cos7 cells expressing ER $\alpha$ -GFP or ER $\beta$ -GFP (Revankar et al. 2005). Previously, this assay had been run as single samples or in a 96-well format but optimization of cell concentration and E2-Alexa concentrations were required for 384-well HTS. This optimization also allowed for verification of other aspects of the assay in the 384 well plate, including the longer time between reading the first and last wells and cell settling due to different well properties.

Following assay optimization, approximately 700 compounds were evaluated for binding against ER $\alpha$  and ER $\beta$ , first at 10  $\mu$ M and then at 100 nM in order to better identify compounds with higher affinity binding to ER $\alpha$  and ER $\beta$ . This screen was also used to perform hit validation in the format of dose-

response curves for compound binding for 48 selected compounds with activity against ER $\alpha$ , ER $\beta$  or both. These results generated a number of preliminary hit compounds with unique activity against one or both receptors.

Activation of ER $\alpha$ , ER $\beta$  or GPR30 by E2 results in the rapid mobilization of calcium from intracellular stores in cells expressing the estrogen receptor of choice. In order to screen compounds for activity against GPR30, a calcium mobilization assay was used to identify compounds with the ability to either act as agonists on their own or to antagonize E2-mediated calcium mobilization. This screen was used on a subset of compounds with scaffolds similar to the known GPR30-selective agonist G-1 as well as compounds which emerged from the dose-response screening of ER $\alpha$  and ER $\beta$  selective compounds.

Finally, compounds which appeared to have either activity selective to a single receptor or unique activities against multiple receptors were screened in a secondary functional assay for PI3K activation. When cells expressing ERs, either ER $\alpha$ , ER $\beta$  or GPR30, and a RFP-fused pleckstrin homology domain of Akt, which binds to PIP3 (PH-RFP), are stimulated with E2 and other estrogenic compounds PI3K is activated and PIP3 is generated in the nucleus, resulting in translocation of the PH-RFP reporter from the cytoplasm to the nucleus (Revankar et al. 2005). This assay was utilized to determine the activity of compounds identified via prior screening methods and identify them as agonists or antagonists of estrogen receptor function.

One compound of particular interest which arose from the Roadmap Initiative screening was an antagonist of GPR30. This compound did not bind

significantly to ER $\alpha$  or ER $\beta$  and did not have any functional effect on either classical ER but is a functional antagonist of GPR30. With the identification of this GPR30 antagonist, there is now a complete set of GPR30-selective compounds with the newly identified antagonist as well as the previously described GPR30-selective agonist G-1 (Bologa et al. 2006). This gives a set of tools for further investigation of GPR30 function, both *in vitro* as well as in *in vivo* assays.

### 7.1.3 Chapter 4

Following the initial identification of a GPR30-selective antagonist in the Roadmap Initiative (Chapter 3), further characterization of this compound was undertaken in order to more fully define its functionality. This chapter focuses on the characterization of this new compound, termed G15. We first investigated the binding of G15 to GPR30, as this question had not been directly addressed in the initial characterization although G15 was non-functional in cells lacking GPR30, suggesting a receptor-mediated mechanism of action. G15 was shown to bind to GPR30 with an affinity similar to that of G-1, the GPR30-selective agonist. Functional assays verified the antagonist character of G15, in PI3K activation assays in cells expressing either GPR30-GFP or ER $\alpha$ -GFP and the PIP3 reporter PH-RFP. In these assays, G15 was shown to specifically block E2 induced PIP3 activation in cells expressing GPR30-GFP but not in cells expressing ER $\alpha$ -GFP, in which E2 activated PI3K regardless of the presence of G15. Additionally, G15 blocked PI3K activation in SKBr3 cells expressing endogenous GPR30 and G15 was capable of blocking G-1 mediated PI3K activation. Finally, this series of

assays allowed for the investigation of the potency of G15, with results indicating that a 10x molar excess of G15 was sufficient to block G-1 or E2 mediated PI3K activation. In addition to blocking PI3K activity mediated by E2 in GPR30 expressing cells, G15 was capable of blocking E2 or G-1 mediated calcium mobilization in GPR30 expressing cells. The G15 block of E2 mediated calcium mobilization also occurred in a dose-dependent manner.

G15 was shown to inhibit GPR30 function *in vivo* as well, both in mouse uteri as well as in a mouse depression assay. E2 has been shown to reduce depression, in humans (Epperson et al. 1999; Genazzani et al. 1999) as well as in a mouse model of depression (Estrada-Camarena et al. 2003). In the model used to investigate the effects of G-1 and G15, mice are suspended by their tail and injection of an antidepressant will cause the mouse to be more immobile than mice injected with control compounds (Cryan et al. 2005). In this assay, E2 and G-1 functioned as antidepressants, and G15 was able to block the antidepressant activity of either E2 or G-1 but not of a control antidepressant, suggesting a role for GPR30 in mediating the antidepressive effects of E2 and G-1. In the mouse uterotrophic assay, ovariectomized mice injected with estrogen exhibit proliferation of the uterine epithelial cells, as well as swelling and water retention (imbibition) of the entire uterus (Owens and Ashby 2002). G-1 promoted epithelial cell proliferation in this model, which G15 was capable of blocking, suggesting a physiological role for GPR30 in this system. G-1 did not promote water imbibition and G15 did not block E2-induced water imbibition, suggesting that this response is due to ER $\alpha$  and/or ER $\beta$ . Together, these results support the

role of G15 as a GPR30-selective antagonist and begin to show how the discovery of selective ligands for GPR30 will assist in untangling the effects of ER $\alpha$ , ER $\beta$  and GPR30 *in vivo*.

The structural similarities between G15 and G-1 suggest that there is a “G-scaffold” of similarity between these compounds and that further modifications to this structure may lead to additional GPR30-selective compounds with greater selectivity for GPR30 or greater potency. With this in mind, an additional series of G-scaffold compounds was synthesized and screened for activity against GPR30 in the calcium mobilization assay. One compound which arose out of this screening was an antagonist of GPR30 with increased selectivity for GPR30 versus ER $\alpha$  and ER $\beta$  and with a very similar structure to G-1 and G15. This antagonist, G36, was further characterized and shown to have similar functional activity to G15 in PI3K and calcium mobilization assays.

#### **7.1.4 Chapter 5**

Gliomas disproportionately affect men, with incidence in women being much lower (Preston-Martin 1996). Additionally, tamoxifen has been shown to inhibit growth of glioma cells *in vitro* (Pollack et al. 1990; Zhang et al. 2000) and to have some therapeutic value (Vertosick et al. 1992; Couldwell et al. 1996; Cloughesy et al. 1997; Mastronardi et al. 1998; Brandes et al. 1999). Interestingly, most gliomas and most glioma cell lines are ER $\alpha$ /ER $\beta$  negative (Plunkett et al. 1999; Hui et al. 2004), bringing into question how E2 and tamoxifen exert their effects on these cell types. Gliomas are the most common type of adult brain tumor and glioblastoma, the most malignant form of

astrocytoma, has one of the worst prognoses of any type of tumor, with median survival less than one year from diagnosis (Jukich et al. 2001; Newton 2004). With these factors in mind, we investigated the role of GPR30 in a glioma cell line.

First, we established that the U87-MG glioblastoma cell line expressed GPR30. These cells stain with a GPR30 antibody and the staining pattern is consistent with GPR30 expression in the endoplasmic reticulum. Additionally, transfection of U87-MG cells with GPR30 siRNA abrogated antibody staining, supporting the expression of GPR30 in these cells. As U87-MG cells are not reported to express either ER $\alpha$  or ER $\beta$  (Hui et al. 2004), GPR30 may represent the estrogen receptor which mediates the effects of tamoxifen in these cells (Pollack et al. 1990; Zhang et al. 2000).

In order to address the functionality of GPR30 in this cell line, the PI3K activation assay was employed. U87-MG cells transfected with PH-RFP and treated with E2 show PI3K activation in the form of nuclear translocation of PH-RFP. The GPR30-selective agonist G-1, as well as tamoxifen, ICI182,780 and raloxifene all activate PI3K, indicating that this activation is through GPR30, as none of these compounds activate PI3K in cells expressing either ER $\alpha$  or ER $\beta$  (Revankar et al. 2005). The GPR30-selective antagonists G15 and G36 also block E2 and G-1 mediated PI3K activation, as does siRNA knockdown of GPR30 expression. Taken together, these functional results strongly support a role for GPR30 as the functional estrogen receptor in U87-MG cells.



Finally, we investigated the expression of GPR30 in human glioblastoma. As glioblastomas are astrocytic tumors, the astrocyte marker GFAP was used to identify astrocytes within brain tissue. In tissue from outside of the tumor margins, which represents more normal brain tissue, sporadic expression of GFAP was seen and all cells expressing GFAP also expressed GPR30. In tumor tissue, nearly all cells expressed both GFAP and GPR30, indicating infiltration of astrocyte-like cells expressing GPR30. Additionally, tumor tissue was much more densely cellular and cell nuclei were highly irregular, indicative of tumor tissue. These results demonstrate that human glioblastomas express GPR30 and that, as this receptor is functional in the U87-MG glioblastoma cell line and is capable of mediating tamoxifen and E2 responses in these cells, GPR30 may be a target for anti-tumor therapies.

#### **7.1.5 Chapter 6**

Imaging of tumors has greatly progressed with the description of targeted radioligands for receptors overexpressed by different tumor types. Initially, the increased metabolic rate of tumor cells was taken advantage of using  $^{18}\text{F}$ -FDG to label cells with increased metabolic activity, including primary tumor cells as well as metastatic sites. This technology has advanced with an array of targeted ligands for both PET and SPECT imaging. As estrogen receptors are often overexpressed by tumors, particularly breast tumors, radiolabeled estrogen conjugates have been developed for imaging of estrogen receptor overexpressing tumors, particularly  $^{18}\text{F}$ -FES which has been utilized to visualize primary tumors as well as metastases (McGuire et al. 1991; Yoshida et al. 2007).

As GPR30 has been better described as an estrogen receptor and the overexpression of GPR30 has been seen in several tumor types, including ovarian (Smith et al. 2009), breast (Filardo et al. 2008) and endometrial (Smith et al. 2007), the utility of a GPR30-selective radioimaging agent has begun to become apparent. As we have previously described the GPR30-selective agonist G-1 (Bologa et al. 2006), we sought to create two series of radioligands based on the G-1 molecule for *in vivo* imaging of GPR30.

The first series of seven G-1 based radioligands were developed for SPECT imaging and are based on the G-1 scaffold with different linkers for incorporation of either cold Iodine or  $^{125}\text{I}$ . Initial biological characterization was completed using the non-radioactive versions of the ligands. These compounds were first analyzed for ER $\alpha$ /ER $\beta$  binding, as a GPR30-selective radioligand should not bind significantly to either ER $\alpha$  or ER $\beta$ . Subsequently, compounds were analyzed for their ability to either activate PI3K or to block the E2-induced activation of PI3K in Cos7 cells expressing either ER $\alpha$ -GFP or GPR30-GFP and PH-RFP. This simple activity assay confirmed the lack of activity of compounds against ER $\alpha$  and also gave insight into their abilities to mediate GPR30 function. GPR30 functionality of these compounds was confirmed using the calcium mobilization assay in which compounds were assessed for their ability to either induce calcium mobilization on their own or to block the E2-induced mobilization. Finally, the binding of several possible radioligand precursors to GPR30 was evaluated. The combination of these results, along with evaluation of solubility and synthetic characteristics, led to the selection of two of these compounds to

be iodinated and tested in *in vivo* imaging assays for GPR30. These imaging studies showed that both radioligands were taken up by Hec50 tumors expressing GPR30 and neither ER $\alpha$  or ER $\beta$ , as well as by reproductive organs and that this uptake could be blocked by injection of E2, indicating receptor mediated uptake. Although the radiotracers were taken up by GPR30-expressing tissues, there was significant background uptake as well and neither first-generation radiotracer is suitable for *in vivo* imaging.

The second series of radiotracers based on G-1 were a series of metal chelators linked to G-1. These compounds could be labeled with  $^{111}\text{In}$  and used for SPECT imaging and, as  $^{111}\text{In}$  has a very short half life of 2.81 days, the radiotracers decay sufficiently after a period of weeks allowing for biological characterization of non-radioactive compounds. These compounds were characterized in the PI3K assay in GPR30-GFP transfected cells and results indicated that, as expected, compounds with either a (-2) or (-1) charge did not elicit a significant response in GPR30-expressing cells, consistent with the intracellular localization of GPR30 and as seen in previous studies utilizing charged G-1 molecules (Revankar et al. 2007). The uncharged G-1 derivative did efficiently activate PI3K, as seen by nuclear translocation of PH-RFP. These results were confirmed using the calcium mobilization assay with SKBr3 cells expressing endogenous GPR30, wherein the charged compounds did not induce calcium mobilization but the uncharged G-1 derivative efficiently mobilized calcium. The *in vivo* imaging studies using these compounds showed that while receptor-mediated uptake occurred, the levels of non-specific background uptake

were too high for good radiotracers and that the compound was metabolized too quickly.

### **7.3 FUTURE DIRECTIONS**

#### **7.3.1 Androgen screen follow-up**

The screening of the ICCVAM library led to the identification of a large number of compounds with novel activities against AR mediated transcription. Subsequent AR-GFP translocation assays further divided these compounds into those which antagonize AR-mediated transcription and translocate AR-GFP and those which antagonize AR-mediated transcription and not inducing translocation of AR-GFP. Furthermore, compounds capable of antagonizing transcription and with inherent ability to translocate AR-GFP can be further divided into those which are capable of blocking R1881-mediated AR-GFP translocation and those which cannot block AR-GFP translocation induced by R1881 treatment. These classes of antagonists certainly deserve further follow-up experiments to determine the mechanism responsible for these distinct results.

Initially, it would be prudent to determine AR binding for all ICCVAM compounds, both those which present interesting cases as antagonists as well as those which act as agonists of AR-mediated transcription. This would grant some insight into how compounds are functioning, and those which act through AR-independent mechanisms could be followed up in different manners than those which interact with the AR to mediate their function. Compounds which do not directly interact with the AR may still have interesting effects, particularly if they lose their efficacy in cells which do not express the AR, suggesting an AR-

independent function which requires AR either upstream or, more likely, downstream of compound function on another target. Compounds which interact directly with the AR to exert their influence could be further optimized for increased AR binding and fewer off-target effects utilizing synthetic chemistry.

After determining AR-binding abilities of ICCVAM compounds, delineation of the different classes of AR functional antagonists could be undertaken. First, a more extensive screen of compounds to determine the ability of all compounds to block R1881-induced AR-GFP translocation would be prudent in order to fully group compounds and identify all phenotypes generated by the ICCVAM library of compounds. For instance, in this work, it appears that cotreatment of cells with tamoxifen and R1881 leads to the sequestration of AR-GFP in the cytosol, with lower levels observed in the nuclei than in unstimulated cells. This is an interesting observation and it would be beneficial to find out if this is a trait unique to tamoxifen or if other compounds behave this way as well. Additionally, it should be verified that effects seen with the AR-GFP complex are seen in cells expressing endogenous AR, by utilizing antibody staining after treating cells as those with AR-GFP and verifying results.

Following this effort, it would be helpful to understand what mechanism(s) are underlying the ability of some compounds to prevent R1881-mediated AR-GFP translocation. For example, it is possible that binding of this class of ligands to the AR prevents disassociation from heat shock proteins or that these binding events prevent dimerization of the AR. Crystallographic studies could provide insight into these questions, as the crystal structures of this class of ligands

bound to the AR may significantly differ from those obtained when the AR binds R1881 or an endogenous ligand. Biochemical experiments could also be conducted, such as treating cells with various ligands, crosslinking proteins and pulling down AR and looking for association of heat shock protein chaperones following ligand binding, as this may give insight into how certain antagonists prevent the AR from translocating into the nucleus. Similarly, Co-IP of AR from stimulated cells and subsequent probing of the pulldown for AR would give insight into if the AR from treated cells existed as dimers or if compound treatment resulted in solely monomeric AR, suggesting a block in nuclear translocation via this mechanism.

Another interesting avenue for follow-up of the ICCVAM screening would be to investigate the differences in activity of BPA, BPB and BPC2. These three bisphenols are closely related structurally although they appear to have different activities against AR, with BPA having the most potent antagonist activity against AR-mediated transcription, BPB having decreased antagonist activity and BPC2 acting as a partial agonist of AR-mediated transcription. Neither BPA or BPB induced translocation of AR-GFP, and BPA effectively blocked R1881-induced AR-GFP translocation. As these compounds are so close structurally, it seems like an opportunity for generating a chemically related set of compounds in order to obtain a more complete understanding of the structure activity relationship between these compounds with regard to their activity against the AR.

### 7.3.2 Identification of important functional groups for GPR30-selective molecules

With the discovery and characterization of G-1, G15 and G36, we have begun to identify important functional groups of the G-scaffold for GPR30 function. An additional series of compounds which includes G-1, G15 and G36 has already been generated, with different modifications to the G-scaffold for delineation of the structure activity relationship between the G-scaffold and GPR30, as well as ER $\alpha$  and ER $\beta$ . These compounds have only been characterized in the briefest of manners, with screening for activity in a calcium mobilization assay in cells expressing only GPR30 as the extent of functional characterization thus far. It is important to determine the ER $\alpha$ /ER $\beta$  binding of this series of compounds, to help define what features of G-1, G15 and G36 make them selective for GPR30 versus the classical ERs. Additionally, more binding studies involving these molecules and GPR30 would generate important information as to which compounds have higher and lower affinity for GPR30 and what impact certain structural changes have on the binding of G-scaffold compounds to GPR30.

Following the completion of binding assays on all of the existing G-scaffold compounds, it would be interesting to see if a second generation of G-scaffold compounds could be synthesized in order to try and find a compound(s) with increased affinity for GPR30 and fewer off-target binding effects. This compound could be useful in the generation of a new series of GPR30-targeted *in vivo* imaging agents to use with similar SPECT-directed radiolabeling strategies as

have been attempted for G-1. A radioligand with greater affinity than G-1-based compounds would reduce the amount of tracer required for imaging and would also possibly reduce the amount of background binding which confounds the use of current G-1 based radiotracers.

### **7.3.3 Characterization of additional roadmap compounds**

Along with G15, there were several other compounds which emerged from Roadmap screening with interesting activities against ER $\alpha$ , ER $\beta$  and/or GPR30. One of these compounds appears to act as an antagonist of all three ERs, which is a type of compound that currently does not exist. This compound has proven to be difficult to characterize in initial follow-up studies, although if the compound which had the initial antagonist activity can be identified, this could be a promising avenue of research including possible clinical endpoints as this would be the first type of compound to block signaling through all three ERs.

Additionally, preliminary findings revealed that there may be compounds with agonist activity against both classical ERs but not GPR30, this type of compound would be similar to G-1 in that it could be used for investigating the activity of classical ERs without direct contribution from GPR30. There also appeared to be an antagonist of ER $\alpha$  which has no activity against either ER $\beta$  or GPR30. This compound would be useful for investigating the relevance of ER $\beta$  and GPR30 in the absence of ER $\alpha$  signaling which could be interesting as ER $\alpha$  is the most well studied ER and there are many instances in which ER $\beta$  is assumed to play no significant role; blocking ER $\alpha$  function in these instances could be



beneficial for determining what role ER $\beta$  plays in a system other than knockout mice or siRNA knockdown of ER $\alpha$  in cells.

#### **7.3.4 Investigating GPR30 function in glioma**

The results described in Chapter 5 that GPR30 is functionally active in a glioblastoma cell line and that it appears to be the only functional estrogen receptor in these cells are intriguing. Gliomas are typically thought of as ER $\alpha$ /ER $\beta$  negative and most glioma cell lines are as well; however, tamoxifen has been shown to be beneficial in preventing growth of glioma cell lines and also has shown some promise in early clinical studies. Additionally, males have a much higher prevalence of glioma and in rodents this has been shown to be dependent on the presence of estrogen, as ovariectomized females lose the protective effect and this effect can be reconstituted by giving these rats estrogen at physiological levels (Plunkett et al. 1999). The fact that both estrogen and tamoxifen act in a similar role in these cells is intriguing and may point to GPR30 being the relevant estrogen receptor in preventing disease as well as in the beneficial effects conferred by tamoxifen, as E2 and tamoxifen are both agonists of GPR30 function.

Significant opportunities for follow-up exist from our small study on GPR30 in glioma. First, it should be confirmed that the cells in which our cell-based assays were done are in fact ER $\alpha$ /ER $\beta$  negative. From functional data, it appears that GPR30 is the only functional estrogen receptor in these cells however it is possible that either ER $\alpha$  or ER $\beta$  are expressed and for some reason not functional in these cells, which would be an interesting finding requiring follow-up

of its own; for instance, if the cells do express ER $\alpha$ , does knocking down ER $\alpha$  change the observed functions of GPR30, suggesting some type of synergistic effect. Additionally, it would be prudent to investigate additional roles of GPR30 in the U87 cell line as well as other models of glioblastoma to verify that our results are not the artifact of a cell line. Assays such as proliferation, migration or invasion assays in the presence of either the GPR30 agonist G-1 or tamoxifen would be useful in determining if activation of GPR30 is responsible, at least in part, for the effects of tamoxifen observed on glial cells. Additionally, knockdown of GPR30 in these same systems would help determine if tamoxifen is acting solely through GPR30 in these instances. Finally, treatment of mice bearing U87 or other glioma xenograft tumors with G-1 or G15/G36 or a combination of these molecules and tamoxifen would provide insight into GPR30 function. Performing these experiments in ovariectomized animals and comparing the G-1 treatment to the previously seen E2 treatment in their ability to prevent tumorigenesis in female animals would also help to elucidate the role of GPR30 in this protective effect.

#### **7.4 CONCLUDING REMARKS**

This study illustrates the identification, characterization and use of small molecule ligands for both the androgen receptor and for estrogen receptors. Selective molecules for visualization of a single type of steroid receptor will be useful in non-invasive determination of receptor expression in tumors and use of these small molecules in the laboratory may lead to greater insights into receptor function. As this work shows, the first generation of ligands developed for any

receptor may not be optimal and additional studies following up this work will be useful for identifying small molecule ligands for each steroid receptor with the greatest specificity and fewest off target effects. Development of selective ligands for delineation of steroid receptor function will be of great use experimentally and also potentially useful in the clinic, as a great number of diseases depend on hormone receptor signaling, including most cancers of both the male and female reproductive systems. We hope that this preliminary work will lead to identification of therapeutically useful ligands for estrogen and androgen receptors.

## APPENDIX: Supplemental Figures

- Figure S1. ICCVAM MARS Agonists.
- Figure S2. ICCVAM MARS Antagonists
- Figure S3A. ER Roadmap Primary Screening
- Figure S3B. ER Roadmap Primary Screening
- Figure S3C. ER Roadmap Primary Screening
- Figure S3D. ER Roadmap Primary Screening
- Figure S3E. ER Roadmap Primary Screening
- Figure S3F. ER Roadmap Primary Screening
- Figure S3G. ER Roadmap Primary Screening
- Figure S3H. ER Roadmap Primary Screening
- Figure S3I. ER Roadmap Primary Screening
- Figure S4A. ER Roadmap Screening dose-responses of selected compounds
- Figure S4B. ER Roadmap Screening dose-responses of selected compounds
- Figure S4C. ER Roadmap Screening dose-responses of selected compounds
- Figure S4D. ER Roadmap Screening dose-responses of selected compounds
- Figure S4E. ER Roadmap Screening dose-responses of selected compounds
- Figure S4F. ER Roadmap Screening dose-responses of selected compounds
- Figure S4G. ER Roadmap screening dose-responses of selected compounds
- Figure S4H. ER Roadmap Screening dose-responses of selected compounds
- Figure S5. Calcium mobilization assay data for G-scaffold Roadmap compounds
- Figure S6. G-Scaffold compounds





Fig. S3A. ER Roadmap Screening at 100nM  
Plate 12911 Rows A-D

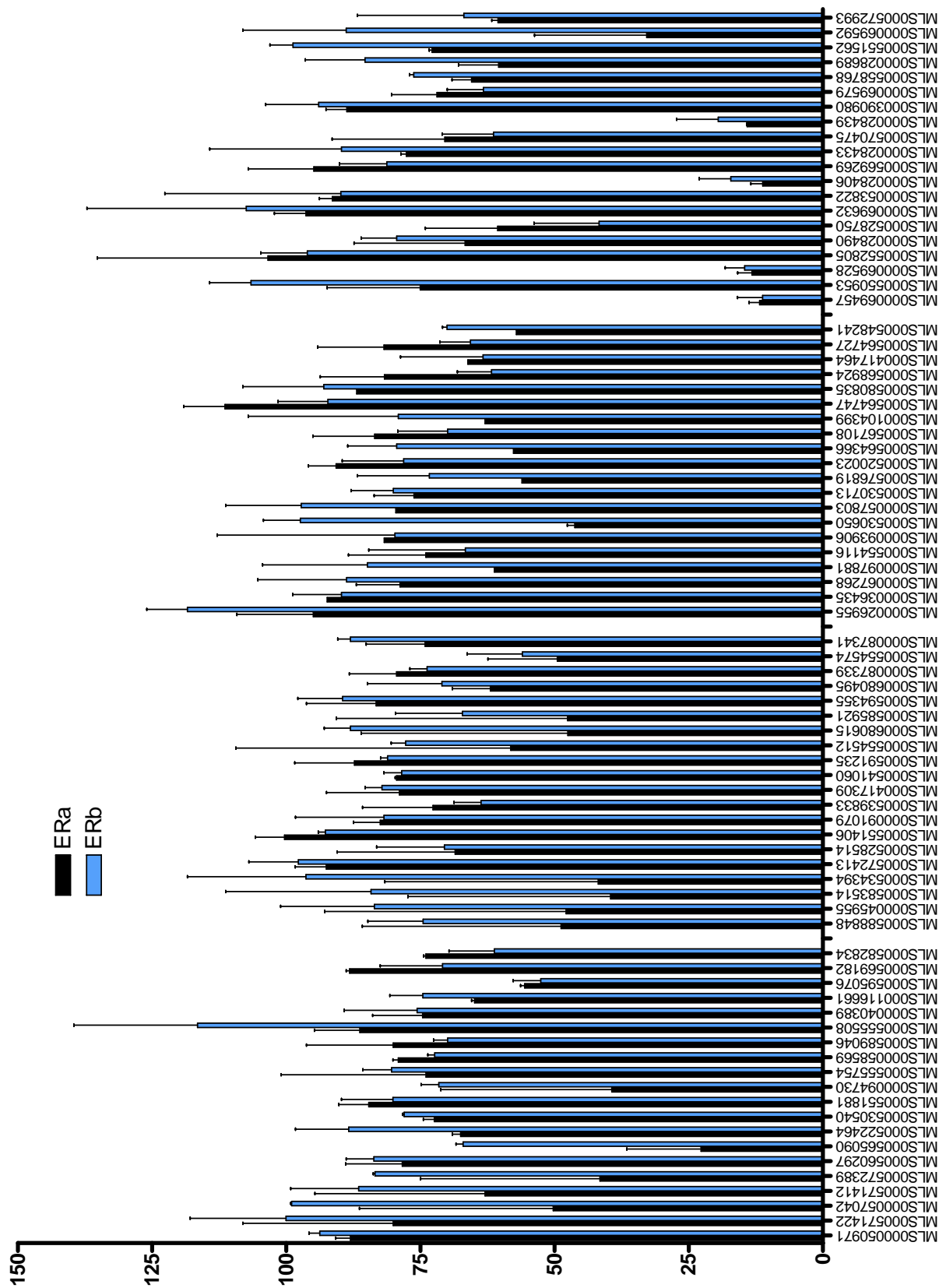


Fig. S3B. ER Roadmap Screening at 100nM

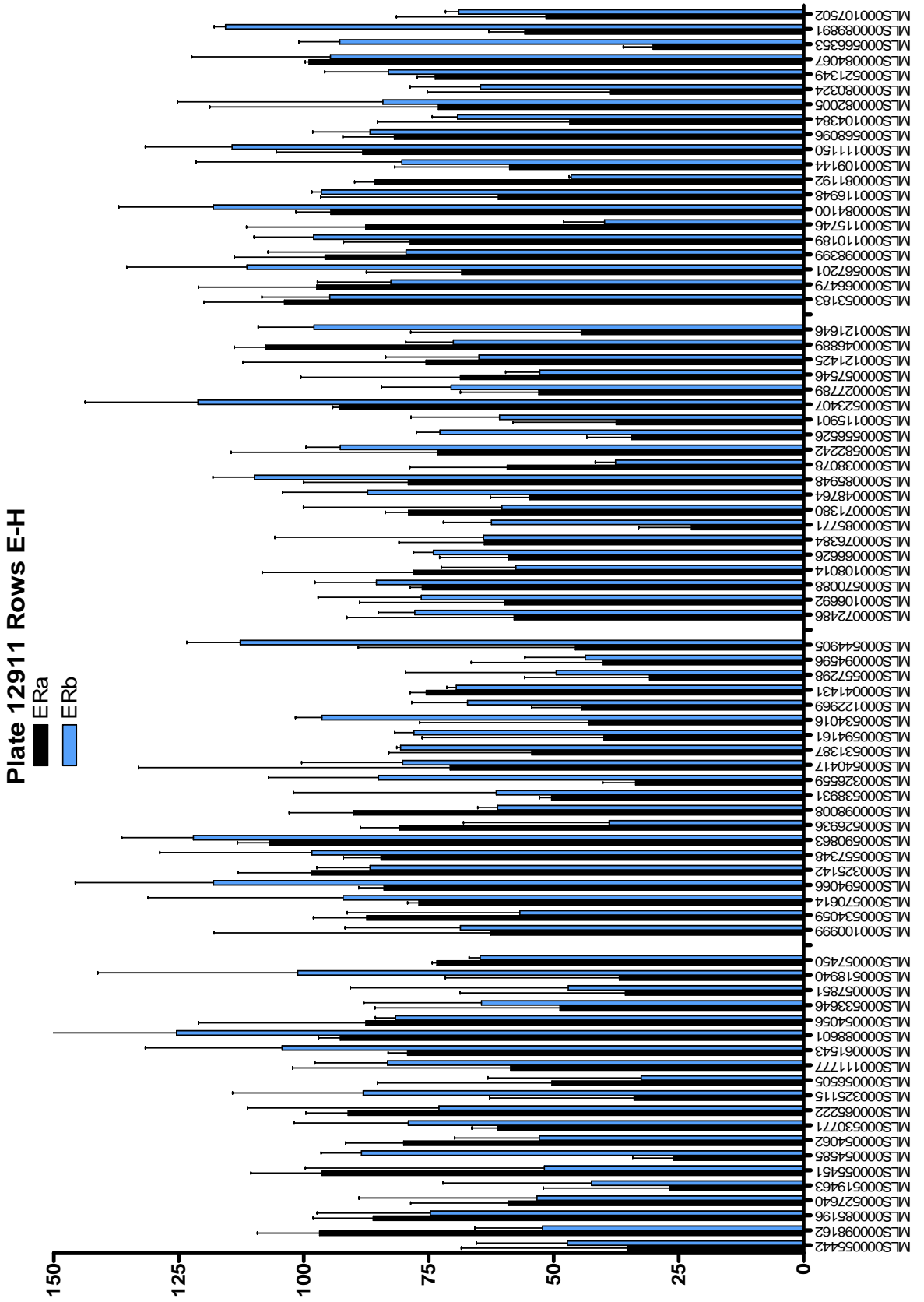




Fig. S3C. ER Roadmap Screening at 100nM

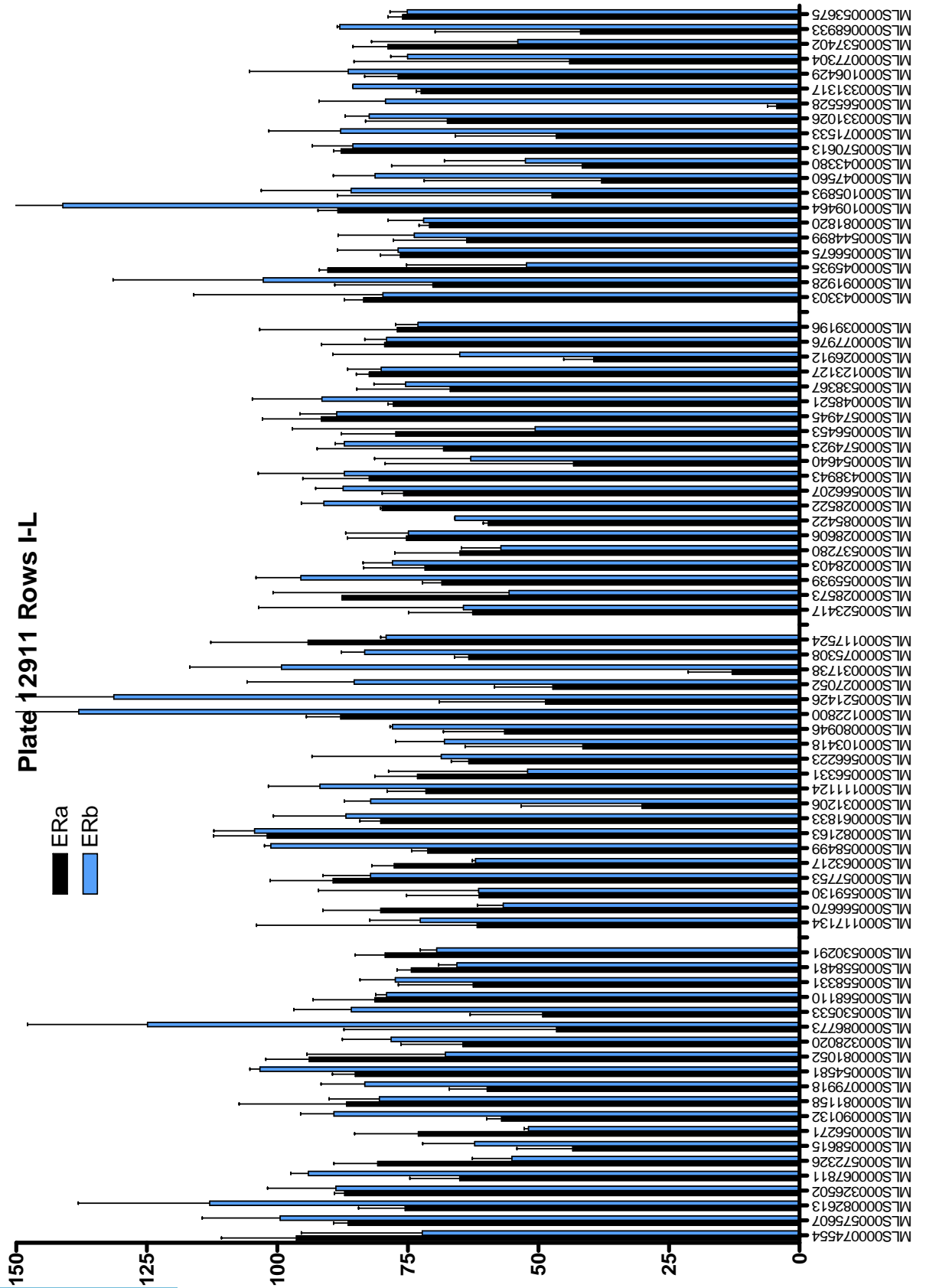


Fig. S3D. ER Roadmap Screening at 100nM

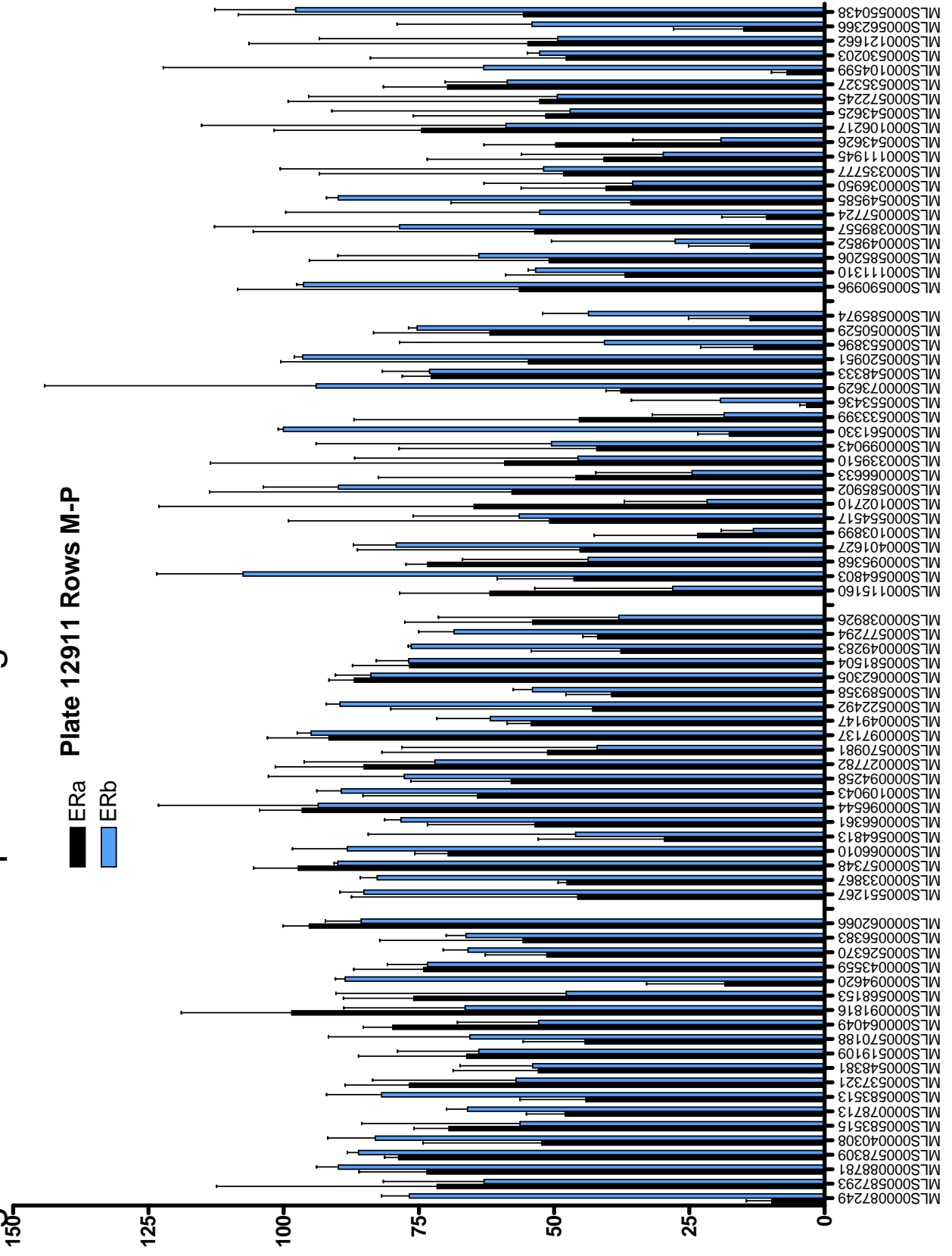


Fig. S3E. ER Roadmap Screening at 100nM

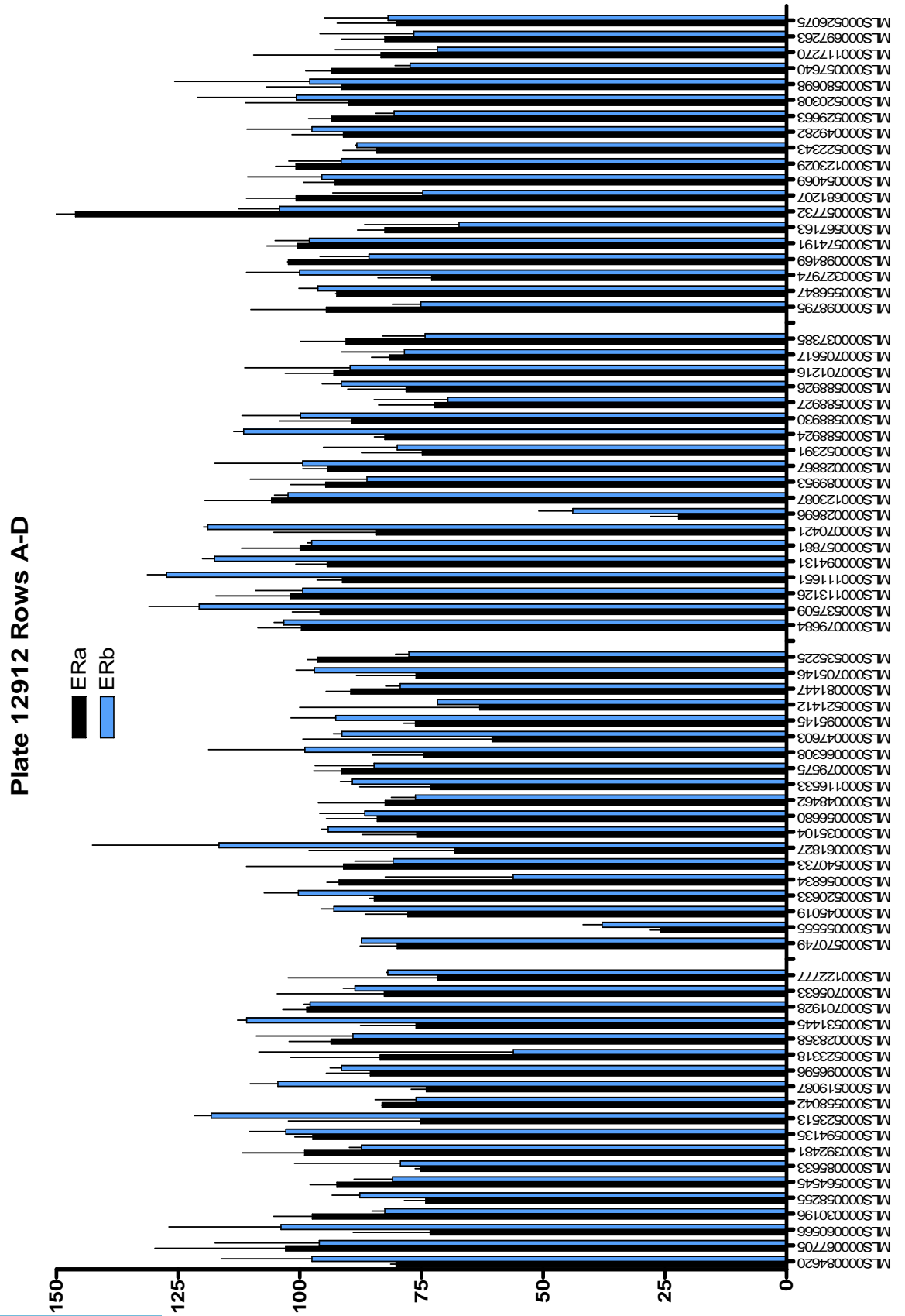




Fig. S3G. ER Roadmap Screening at 100nM  
Plate 12912 Rows I-L

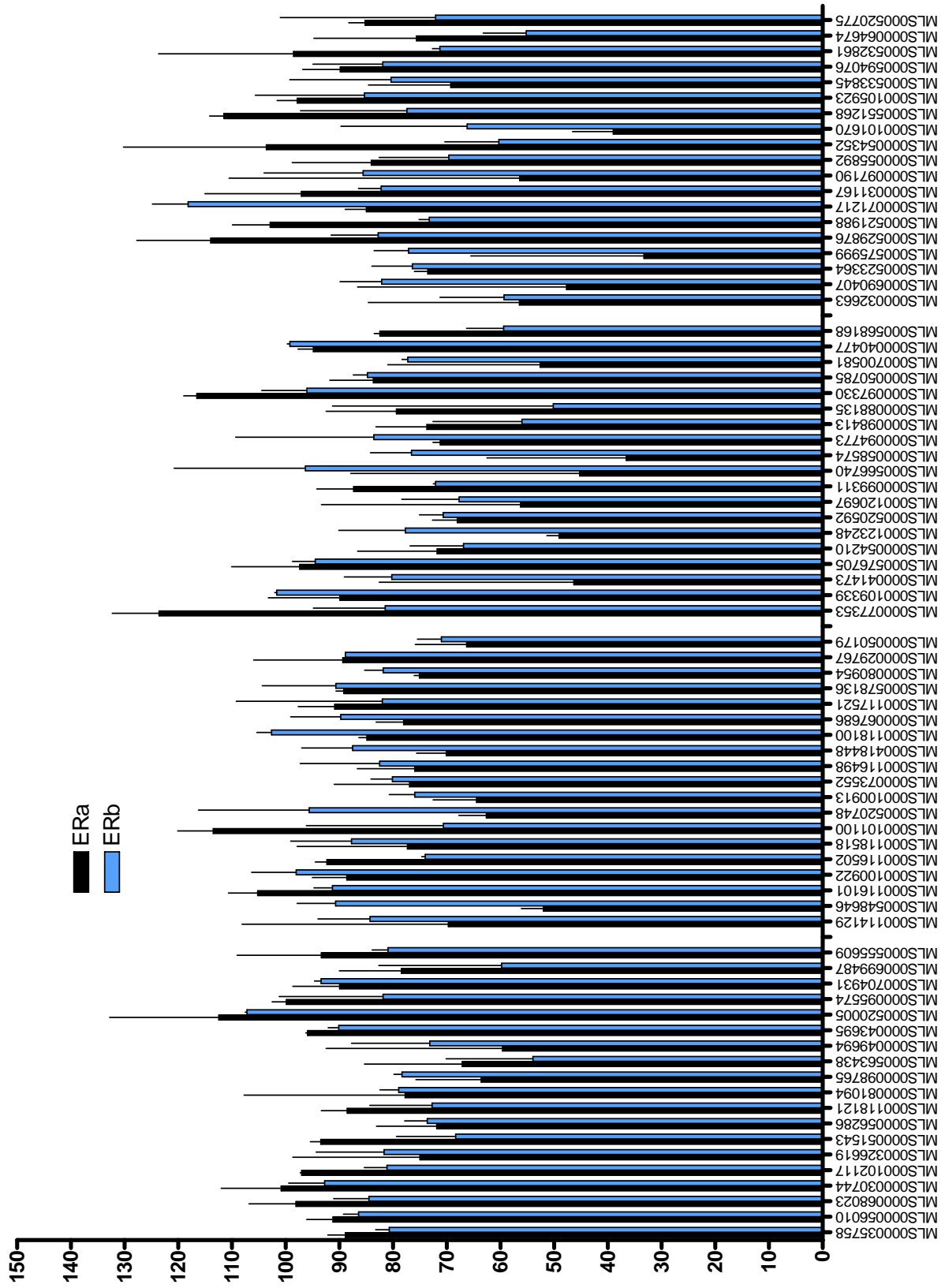


Fig. S3H. ER Roadmap Screening at 100nM

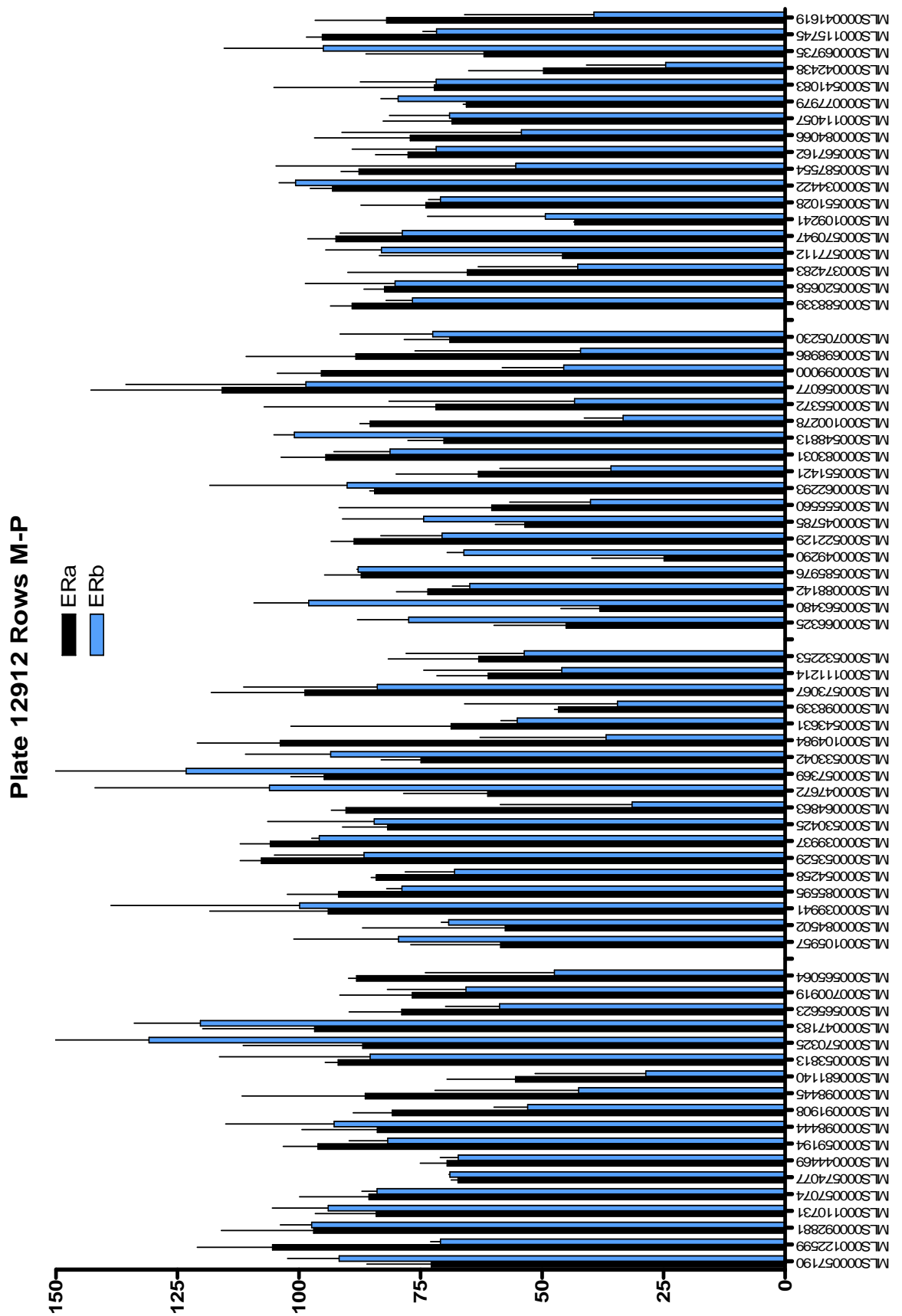


Fig. S31. ER Roadmap Screening at 100nM. Green box is highlighting G15. 20070928 G15-like compounds

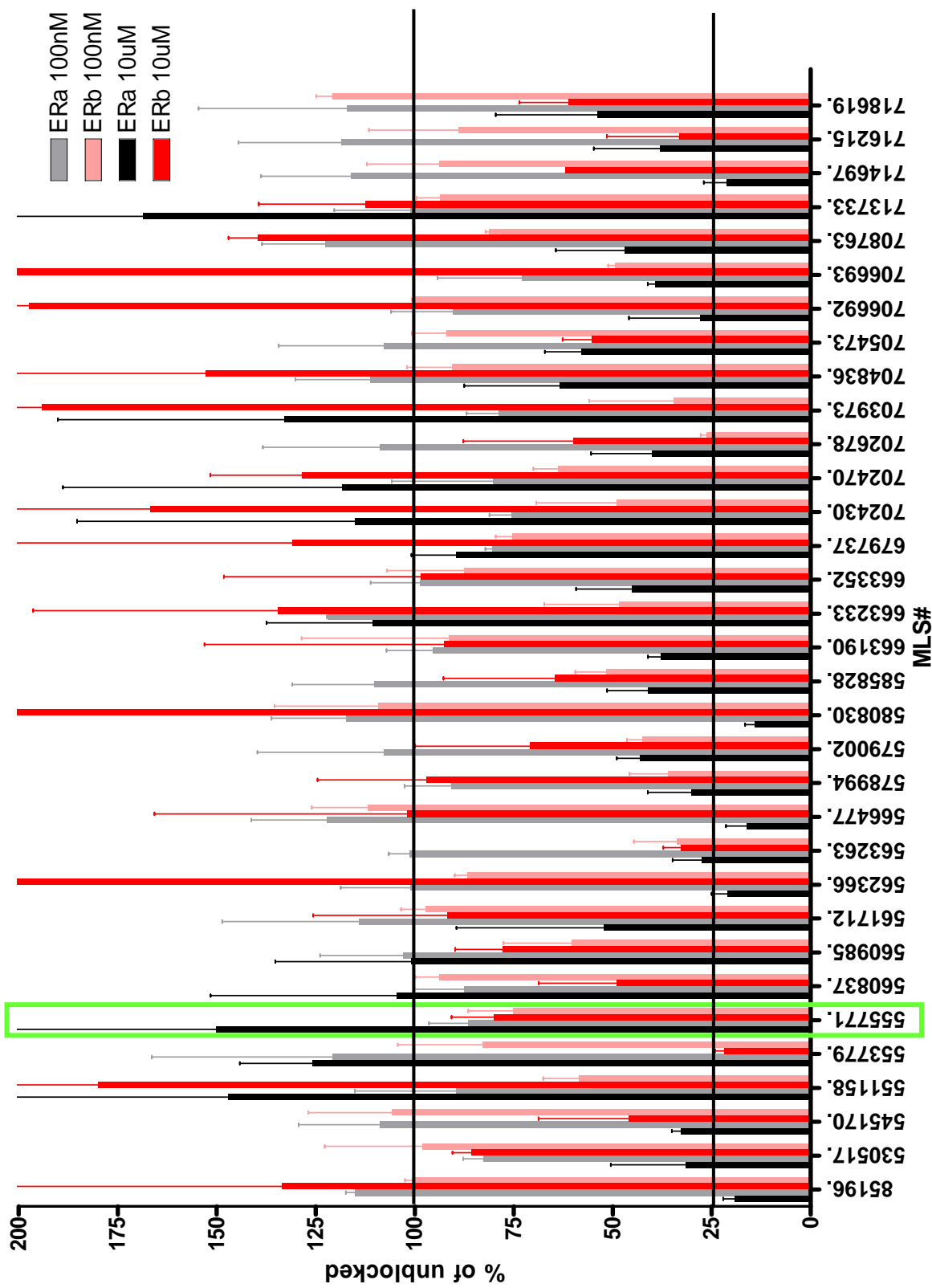


Fig. S4A. ER Roadmap Screening dose-responses of selected compounds.

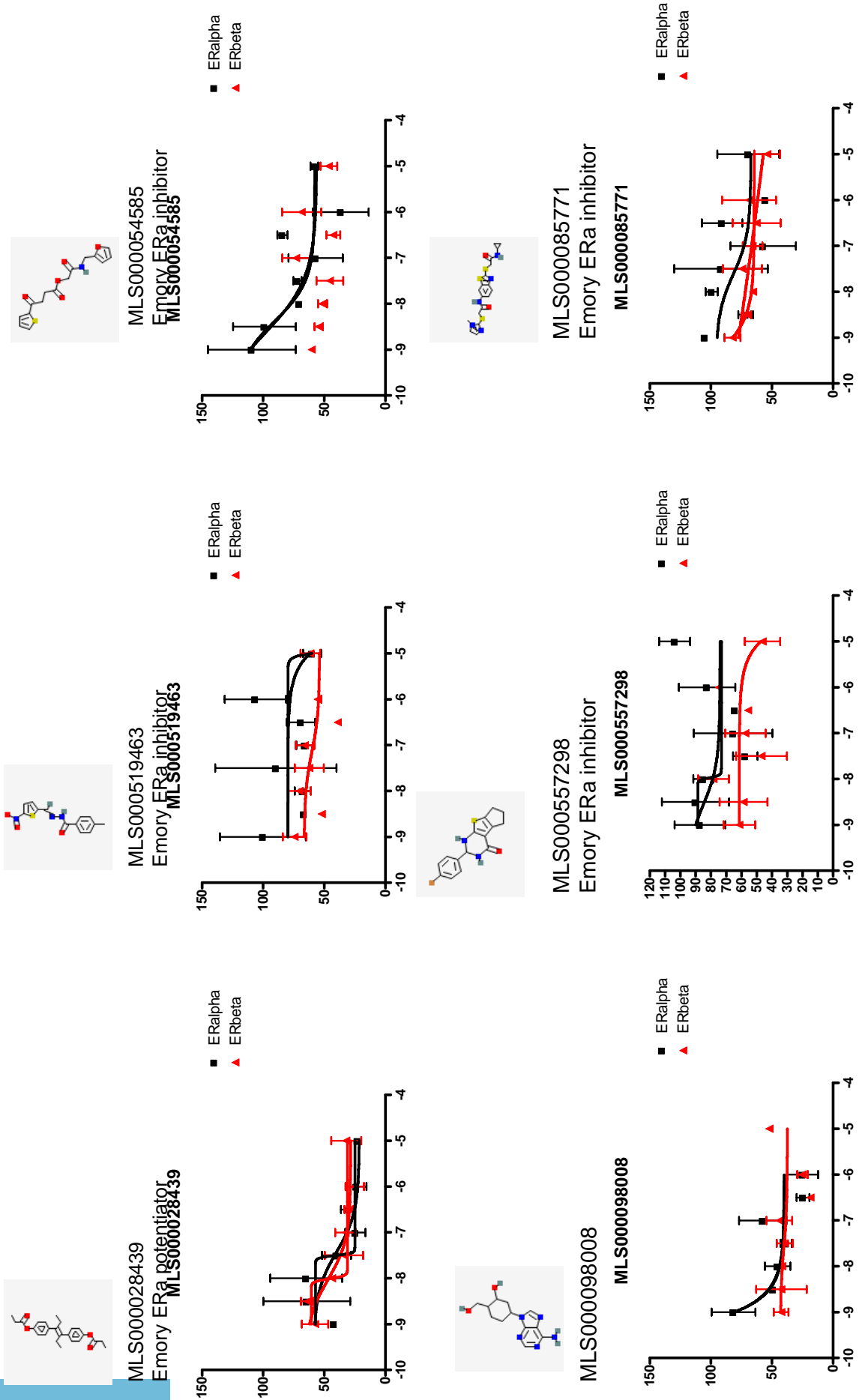
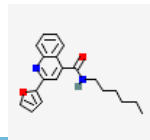
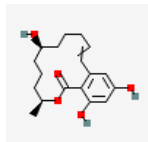
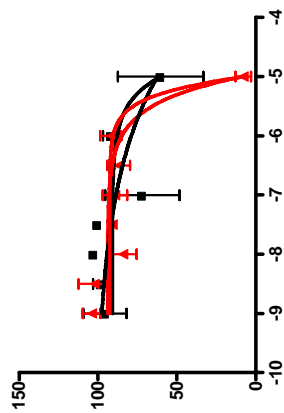




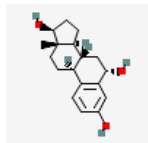
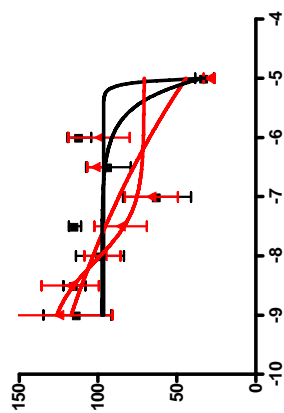
Fig. S4B. ER Roadmap Screening dose-responses of selected compounds.



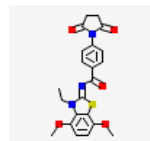
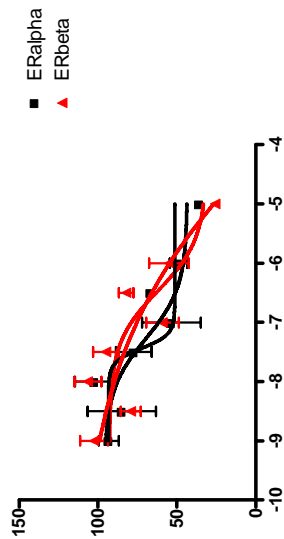
MLS000550438  
Emory ERb inhibitor



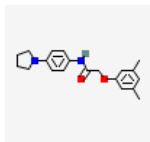
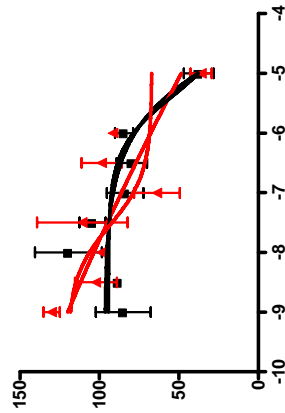
MLS000055555  
Emory ERa potentiator



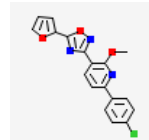
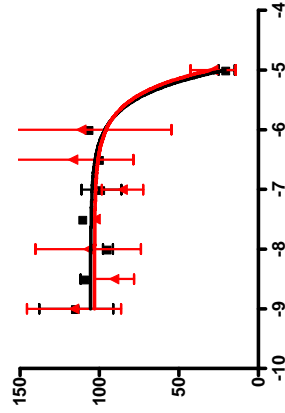
MLS000028696  
Emory ERa potentiator



MLS000103757  
Emory ERa potentiator



MLS000112626  
Emory ERb inhibitor



MLS000076062  
Emory ERa potentiator

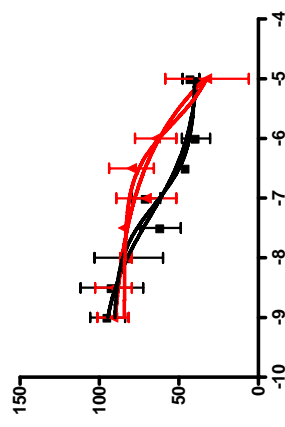


Fig. S4C. ER Roadmap Screening dose-responses of selected compounds.

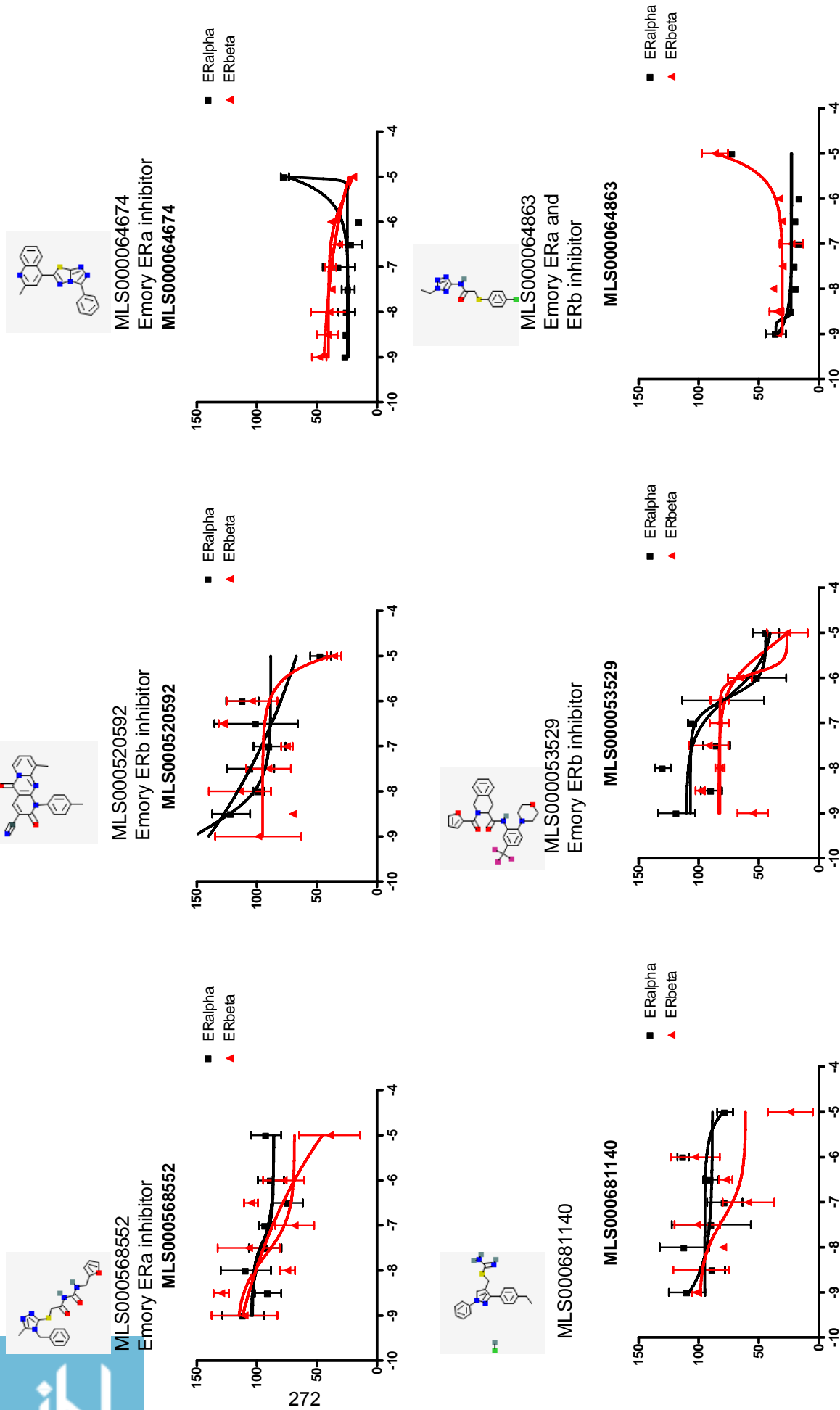
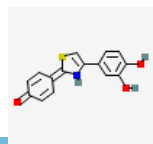
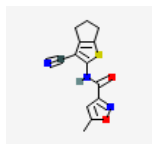
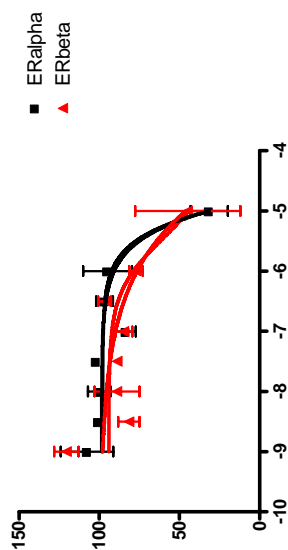


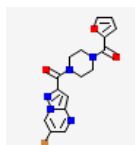
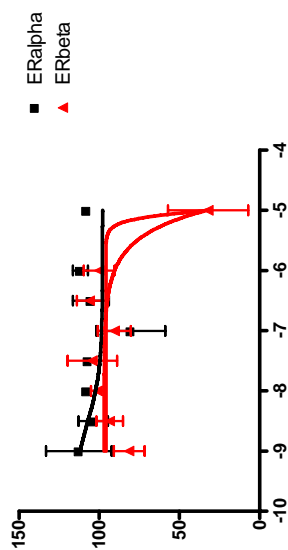
Fig. S4D. ER Roadmap Screening dose-responses of selected compounds.



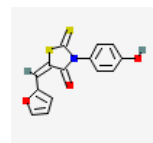
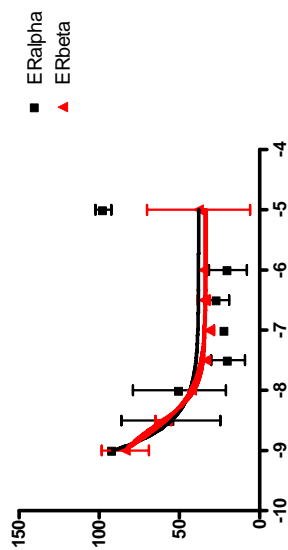
MLS00011214  
Emory ERb inhibitor  
MLS00011214



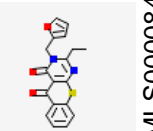
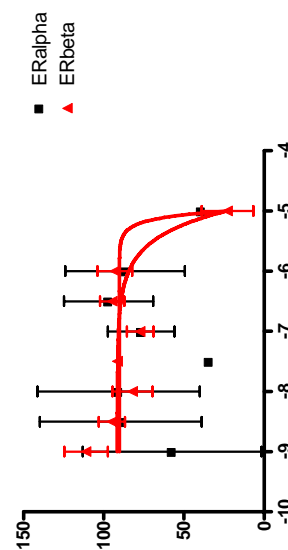
MLS000066325  
Emory ERb inhibitor  
MLS000066325



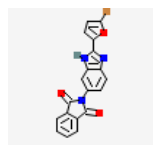
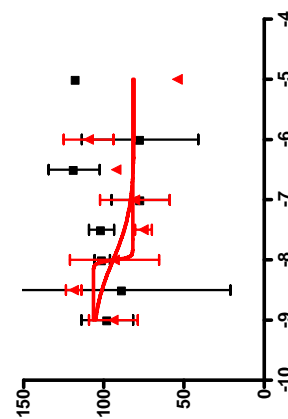
MLS000100278  
Emory ERA and  
ERb inhibitor  
MLS000100278



MLS000705230  
MLS000705230



MLS000084066  
Emory ERb inhibitor  
MLS000084066



MLS000041619  
Emory ERA inhibitor  
MLS000041619

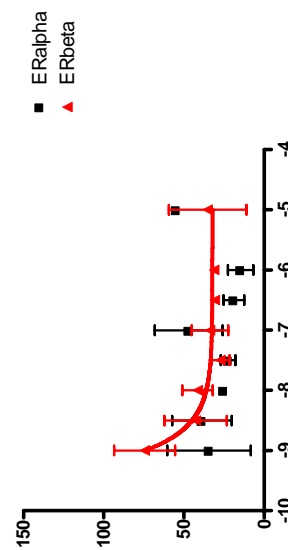


Fig. S4E. ER Roadmap Screening dose-responses of selected compounds.

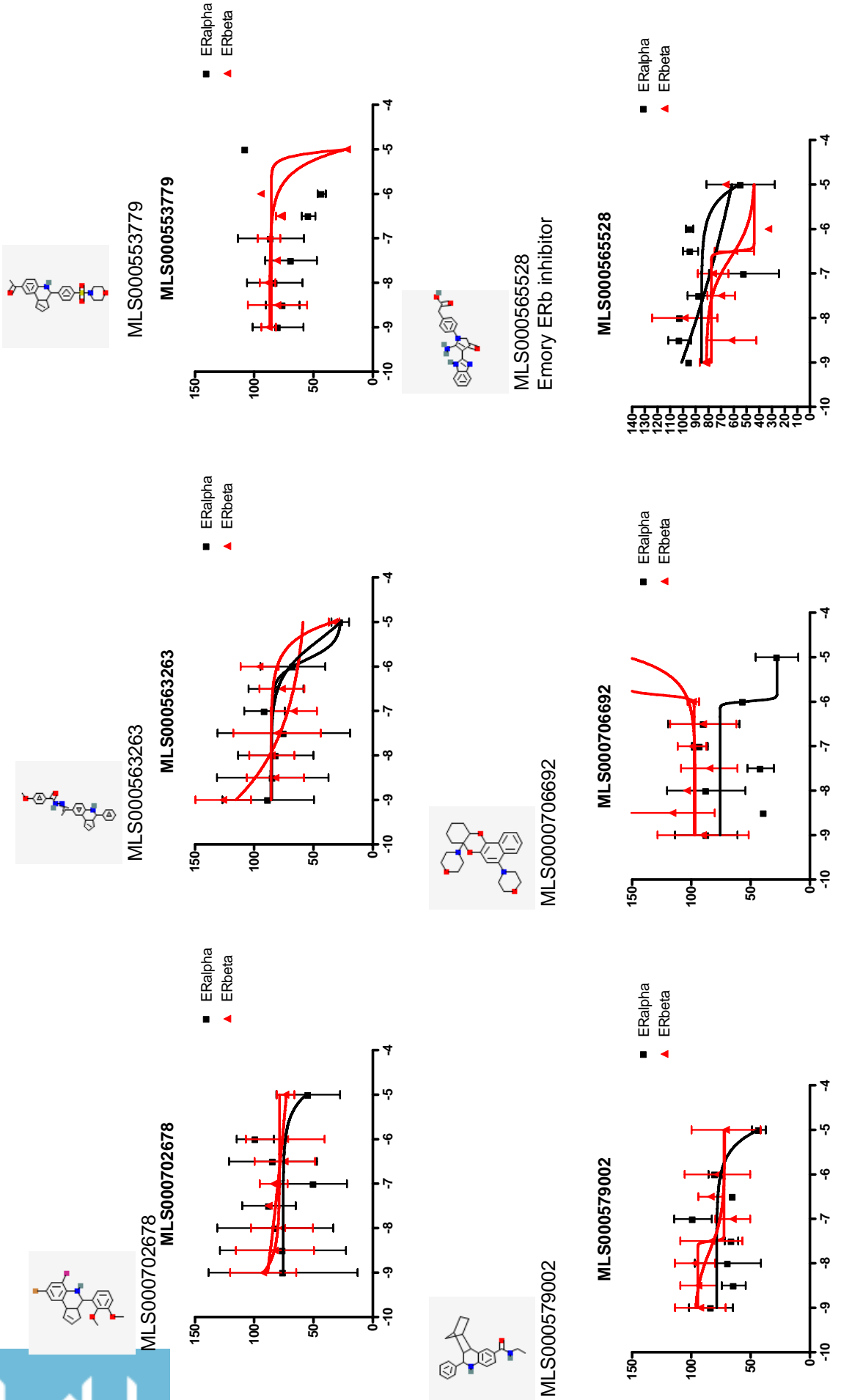


Fig. S4F. ER Roadmap Screening dose-responses of selected compounds.

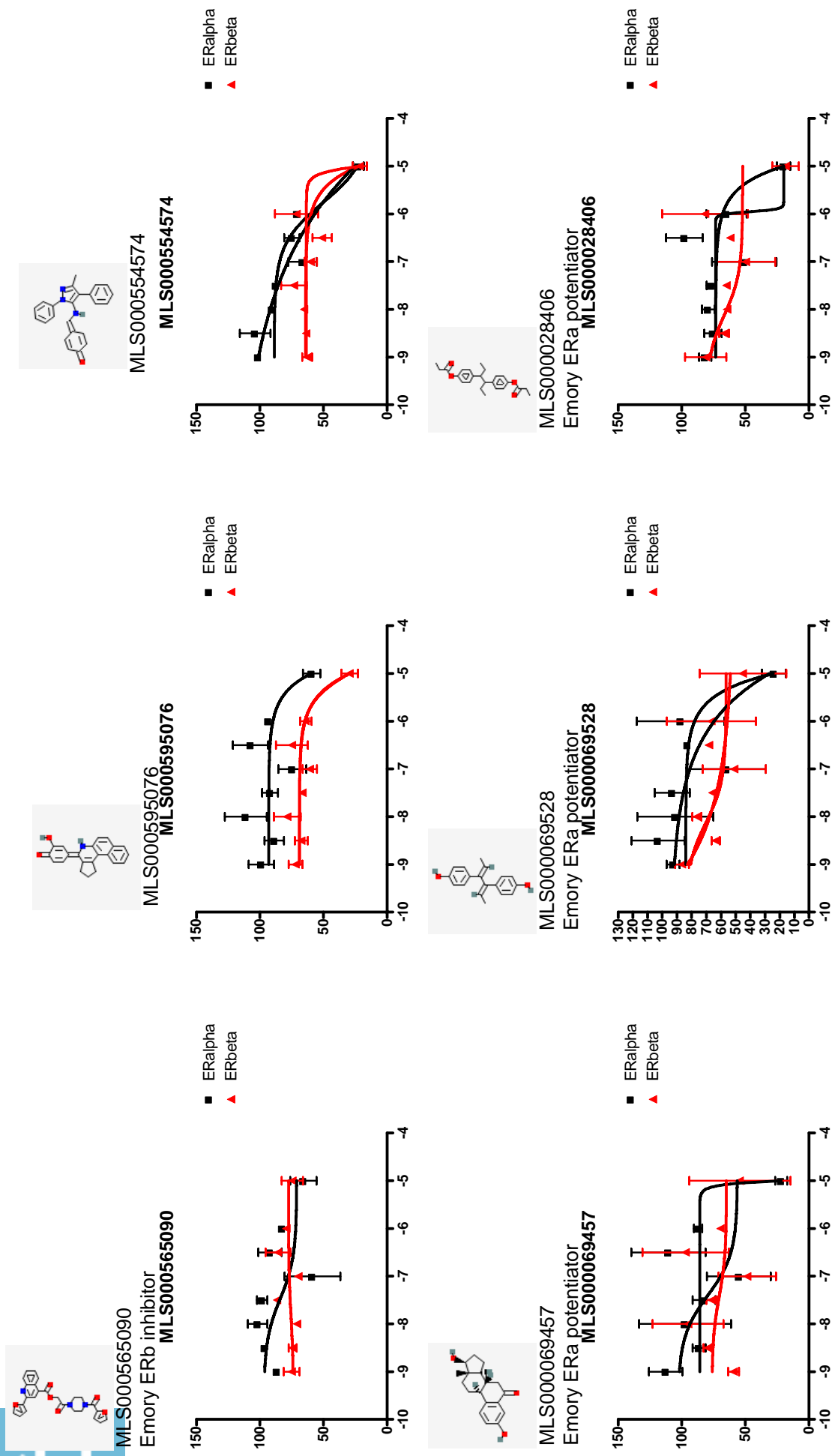


Fig. S4G. ER Roadmap Screening dose-responses of selected compounds.

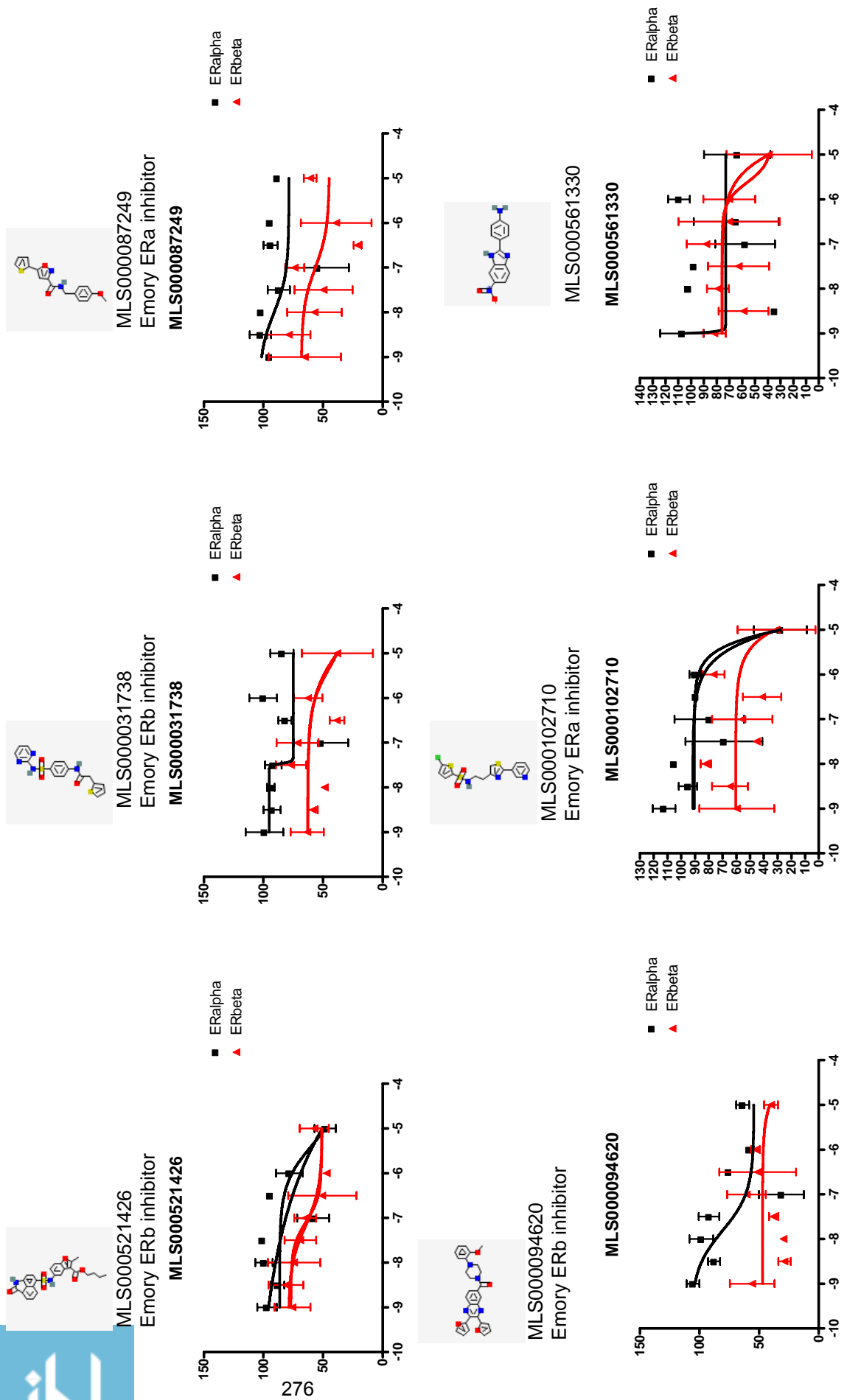
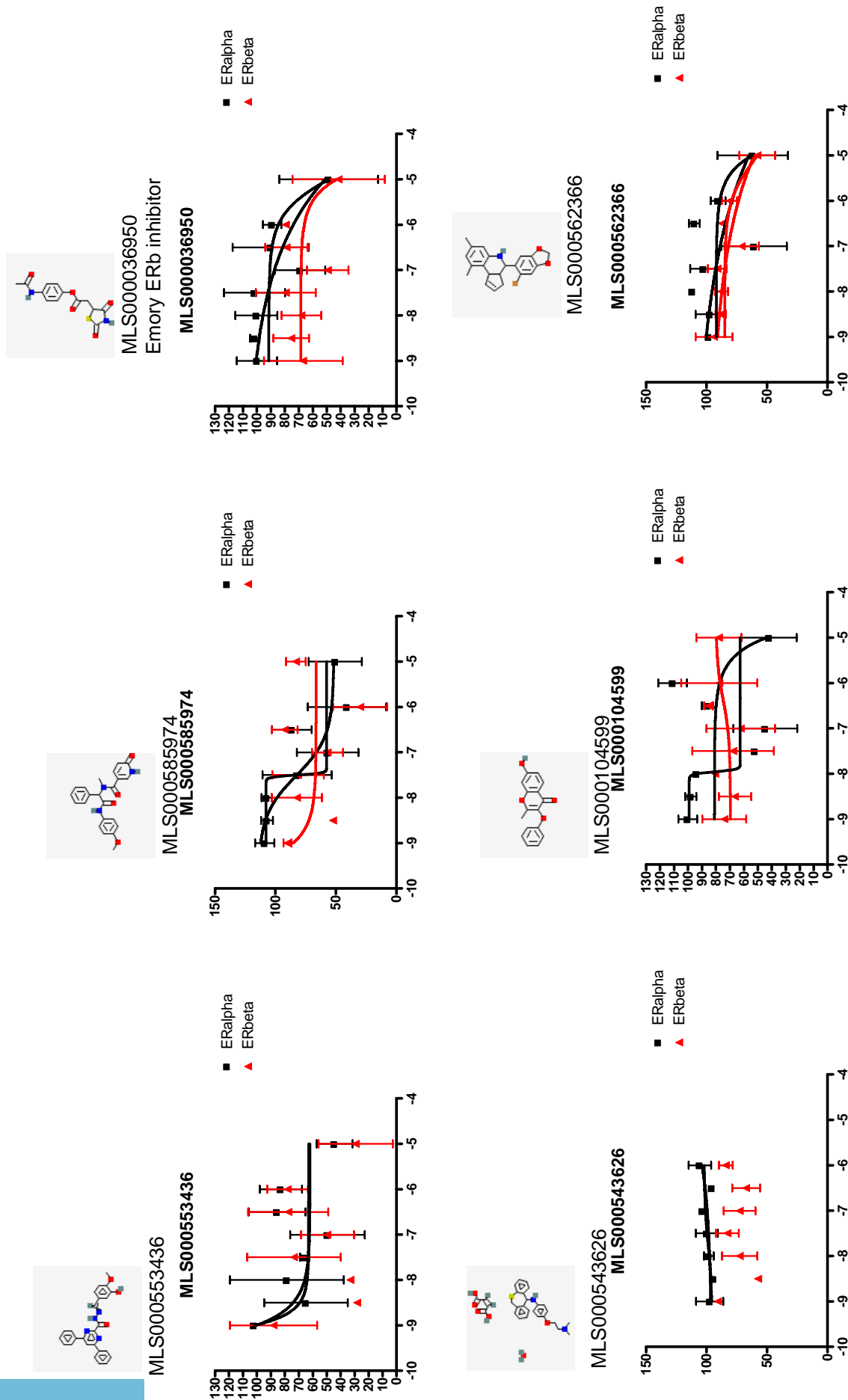


Fig. S4H. ER Roadmap Screening dose-responses of selected compounds.



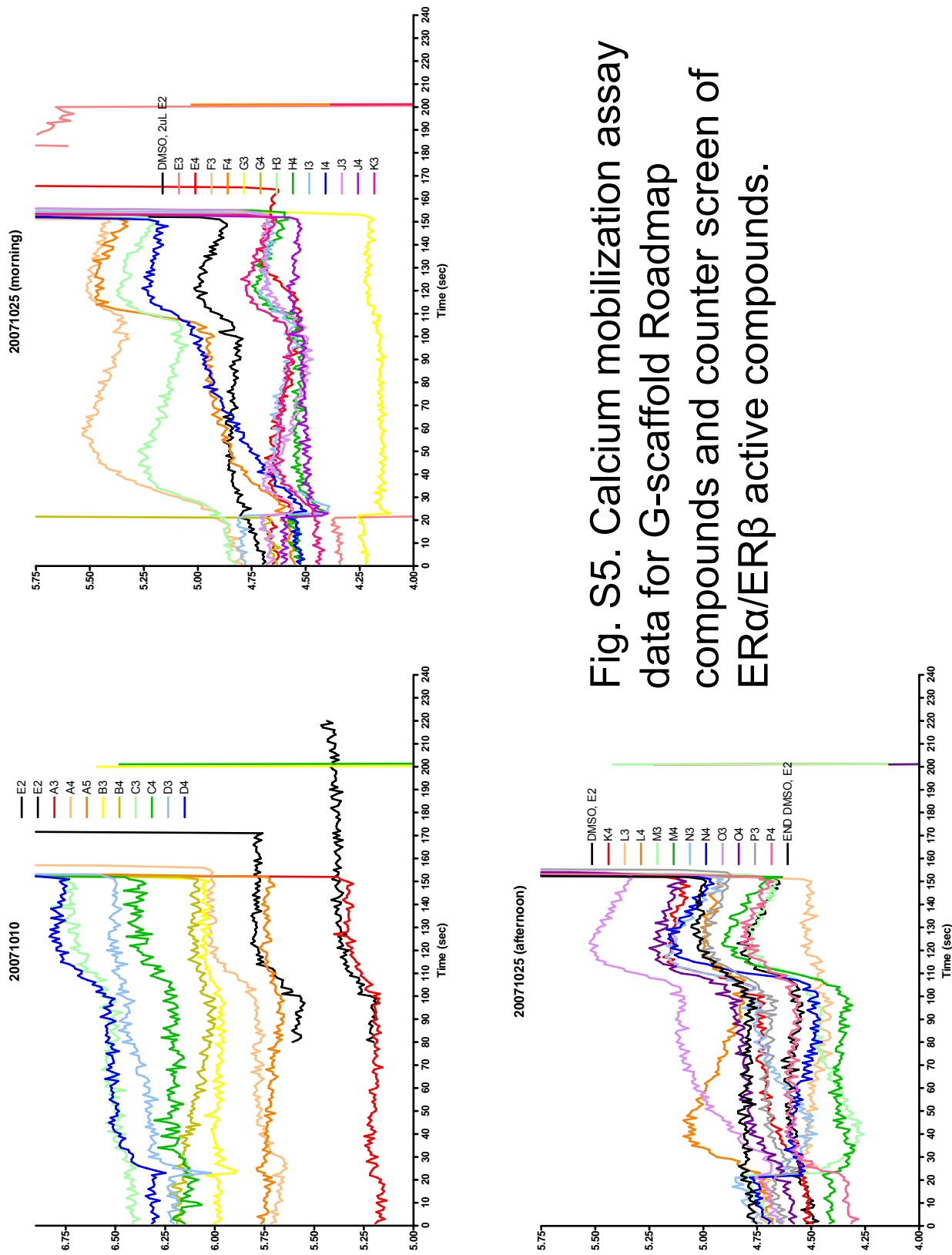
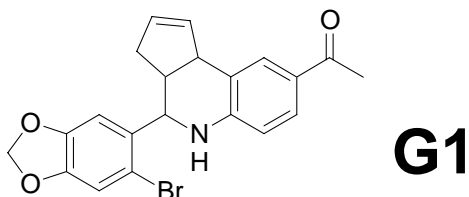


Fig. S5. Calcium mobilization assay data for G-scaffold Roadmap compounds and counter screen of ER $\alpha$ /ER $\beta$  active compounds.

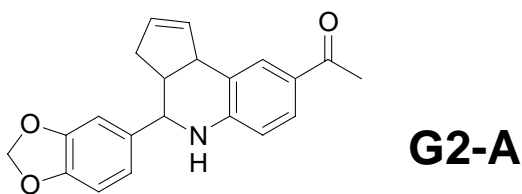


**Fig. S6. G-scaffold compounds.**



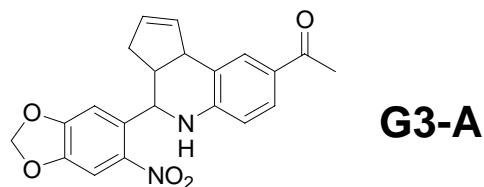
1-[4-(6-Bromo-benzo[1,3]dioxol-5-yl)-3a,4,5,9b-tetrahydro-3H-cyclopenta[c]quinolin-8-yl]-ethanone

$C_{21}H_{18}BrNO_3$   
Exact Mass: 411.05  
Mol. Wt.: 412.28  
C, 61.18; H, 4.40; Br, 19.38; N, 3.40; O, 11.64



1-(4-Benzo[1,3]dioxol-5-yl)-3a,4,5,9b-tetrahydro-3H-cyclopenta[c]quinolin-8-yl)-ethanone

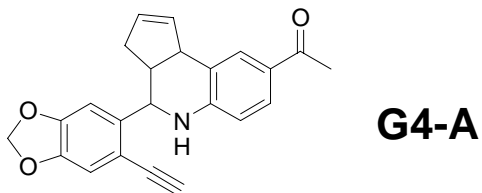
$C_{21}H_{19}NO_3$   
Exact Mass: 333.14  
Mol. Wt.: 333.38  
C, 75.66; H, 5.74; N, 4.20; O, 14.40



1-[4-(6-Nitro-benzo[1,3]dioxol-5-yl)-3a,4,5,9b-tetrahydro-3H-cyclopenta[c]quinolin-8-yl]-ethanone

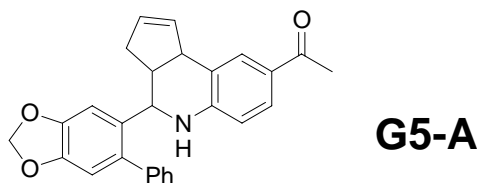
$C_{21}H_{18}N_2O_5$   
Exact Mass: 378.12  
Mol. Wt.: 378.38  
C, 66.66; H, 4.79; N, 7.40; O, 21.14

**Fig. S6. G-scaffold compounds.**



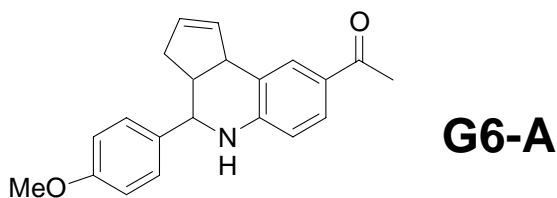
1-[4-(6-Ethynyl-benzo[1,3]dioxol-5-yl)-3a,4,5,9b-tetrahydro-3H-cyclopenta[c]quinolin-8-yl]-ethanone

$C_{23}H_{19}NO_3$   
Exact Mass: 357.14  
Mol. Wt.: 357.40  
C, 77.29; H, 5.36; N, 3.92; O, 13.43



1-[4-(6-Phenyl-benzo[1,3]dioxol-5-yl)-3a,4,5,9b-tetrahydro-3H-cyclopenta[c]quinolin-8-yl]-ethanone

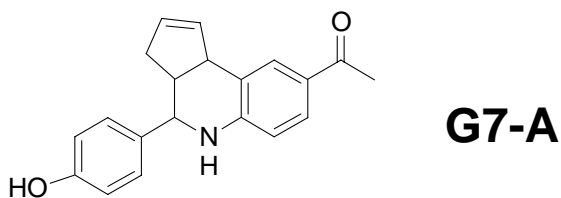
$C_{27}H_{23}NO_3$   
Exact Mass: 409.17  
Mol. Wt.: 409.48  
C, 79.20; H, 5.66; N, 3.42; O, 11.72



1-[4-(4-Methoxy-phenyl)-3a,4,5,9b-tetrahydro-3H-cyclopenta[c]quinolin-8-yl]-ethanone

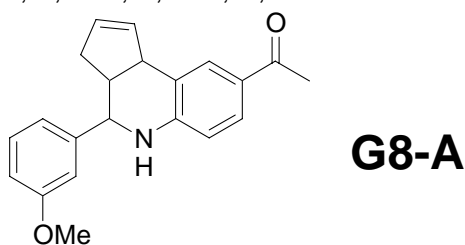
$C_{21}H_{21}NO_2$   
Exact Mass: 319.16  
Mol. Wt.: 319.40  
C, 78.97; H, 6.63; N, 4.39; O, 10.02

**Fig. S6. G-scaffold compounds.**



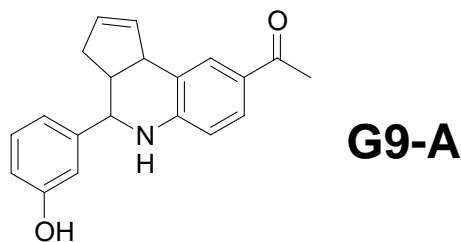
1-[4-(4-Hydroxy-phenyl)-3a,4,5,9b-tetrahydro-3H-cyclopenta[c]quinolin-8-yl]-ethanone

$C_{20}H_{19}NO_2$   
Exact Mass: 305.14  
Mol. Wt.: 305.37  
C, 78.66; H, 6.27; N, 4.59; O, 10.48



1-[4-(3-Methoxy-phenyl)-3a,4,5,9b-tetrahydro-3H-cyclopenta[c]quinolin-8-yl]-ethanone

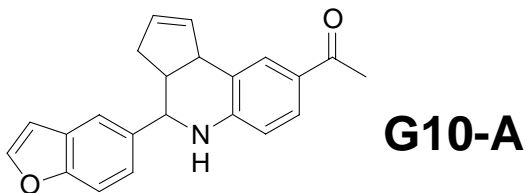
$C_{21}H_{21}NO_2$   
Exact Mass: 319.16  
Mol. Wt.: 319.40  
C, 78.97; H, 6.63; N, 4.39; O, 10.02



1-[4-(3-Hydroxy-phenyl)-3a,4,5,9b-tetrahydro-3H-cyclopenta[c]quinolin-8-yl]-ethanone

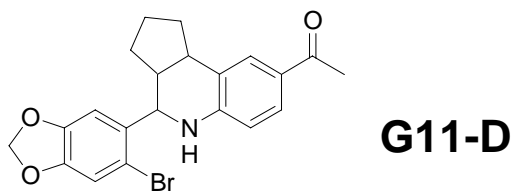
$C_{20}H_{19}NO_2$   
Exact Mass: 305.14  
Mol. Wt.: 305.37  
C, 78.66; H, 6.27; N, 4.59; O, 10.48

**Fig. S6. G-scaffold compounds.**



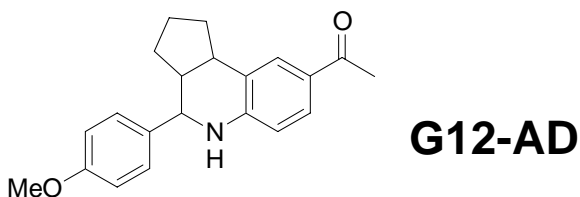
1-(4-Benzofuran-5-yl)-2,3,3a,4,5,9b-tetrahydro-3H-cyclopenta[c]quinolin-8-yl-ethanone

$C_{22}H_{19}NO_2$   
Exact Mass: 329.14  
Mol. Wt.: 329.39  
C, 80.22; H, 5.81; N, 4.25; O, 9.71



1-[4-(6-Bromo-benzo[1,3]dioxol-5-yl)]-2,3,3a,4,5,9b-hexahydro-1H-cyclopenta[c]quinolin-8-yl-ethanone

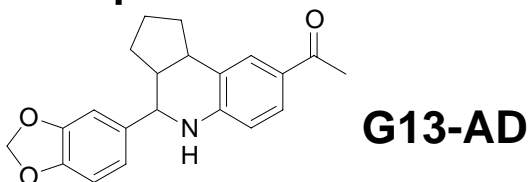
$C_{21}H_{20}BrNO_3$   
Exact Mass: 413.06  
Mol. Wt.: 414.29  
C, 60.88; H, 4.87; Br, 19.29; N, 3.38; O, 11.59



1-[4-(4-Methoxy-phenyl)]-2,3,3a,4,5,9b-hexahydro-1H-cyclopenta[c]quinolin-8-yl-ethanone

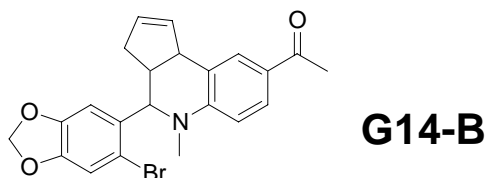
$C_{21}H_{23}NO_2$   
Exact Mass: 321.17  
Mol. Wt.: 321.41  
C, 78.47; H, 7.21; N, 4.36; O, 9.96

**Fig. S6. G-scaffold compounds.**



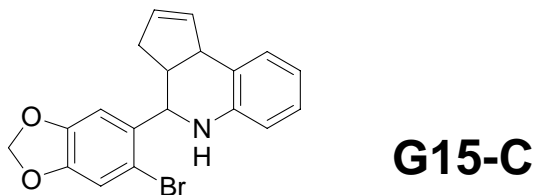
1-(4-Benzo[1,3]dioxol-5-yl)-2,3,3a,4,5,9b-hexahydro-1H-cyclopenta[c]quinolin-8-yl)-ethanone

$C_{21}H_{21}NO_3$   
Exact Mass: 335.15  
Mol. Wt.: 335.40  
C, 75.20; H, 6.31; N, 4.18; O, 14.31



1-[4-(6-Bromo-benzo[1,3]dioxol-5-yl)-5-methyl-3a,4,5,9b-tetrahydro-3H-cyclopenta[c]quinolin-8-yl]-ethanone

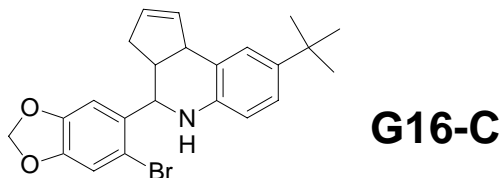
$C_{22}H_{20}BrNO_3$   
Exact Mass: 425.06  
Mol. Wt.: 426.30  
C, 61.98; H, 4.73; Br, 18.74; N, 3.29; O, 11.26



4-(6-Bromo-benzo[1,3]dioxol-5-yl)-3a,4,5,9b-tetrahydro-3H-cyclopenta[c]quinoline

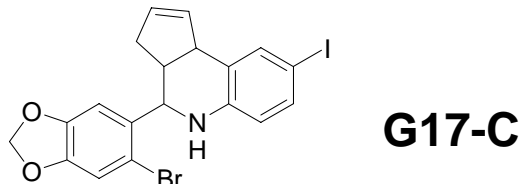
$C_{19}H_{16}BrNO_2$   
Exact Mass: 369.04  
Mol. Wt.: 370.24  
C, 61.64; H, 4.36; Br, 21.58; N, 3.78; O, 8.64

**Fig. S6. G-scaffold compounds.**



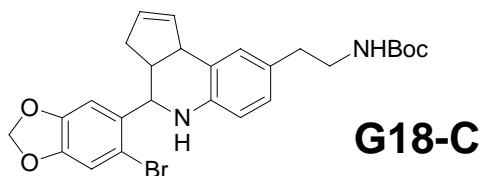
4-(6-Bromo-benzo[1,3]dioxol-5-yl)-8-*tert*-butyl-3a,4,5,9b-tetrahydro-3H-cyclopenta[*c*]quinoline

$C_{23}H_{24}BrNO_2$   
Exact Mass: 425.10  
Mol. Wt.: 426.35  
C, 64.79; H, 5.67; Br, 18.74; N, 3.29; O, 7.51



4-(6-Bromo-benzo[1,3]dioxol-5-yl)-8-iodo-3a,4,5,9b-tetrahydro-3H-cyclopenta[*c*]quinoline

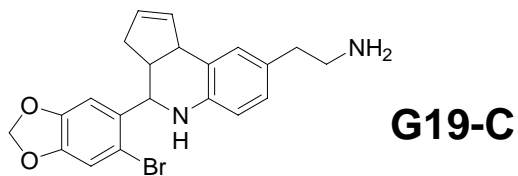
$C_{19}H_{15}BrINO_2$   
Exact Mass: 494.93  
Mol. Wt.: 496.14  
C, 46.00; H, 3.05; Br, 16.11; I, 25.58; N, 2.82; O, 6.45



{2-[4-(6-Bromo-benzo[1,3]dioxol-5-yl)-3a,4,5,9b-tetrahydro-3H-cyclopenta[*c*]quinolin-8-yl]-ethyl}  
-carbamic acid *tert*-butyl ester

$C_{26}H_{29}BrN_2O_4$   
Exact Mass: 512.13  
Mol. Wt.: 513.42  
C, 60.82; H, 5.69; Br, 15.56; N, 5.46; O, 12.46

**Fig. S6. G-scaffold compounds.**

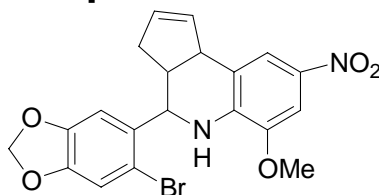


2-[4-(6-Bromo-benzo[1,3]dioxol-5-yl)-3a,4,5,9b-tetrahydro-3H-cyclopenta[c]quinolin-8-yl]-ethylamine

C<sub>21</sub>H<sub>21</sub>BrN<sub>2</sub>O<sub>2</sub>  
Exact Mass: 412.08  
Mol. Wt.: 413.31

C, 61.03; H, 5.12; Br, 19.33; N, 6.78; O, 7.74

**Fig. S6. G-scaffold compounds.**



**G20-C**

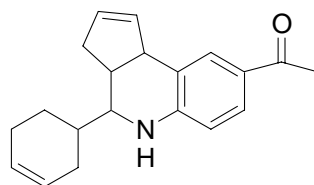
4-(6-Bromo-benzo[1,3]dioxol-5-yl)-6-methoxy-8-nitro-3a,4,5,9b-tetrahydro-3H-cyclopenta[c]quinoline

$C_{20}H_{17}BrN_2O_5$

Exact Mass: 444.03

Mol. Wt.: 445.26

C, 53.95; H, 3.85; Br, 17.95; N, 6.29; O, 17.97



**G21-A**

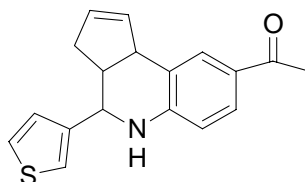
1-(4-Cyclohex-3-enyl-3a,4,5,9b-tetrahydro-3H-cyclopenta[c]quinolin-8-yl)-ethanone

$C_{20}H_{23}NO$

Exact Mass: 293.18

Mol. Wt.: 293.40

C, 81.87; H, 7.90; N, 4.77; O, 5.45



**G22-A**

1-(4-Thiophen-3-yl-3a,4,5,9b-tetrahydro-3H-cyclopenta[c]quinolin-8-yl)-ethanone

$C_{18}H_{17}NOS$

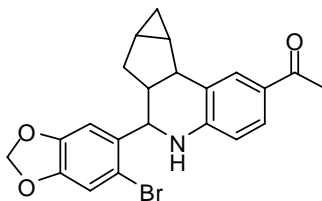
Exact Mass: 295.10

Mol. Wt.: 295.40

C, 73.19; H, 5.80; N, 4.74; O, 5.42; S, 10.86



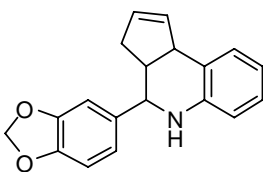
**Fig. S6. G-scaffold compounds.**



**G23-D**

1-[6-(6-Bromo-benzo[1,3]dioxol-5-yl)-5,6,6a,7,7a,8,8a,8b-octahydro-5-aza-cyclopropa[4,5]cyclopenta[1,2-a]naphthalen-2-yl]-ethanone

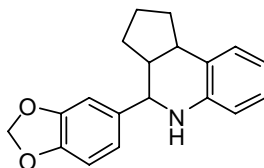
$C_{22}H_{20}BrNO_3$   
Exact Mass: 425.06  
Mol. Wt.: 426.30  
C, 61.98; H, 4.73; Br, 18.74; N, 3.29; O, 11.26



**G24-AC**

4-Benzo[1,3]dioxol-5-yl-3a,4,5,9b-tetrahydro-3H-cyclopenta[c]quinoline

$C_{19}H_{17}NO_2$   
Exact Mass: 291.13  
Mol. Wt.: 291.34  
C, 78.33; H, 5.88; N, 4.81; O, 10.98

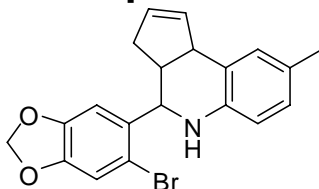


**G25-ACD**

4-Benzo[1,3]dioxol-5-yl-2,3,3a,4,5,9b-hexahydro-1H-cyclopenta[c]quinoline

$C_{19}H_{19}NO_2$   
Exact Mass: 293.14  
Mol. Wt.: 293.36  
C, 77.79; H, 6.53; N, 4.77; O, 10.91

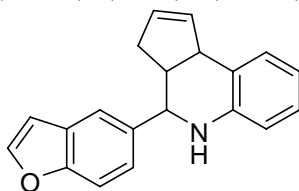
**Fig. S6. G-scaffold compounds.**



**G26-C**

4-(6-Bromo-benzo[1,3]dioxol-5-yl)-8-methyl-3a,4,5,9b-tetrahydro-3H-cyclopenta[c]quinoline

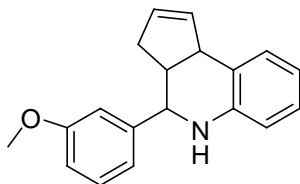
$C_{20}H_{18}BrNO_2$   
Exact Mass: 383.05  
Mol. Wt.: 384.27  
C, 62.51; H, 4.72; Br, 20.79; N, 3.65; O, 8.33



**G27-AC**

4-Benzofuran-5-yl-3a,4,5,9b-tetrahydro-3H-cyclopenta[c]quinoline

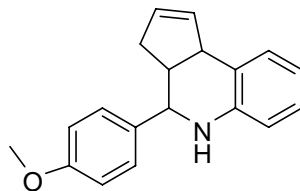
$C_{20}H_{17}NO$   
Exact Mass: 287.13  
Mol. Wt.: 287.36  
C, 83.59; H, 5.96; N, 4.87; O, 5.57



**G28-AC**

4-(3-Methoxy-phenyl)-3a,4,5,9b-tetrahydro-3H-cyclopenta[c]quinoline

$C_{19}H_{19}NO$   
Exact Mass: 277.15  
Mol. Wt.: 277.36  
C, 82.28; H, 6.90; N, 5.05; O, 5.77

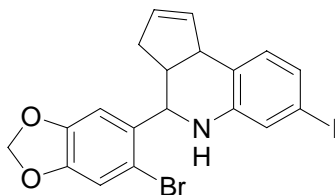


**G29-AC**

4-(4-Methoxy-phenyl)-3a,4,5,9b-tetrahydro-3H-cyclopenta[c]quinoline

$C_{19}H_{19}NO$   
Exact Mass: 277.15  
Mol. Wt.: 277.36  
C, 82.28; H, 6.90; N, 5.05; O, 5.77

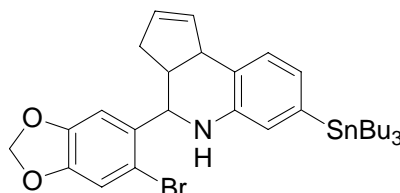
**Fig. S6. G-scaffold compounds.**



**G30-C**

4-(6-Bromo-benzo[1,3]dioxol-5-yl)-7-iodo-3a,4,5,9b-tetrahydro-3H-cyclopenta[c]quinoline

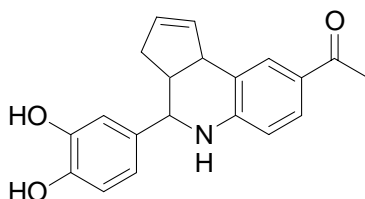
$C_{19}H_{15}BrINO_2$   
Exact Mass: 494.93  
Mol. Wt.: 496.14  
C, 46.00; H, 3.05; Br, 16.11; I, 25.58; N, 2.82; O, 6.45



**G31-C**

4-(6-Bromo-benzo[1,3]dioxol-5-yl)-7-tributylstannanyl-3a,4,5,9b-tetrahydro-3H-cyclopenta[c]quinoline

$C_{31}H_{42}BrNO_2Sn$   
Exact Mass: 659.14  
Mol. Wt.: 659.28  
C, 56.48; H, 6.42; Br, 12.12; N, 2.12; O, 4.85; Sn, 18.01

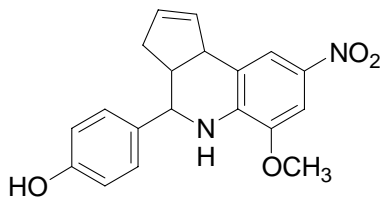


**G32-A**

1-[4-(3,4-Dihydroxy-phenyl)-3a,4,5,9b-tetrahydro-3H-cyclopenta[c]quinolin-8-yl]-ethanone

$C_{20}H_{19}NO_3$   
Exact Mass: 321.14  
Mol. Wt.: 321.37  
C, 74.75; H, 5.96; N, 4.36; O, 14.94

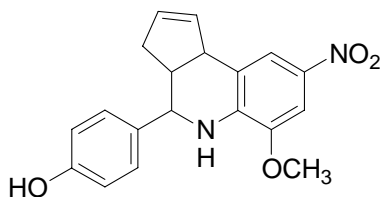
**Fig. S6. G-scaffold compounds.**



**G33-AC**

4-(6-Methoxy-8-nitro-3a,4,5,9b-tetrahydro-3H-cyclopenta[c]quinolin-4-yl)-phenol

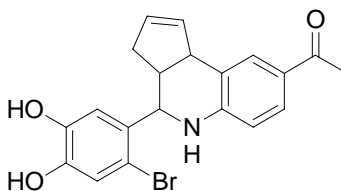
$C_{19}H_{18}N_2O_4$   
Exact Mass: 338.13  
Mol. Wt.: 338.36  
C, 67.44; H, 5.36; N, 8.28; O, 18.91



**G34-AC**

4-(6-Methoxy-8-nitro-3a,4,5,9b-tetrahydro-3H-cyclopenta[c]quinolin-4-yl)-phenol

$C_{19}H_{18}N_2O_4$   
Exact Mass: 338.13  
Mol. Wt.: 338.36  
C, 67.44; H, 5.36; N, 8.28; O, 18.91

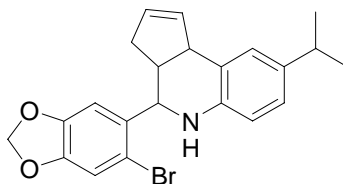


**G35-A**

1-[4-(2-Bromo-4,5-dihydroxy-phenyl)-3a,4,5,9b-tetrahydro-3H-cyclopenta[c]quinolin-8-yl]-ethanone

$C_{20}H_{18}BrNO_3$   
Exact Mass: 399.05  
Mol. Wt.: 400.27  
C, 60.01; H, 4.53; Br, 19.96; N, 3.50; O, 11.99

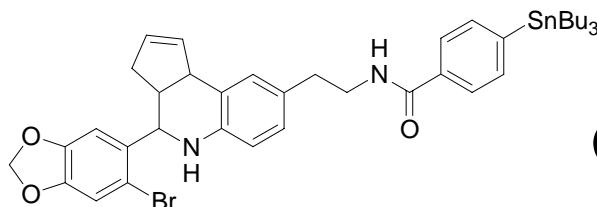
**Fig. S6. G-scaffold compounds.**



**G36-C**

4-(6-Bromo-benzo[1,3]dioxol-5-yl)-8-isopropyl-3a,4,5,9b-tetrahydro-3H-cyclopenta[c]quinoline

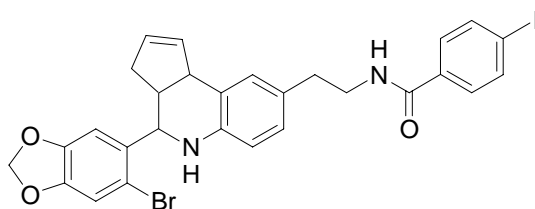
$C_{22}H_{22}BrNO_2$   
Exact Mass: 411.08  
Mol. Wt.: 412.32  
C, 64.09; H, 5.38; Br, 19.38; N, 3.40; O, 7.76



**G37-C**

*N*-{2-[4-(6-Bromo-benzo[1,3]dioxol-5-yl)-3a,4,5,9b-tetrahydro-3H-cyclopenta[c]quinolin-8-yl]-ethyl}-4-tributylstannanyl-benzamide

$C_{40}H_{51}BrN_2O_3Sn$   
Exact Mass: 806.21  
Mol. Wt.: 806.46  
C, 59.57; H, 6.37; Br, 9.91; N, 3.47; O, 5.95; Sn, 14.72



**G38-C**

*N*-{2-[4-(6-Bromo-benzo[1,3]dioxol-5-yl)-3a,4,5,9b-tetrahydro-3H-cyclopenta[c]quinolin-8-yl]-ethyl}-4-iodo-benzamide

$C_{28}H_{24}BrIN_2O_3$   
Exact Mass: 642.00  
Mol. Wt.: 643.31  
C, 52.28; H, 3.76; Br, 12.42; I, 19.73; N, 4.35; O, 7.46

## REFERENCES

- Albanito, L., R. Lappano, et al. (2008). "G-protein-coupled receptor 30 and estrogen receptor-alpha are involved in the proliferative effects induced by atrazine in ovarian cancer cells." Environ Health Perspect **116**(12): 1648-55.
- Albanito, L., A. Madeo, et al. (2007). "G protein-coupled receptor 30 (GPR30) mediates gene expression changes and growth response to 17beta-estradiol and selective GPR30 ligand G-1 in ovarian cancer cells." Cancer Res **67**(4): 1859-66.
- Alyea, R. A., S. E. Laurence, et al. (2008). "The roles of membrane estrogen receptor subtypes in modulating dopamine transporters in PC-12 cells." J Neurochem **106**(4): 1525-33.
- An, W. F. (2009). "Fluorescence-based assays." Methods Mol Biol **486**: 97-107.
- An, W. F. and N. J. Tolliday (2009). "Introduction: cell-based assays for high-throughput screening." Methods Mol Biol **486**: 1-12.
- Andreatta, C., P. Nahreini, et al. (2001). "Use of short-lived green fluorescent protein for the detection of proteasome inhibition." Biotechniques **30**(3): 656-60.
- Aneck-Hahn, N. H., G. W. Schulenburg, et al. (2007). "Impaired semen quality associated with environmental DDT exposure in young men living in a malaria area in the Limpopo Province, South Africa." J Androl **28**(3): 423-34.
- Araki, N., K. Ohno, et al. (2005). "Evaluation of a rapid in vitro androgen receptor transcriptional activation assay using AR-EcoScreen cells." Toxicol In Vitro **19**(3): 335-52.
- Arias-Pulido, H., M. Royce, et al. (2009). "GPR30 and estrogen receptor expression: new insights into hormone dependence of inflammatory breast cancer." Breast Cancer Res Treat.
- Ariazi, E. A., J. L. Ariazi, et al. (2006). "Estrogen receptors as therapeutic targets in breast cancer." Curr Top Med Chem **6**(3): 181-202.
- Arnone, M. I., I. J. Dmochowski, et al. (2004). "Using reporter genes to study cis-regulatory elements." Methods Cell Biol **74**: 621-52.
- Bakken, K., E. Alsaker, et al. (2004). "Hormone replacement therapy and incidence of hormone-dependent cancers in the Norwegian Women and Cancer study." Int J Cancer **w112**(1): 130-4.

- Balla, T. and P. Varnai (2002). "Visualizing cellular phosphoinositide pools with GFP-fused protein-modules." Sci STKE **2002**(125): PL3.
- Banerjee, S., T. Das, et al. (2005). "An estradiol-conjugate for radiolabelling with <sup>177</sup>Lu: an attempt to prepare a radiotherapeutic agent." Bioorg Med Chem **13**(13): 4315-22.
- Barletta, F., C. W. Wong, et al. (2004). "Characterization of the interactions of estrogen receptor and MNAR in the activation of cSrc." Mol Endocrinol **18**(5): 1096-108.
- Barone, T. A., J. W. Gorski, et al. (2009). "Estrogen increases survival in an orthotopic model of glioblastoma." J Neurooncol **95**(1): 37-48.
- Barrett-Connor, E., J. E. Mueller, et al. (2000). "Low levels of estradiol are associated with vertebral fractures in older men, but not women: the Rancho Bernardo Study." J Clin Endocrinol Metab **85**(1): 219-23.
- Baumgartner, R. N., R. R. Ross, et al. (1999). "Serum leptin in elderly people: associations with sex hormones, insulin, and adipose tissue volumes." Obes Res **7**(2): 141-9.
- Beato, M. and J. Klug (2000). "Steroid hormone receptors: an update." Hum Reprod Update **6**(3): 225-36.
- Benten, W. P., M. Lieberherr, et al. (1999). "Testosterone signaling through internalizable surface receptors in androgen receptor-free macrophages." Mol Biol Cell **10**(10): 3113-23.
- Bergerat, J. P. and J. Ceraline (2009). "Pleiotropic functional properties of androgen receptor mutants in prostate cancer." Hum Mutat **30**(2): 145-57.
- Berno, V., C. A. Hinojos, et al. (2006). "High-resolution, high-throughput microscopy analyses of nuclear receptor and coregulator function." Methods Enzymol **414**: 188-210.
- Bi, J. X., M. Wirth, et al. (2002). "Dynamic characterization of recombinant Chinese hamster ovary cells containing an inducible c-fos promoter GFP expression system as a biomarker." J Biotechnol **93**(3): 231-42.
- Bianco, J. J., D. J. Handelsman, et al. (2002). "Direct response of the murine prostate gland and seminal vesicles to estradiol." Endocrinology **143**(12): 4922-33.
- Blasko, E., C. A. Haskell, et al. (2009). "Beneficial role of the GPR30 agonist G-1 in an animal model of multiple sclerosis." J Neuroimmunol.

- Bologa, C. G., C. M. Revankar, et al. (2006). "Virtual and biomolecular screening converge on a selective agonist for GPR30." Nature Chemical Biology **2**(4): 207-12.
- Bologa, C. G., C. M. Revankar, et al. (2006). "Virtual and biomolecular screening converge on a selective agonist for GPR30." Nat Chem Biol **2**(4): 207-12.
- Brailoiu, E., S. L. Dun, et al. (2007). "Distribution and characterization of estrogen receptor G protein-coupled receptor 30 in the rat central nervous system." J. Endocrinol. **193**(2): 311-321.
- Brandes, A. A., M. Ermani, et al. (1999). "Procarbazine and high-dose tamoxifen as a second-line regimen in recurrent high-grade gliomas: a phase II study." J Clin Oncol **17**(2): 645-50.
- Brass, A. L., J. Barnard, et al. (1995). "Androgen up-regulates epidermal growth factor receptor expression and binding affinity in PC3 cell lines expressing the human androgen receptor." Cancer Res **55**(14): 3197-203.
- Brass, L. M. (2004). "Hormone replacement therapy and stroke: clinical trials review." Stroke **35**(11 Suppl 1): 2644-7.
- Brooks, J. H. and J. R. Reddon (1996). "Serum testosterone in violent and nonviolent young offenders." J Clin Psychol **52**(4): 475-83.
- Castoria, G., A. Migliaccio, et al. (2001). "PI3-kinase in concert with Src promotes the S-phase entry of oestradiol-stimulated MCF-7 cells." Embo J **20**(21): 6050-9.
- Chang, C. Y., Y. D. Hsuuw, et al. (2006). "Androgenic and antiandrogenic effects and expression of androgen receptor in mouse embryonic stem cells." Fertil Steril **85 Suppl 1**: 1195-203.
- Chen, C. D., D. S. Welsbie, et al. (2004). "Molecular determinants of resistance to antiandrogen therapy." Nat Med **10**(1): 33-9.
- Cheng, J., S. C. Watkins, et al. (2007). "Testosterone activates mitogen-activated protein kinase via Src kinase and the epidermal growth factor receptor in sertoli cells." Endocrinology **148**(5): 2066-74.
- Chodosh, L. A. and R. D. Cardiff (2006). "In vivo imaging of the mammary gland: the shape of things to come." J Mammary Gland Biol Neoplasia **11**(2): 101-2.
- Christian, H. C., N. J. Rolls, et al. (2000). "Nongenomic actions of testosterone on a subset of lactotrophs in the male rat pituitary." Endocrinology **141**(9): 3111-9.



- Church, D. R., E. Lee, et al. (2005). "Induction of AP-1 activity by androgen activation of the androgen receptor in LNCaP human prostate carcinoma cells." Prostate **63**(2): 155-68.
- Cloughesy, T. F., R. P. Woods, et al. (1997). "Prolonged treatment with biologic agents for malignant glioma: a case study with high dose tamoxifen." J Neurooncol **35**(1): 39-45.
- Coleman, R. E. (2000). "FDG imaging." Nucl Med Biol **27**(7): 689-90.
- Coughlin, S. S., A. Giustozzi, et al. (2000). "A meta-analysis of estrogen replacement therapy and risk of epithelial ovarian cancer." J Clin Epidemiol **53**(4): 367-75.
- Couldwell, W. T., D. R. Hinton, et al. (1996). "Treatment of recurrent malignant gliomas with chronic oral high-dose tamoxifen." Clin Cancer Res **2**(4): 619-22.
- Couse, J. F. and K. S. Korach (1999). "Estrogen receptor null mice: what have we learned and where will they lead us?" Endocrine Rev. **20**(3): 358-417.
- Cryan, J. F., C. Mombereau, et al. (2005). "The tail suspension test as a model for assessing antidepressant activity: review of pharmacological and genetic studies in mice." Neurosci Biobehav Rev **29**(4-5): 571-625.
- Cummins, C. H. (1993). "Radiolabeled steroidal estrogens in cancer research." Steroids **58**(6): 245-59.
- Currie, L. J., M. B. Harrison, et al. (2004). "Postmenopausal estrogen use affects risk for Parkinson disease." Arch Neurol **61**(6): 886-8.
- Curtis, S. W., J. Clark, et al. (1999). "Disruption of estrogen signaling does not prevent progesterone action in the estrogen receptor alpha knockout mouse uterus." Proc Natl Acad Sci U S A **96**(7): 3646-51.
- Dai, R., R. A. Phillips, et al. (2009). "Estrogen Regulates Transcription Factors STAT-1 and NF- $\kappa$ B to Promote Inducible Nitric Oxide Synthase and Inflammatory Responses." J Immunol.
- Dehdashti, F., J. E. Mortimer, et al. (2009). "PET-based estradiol challenge as a predictive biomarker of response to endocrine therapy in women with estrogen-receptor-positive breast cancer." Breast Cancer Res Treat **113**(3): 509-17.
- Dehm, S. M. and D. J. Tindall (2006). "Molecular regulation of androgen action in prostate cancer." J Cell Biochem **99**(2): 333-44.

- Delpassand, E. S., D. J. Yang, et al. (1996). "Synthesis, biodistribution, and estrogen receptor scintigraphy of indium-111-diethylenetriaminepentaacetic acid-tamoxifen analogue." J Pharm Sci **85**(6): 553-9.
- Dennis, M. K., H. J. Bowles, et al. (2008). "A multifunctional androgen receptor screening assay using the high-throughput Hypercyt((R)) flow cytometry system." Cytometry A.
- Dennis, M. K., R. Burai, et al. (2009). "In vivo effects of a GPR30 antagonist." Nat Chem Biol **5**(6): 421-7.
- Deroo, B. J. and K. S. Korach (2006). "Estrogen receptors and human disease." J Clin Invest **116**(3): 561-70.
- Dhandapani, K. M. and D. W. Brann (2002). "Protective effects of estrogen and selective estrogen receptor modulators in the brain." Biol Reprod **67**(5): 1379-85.
- Diel, P., R. B. Geis, et al. (2004). "The differential ability of the phytoestrogen genistein and of estradiol to induce uterine weight and proliferation in the rat is associated with a substance specific modulation of uterine gene expression." Molecular and Cellular Endocrinology **221**(1-2): 21-32.
- Domingo-Domenech, J., P. L. Fernandez, et al. (2008). "Serum HER2 extracellular domain predicts an aggressive clinical outcome and biological PSA response in hormone-independent prostate cancer patients treated with docetaxel." Ann Oncol **19**(2): 269-75.
- Dubal, D. B., H. Zhu, et al. (2001). "Estrogen receptor alpha, not beta, is a critical link in estradiol-mediated protection against brain injury." Proc Natl Acad Sci U S A **98**(4): 1952-7.
- Dun, S. L., G. C. Brailoiu, et al. (2009). "Expression of estrogen receptor GPR30 in the rat spinal cord and in autonomic and sensory ganglia." J Neurosci Res **87**: 1610-1619.
- Edwards, B. S., T. Oprea, et al. (2004). "Flow cytometry for high-throughput, high-content screening." Curr Opin Chem Biol **8**(4): 392-8.
- Edwards, B. S., S. M. Young, et al. (2009). "High-content screening: flow cytometry analysis." Methods Mol Biol **486**: 151-65.
- Edwards, B. S., S. M. Young, et al. (2007). "High-throughput flow cytometry for drug discovery." Expert Opinion on Drug Discovery **2**(5): 685-696.
- Edwards, D. P. (2005). "Regulation of signal transduction pathways by estrogen and progesterone." Annu Rev Physiol **67**: 335-76.

- Ellem, S. J., J. F. Schmitt, et al. (2004). "Local aromatase expression in human prostate is altered in malignancy." J Clin Endocrinol Metab **89**(5): 2434-41.
- Epperson, C. N., K. L. Wisner, et al. (1999). "Gonadal steroids in the treatment of mood disorders." Psychosom Med **61**(5): 676-97.
- Estrada-Camarena, E., A. Fernandez-Guasti, et al. (2003). "Antidepressant-like effect of different estrogenic compounds in the forced swimming test." Neuropsychopharmacology **28**(5): 830-8.
- Fang, H., W. Tong, et al. (2003). "Study of 202 natural, synthetic, and environmental chemicals for binding to the androgen receptor." Chem Res Toxicol **16**(10): 1338-58.
- Ferguson, A. T., R. G. Lapidus, et al. (1995). "Demethylation of the estrogen receptor gene in estrogen receptor-negative breast cancer cells can reactivate estrogen receptor gene expression." Cancer Res **55**(11): 2279-83.
- Filardo, E., J. Quinn, et al. (2007). "Activation of the novel estrogen receptor G protein-coupled receptor 30 (GPR30) at the plasma membrane." Endocrinology **148**(7): 3236-45.
- Filardo, E. J., C. T. Graeber, et al. (2006). "Distribution of GPR30, a seven membrane-spanning estrogen receptor, in primary breast cancer and its association with clinicopathologic determinants of tumor progression." Clin Cancer Res **12**(21): 6359-66.
- Filardo, E. J., J. A. Quinn, et al. (2000). "Estrogen-induced activation of Erk-1 and Erk-2 requires the G protein-coupled receptor homolog, GPR30, and occurs via trans-activation of the epidermal growth factor receptor through release of HB-EGF." Mol Endocrinol **14**(10): 1649-60.
- Filardo, E. J., J. A. Quinn, et al. (2002). "Estrogen action via the G protein-coupled receptor, GPR30: stimulation of adenylyl cyclase and cAMP-mediated attenuation of the epidermal growth factor receptor-to-MAPK signaling axis." Mol Endocrinol **16**(1): 70-84.
- Filardo, E. J., J. A. Quinn, et al. (2008). "Association of the membrane estrogen receptor, GPR30, with breast tumor metastasis and transactivation of the epidermal growth factor receptor." Steroids **73**(9-10): 870-3.
- Foley, E. F., A. A. Jazaeri, et al. (2000). "Selective loss of estrogen receptor beta in malignant human colon." Cancer Res **60**(2): 245-8.
- Frasor, J., D. H. Barnett, et al. (2003). "Response-specific and ligand dose-dependent modulation of estrogen receptor (ER) alpha activity by ERbeta in the uterus." Endocrinology **144**(7): 3159-66.

- Friedrich, E. B., Y. P. Clever, et al. (2006). "17Beta-estradiol inhibits monocyte adhesion via down-regulation of Rac1 GTPase." J Mol Cell Cardiol **40**(1): 87-95.
- Fu, X. D. and T. Simoncini (2008). "Extra-nuclear signaling of estrogen receptors." IUBMB Life **60**(8): 502-10.
- Fujimoto, M., E. Yoshino, et al. (1984). "Estrogen receptors in brain tumors." Clin Neuropharmacol **7**(4): 357-62.
- Funakoshi, T., A. Yanai, et al. (2006). "G protein-coupled receptor 30 is an estrogen receptor in the plasma membrane." Biochem Biophys Res Commun **346**(3): 904-10.
- Fuse, H., S. Korenaga, et al. (2007). "Non-steroidal antiandrogens act as AF-1 agonists under conditions of high androgen-receptor expression." Prostate **67**(6): 630-7.
- Gann, P. H., C. H. Hennekens, et al. (1996). "Prospective study of sex hormone levels and risk of prostate cancer." J Natl Cancer Inst **88**(16): 1118-26.
- Gelmann, E. P. (2002). "Molecular biology of the androgen receptor." J Clin Oncol **20**(13): 3001-15.
- Genazzani, A. R., A. Spinetti, et al. (1999). "Menopause and the central nervous system: intervention options." Maturitas **31**(2): 103-10.
- Gill, A., M. Jamnongjit, et al. (2004). "Androgens promote maturation and signaling in mouse oocytes independent of transcription: a release of inhibition model for mammalian oocyte meiosis." Mol Endocrinol **18**(1): 97-104.
- GPER/GPR30. from <http://www.iuphar-db.org/GPCR/ReceptorDisplayForward?receptorID=3055>.
- Grady, D., T. Gebretsadik, et al. (1995). "Hormone replacement therapy and endometrial cancer risk: a meta-analysis." Obstet Gynecol **85**(2): 304-13.
- Grunert, G., M. Porcia, et al. (1986). "Differential potency of oestradiol-17 beta and diethylstilboestrol on separate groups of responses in the rat uterus." Journal of Endocrinology **110**(1): 103-14.
- Gunanathan, C., A. Pais, et al. (2007). "Water-soluble contrast agents targeted at the estrogen receptor for molecular magnetic resonance imaging." Bioconjug Chem **18**(5): 1361-5.
- Guzzo, J. A. (2000). "Selective estrogen receptor modulators--a new age of estrogens in cardiovascular disease?" Clin Cardiol **23**(1): 15-7.

- Gyllenborg, J., S. L. Rasmussen, et al. (2001). "Cardiovascular risk factors in men: The role of gonadal steroids and sex hormone-binding globulin." Metabolism **50**(8): 882-8.
- Haas, D., S. N. White, et al. (2005). "The modulator of nongenomic actions of the estrogen receptor (MNAR) regulates transcription-independent androgen receptor-mediated signaling: evidence that MNAR participates in G protein-regulated meiosis in *Xenopus laevis* oocytes." Mol Endocrinol **19**(8): 2035-46.
- Haas, E., I. Bhattacharya, et al. (2009). "Regulatory Role of G Protein-Coupled Estrogen Receptor for Vascular Function and Obesity." Circ Res.
- Haas, E., I. Bhattacharya, et al. (2009). "Regulatory role of G protein-coupled estrogen receptor for vascular function and obesity." Circ Res **104**(3): 288-91.
- Hall, J., R. D. Jones, et al. (2006). "Selective inhibition of L-type Ca<sup>2+</sup> channels in A7r5 cells by physiological levels of testosterone." Endocrinology **147**(6): 2675-80.
- Hanson, R. N. (2000). "Synthesis of Auger electron-emitting radiopharmaceuticals." Curr Pharm Des **6**(14): 1457-68.
- Hara, T., J. Miyazaki, et al. (2003). "Novel mutations of androgen receptor: a possible mechanism of bicalutamide withdrawal syndrome." Cancer Res **63**(1): 149-53.
- Harris, H. A., L. M. Albert, et al. (2003). "Evaluation of an estrogen receptor-beta agonist in animal models of human disease." Endocrinology **144**(10): 4241-9.
- Hatch, E. E., M. S. Linet, et al. (2005). "Reproductive and hormonal factors and risk of brain tumors in adult females." Int J Cancer **114**(5): 797-805.
- Hazell, G. G., S. T. Yao, et al. (2009). "Localisation of GPR30, a novel G protein-coupled oestrogen receptor, suggests multiple functions in rodent brain and peripheral tissues." J Endocrinol **202**(2): 223-36.
- He, B., J. A. Kempainen, et al. (1999). "Activation function 2 in the human androgen receptor ligand binding domain mediates interdomain communication with the NH(2)-terminal domain." J Biol Chem **274**(52): 37219-25.
- Heinlein, C. A. and C. Chang (2002). "The roles of androgen receptors and androgen-binding proteins in nongenomic androgen actions." Mol Endocrinol **16**(10): 2181-7.

- Hellweg, C. E., C. Baumstark-Khan, et al. (2003). "Generation of stably transfected Mammalian cell lines as fluorescent screening assay for NF-kappaB activation-dependent gene expression." J Biomol Screen **8**(5): 511-21.
- Henderson, B. E. and H. S. Feigelson (2000). "Hormonal carcinogenesis." Carcinogenesis **21**(3): 427-33.
- Hensley, M. L. (2002). "Epithelial ovarian cancer." Curr Treat Options Oncol **3**(2): 131-41.
- Herrmann, B. L., B. Saller, et al. (2002). "Impact of estrogen replacement therapy in a male with congenital aromatase deficiency caused by a novel mutation in the CYP19 gene." J Clin Endocrinol Metab **87**(12): 5476-84.
- Hess-Wilson, J. K. and K. E. Knudsen (2006). "Endocrine disrupting compounds and prostate cancer." Cancer Lett **241**(1): 1-12.
- Hewitt, S. C., E. H. Goulding, et al. (2002). "Studies using the estrogen receptor alpha knockout uterus demonstrate that implantation but not decidualization-associated signaling is estrogen dependent." Biol Reprod **67**(4): 1268-77.
- Hewitt, S. C., J. C. Harrell, et al. (2005). "Lessons in estrogen biology from knockout and transgenic animals." Annual Review of Physiology **67**: 285-308.
- Ho, S. M. (2003). "Estrogen, progesterone and epithelial ovarian cancer." Reprod Biol Endocrinol **1**: 73.
- Hochberg, R. B. and W. Rosner (1980). "Interaction of 16 alpha-[125I]iodo-estradiol with estrogen receptor and other steroid-binding proteins." Proc Natl Acad Sci U S A **77**(1): 328-32.
- Holzbeierlein, J., P. Lal, et al. (2004). "Gene expression analysis of human prostate carcinoma during hormonal therapy identifies androgen-responsive genes and mechanisms of therapy resistance." Am J Pathol **164**(1): 217-27.
- Huang, K., E. A. Whelan, et al. (2004). "Reproductive factors and risk of glioma in women." Cancer Epidemiol Biomarkers Prev **13**(10): 1583-8.
- Hui, A. M., W. Zhang, et al. (2004). "Agents with selective estrogen receptor (ER) modulator activity induce apoptosis in vitro and in vivo in ER-negative glioma cells." Cancer Res **64**(24): 9115-23.
- Hurn, P. D. and I. M. Macrae (2000). "Estrogen as a neuroprotectant in stroke." J Cereb Blood Flow Metab **20**(4): 631-52.

- Ito, K. (2007). "Hormone replacement therapy and cancers: the biological roles of estrogen and progesterin in tumorigenesis are different between the endometrium and breast." Tohoku J Exp Med **212**(1): 1-12.
- Jukich, P. J., B. J. McCarthy, et al. (2001). "Trends in incidence of primary brain tumors in the United States, 1985-1994." Neuro Oncol **3**(3): 141-51.
- Kaighn, M. E., K. S. Narayan, et al. (1979). "Establishment and characterization of a human prostatic carcinoma cell line (PC-3)." Invest Urol **17**(1): 16-23.
- Kamanga-Sollo, E., M. E. White, et al. (2008). "Potential role of G-protein-coupled receptor 30 (GPR30) in estradiol-17beta-stimulated IGF-I mRNA expression in bovine satellite cell cultures." Domest Anim Endocrinol **35**(3): 254-62.
- Kampa, M., E. A. Papakonstanti, et al. (2002). "The human prostate cancer cell line LNCaP bears functional membrane testosterone receptors that increase PSA secretion and modify actin cytoskeleton." Faseb J **16**(11): 1429-31.
- Kanda, N. and S. Watanabe (2003). "17Beta-estradiol enhances the production of nerve growth factor in THP-1-derived macrophages or peripheral blood monocyte-derived macrophages." J Invest Dermatol **121**(4): 771-80.
- Kanda, N. and S. Watanabe (2003). "17beta-estradiol inhibits oxidative stress-induced apoptosis in keratinocytes by promoting Bcl-2 expression." J Invest Dermatol **121**(6): 1500-9.
- Kanda, N. and S. Watanabe (2004). "17beta-estradiol stimulates the growth of human keratinocytes by inducing cyclin D2 expression." J Invest Dermatol **123**(2): 319-28.
- Kato, S., T. Sato, et al. (2005). "Function of nuclear sex hormone receptors in gene regulation." Cancer Chemother Pharmacol **56 Suppl 1**: 4-9.
- Katzenellenbogen, J. A., K. E. Carlson, et al. (1980). "Receptor-binding radiopharmaceuticals for imaging breast tumors: estrogen-receptor interactions and selectivity of tissue uptake of halogenated estrogen analogs." Journal of Nuclear Medicine **21**(6): 550-558.
- Khosla, S., L. J. Melton, 3rd, et al. (2001). "Relationship of serum sex steroid levels to longitudinal changes in bone density in young versus elderly men." J Clin Endocrinol Metab **86**(8): 3555-61.
- Kiss-Toth, E., F. M. Guesdon, et al. (2000). "A novel mammalian expression screen exploiting green fluorescent protein-based transcription detection in single cells." J Immunol Methods **239**(1-2): 125-35.



- Kizu, R., N. Otsuki, et al. (2004). "A new luciferase reporter gene assay for the detection of androgenic and antiandrogenic effects based on a human prostate specific antigen promoter and PC3/AR human prostate cancer cells." Anal Sci **20**(1): 55-9.
- Kobayashi, S., H. Ishitani, et al. (1995). "Lanthanide triflate catalyzed imino Diels-Alder reactions; convenient synthesis of pyridine and quinoline derivatives." Synthesis(9): 1195-1202.
- Korach, K. S. (1994). "Insights from the study of animals lacking functional estrogen receptor." Science **266**(5190): 1524-7.
- Kousteni, S., T. Bellido, et al. (2001). "Nongenotropic, sex-nonspecific signaling through the estrogen or androgen receptors: dissociation from transcriptional activity." Cell **104**(5): 719-30.
- Kuckuck, F. W., B. S. Edwards, et al. (2001). "High throughput flow cytometry." Cytometry **44**(1): 83-90.
- Kuhn, J., O. A. Dina, et al. (2008). "GPR30 estrogen receptor agonists induce mechanical hyperalgesia in the rat." Eur J Neurosci **27**(7): 1700-9.
- Kuiper, G. G., E. Enmark, et al. (1996). "Cloning of a novel receptor expressed in rat prostate and ovary." Proc Natl Acad Sci U S A **93**(12): 5925-30.
- Kuiper, G. G., P. J. Shughrue, et al. (1998). "The estrogen receptor beta subtype: a novel mediator of estrogen action in neuroendocrine systems." Front Neuroendocrinol **19**(4): 253-86.
- Kumar, P., Q. Wu, et al. (2007). "Direct Interactions with Gai and Gβγ Mediate Nongenomic Signaling by ERα." Mol Endocrinol.
- Kushner, P. J., D. A. Agard, et al. (2000). "Estrogen receptor pathways to AP-1." J Steroid Biochem Mol Biol **74**(5): 311-7.
- Lamb, D. J., N. L. Weigel, et al. (2001). "Androgen receptors and their biology." Vitam Horm **62**: 199-230.
- Lange, C. A., D. Gioeli, et al. (2007). "Integration of rapid signaling events with steroid hormone receptor action in breast and prostate cancer." Annu Rev Physiol **69**: 171-199.
- Lange, C. A., J. K. Richer, et al. (1998). "Convergence of progesterone and epidermal growth factor signaling in breast cancer. Potentiation of mitogen-activated protein kinase pathways." J Biol Chem **273**(47): 31308-16.
- Lannigan, D. A. (2003). "Estrogen receptor phosphorylation." Steroids **68**(1): 1-9.



- Lashley, M. R., E. J. Niedzinski, et al. (2002). "Synthesis and estrogen receptor affinity of a 4-hydroxytamoxifen-labeled ligand for diagnostic imaging." Bioorg Med Chem **10**(12): 4075-82.
- Lax, S. F. (2004). "Molecular genetic pathways in various types of endometrial carcinoma: from a phenotypical to a molecular-based classification." Virchows Arch **444**(3): 213-23.
- Leav, I., F. B. Merk, et al. (1989). "Androgen-supported estrogen-enhanced epithelial proliferation in the prostates of intact Noble rats." Prostate **15**(1): 23-40.
- Leslie, K. K., D. Keefe, et al. (1994). "Estrogen receptors are identified in the glioblastoma cell line U138MG." J Soc Gynecol Investig **1**(3): 238-44.
- Li, A. J., R. L. Baldwin, et al. (2003). "Estrogen and progesterone receptor subtype expression in normal and malignant ovarian epithelial cell cultures." Am J Obstet Gynecol **189**(1): 22-7.
- Li, X., X. Zhao, et al. (1998). "Generation of destabilized green fluorescent protein as a transcription reporter." J Biol Chem **273**(52): 34970-5.
- Linden, H. M., S. A. Stekhova, et al. (2006). "Quantitative fluoroestradiol positron emission tomography imaging predicts response to endocrine treatment in breast cancer." J Clin Oncol **24**(18): 2793-9.
- Lino, M. and A. Merlo (2009). "Translating biology into clinic: the case of glioblastoma." Curr Opin Cell Biol **21**(2): 311-6.
- Liu, A. M., D. C. New, et al. (2009). "Reporter gene assays." Methods Mol Biol **486**: 109-23.
- Liu, H. S., M. S. Jan, et al. (1999). "Is green fluorescent protein toxic to the living cells?" Biochem Biophys Res Commun **260**(3): 712-7.
- Liu, S. (2008). "Bifunctional coupling agents for radiolabeling of biomolecules and target-specific delivery of metallic radionuclides." Adv Drug Deliv Rev **60**(12): 1347-70.
- Liu, X., X. L. Fan, et al. (2005). "Estrogen provides neuroprotection against activated microglia-induced dopaminergic neuronal injury through both estrogen receptor-alpha and estrogen receptor-beta in microglia." J Neurosci Res **81**(5): 653-65.
- Liu, Y., S. Majumder, et al. (2005). "Inhibition of HER-2/neu kinase impairs androgen receptor recruitment to the androgen responsive enhancer." Cancer Res **65**(8): 3404-9.

- Losel, R. M., E. Falkenstein, et al. (2003). "Nongenomic steroid action: controversies, questions, and answers." Physiol Rev **83**(3): 965-1016.
- Loss, E. S., M. Jacobsen, et al. (2004). "Testosterone modulates K(+)ATP channels in Sertoli cell membrane via the PLC-PIP2 pathway." Horm Metab Res **36**(8): 519-25.
- Louis, D. N. (2006). "Molecular pathology of malignant gliomas." Annu Rev Pathol **1**: 97-117.
- Luine, V. N. (1985). "Estradiol increases choline acetyltransferase activity in specific basal forebrain nuclei and projection areas of female rats." Exp Neurol **89**(2): 484-90.
- Lutz, L. B., L. M. Cole, et al. (2001). "Evidence that androgens are the primary steroids produced by *Xenopus laevis* ovaries and may signal through the classical androgen receptor to promote oocyte maturation." Proc Natl Acad Sci U S A **98**(24): 13728-33.
- Lyng, F. M., G. R. Jones, et al. (2000). "Rapid androgen actions on calcium signaling in rat sertoli cells and two human prostatic cell lines: similar biphasic responses between 1 picomolar and 100 nanomolar concentrations." Biol Reprod **63**(3): 736-47.
- Madak-Erdogan, Z., K. J. Kieser, et al. (2008). "Nuclear and extranuclear pathway inputs in the regulation of global gene expression by estrogen receptors." Mol Endocrinol **22**(9): 2116-27.
- Maggiolini, M., A. Vivacqua, et al. (2004). "The G protein-coupled receptor GPR30 mediates c-fos up-regulation by 17beta-estradiol and phytoestrogens in breast cancer cells." J Biol Chem **279**: 27008-27016.
- Mankoff, D. A., J. M. Link, et al. (2008). "Tumor receptor imaging." J Nucl Med **49 Suppl 2**: 149S-63S.
- Marcelli, M., D. L. Stenoien, et al. (2006). "Quantifying effects of ligands on androgen receptor nuclear translocation, intranuclear dynamics, and solubility." J Cell Biochem **98**(4): 770-88.
- Marin, R., B. Guerra, et al. (2003). "Estradiol prevents amyloid-beta peptide-induced cell death in a cholinergic cell line via modulation of a classical estrogen receptor." Neuroscience **121**(4): 917-26.
- Marques, R. B., S. Erkens-Schulze, et al. (2005). "Androgen receptor modifications in prostate cancer cells upon long-term androgen ablation and antiandrogen treatment." Int J Cancer **117**(2): 221-9.

- Mastronardi, L., F. Puzzilli, et al. (1998). "Tamoxifen and carboplatin combinational treatment of high-grade gliomas. Results of a clinical trial on newly diagnosed patients." J Neurooncol **38**(1): 59-68.
- Matsuda, K., I. Ochiai, et al. (2002). "Colocalization and ligand-dependent discrete distribution of the estrogen receptor (ER)alpha and ERbeta." Mol Endocrinol **16**(10): 2215-30.
- McGuire, A. H., F. Dehdashti, et al. (1991). "Positron tomographic assessment of 16 alpha-[18F] fluoro-17 beta-estradiol uptake in metastatic breast carcinoma." J Nucl Med **32**(8): 1526-31.
- Mellado, B., J. Codony, et al. (2009). "Molecular biology of androgen-independent prostate cancer: the role of the androgen receptor pathway." Clin Transl Oncol **11**(1): 5-10.
- Mendelsohn, M. E. (2000). "Mechanisms of estrogen action in the cardiovascular system." J Steroid Biochem Mol Biol **74**(5): 337-43.
- Migliaccio, A., G. Castoria, et al. (2000). "Steroid-induced androgen receptor-oestradiol receptor beta-*Src* complex triggers prostate cancer cell proliferation." Embo J **19**(20): 5406-17.
- Moll, F., D. Katsaros, et al. (2002). "Estrogen induction and overexpression of fibulin-1C mRNA in ovarian cancer cells." Oncogene **21**(7): 1097-107.
- Monge, A., M. Jagla, et al. (2006). "Unfaithfulness and promiscuity of a mutant androgen receptor in a hormone-refractory prostate cancer." Cell Mol Life Sci **63**(4): 487-97.
- Montgomery, R. B., E. A. Mostaghel, et al. (2008). "Maintenance of intratumoral androgens in metastatic prostate cancer: a mechanism for castration-resistant tumor growth." Cancer Res **68**(11): 4447-54.
- Mortimer, J. E., F. Dehdashti, et al. (1996). "Positron emission tomography with 2-[18F]Fluoro-2-deoxy-D-glucose and 16alpha-[18F]fluoro-17beta-estradiol in breast cancer: correlation with estrogen receptor status and response to systemic therapy." Clin Cancer Res **2**(6): 933-9.
- Mosca, L. (2001). "Rationale and overview of the Raloxifene Use for the Heart (RUTH) trial." Ann N Y Acad Sci **949**: 181-5.
- Nakhla, A. M., M. S. Khan, et al. (1990). "Biologically active steroids activate receptor-bound human sex hormone-binding globulin to cause LNCaP cells to accumulate adenosine 3',5'-monophosphate." J Clin Endocrinol Metab **71**(2): 398-404.

- Nakhla, A. M., J. Leonard, et al. (1999). "Sex hormone-binding globulin receptor signal transduction proceeds via a G protein." Steroids **64**(3): 213-6.
- Nash, J. D., R. F. Ozols, et al. (1989). "Estrogen and anti-estrogen effects on the growth of human epithelial ovarian cancer in vitro." Obstet Gynecol **73**(6): 1009-16.
- Nayak, T. K., H. J. Hathaway, et al. (2008). "Preclinical development of a neutral, estrogen receptor-targeted, tridentate <sup>99m</sup>Tc(I)-estradiol-pyridin-2-yl hydrazine derivative for imaging of breast and endometrial cancers." Journal of Nuclear Medicine **49**(6): 978-86.
- Necela, B. M. and J. A. Cidlowski (2003). "Development of a flow cytometric assay to study glucocorticoid receptor-mediated gene activation in living cells." Steroids **68**(4): 341-50.
- Newton, H. B. (2004). "Molecular neuro-oncology and the development of targeted therapeutic strategies for brain tumors. Part 3: brain tumor invasiveness." Expert Rev Anticancer Ther **4**(5): 803-21.
- NIH. (2003). "ICCVAM Evaluation of *In Vitro* Test Methods for Detecting Potential Endocrine Disruptors: Estrogen Receptor and Androgen Receptor Binding and Transcriptional Activation Assays." from [http://iccvam.niehs.nih.gov/docs/endo\\_docs/edfinalrpt0503/edfinalrpt.pdf](http://iccvam.niehs.nih.gov/docs/endo_docs/edfinalrpt0503/edfinalrpt.pdf).
- Nilsson, S., S. Makela, et al. (2001). "Mechanisms of estrogen action." Physiol Rev **81**(4): 1535-65.
- Noel, S. D., K. L. Keen, et al. (2009). "Involvement of G-Protein Coupled Receptor 30 (GPR30) in Rapid Action of Estrogen in Primate LHRH Neurons." Mol Endocrinol **23**: 349-359.
- O'Donnell, A. J., K. G. Macleod, et al. (2005). "Estrogen receptor-alpha mediates gene expression changes and growth response in ovarian cancer cells exposed to estrogen." Endocr Relat Cancer **12**(4): 851-66.
- O'Rourke, E. J., A. L. Conery, et al. (2009). "Whole-animal high-throughput screens: the *C. elegans* model." Methods Mol Biol **486**: 57-75.
- Otto, C., B. Rohde-Schulz, et al. (2008). "GPR30 localizes to the endoplasmic reticulum and is not activated by estradiol." Endocrinology **149**: 4846-4856.
- Owens, J. W. and J. Ashby (2002). "Critical review and evaluation of the uterotrophic bioassay for the identification of possible estrogen agonists and antagonists: in support of the validation of the OECD uterotrophic protocols for the laboratory rodent. Organisation for Economic Co-operation and Development." Crit Rev Toxicol **32**(6): 445-520.

- Pandey, D. P., R. Lappano, et al. (2009). "Estrogenic GPR30 signalling induces proliferation and migration of breast cancer cells through CTGF." EMBO Journal **28**(5): 523-532.
- Pang, Y., J. Dong, et al. (2008). "Estrogen signaling characteristics of Atlantic croaker G protein-coupled receptor 30 (GPR30) and evidence it is involved in maintenance of oocyte meiotic arrest." Endocrinology **149**(7): 3410-26.
- Pappas, T. C., B. Gametchu, et al. (1995). "Membrane estrogen receptors identified by multiple antibody labeling and impeded-ligand binding." Faseb J **9**(5): 404-10.
- Park, S. H., L. W. Cheung, et al. (2008). "Estrogen regulates Snail and Slug in the down-regulation of E-cadherin and induces metastatic potential of ovarian cancer cells through estrogen receptor alpha." Mol Endocrinol **22**(9): 2085-98.
- Pinkerton, J. V. and V. W. Henderson (2005). "Estrogen and cognition, with a focus on Alzheimer's disease." Semin Reprod Med **23**(2): 172-9.
- Plunkett, R. J., A. Lis, et al. (1999). "Hormonal effects on glioblastoma multiforme in the nude rat model." J Neurosurg **90**(6): 1072-7.
- Pollack, I. F., M. S. Randall, et al. (1990). "Effect of tamoxifen on DNA synthesis and proliferation of human malignant glioma lines in vitro." Cancer Res **50**(22): 7134-8.
- Porsolt, R. D., G. Anton, et al. (1978). "Behavioural despair in rats: a new model sensitive to antidepressant treatments." Eur J Pharmacol **47**(4): 379-91.
- Prakash Pandey, D., R. Lappano, et al. (2009). "Estrogenic GPR30 signalling induces proliferation and migration of breast cancer cells through CTGF." EMBO J.
- Preston-Martin, S. (1996). "Epidemiology of primary CNS neoplasms." Neurol Clin **14**(2): 273-90.
- Prossnitz, E. R., J. B. Arterburn, et al. (2008). "Estrogen signaling through the transmembrane G protein-coupled receptor GPR30." Annu Rev Physiol **70**: 165-190.
- Prossnitz, E. R., L. A. Sklar, et al. (2008). "GPR30: a novel therapeutic target in estrogen-related disease." Trends Pharmacol Sci **29**(3): 116-23.
- Rahman, F. and H. C. Christian (2007). "Non-classical actions of testosterone: an update." Trends Endocrinol Metab **18**(10): 371-8.

- Ramesh, C., B. Bryant, et al. (2006). "Linkage effects on binding affinity and activation of GPR30 and estrogen receptors ERalpha/beta with tridentate pyridin-2-yl hydrazine tricarbonyl-Re/(99m)Tc(I) chelates." J Am Chem Soc **128**(45): 14476-7.
- Ramesh, C., T. K. Nayak, et al. (2009). "Synthesis and Characterization of Iodinated Tetrahydroquinolines Targeting the G Protein-Coupled Estrogen Receptor GPR30." J Med Chem.
- Ramirez, S., C. T. Aiken, et al. (2003). "High-throughput flow cytometry: validation in microvolume bioassays." Cytometry A **53**(1): 55-65.
- Rasband, W. (2007). ImageJ. Bethesda, MD, NIH.
- Razandi, M., A. Pedram, et al. (2003). "Proximal events in signaling by plasma membrane estrogen receptors." J Biol Chem **278**(4): 2701-12.
- Revankar, C. M., D. F. Cimino, et al. (2005). "A transmembrane intracellular estrogen receptor mediates rapid cell signaling." Science **307**(5715): 1625-30.
- Revankar, C. M., H. D. Mitchell, et al. (2007). "Synthetic estrogen derivatives demonstrate the functionality of intracellular GPR30." ACS Chem Biol **2**(8): 536-44.
- Richer, J. K., C. A. Lange, et al. (1998). "Convergence of progesterone with growth factor and cytokine signaling in breast cancer. Progesterone receptors regulate signal transducers and activators of transcription expression and activity." J Biol Chem **273**(47): 31317-26.
- Ricke, W. A., K. Ishii, et al. (2006). "Steroid hormones stimulate human prostate cancer progression and metastasis." Int J Cancer **118**(9): 2123-31.
- Rijks, L. J., G. J. Boer, et al. (1997). "The Z-isomer of 11 beta-methoxy-17 alpha-[123I]iodovinylestradiol is a promising radioligand for estrogen receptor imaging in human breast cancer." Nucl Med Biol **24**(1): 65-75.
- Riman, T., P. W. Dickman, et al. (2002). "Hormone replacement therapy and the risk of invasive epithelial ovarian cancer in Swedish women." J Natl Cancer Inst **94**(7): 497-504.
- Risbridger, G., H. Wang, et al. (2001). "Evidence that epithelial and mesenchymal estrogen receptor-alpha mediates effects of estrogen on prostatic epithelium." Dev Biol **229**(2): 432-42.
- Risbridger, G. P., S. J. Ellem, et al. (2007). "Estrogen action on the prostate gland: a critical mix of endocrine and paracrine signaling." J Mol Endocrinol **39**(3): 183-8.

- Rocheffort, H., M. Glondu, et al. (2003). "How to target estrogen receptor-negative breast cancer?" Endocr Relat Cancer **10**(2): 261-6.
- Rodriguez, C., A. V. Patel, et al. (2001). "Estrogen replacement therapy and ovarian cancer mortality in a large prospective study of US women." Jama **285**(11): 1460-5.
- Rogan, W. J. and N. B. Ragan (2003). "Evidence of effects of environmental chemicals on the endocrine system in children." Pediatrics **112**(1 Pt 2): 247-52.
- Rosano, G. M., F. Leonardo, et al. (1999). "Acute anti-ischemic effect of testosterone in men with coronary artery disease." Circulation **99**(13): 1666-70.
- Ross, R. (1999). "Atherosclerosis--an inflammatory disease." N Engl J Med **340**(2): 115-26.
- Rossouw, J. E., G. L. Anderson, et al. (2002). "Risks and benefits of estrogen plus progestin in healthy postmenopausal women: principal results From the Women's Health Initiative randomized controlled trial." Jama **288**(3): 321-33.
- Roy, A. K., Y. Lavrovsky, et al. (1999). "Regulation of androgen action." Vitam Horm **55**: 309-52.
- Roy, A. K., R. K. Tyagi, et al. (2001). "Androgen receptor: structural domains and functional dynamics after ligand-receptor interaction." Ann N Y Acad Sci **949**: 44-57.
- Roy, P., S. Franks, et al. (2006). "Determination of androgen bioactivity in human serum samples using a recombinant cell based in vitro bioassay." J Steroid Biochem Mol Biol **101**(1): 68-77.
- Sampei, K., S. Goto, et al. (2000). "Stroke in estrogen receptor-alpha-deficient mice." Stroke **31**(3): 738-43; discussion 744.
- Sawada, H., M. Ibi, et al. (1998). "Estradiol protects mesencephalic dopaminergic neurons from oxidative stress-induced neuronal death." J Neurosci Res **54**(5): 707-19.
- Sawada, H., M. Ibi, et al. (2000). "Mechanisms of antiapoptotic effects of estrogens in nigral dopaminergic neurons." Faseb J **14**(9): 1202-14.
- Schaufele, F., X. Carbonell, et al. (2005). "The structural basis of androgen receptor activation: intramolecular and intermolecular amino-carboxy interactions." Proc Natl Acad Sci U S A **102**(28): 9802-7.



- Sherwin, B. B. (2003). "Estrogen and cognitive functioning in women." Endocr Rev **24**(2): 133-51.
- Simon, J. A., J. Hsia, et al. (2001). "Postmenopausal hormone therapy and risk of stroke: The Heart and Estrogen-progestin Replacement Study (HERS)." Circulation **103**(5): 638-42.
- Simon, S. and S. O. Mueller (2006). "Human reporter gene assays: transcriptional activity of the androgen receptor is modulated by the cellular environment and promoter context." Toxicology **220**(2-3): 90-103.
- Simoncini, T., A. Hafezi-Moghadam, et al. (2000). "Interaction of oestrogen receptor with the regulatory subunit of phosphatidylinositol-3-OH kinase." Nature **407**(6803): 538-41.
- Sirianni, R., A. Chimento, et al. (2008). "The novel estrogen receptor, G protein-coupled receptor 30, mediates the proliferative effects induced by 17beta-estradiol on mouse spermatogonial GC-1 cell line." Endocrinology **149**(10): 5043-51.
- Smith, E. P., J. Boyd, et al. (1994). "Estrogen resistance caused by a mutation in the estrogen-receptor gene in a man." N Engl J Med **331**(16): 1056-61.
- Smith, H. O., H. Arias-Pulido, et al. (2009). "GPR30 predicts poor survival for ovarian cancer." Gynecol Oncol.
- Smith, H. O., K. K. Leslie, et al. (2007). "GPR30: a novel indicator of poor survival for endometrial carcinoma." Am J Obstet Gynecol **196**(4): 386 e1-9; discussion 386 e9-11.
- Smith, H. O., K. K. Leslie, et al. (2007). "GPR30: a novel indicator of poor survival for endometrial carcinoma." Am J Obstet Gynecol **196**(4): 386.e1-11.
- Song, R. X. (2007). "Membrane-initiated steroid signaling action of estrogen and breast cancer." Semin Reprod Med **25**(3): 187-97.
- Song, R. X., Z. Zhang, et al. (2005). "Estrogen rapid action via protein complex formation involving ERalpha and Src." Trends Endocrinol Metab **16**(8): 347-53.
- Soto, A. M., M. V. Maffini, et al. (2006). "Strengths and weaknesses of in vitro assays for estrogenic and androgenic activity." Best Pract Res Clin Endocrinol Metab **20**(1): 15-33.
- Stanbrough, M., G. J. Bubley, et al. (2006). "Increased expression of genes converting adrenal androgens to testosterone in androgen-independent prostate cancer." Cancer Res **66**(5): 2815-25.



- Steru, L., R. Chermat, et al. (1987). "The automated Tail Suspension Test: a computerized device which differentiates psychotropic drugs." Prog Neuropsychopharmacol Biol Psychiatry **11**(6): 659-71.
- Steru, L., R. Chermat, et al. (1985). "The tail suspension test: a new method for screening antidepressants in mice." Psychopharmacology (Berl) **85**(3): 367-70.
- Syed, V., G. Ulinski, et al. (2001). "Expression of gonadotropin receptor and growth responses to key reproductive hormones in normal and malignant human ovarian surface epithelial cells." Cancer Res **61**(18): 6768-76.
- Tanenbaum, D. M., Y. Wang, et al. (1998). "Crystallographic comparison of the estrogen and progesterone receptor's ligand binding domains." Proceedings of the National Academy of Sciences of the United States of America **95**(11): 5998-6003.
- Taplin, M. E., B. Rajeshkumar, et al. (2003). "Androgen receptor mutations in androgen-independent prostate cancer: Cancer and Leukemia Group B Study 9663." J Clin Oncol **21**(14): 2673-8.
- Teng, J., Z. Y. Wang, et al. (2008). "The G protein-coupled receptor GPR30 inhibits human urothelial cell proliferation." Endocrinology **149**(8): 4024-34.
- Termine, J. D. and M. Wong (1998). "Post-menopausal women and osteoporosis: available choices for maintenance of skeletal health." Maturitas **30**(3): 241-5.
- Terouanne, B., B. Tahiri, et al. (2000). "A stable prostatic bioluminescent cell line to investigate androgen and antiandrogen effects." Mol Cell Endocrinol **160**(1-2): 39-49.
- Thomas, P. and J. Dong (2006). "Binding and activation of the seven-transmembrane estrogen receptor GPR30 by environmental estrogens: a potential novel mechanism of endocrine disruption." J Steroid Biochem Mol Biol **102**(1-5): 175-9.
- Thomas, P., Y. Pang, et al. (2005). "Identity of an estrogen membrane receptor coupled to a G-protein in human breast cancer cells." Endocrinology **146**(2): 624-32.
- Thomas, P., Y. Pang, et al. (2005). "Identity of an estrogen membrane receptor coupled to a G protein in human breast cancer cells." Endocrinology **146**(2): 624-32.
- Thompson, T. A., M. N. Gould, et al. (1993). "Transient promoter activity in primary rat mammary epithelial cells evaluated using particle bombardment gene transfer." In Vitro Cell Dev Biol **29A**(2): 165-70.

- Titus, M. A., C. W. Gregory, et al. (2005). "Steroid 5alpha-reductase isozymes I and II in recurrent prostate cancer." Clin Cancer Res **11**(12): 4365-71.
- Titus, M. A., M. J. Schell, et al. (2005). "Testosterone and dihydrotestosterone tissue levels in recurrent prostate cancer." Clin Cancer Res **11**(13): 4653-7.
- Toran-Allerand, C. D. (2004). "Minireview: A plethora of estrogen receptors in the brain: where will it end?" Endocrinology **145**(3): 1069-74.
- Toran-Allerand, C. D., X. Guan, et al. (2002). "ER-X: a novel, plasma membrane-associated, putative estrogen receptor that is regulated during development and after ischemic brain injury." J Neurosci **22**(19): 8391-401.
- Traupe, T., C. D. Stettler, et al. (2007). "Distinct roles of estrogen receptors alpha and beta mediating acute vasodilation of epicardial coronary arteries." Hypertension **49**(6): 1364-70.
- Tsujikawa, T., Y. Yoshida, et al. (2008). "Uterine tumors: pathophysiologic imaging with 16alpha-[18F]fluoro-17beta-estradiol and 18F fluorodeoxyglucose PET--initial experience." Radiology **248**(2): 599-605.
- Tummala, M. K. and W. P. McGuire (2005). "Recurrent ovarian cancer." Clin Adv Hematol Oncol **3**(9): 723-36.
- Van de Wiele, C., F. De Vos, et al. (2000). "Radiolabeled estradiol derivatives to predict response to hormonal treatment in breast cancer: a review." Eur J Nucl Med **27**(9): 1421-33.
- Van Den Bossche, B. and C. Van de Wiele (2004). "Receptor imaging in oncology by means of nuclear medicine: current status." J Clin Oncol **22**(17): 3593-607.
- Velema, J. P. and C. L. Percy (1987). "Age curves of central nervous system tumor incidence in adults: variation of shape by histologic type." J Natl Cancer Inst **79**(4): 623-9.
- Venners, S. A., S. Korricks, et al. (2005). "Preconception serum DDT and pregnancy loss: a prospective study using a biomarker of pregnancy." Am J Epidemiol **162**(8): 709-16.
- Vertosick, F. T., Jr., R. G. Selker, et al. (1992). "The treatment of intracranial malignant gliomas using orally administered tamoxifen therapy: preliminary results in a series of "failed" patients." Neurosurgery **30**(6): 897-902; discussion 902-3.

- Visvader, J. E. and G. J. Lindeman (2003). "Transcriptional regulators in mammary gland development and cancer." Int J Biochem Cell Biol **35**(7): 1034-51.
- Wada-Hiraike, O., H. Hiraike, et al. (2006). "Role of estrogen receptor beta in uterine stroma and epithelium: Insights from estrogen receptor beta-/- mice." Proc Natl Acad Sci U S A **103**(48): 18350-5.
- Wang, C., B. Dehghani, et al. (2009). "Membrane estrogen receptor regulates experimental autoimmune encephalomyelitis through up-regulation of programmed death 1." J Immunol **182**(5): 3294-303.
- Wang, C., B. Dehghani, et al. (2008). "GPR30 contributes to estrogen-induced thymic atrophy." Mol Endocrinol **22**(3): 636-48.
- Wang, C., E. R. Prossnitz, et al. (2008). "G protein-coupled receptor 30 expression is required for estrogen stimulation of primordial follicle formation in the hamster ovary." Endocrinology **149**(9): 4452-61.
- Webb, C. M., D. L. Adamson, et al. (1999). "Effect of acute testosterone on myocardial ischemia in men with coronary artery disease." Am J Cardiol **83**(3): 437-9, A9.
- Webb, C. M., J. G. McNeill, et al. (1999). "Effects of testosterone on coronary vasomotor regulation in men with coronary heart disease." Circulation **100**(16): 1690-6.
- White, S. N., M. Jamnongjit, et al. (2005). "Specific modulation of nongenomic androgen signaling in the ovary." Steroids **70**(5-7): 352-60.
- Wilding, G. (1995). "Endocrine control of prostate cancer." Cancer Surv **23**: 43-62.
- Wilding, G., M. Chen, et al. (1989). "Aberrant response in vitro of hormone-responsive prostate cancer cells to antiandrogens." Prostate **14**(2): 103-15.
- Willner, P. (1990). "Animal models of depression: an overview." Pharmacol Ther **45**(3): 425-55.
- Wyller, M. R., D. H. Smith, et al. (2009). "Cell-based assays to probe the ERK MAP kinase pathway in endothelial cells." Methods Mol Biol **486**: 29-41.
- Yamauchi, H., M. Cristofanilli, et al. (2009). "Molecular targets for treatment of inflammatory breast cancer." Nat Rev Clin Oncol **6**(7): 387-94.
- Yoo, J., C. S. Dence, et al. (2005). "Synthesis of an estrogen receptor beta-selective radioligand: 5-[18F]fluoro-(2R,3S)-2,3-bis(4-

hydroxyphenyl)pentanenitrile and comparison of in vivo distribution with 16alpha-[18F]fluoro-17beta-estradiol." Journal of medicinal chemistry **48**(20): 6366-6378.

Yoshida, Y., T. Kurokawa, et al. (2007). "The positron emission tomography with F18 17beta-estradiol has the potential to benefit diagnosis and treatment of endometrial cancer." Gynecol Oncol **104**(3): 764-6.

Yoshida, Y., T. Kurokawa, et al. (2009). "Positron emission tomography in ovarian cancer: 18F-deoxy-glucose and 16alpha-18F-fluoro-17beta-estradiol PET." J Ovarian Res **2**(1): 7.

Yue, W., J. P. Wang, et al. (2005). "Tamoxifen versus aromatase inhibitors for breast cancer prevention." Clin Cancer Res **11**(2 Pt 2): 925s-30s.

Zeng, J., W. Li, et al. (2008). "Insights into ligand selectivity in estrogen receptor isoforms: molecular dynamics simulations and binding free energy calculations." J Phys Chem B **112**(9): 2719-26.

Zhang, W., W. T. Couldwell, et al. (2000). "Tamoxifen-induced enhancement of calcium signaling in glioma and MCF-7 breast cancer cells." Cancer Res **60**(19): 5395-400.

}